UNIVERSITÀ DEGLI STUDI DI MILANO

Graduate School in Pharmacological Sciences

Department of Pharmacological and Biomolecular Sciences

XXVIII cycle

PhD Thesis

Molecular aspects of Alzheimer's Disease pathogenesis: from local spine trafficking to long distance spine to nucleus signalling.
"Towards new therapeutic intervention"

BIO/14

Stefano Musardo
MATRICOLA: R10237

TUTOR: ***Prof.ssa Monica Di Luca***
COORDINATORE: ***Prof. Alberto Corsini***

ANNO ACCADEMICO 2014-2015

Questa è l'essenza della scienza: fate una domanda impertinente

e preparatevi a ricevere una risposta pertinente

.

Jacob Bronowski

INDEX

INTRUDUCTION

INTRODUCTION

1 ALZHEIMER'S DISEASE: WHAT IS KNOWN AND WHAT IS UNKNOWN

Alzheimer's disease (AD) is the most common form of dementia characterized by progressive cognitive dysfunctions and loss of memory. AD has a high impact on public health in Europe: a recent study has highlighted the burden of brain diseases, showing that AD costs an estimated €55 billion per year (Di Luca et al 2011), and represents the second-leading cause of brain disorders after affective disorders and equal with addiction disorders (Andlin-Sobocki et al 2005). In Europe, the dementia affects the 6-7% of the population over 65, and the estimated number of the patients with dementia is around 5 million. These numbers, together with the burden on public health, are expected to dramatically increase, and this is due to the progressive rise of the life expectancy during the last century (Andlin-Sobocki et al 2005, Di Luca et al 2011). Up to date this tremendous disorder is incurable because of the scarce knowledge of the molecular events that drive the onset of the disease.

Alois Alzheimer, a Bavarian psychiatric, first described the disease in 1906 in a 51-years-old woman, Auguste D.[1] The autopsy showed an evenly affected atrophic brain without macroscopic foci, while the larger cerebral vessels showed arteriosclerotic changes. In all AD patients, the macroscopic characteristics come along with two microscopic hallmarks: intracellular neurofibrillary tangles (NFTs) and extracellular senile plaques that are deposits of β-amyloid (Aβ) (Price et al 1998), and these two features are still considered the prerequisites for a confirmed AD diagnosis (figure 1).

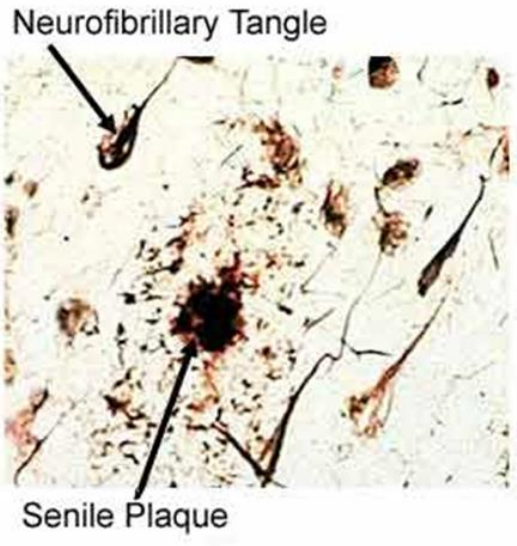

Figure 1 *Neurofibrillar tangles and senile plaque in AD cortex*

[1] Alzheimer A, Uber eine eigenartige Erkankung der Hirnrinde. Allg. Zschr. F Psychiatr. Psychisch-Gerichtl Mediz, 1907 64:p. 146-8.

Based on the age of onset, AD can be divided in two groups: the early-onset AD (EOAD) and late-onset AD (LOAD). The EOAD is diagnosed before the age of 65 and represents only the 2% of all cases, hence is considered extremely rare (Rossor et al 1996). EOAD is a familiar form of AD caused by autosomal dominant mutations. Such mutations occur in three genes: presenilin 1 (PSEN1), PSEN2 and amyloid precursor protein (APP). On the contrary, the LOAD is the most common form of the disease, characterized by genetic predisposition that involves several genes polymorphisms (for instance Apolipoprotein E) (Burke & Roses 1991), that are associated with an increased risk for AD, but are not sufficient to cause it (Ridge et al 2013, Rossor et al 1996).

1.1 The Amyloid Cascade

For more than one century, NTF and senile plaques have dominated the AD research, supported by epidemiological-clinical studies and by genetic and biochemical evidence (Puzzo et al 2015). Originally, AD research was focused on β-amyloid, which deposition has considered the driving force of the pathogenesis, responsible for synaptic dysfunction and memory loss as well as brain damage (Hardy & Allsop 1991). The increase of Aβ leads to a cascade of events consisting in formation of plaques, hyperphosphorylation of tau protein that aggregates in NFTs, neuronal death and inflammatory response: such evidence led to a formulation of the amyloid cascade hypothesis (Hardy & Higgins 1992), that for 25 years has represented the *primum movens* of AD. Aβ derives from Amyloid precursor protein (APP), a type-1 transmembrane glycoprotein, whose gene can give origin to three isoforms of the protein, with the APP695 isoform highly expressed in neuronal tissue (Tanaka et al 1988). APP undergoes a shedding process leading to the release of the ectodomain in extracellular matrix, and then the membrane-retained stub is subjected to a second cleavage to release the C-terminal tail. This complex metabolism involves different secretases (α-, β-, and γ-secretase), whose activity leads to a different destiny of APP (Haass & Selkoe 1993). In the physiological metabolic pathway of APP the α-secretase A Disintregrin And Metalloprotease 10 (ADAM10), a member of the disintegrin and metalloprotease family, represents the main protagonist of the non-amyloidogenic metabolism (Jorissen et al 2010, Kuhn et al 2010). The ADAM10-mediated ectodomain shedding of APP leads to the formation of a soluble and neuroprotective fragment called sAPPα and a membrane-retained stub named CTF83. The latter fragment is further cut by the γ-secretase, a multimeric complex composed of presenelin 1 (PS1), presenelin 2 (PS2), nicastrin, APH1 and PEN2 (Edbauer et al 2003, Musardo et al 2013). The activity of this complex generates the small peptides p3 and the amyloid intracellular domain (AICD) (Passer et al 2000). On the other hand, the production of Aβ is mediated by the concerted action of β-secratese BACE1 (β-site APP cleaving enzyme) (Vassar et al 1999), and γ-

secretase. In the amyloidogenic pathway, BACE1 cleaves APP at the N-terminus of Aβ domain, releasing the sAPPβ extracellular fragment and leaving the CTF99 hook up to the membrane. This fragment is subsequently cleaved by the γ-secretase leading to Aβ production and AICD formation (figure 2).

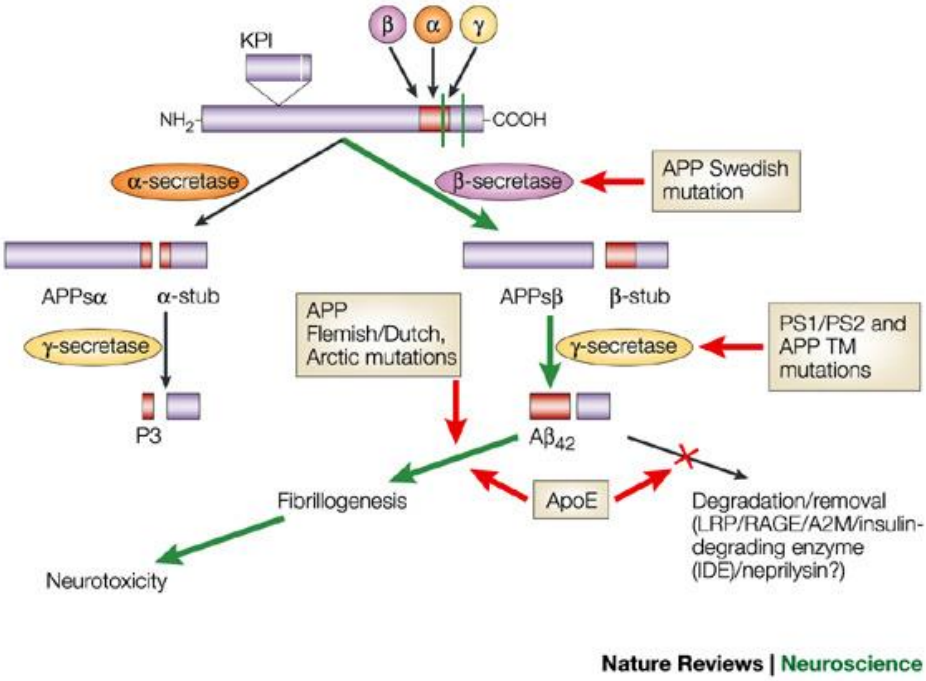

Figure 2 *Schematic of the proteolytic events and cleavage products that are generated during the processing of APP. The amyloid precursor protein (APP) Swedish mutation makes APP a more favoured substrate for beta-secretase (beta-site APP-cleaving enzyme, or BACE) cleavage, thereby increasing the flux of APP down the beta-secretase–gamma-secretase cleavage pathway to generate amyloid-beta (Abeta) (wild-type APP is predominantly processed by the alpha-secretase pathway). The mutations in presenilin 1 (PS1) and PS2 alter gamma-secretase cleavage and promote the overproduction of Abeta42.*

One of the most interesting features of APP metabolism is that Aβ is synthetized also under physiological condition and the abnormal accumulation in AD patients is due to an unbalance of Aβ production and clearance (Marcello et al 2012a). Which are the molecular events that orchestrate this unbalance? The answer is still unknown and represents a hard challenge for all the neuroscientists. The belief that Aβ can be the driving force of AD pathogenesis rises from a lot of evidence. Firstly, different research groups have identified specific mutations in APP gene in patients with FAD (Goate et al 1991, Hardy 1992, Hendriks et al 1992, Mullan et al 1992). Secondly, the finding that Aβ is a physiological product of APP metabolism, and that could be measured in several biological samples (Haass et al 1992, Seubert et al 1992, Shoji et al 1992), allowed neuroscientist to strongly correlate Aβ deposition with APP mutation. Moreover, it has been shown that a specific mutation in APP gene with neuroprotective activity against cognitive dysfunction in aged people results in a reduction in the formation of Aβ (Jonsson et al 2012). This mutation (A673T) is adjacent to the BACE-site in APP, and

results in an approximately 40% reduction in the formation of amyloidogenic peptides *in vitro*. On the contrary, up to date several mutations have been identified close to the cleavage sites of β- or γ-secretase that promote the generation of Aβ (Cai et al 1993, Citron et al 1992, Suzuki et al 1994). Several mutations in PS1 and PS2 were also observed in AD families. Such mutations affected γ-secretase complex activity, leading to the alteration of APP metabolism and to an increase of the formation of the 42 aminoacids Aβ that is more prone to aggregate (Borchelt et al 1996, Citron et al 1997, Duff et al 1996) (figure 2)

All these considerations had strongly supported the amyloid hypothesis; furthermore, the identification of different mutations in APP, PS1 and PS2 genes related to FAD, led to the generation of different transgenic animal models that are still in use to investigate the pathogenic mechanisms and the progression of the disease (Saraceno et al 2013). The amyloidocentric theory of AD is supported also by the observation that mutations in tau protein cause frontotemporal dementia (FTD) (Hutton et al 1998, Poorkaj et al 1998, Spillantini et al 1998), a neurodegenerative disorder characterized by harsh deposition of tau protein in NFTs without deposition of amyloid. This observation suggests that NFTs deposition in AD patients (that are composed of hyperphosphorylated wild-type tau protein) is a secondary process that comes only after changes in Aβ metabolism and plaques deposition (Hardy et al 1998, Lewis et al 2001, Rapoport et al 2002), even if the precise temporal and mechanistic relationships between Aβ deposition and tau pathology remain to be resolved. In summary, the first version of the amyloid cascade hypothesis posits that the insoluble extracellular deposition of the Aβ peptide in the brain parenchyma is a crucial step that ultimately leads to AD (figure 3).

Another piece of evidence supporting this theory came from several studies in which the application of Aβ fibrils to cultured neurons was highly toxic *in vitro* (Lorenzo & Yankner 1996) and that intracerebral injection of Aβ fibril caused a neurodegeneration-associated disruption of performance of cognitive tasks in animals (Maurice et al 1996, McDonald et al 1994, Nitta et al 1994, Stephan et al 2001).

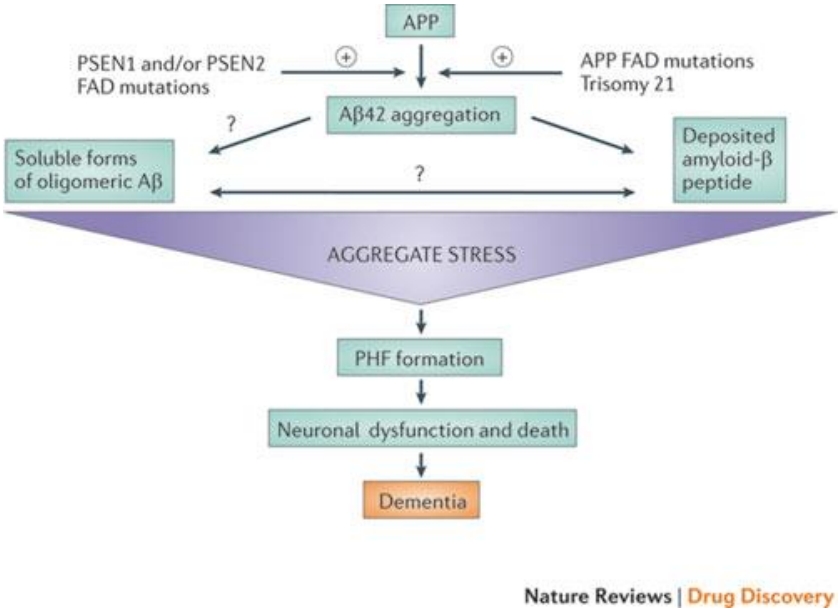

Figure 3 *The amyloid cascade hypothesis posits that the deposition of the amyloid-β peptide in the brain parenchyma is a crucial step that ultimately leads to Alzheimer's disease. Autosomal dominant mutations that cause early onset familial Alzheimer's disease (FAD) occur in three genes: presenilin 1 (PSEN1), PSEN2 and amyloid precursor protein (APP). This hypothesis has been modified over the years as it has become clear that the correlation between dementia or other cognitive alterations and amyloid-β accumulation in the brain in the form of amyloid plaques is not linear, neither in humans nor in mice. The concept of amyloid-β-derived diffusible ligands or soluble toxic oligomers, has been proposed to account for the neurotoxicity of the amyloid-β peptide.*

However, accumulating evidence suggest that senile plaques or NFTs volume poorly correlate with the severity of dementia. Several studies have demonstrated that the correlation between dementia and Aβ accumulation in the brain in the form of amyloid plaques is not linear, neither in humans nor in mice (Price et al 1998, Terry 1996, Walsh & Selkoe 2007). On the contrary many studies demonstrated the correlation between measures of synaptic density and degree of dementia (DeKosky & Scheff 1990, Terry et al 1991). Electron microscopy, immunocytochemical and biochemical analyses on synaptic marker proteins in AD biopsies and autopsies (Dickson et al 1995, Honer et al 1992, Terry et al 1991) indicate that synaptic loss in the hippocampus and neocortex is an early event (Masliah et al 1994). Moreover, different research groups have shown that the decrease in synapse number and density is not proportional to the loss of neuronal cell bodies (Bertoni-Freddari et al 1996, Davies et al 1987, DeKosky & Scheff 1990), suggesting that during the disease process the lack of synaptic endings may precede the collapse of the neuron. Recently, different neuroscientists have discovered some modifications in the brains of AD patients and APP transgenic mice, consolidating the idea that synaptic function is compromised prior to the physical deterioration of neuronal structures (Oddo et al 2003, Palop et al 2003, Westphalen et al 2003, Yao et al 2003).

1.2 The Amyloid Hypothesis: An Update

This revisited amyloid hypothesis that points out to a pivotal role of Aβ oligomers could have a mechanistic explanation. The senile plaques, which are composed of fibrillar aggregates, present less β-amyloid surface area to neuronal membranes, compared to small oligomers, which can diffuse into synaptic clefts. This soluble assembly forms are better candidates for inducing neuronal and/or synaptic dysfunction rather than plaques load. Indeed, soluble molecular species generated at early stages of the disease could be involved in synaptic failure (Hardy & Selkoe 2002, Klein et al 2001). Human Aβ can exist in diverse assembly states, including monomers, dimers, trimers, tetramers, dodecamers, higher-order oligomers and protofibrils, as well as mature fibrils, which can form microscopically visible amyloid plaques in brain tissues (Glabe 2008). The soluble assemblies of β-amyloid, also known as Aβ-derived diffusible ligands (ADDLs), can cause cognitive problems by disrupting synaptic function in the absence of significant neurodegeneration, and only at more advanced stages are deposited in senile plaques (Hardy & Selkoe 2002, Klein et al 2001).

The correlation between Aβ species and age-dependent memory loss firstly arose from a study carried out in Tg2576 transgenic mice expressing human APP695 with Swedish mutation (K670N/M671L) (Hsiao et al 1995). These animals show elevated levels of $A\beta_{1-42}$ in the brain and perform badly during spatial memory test (Morris water maze) (Westerman et al 2002). Subsequently, as a consequence of these results, several researchers demonstrated this association also in other transgenic animal models such as 3XTg-AD mice (Oddo et al 2003), which harbour three human mutation (PS1M146V, APP_{SWE} and tauP301L), and the J20 mouse model that overexpresses human APP with Swedish and Indiana (V717F) mutations (Mucke et al 2000). All these studies showed that synaptic failure and cognitive impairment strongly correlate with the increase of soluble oligomeric Aβ species, and this phenotype is evident prior to the deposition of senile plaques and NFTs.

Although which mechanism triggers the synaptic failure is still poorly understood, all the considerations described above clearly point out the Aβ oligomers as the species responsible for synaptic plasticity modifications. Therefore, several studies carried out electrophysiological measurements of synaptic plasticity in different AD animal models.

The two main paradigms of activity-dependent synaptic plasticity that describe the capability of the excitatory synapses to adapt their activity in response to specific stimuli are the long-term potentiation (LTP) and long-term depression (LTD). LTP induction increases the efficacy and strength of the synapse and requires activation of the N-methyl-D-aspartate receptors (NMDARs). Such activation leads to a signalling cascade that induces the insertion of α-amino-3-hydroxy-5-methyl-4-isoxazolepropionic acid receptors (AMPARs) into the postsynaptic membrane (Malenka & Bear 2004). On the contrary, LTD

induction leads to a decrease of synapse efficacy and is mediated by the endocytosis on AMPARs (Malenka & Bear 2004).

Several studies have shown that Aβ application on hippocampal cultures on one side impaires the LTP, acting on NMDARs-dependent downstream signalling, and on the other side it enhances the LTD (Hsieh et al 2006, Shankar et al 2008, Walsh et al 2002a, Walsh et al 2002c)This evidence pushed the neuroscientists to investigate which β-amyloid-dependent molecular events drive synaptic dysfunction. Diverse scientific reports suggest that synaptic dysfunction is dependent on NMDARs-mediated activity that leads to an increase in cytoplasmic levels of Ca^{2+} and activation of Ca^{2+}-dependent downstream pathways (Kamenetz et al 2003, Shankar et al 2007). In this frame, one of the downstream proteins is calcineurin and its activation leads to cofilin dephosphorylation, and indeed activation. Cofilin is an actin filament severing protein and its activation results in dendritic spine loss (Shankar et al 2007). A recent study has also demonstrated that Aβ oligomers can interact with human leukocyte immunoglobulin-like receptor B2 (LilrB2) leading to the enhancement of cofilin signalling (Kim et al 2013). Moreover, Aβ can interact with the mouse orthologue paired immunoglobulin-like receptor B (PirB) and this interaction increase memory loss in AD animal models (Kim et al 2013). The synaptic failure induced by Aβ involves also the removal of AMPARs from the synaptic membrane and the degradation of postsynaptic density-95 (PSD-95) protein at glutamatergic synapses (Almeida et al 2005, Roselli et al 2005). The application of Aβ to wild-type hippocampal neurons increases the endocytosis of AMPARs; moreover neuronal cultures obtained from Tg2576 mice have selective alterations in pre- and post-synaptic compartments compared to wild-type neurons (Almeida et al 2005). The authors observed early reductions in surface expression of AMPARs subunit GluA1 in Tg2576 neurons. Moreover, they provide evidence that Aβis specifically involved in these alterations in synaptic biology, since alterations in PSD-95 and GluA1 are blocked by γ-secretase inhibition. The unbalance of AMPARs endocytosis and the consequent removal from synaptic membrane is due to the dysregulated activation of calcineurin/PP2B and downregulation of Ca2+/calmodulin-dependent protein kinase II (CamKII) mediated by Aβ (Gu et al 2009, Zhao et al 2010). This applies also to NMDARs: Aβ fosters surface removal of NMDARs that is triggered by the dephosphorylation at the tyrosine 1472 of the GluN2B subunit. This process is mediated by the activation of the phosphatase STEP (Kurup et al 2010, Snyder et al 2005), and the dephosphorylation of the Tyr1472 leads to a decrease of the association of NMDARs with PSD-95 and to a concomitant increase of the association with the clathrin adaptor protein AP-2 directly involved in endocytosis machinery (Snyder et al 2005). Such evidence demonstrated that Aβ can affect NMDARs or AMPARs endocytosis and, thereby, it can influence the glutamatergic transmission.

In physiological conditions, the internalization of AMPARs requires the activation of the apoptotic effector component caspase-3 (Li et al 2010); this protein activates calcineurin that is involved, as described above, in the dephosphorylation of GluA1. In pathological conditions, like AD, caspase 3 has been found enriched in the postsynaptic density (Louneva et al 2008) and this suggested a pathological role in early synaptic failure. Indeed, in Tg2576 mice an enhancement of the activity of caspase 3 has been found at the onset of memory decline. The molecular modifications mediated by caspase 3 led to alterations of glutamatergic synaptic transmission and plasticity and correlated with spine degeneration and a deficits in hippocampal-dependent memory (D'Amelio et al 2011).

In addition to NMDARs and AMPARs an involvement of the metabotropic glutamate receptor (mGluRs) in Aβ mediated synaptic dysfunction has been suggested (Shankar et al 2008), since it is well established that activation of mGluRs leads to induction of LTD (malenka et al 2004, bellone et al 2008). The experiment of Shankar and colleagues demonstrates that different sources of Aβ (synthetic, extracted from human brain or from cells) can facilitate mGluR-mediated LTD and can inhibit LTP leading to a reduced dendritic spine density. Such considerations support the idea that soluble Aβ can play a central role in synaptic failure.

How can Aβ impair LTP and facilitate LTD? It has been shown that the oligomers can interfere with the glutamate uptake process (Li et al 2009). The glutamic acid represents the most abundant excitatory neurotransmitter in the nervous system (Meldrum 2000) that binds and activates the ionotropic receptor, such as NMDARs or AMPARs, or the metabotropic receptors mGluR. Glutamate is stored in presynaptic vesicles and under specific impulses is released in the synaptic cleft. An excess of glutamate levels can overstimulate the receptors leading to a damage of the neurons or to the activation of cell death systems (Mehta et al 2013). In AD patients it has been found that the glutamate transporter EEAT1 and EEAT2, which are responsible for glutamate uptake, are downregulated in the hippocampus (Jacob et al 2007). The spill-out of glutamate leads to the accumulation of the neurotransmitter into the extrasynaptic space, where it can overactivates the extrasynaptic GluN2B-containing NMDARs (Li et al 2011). The presence of soluble Aβ oligomers can foster the release of glutamate from astrocytes with a subsequent accumulation in extrasynaptic compartments and aberrant activation of extrasynaptic NMDARs (Talantova et al 2013). This results in a complex activation of different signalling pathways that lead to neuronal loss. One of the altered pathways is the oxidation reactions chain: the hyperactivation of neuronal nitric oxidase synthase (nNOS) and the overload of calcium in mitochondria generate an excess of reactive nitrogen and oxygen species (RNS/ROS) (Molokanova et al 2014). Consequently, different proteins can undergo an aberrant oxidation reaction disrupting their normal function. One example is the S-nitrosylation of sulfonation of the myocyte enhancer factor 2 (MEF2), a (Potthoff & Olson 2007). The altered S-nitrosylation

disrupts the MEF2-DNA binding and transcriptional activity, leading to impaired neurogenesis and cell survival (Okamoto et al 2014). Another target protein of the S-nitrosylation process is Cdk5, a kinase whose activity is known to regulate the morphogenesis of dendritic spines, thus influencing the function of neuronal circuits (Fu et al 2007). Aberrant redox regulation of Cdk5 activity triggered by S-nitrosylation has been found in both AD animal models and patients, and contributes to Aβ induced dendritic spine loss (Qu et al 2011).

The integrity and morphology of the spines are guaranteed by several scaffold proteins, such as PSD-95, which play a central role in protein assembly, synaptic development and neural plasticity (Kim & Sheng 2004, Sheng & Hoogenraad 2007). In particular, PSD-95 binds and directly influences the activity of the NMDARs and AMPARs; in the brain of post-mortem AD patients it has been found that the levels of PSD-95 are downregulated and this decrease correlates with the amount of Aβ oligomers and severity of dementia (Gylys et al 2004). Similar data come from studies carried out on AD animal models (Almeida et al 2005, Spires & Hyman 2005) and on neurons exposed to Aβ (Roselli et al 2005). In both cases, the disruption of PSD-95 is accompanied by spine loss and AMPARs removal from synaptic membranes, thus suggesting a role in the pathogenesis of AD. Furthermore, several authors found that Aβ co-localizes with PSD-95 at the excitatory synapses in human AD brains and in neuronal cultures exposed to Aβ (Lacor et al 2004, Pham et al 2010), suggesting that Aβmay interact with PSD-95 and interfere with its activity, leading to synaptic damage.

Such evidence revealed the capability of Aβ to bind different synaptic receptors and to affect their physiological activity. However, several studies demonstrated that synaptic failure could be mediated by activation of molecules, and their related intracellular pathway, that are not directly associated with ionotropic receptors activity. One example is the low-affinity p75 neurotrophin receptor ($p75^{NTR}$); it has been demonstrated that Aβ can bind $p75^{NTR}$ whose activation induces apoptosis (Chakravarthy et al 2010, Yaar et al 1997). Moreover, in hippocampal neurons of AD animals and in human post-mortem AD hippocampi, it has been found an upregulation of surface expression of $p75^{NTR}$ (Chakravarthy et al 2010, Chakravarthy et al 2012) and a downregulation of the neurotrophin high-affinity receptor TrkA (Costantini et al 2006). The opposite regulation of these two neurotrophin receptors can shift APP metabolism towards the amyloidogenic pathway. In fact, $p75^{NTR}$ promotes the activity of BACE-1 while TrkA decrease it (Costantini et al 2006, Costantini et al 2005). Therefore, in a pathological context such as AD, the upregulation of $p75^{NTR}$ and the downregulation of TrkA promote the activity of BACE-1, leading to an overproduction of Aβ that can generate a vicious circle.

In addition to neurotrophin receptors, insulin and insulin-like growth factor receptors and their related signalling pathways play a critical role in synaptic plasticity and cognitive function by affecting both excitatory and inhibitory synaptic activity (Zhao & Alkon 2001, Zhao et al 2004). In the last 10 years, it

is increasingly gaining ground the hypothesis that AD may represent a metabolic disease of the brain associated with brain insulin and insulin-like growth factor-I (IGF-I) resistance and deficiency. Alterations of insulin signalling may contribute to dysregulation of downstream pro-survival pathways, including decreased signalling mediated by PI3K, Akt, and Wnt/β-catenin; moreover, disrupted insulin-related signalling may enhance pathogenic pathways such as glycogen synthase kinase 3 (GSK-3β) to trigger tau hyperphosphorylation (de la Monte et al 2010, Liao & Xu 2009). As described in paragraph 1.1, hyperphosphorylated tau (p-tau) is the main component of NFTs, one of the hallmarks of AD. Tau is a microtubule-associated protein (MAP) that was originally identified as the driving force of microtubule assembly and network stabilization (Lee & Rook 1992, Weingarten et al 1975). In pathological conditions, the hyperphosphorylation of tau leads to dissociation from microtubules and aggregation in tangles, a common feature of several neurological disorders. Initially tau was known as an axonal protein, but a recent study demonstrated that tau is also expressed in dendrites and postsynaptic density although at lower levels (Ittner et al 2010). Moreover, several studies demonstrated that p-tau colocalizes with Aβ in synaptic terminals in both AD patients and AD animal models (Fein et al 2008, Takahashi et al 2010) and this correlates with synapses loss and with disease progression (Manczak & Reddy 2013). Aβ and p-tau can have a negative synergic action with a positive feedback; as described above, Aβ can stimulate astrocytes to release glutamate, whose accumulation in turn activates the extrasynaptic NMDARs, ultimately leading to an over production of p-tau (Talantova et al 2013). This causal association is further confirmed by studies demonstrating that Aβ synaptic loss is tau-dependent, since the deletion or reduction of tau protein can rescue Aβ mediate synaptic loss and cognitive impairment in AD animal models (Ittner et al 2010, Roberson et al 2007). Shipton and colleagues (Shipton et al 2011) demonstrated that the absence of tau protein prevents β-amyloid-induced impairment of LTP. Moreover, they showed that Aβ increases tau phosphorylation and that a specific inhibitor of the tau kinase GSK3β blocks the increased tau phosphorylation induced by Aβ and prevents β-amyloid-induced impairment of LTP in wild-type mice. Together, these findings show that tau protein is required for Aβ triggered synaptic failure in the hippocampus and suggest that the β-amyloid-induced impairment of LTP is mediated by tau phosphorylation. Moreover, hippocampal primary neurons exposed to Aβ oligomers show an evident missorting of endogenous tau into the somatodendritic compartment (Zempel et al 2010). In missorted dendritic regions, there is a depletion of spines, a local increase in Ca^{2+} and the breakdown of microtubules, which leads to impairment of AMPARs surface expression and synaptic transmission (Hoover et al 2010).

All these pieces of evidence clearly point out Aβ oligomers as central player in AD pathogenesis, representing the driving force of synaptic dysfunction and cognitive decline. Aβ-mediated synaptic

dysfunction involves several signalling pathways, including the glutamate receptors and the related downstream signalling, the spill-out of glutamate and its accumulation in extrasynaptic compartments with a subsequent over activation of extrasynaptic NMDARs, and the hyperphosphorylation of tau. Even if a lot of evidence highlights the involvement of different and complex pathological events, the details of molecular mechanisms are still poorly understood.

2 THE α-SECRETASE ADAM10

ADAM10 is a 748 amino acid type I membrane glycoprotein, which is ubiquitously expressed (Wolfsberg et al 1995). Members of the ADAM family are characterized by a defined domain structure, including a signal sequence, a N-terminal prodomain, followed by a catalytic proteinase domain containing a zinc-binding motif, a disintegrin, a cysteine-rich transmembrane, and a cytoplasmatic domain (Weskamp et al 1996, Wolfsberg et al 1995). The nascent protein itself is not functional and is produced as a zymogene. ADAM10 is predominantly found as a proenzyme intracellularly in the Golgi, presumably in an inactive form (Lammich et al 1999). After the cleavage of the signal sequence, ADAM10 enters the secretory pathway to be processed and thereby activated by the proprotein convertases furin or PC7 (Anders et al 2001), as demonstrated for the prodomains of several ADAMs (Loechel et al 1998, Lum et al 1998, Roghani et al 1999). Furin and PC7 are calcium-dependent endoproteases responsible for proteolytic cleavage of cellular and viral proteins
transported via the constitutive secretory pathway. Cleavage occurs at the C-terminus of basic amino acid sequences, such as R–X–K/R–R and R–X–X–R. The furin was found predominantly in the TGN, but also in clathrin-coated vesicles dispatched from the TGN, on the plasma membrane as an integral membrane protein and in the medium as an anchorless enzyme (Schafer et al 1995). ADAM10 prodomain exhibits a dual function: the separately expressed prodomain is capable of inactivating endogenous ADAM10 in cell cultures while overexpressed ADAM10 without its prodomain is inactive (Anders et al 2001). By contrast, coexpression of the prodomain in trans rescues the activity of the deletion mutant of ADAM10 without the intracellular prodomain (Anders et al 2001). In addition, the recombinant murine prodomain purified from Escherichia coli acts as a potent and selective competitive inhibitor in experiments performed *in vitro* (Moss et al 2007). This implicates that the prodomain of ADAM10 acts not only as a transient inhibitor, but also as an internal chaperone in the maturation of the enzyme. The catalytic domain of ADAM10 contains a typical zinc-binding consensus motif (HEXGHXX GXXHD); the mutation E384A, compromising this motif, leads to a substantial decrease in sAPPα secretion (Fahrenholz et al 2000, Postina et al 2004). Although the removal of the disintegrin domain of ADAM10 did not grossly affect shedding of APP in cell cultures (Fahrenholz et al

2000), the cleavage of some substrates molecule is likely to be influenced by non-catalytic domains. For example, epidermal growth factor cleavage is at least partially impaired in ADAM10 knockout cells overexpressing a cytoplasmic domain deletion mutant of ADAM10 (Horiuchi et al 2007). During transport through the secretory pathway, ADAM10 is complex N-glycosylated resulting in the active protease, which mediates proteolysis in the late compartments of the secretory pathway and at the plasma membrane. Cell surface biotinylation experiments demonstrated that the proteolytically activated form of ADAM10 is localized mainly in the plasma membrane (Lammich et al 1999).

3 THE GLUTAMATERGIC EXCITATORY SYNAPSE

The human brain is the most complex biological system in the universe and consists of a billion of neurons, each forming up to 100.000 synaptic connections. These connections represent the cell-cell communication sites in the central nervous system and are mainly constituted by specialized contact zones between neurons called chemical synapses. The term “synapse” indicates a simply contact between two nerve cells without the continuity of substance. In the first half of the 1900, the synapses were described as polarized neuronal cell junctions with specific membrane specializations at transmitter-releasing presynaptic site and with, in close opposition, the afferent postsynaptic part. In the excitatory synapse, the membrane of postsynaptic compartment appears thickened and electron-dense and, because of these two features, this compartment was defined postsynaptic density (PSD). Subsequently, the rise of high-resolution electron microscopy and elaborated cryo-fixation techniques have defined the ultrastructure of the synaptic contact zone (figure 4):

- *Presynaptic active zone*: a cluster of dense granular presynaptic particles and synaptic vesicles characterizes this compartment. Some of the vesicles are closely associated with the presynaptic membrane and undergo exocytosis process (Sudhof 2004);
- *Synaptic cleft*: it is a very narrow space with a width of 23.8 nm in which different cell-adhesion molecules hold pre- and postsynaptic membranes together, guaranteeing the proper distance and separation (Scheiffele 2003);
- *PSD*: it is a portion of the post-synaptic membrane that is directly opposed to the active zone and ensures that receptors are in close proximity to presynaptic neurotransmitter release sites. Hundreds of proteins have been identified in the postsynaptic density including glutamate receptors, scaffold proteins, and many signaling molecules. The PSD results in an assembly of proline-rich synapse-associated protein/SH3 and ankyrin repeat-containing proteins (ProSAP/Shank) (Baron 2006, Zuber et al 2005).

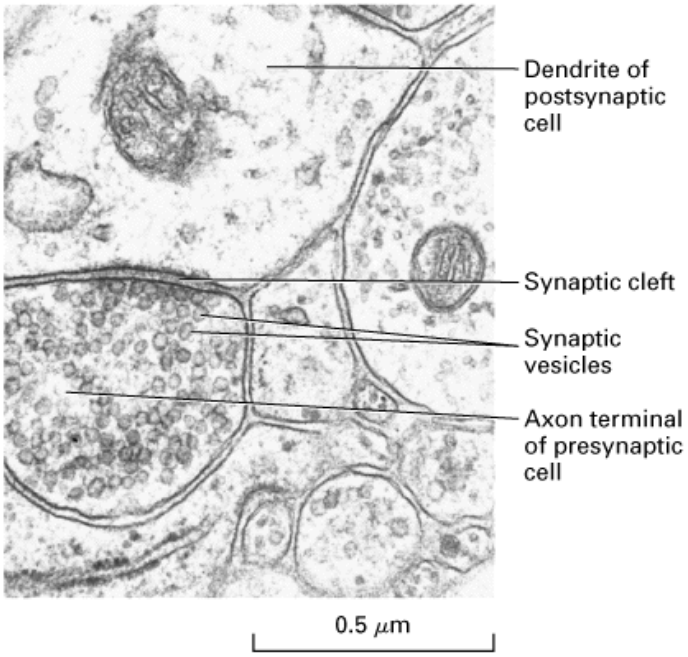

Figure 4 *Electron micrograph showing a cross section of a dendrite synapsing with an axon terminal filled with synaptic vesicles. In the synaptic region, the plasma membrane of the presynaptic cell is specialized for vesicle exocytosis; synaptic vesicles, which contain a neurotransmitter, are clustered in these regions. The opposing membrane of the postsynaptic cell contains receptors for the neurotransmitter.*

In addition to this electron-dense region, the postsynaptic compartment can be divided in two other specialized regions called perisynaptic and extrasynaptic regions.

The extrasynaptic regions are enriched with a distinctive set of proteins, such as metabotropic glutamate receptors (Baude et al 1993) and proteins involved in endocytosis (Racz et al 2004).

Excitatory synapses are characterized by different glutamate receptors (GluRs), AMPARs, NMDARs and mGluRs, which are specifically targeted and clustered at the PSD (Mayer & Armstrong 2004). All these receptors are components of individual, tightly associated, multiprotein complexes that regulate synaptic targeting or removal from synaptic sites, local expression, signal transduction and clustering (Kim & Sheng 2004). With increasing knowledge about protein composition, it became even more pressing to understand the spatial organization of molecules within the PSD.

The PSD of excitatory synapses seems to be arranged in a clear-cut laminar hierarchical structure (Zuber et al 2005). This hierarchy appears to be determined by the targeting and binding characteristics of the individual proteins. At the membrane, receptors are organized in distinct subcompartments combined into larger protein units, which are finally attached to the local cytoskeleton. As a consequence, PSD proteins can be divided in different groups: membrane-bound receptors and channels (i.e. GluRs) scaffolding proteins (i.e. members of the MAGUK family), signalling and regulatory proteins (i.e. Calcium-calmodulin-dependent Kinase II (CaMKII) and cell adhesion proteins.

3.1 Glutamate Receptors

Glutamate is generally acknowledged to be the most important neurotransmitter for normal brain function. It is released from vesicles from pre-synaptic sites and interacts with its receptors on the post-synaptic site. There are two major classes of GluRs: ionotropic receptors are cation channels whose opening is favored (over the closed state) when glutamate binds to the receptor, while metabotropic receptors do not conduct ion fluxes. When they bind glutamate, they activate intracellular enzymes through G proteins. Several types of iGluRs have been identified: AMPARs, NMDARs and kainate receptors. The cloning of iGluRs immediately led to correlate their amminoacid sequence to function and mechanism. Contrary to expectations, iGluRs proved to have only three transmembrane domains (M1, M3 and M4) plus a cytoplasm-facing re-entrant membrane loop (M2). Thus the N-terminus is located extracellularly and the C-terminus intracellularly.

For ionotropic glutamate receptors, the agonist binding sites and associated ion channel are incorporated into the same macromolecular complex. Agonist binding forces a conformational change in the receptor that increases the probability of channel opening. The affinity for glutamate is different for the different glutamate receptors. The EC50 (half maximal effective concentration) of glutamate at NMDA receptors is approximately 1 µmol/l, while at AMPA receptors it is approximately 400 µmol/l (Traynelis et al 2010).

3.1.1 AMPA Receptors

AMPARs are heterotetramers composed of a combination of GluAs 1 to 4 (GluA1-4) subunits that assemble in a combinatorial fashion to form a functional receptor channel (Nakanishi et al 1990). They are activated by glutamate and antagonized by 6-ciano-7-nitroquinoxaline-2,3-dione (CNQX) and 2,3-dihydroxy-6-nitro-7-sulfamoylbenzo(f)quinoxaline (NBQX). These receptors are the major mediators of fast glutamatergic excitatory synaptic transmission in the CNS. Structural studies suggest that tetrameric assemblies of AMPARs are achieved in a dimer-of-dimers fashion (Madden 2002). Different subunits of AMPARs display distinct spatial and temporal pattern of expression and endow specific properties to AMPAR complexes: AMPARs containing GluA2 subunits show lower permeability to Ca^{2+} while receptors assembled from GluA1, GluA3 and GluA4 are highly permeable to Ca^{2+} (Burnashev et al 1992). Alternative splicing and RNA editing provide further variability of the functional receptor characteristics. GluA2 subunit, for example, undergoes RNA editing which prevents Ca^{2+} permeability, contributes to linear I-V relationship of current flux and confers insensitivity to intracellular spermine (Boulter et al 1990, Keller et al 1992, Washburn et al 1997) (figure 5).

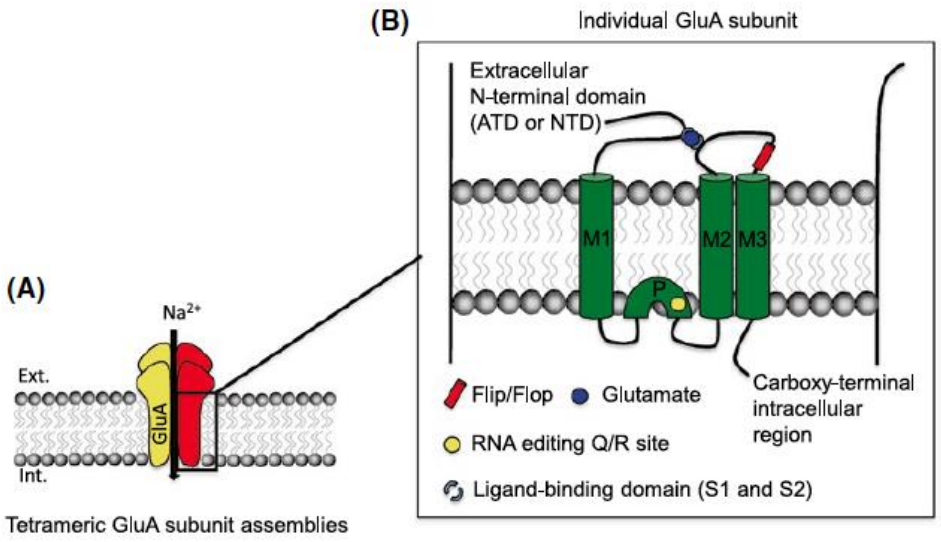

Figure 5 *AMPARs structure and subunits composition. AllAMPAR subunits consist of an extracellular amino terminal domain (ATD or NTD), a ligand-binding domain (LBD) (S1 and S2), three membrane-spanning domains (M1, M2 and M3), one cytoplasmic re-entrant loop (P), and a carboxy-terminal intracellular region. The extracellular and transmembrane regions of all GluAs are highly homologous and the four GluAs differ from each other mainly in terms of their intracellular cytoplasmic tails*

Protein quantification study on the purified PSD fraction reported the ratio among different GluA subunits suggesting that the major AMPARs in the forebrain are likely to be GluA1- and GluA2-containing (Cheng et al 2006).

All four subunits of AMPARs have several identified phosphorylation sites on their intracellular C-termini that regulate their function and that seem to be involved in the regulation of various form of synaptic plasticity.

GluA1 is one of the most abundantly expressed subunit of AMPARs in hippocampal and neocortical neurons (Martin et al 1993). Most of the phosphorylation on GluA1 occurs on serine and threonine residues (Blackstone et al 1994), but tyrosine phosphorylation has also been observed under certain circumstances (Moss et al 1993). Ser831 and Ser845 have been implicated in the expression of LTP and LTD (Barria et al 1997). Phosphorylation on GluA1-Ser831 is mediated by PKC and CaMKII (Roche et al 1996), while GluA1-Ser845 is phosphorylated by protein kinase A (PKA) (Roche et al 1996). Phosphorylation on both of these residues can enhance current through AMPARs, albeit via distinct mechanisms (Derkach et al 1999).

GluA2 is a key subunit which renders AMPARs channel impermeable to Ca^{2+} and confers specific biophysical properties (Tanaka et al 2000). There are several serine phosphorylation sites (Ser863 and Ser880) mapped on the intracellular C-terminal of GluA2 that are phosphorylated by PKC (Matsuda et al 1999). Among these, Ser880 has been implicated to play a role in synaptic plasticity. When

unphosphorylated at Ser880, GluA2 can interact with PDZ domains of glutamate receptor interacting protein GRIP/ABP (AMPARs Binding Protein) or interacting with PICK-1 (Matsuda et al 1999). Interaction between GluA2 and GRIP family of proteins has been shown to stabilize AMPARs at synaptic locations (Dong et al 1997) or intracellular pools (Daw et al 2000). On the other hand, phosphorylated Ser880 allows preferential binding to PICK-1. Interaction of Ser880 phosphorylated GluA2 to PICK-1 has been demonstrated either to promote endocytosis (Chung et al 2000) or allow trafficking of receptors to the plasma membrane (Daw et al 2000).

GluA3 and GluA4 are highly expressed in the adult forebrain structures compared to GluA1 and GluA2 subunits (Petralia & Wenthold 1992). They contain homologous phosphorylation sites corresponding to those on GluA1 and GluA2, which have been implicated in synaptic plasticity mechanisms. GluA4 can be inserted into synapses by spontaneous activity and its expression in the hippocampus is limited to the early post-natal period development (Zhu et al 2000).

3.1.2. NMDA Receptors

NMDARs are cationic channels which are permeable to sodium (Na^+), potassium (K^+) and calcium (Ca^{2+}) ions. In particular, Ca^{2+} influx is the critical factor mediating many of the NMDAR-specific physiological and pathological events (Holtmaat & Svoboda 2009). NMDARs are heterotetramers that differ according to their subunit composition. To date, 7 different NMDAR subunits have been identified and have been classified in 3 subfamilies according to their sequence homology, one represented by a single gene (GluN1, encoding a protein of ~900 amino acids), the second by four genes (GluN2A-GluN2D, ~1450 amino acids) and the third by two known genes (GluN3A-GluN3B, about 1000 amino acids) (Paoletti et al 2013). NMDARs classically consist of 2 obligatory GluN1 subunits and 2 regulatory subunits either 2 GluN2 or a mixture of GluN2 and GluN3 subunits (Sanz-Clemente et al 2013). The different combination of NMDAR subunits has the advantage of providing a multiplicity of receptor subtypes in the CNS. NMDAR subunits share a similar modular architecture. They consist of a large extracellular amino-terminal domain (NTD), 3 membrane-spanning regions (M1, M3 and M4), a re-entry loop (M2) and an intracellular carboxy-terminal domain (CTD) (Dingledine et al 1999, Mayer 2006). The extracellular S1 loop in the NTD and the S2 loop in the extracellular region between M3 and M4 form a bilobed structure which represent the binding site for the 2 co-agonists, glycine or D-serine for GluN1 and GluN3 and glutamate for GluN2. Simultaneous binding of these 2 ligands is required for NMDAR activation (Mayer 2006). The re-entry loop M2 forms the channel pore which is highly permeable to Ca^{2+} (figure 6). In particular, critical asparagines residues within this loop determine Ca^{2+} permeability and mediate the magnesium (Mg^{2+}) blockade. Ca^{2+} influx through NMDARs is essential for

synaptogenesis, experience-dependent synaptic remodeling and long-lasting changes in synaptic efficacy such as LTP and LTD (Lau & Zukin 2007). Finally, the CTD, which varies depending upon the subunit, is fundamental for NMDAR regulation. It contains multiple phosphorylation sites including those for protein kinase A (PKA) and C (PKC) and Ca^{2+}/calmodulin-dependent kinase II (CaMKII) (Chen & Roche 2007). These phosphorylation sites are critical for activity-dependent regulation of the receptor trafficking and function. Moreover, CTD also contains various binding sites for several postsynaptic density proteins (scaffolding and adaptor proteins) and signaling effectors (Lau & Zukin 2007).

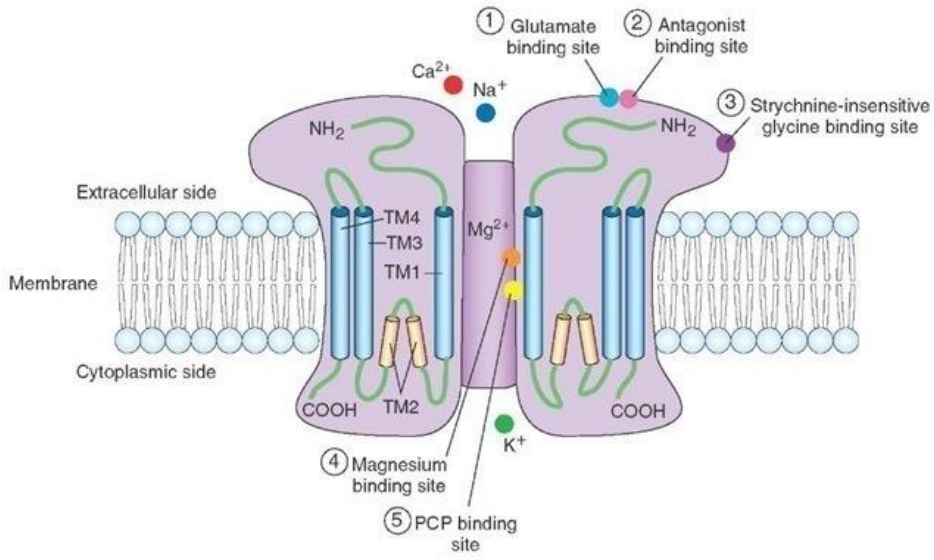

Figure 6 *Model of the NMDA receptor. Activation of the receptor is complex. The integral ion channel is blocked by magnesium in a voltage-dependent manner; depolarization of the neuron (for example, by the action of glutamate at other classes of ion channel) removes this block. Binding of both glutamate and glycine results in the opening of the channel, allowing calcium to enter.*

Most of the NMDA receptors in the brain are heteromeric receptors, as AMPA and kainate receptors. The mRNAs encoding the NMDAR subunits are differentially distributed, as are those of other glutamate receptors. Expression of GluN1 mRNA is nearly ubiquitous in the CNS. In contrast, the four GluN2 subunits show differential patterns of expression. GluN2A is present throughout the forebrain and the cerebellum. GluN2B and GluN2C, however, have a more limited distribution- GluN2B is expressed in highest levels in the forebrain and GluN2C in the cerebellum where GluN2B mRNA in not detected. GluN2D expression seems to be virtually complementary to that of GluN2A in being high in the midbrain and hindbrain but low in the forebrain. GluN3A is expressed in the spinal cord and cortex, whereas GluN3B is found mainly in motor neurons in the spinal cord, pons and medulla (Paoletti et al 2013, Sanz-Clemente et al 2013). NMDARs are some of the most tightly regulated neurotransmitter

receptors. There are at least six distinct binding sites for endogenous ligands that influence the probability of ion channel opening. These consist of recognition sites for two different agonists (glutamate and glycine) and a polyamine regulatory site. Such sites promote receptor activation, while separate recognition sites for Mg^{2+}, Zn^{2+} and H^{+} inhibit ion flux through receptors. The redox state of the receptor also affects NMDARs-mediated responses. One of the three pairs of cysteine residues may either be reduced (thus enhancing NMDAR-mediated currents) or oxidized to form disulfide bridges (reducing currents). NMDAR agonist are typically short-chain dicarboxylic amino acids such glutamate, aspartate and NMDA. Acting at a site on the GluN2 subunit, glutamate is the most potent endogenous agonist in the mammalian brain. NMDA itself, although it is a very selective agonist of these receptors, is 30 times less potent than glutamate in electrophysiological assays. Competitive antagonists of the glutamate recognition site are formed from the corresponding agonists by extending the carbon chain, sometimes in a ring structure and often including replacement of the w-carboxyl group with a phosphonic acid group (Traynelis et al 2010). Numerous competitive antagonists of this recognition site are available, notably d-2-amino-5-phosphonopentanoic acid (D-AP5) and 3-(2-carboxypiperazin-4-yl)1-propeny-1-phosphonic acid (2R-CPPene), the latter having a Kd of approximately 40 nmol/l in binding and functional studies. These compounds are polar and poorly penetrate the blood–brain barrier, although recently several NMDA receptor blockers have been developed that have better access to the brain from the blood.

The NMDAR is unique among all known neurotransmitter receptors in its requirement for the simultaneous binding of two different agonists for activation. In addition to the conventional agonist binding site typically occupied by glutamate, the binding of glycine to a site on the GluN1 subunit is required for receptor activation (Kleckner & Dingledine 1988, Traynelis et al 2010). Because neither glycine nor glutamate acting alone can open this ion channel, they are referred to as coagonists of the NMDA receptor (Kleckner & Dingledine 1988). The glycine site on the NMDA receptor is pharmacologically distinct from the classical inhibitory glycine in that it is not blocked by strychnine and is not activated by β-alanine. Several small analogs of glycine, including serine and alanine, also act as agonists at this site. In both cases the D-isomer is 20–30 fold more potent than the L-isomer. D-serine, formed by serine racemase, is a potent endogenous agonist at the glycine site (Wolosker et al 1999). Bicyclic compounds and many derivatives of either kynurenic acid or quinoxalinedicarboxylic acid are competitive antagonists at the glycine site. Interestingly, most glycine site antagonists in these two series also block competitively the glutamate recognition site of AMPA receptors, suggesting possible structural similarities in the two ligand-recognition sites. Thus, glutamate and glycine act in concert to open NMDA receptor ion channels. In contrast, a very important brake on NMDA receptor activation is provided by extracellular Mg^{2+}, which exerts a voltage-dependent block on the open ion

channel (Nowak et al 1984). Other voltage-dependent blockers of NMDA receptor channels include MK-801, the anesthetic ketamine and the recreational drug of abuse phencyclidine (PCP). These blockers (and Mg^{2+}) exhibit varying degrees of voltage dependence and therefore probably recognize somewhat different domains in the channel of the NMDA receptor. Interestingly, the GluN3A/GluN3B subunits also possess a glycine binding site. Incorporation of a GluN3 subunit into NMDA receptors reduces Ca^{2+} permeability of the receptor channel.

Another important endogenous allosteric inhibitor of NMDA receptor activation is H^+. Protons reduce the frequency of channel opening at GluN2B-containing receptors over the physiological pH range, with a midpoint at pH 7.4. At pH 6.0, receptor activation is nearly completely suppressed (Traynelis et al 2010). This suggests that an ionizable histidine or cysteine may play a key role in receptor activation. This regulatory mechanism may be especially important in acute stroke and other conditions that lead to accumulation of protons (tissue acidosis). One or more modulatory sites that bind polyamines such as spermine and spermidine are also found on NMDARs. Occupancy of one of the polyamine sites relieves tonic proton block and thus potentiates NMDA receptor activation in a pH-dependent manner (Traynelis et al 1995). At higher concentrations, however, polyamines produce a voltage-dependent block of the ion channel and thus inhibit ion flux through activated receptors.

In addition to the regulatory mechanisms discussed above, an interesting form of Ca^{2+}-dependent inactivation of NMDA receptors is brought about by calmodulin. Activated by Ca^{2+} entry, calmodulin interacts with the C-terminal domain of the GluN1 subunit (Fig. 17-4B); this interaction causes inactivation of the receptor manifested by reduced channel opening frequency and reduced channel open time (Ehlers et al 1996). The Ca^{2+}-calmodulin-dependent phosphatase, calcineurin, was also shown to inactivate NMDA receptors (Tong et al 1995), suggesting a two-step process for modulation involving dephosphorylation of the NMDA receptor followed by binding of the Ca^{2+}-calmodulin complex.

3.1.3 Metabotropic Glutamate Receptors

Metabotropic glutamate receptors are linked by trimeric G proteins to cytoplasmic enzymes (Conn 2003). To date eight mGlu receptors have been cloned and named mGlu1–mGlu8. The corresponding genes encode proteins that are thought to span the plasma membrane seven times and, like the ionotropic receptors, they possess an unusually large N-terminal extracellular domain preceding the membrane-spanning segments. mGlu receptors have been grouped into three functional classes based on amino-acid sequence homology, agonist pharmacology and the signal transduction pathways to which they are coupled. Members of each class share ~70% sequence homology, with about 45%

homology between classes. Alternatively spliced variants have been described for mGlu1, mGlu4, mGlu5 and mGlu7. Glutamate itself activates all of the recombinant mGlu receptors, but with widely varying potencies ranging from 2 nmol/l (mGlu8) to 1 mmol/l (mGlu7). Highly selective agonists for each of the three groups have been identified. 3,5-dihydroxyphenylglycine (DHPG) appears to be a selective group I agonist, 2R,4R-4-aminopyrrolidine- 2–4-dicarboxylate (APDC) is highly selective and reasonably potent (400 nmol/l) agonist for group II, whereas l-amino-4-phosphonobutyrate (l-AP4) is a selective agonist of group III mGlu receptors. Some phenylglycine derivatives are mGlu receptor antagonists but highly group-selective antagonists remain to be identified. The classification of mGlu receptors into three groups is further supported by a consideration of their signal transduction mechanisms. Group I mGlu receptors stimulate phospholipase C activity to produce IP3, which causes the release of Ca^{2+} from cytoplasmic stores. The ability to increase intracellular Ca^{2+} levels differs between the members of this class and their splice variants, a property probably attributable to the different affinities each receptor has for its G protein (figure 7). Activation of phospholipase C leads not only to the formation of IP3 but also diacylglycerol, which in turn activates protein kinase C. Activation of group II and group III mGlu receptors results in the inhibition of adenylate cyclase. This response is blocked by pertussis toxin, which suggests that a G protein of the Gi family is involved. mGlu receptors located on the postsynaptic membrane modulate a wide variety of ligand- and voltage-gated ion channels expressed on central neurons, as would be expected if receptor activation is coupled to multiple effector enzymes. Activation of all three classes of mGlu receptor has been shown to inhibit L-type voltage-dependent Ca^{2+} channels, and both group I and II mGlu receptors inhibit N-type Ca^{2+} channels. mGlu receptor activation also decreases a high-threshold Ca^{2+} current in spiking neurons of Xenopus retina. Activation of mGlu receptors closes voltage-dependent, Ca^{2+}-dependent K1 channels in hippocampal and other cortical neurons, leading to slow depolarization and consequent neuronal excitation. The exact mechanism of modulation of K^+ currents by mGlu receptors is at present unclear but could occur through activation of CaMKII. In cerebellar granule cells, mGlu receptor activation increases the activity of Ca^{2+}- dependent and inwardly rectifying K^1 channels, leading to a reduction in excitability.

A large number of ligand-gated channels are also modulated by mGlu receptor activation including NMDA and kainate receptors as well as dopamine, GABA-A and norepinephrine receptors. Whether activation of mGlu receptors acts to inhibit or potentiate an ionotropic receptor depends on what component of the signal transduction mechanism is affected and this is often tissue specific. For example, in hippocampal pyramidal cells, group I mGlu receptor activation potentiates currents through NMDA receptors. This effect is reduced by inhibitors of either protein kinase C or Src kinase, and may proceed through dual signaling pathways. In contrast, in cerebellar granule cells, mGlu

receptor activation inhibits NMDA-receptor-induced elevations of intracellular calcium, also by a mechanism thought to involve PKC.

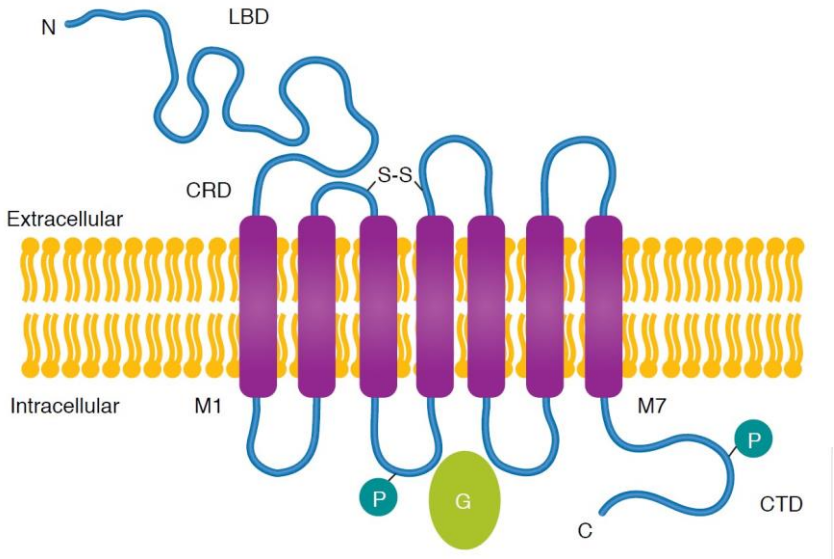

Figure 7 *Metabotropic glutamate (mGlu) receptors are G-protein coupled receptors (GPCRs) that have been subdivided into three groups, based on sequence similarity, pharmacology and intracellular signalling mechanisms. Group I mGlu receptors (**mGlu1** and **mGlu5**) are coupled to PLC and intracellular calcium signalling, while group II (**mGlu2** and **mGlu3**) and group III receptors (**mGlu4**,**mGlu6**, **mGlu7** and **mGlu8**) are negatively coupled to adenylyl cyclase. mGlu possess a 7-transmembrane domain motif (TMD) and a larger N-terminal domain. Alternative splice variants are also found for $mGlu_1$, $mGlu_3$, $mGlu_5$, $mGlu_6$, $mGlu_7$ and $mGlu_8$ receptors***.

3.2 Scaffolding Proteins of PSD

NMDA and AMPA receptors are spread across PSD, whereas metabotropic glutamate receptors (except mGlu7) are located along the periphery of the PSD. NMDARs appear to be present at most or all glutamatergic synapses whereas the content of AMPARs is variable—from 0 to about 50 receptors per PSD (Kennedy et al 2005). Some synapses are 'silent', meaning that their activation does not elicit AMPA receptor currents when the plasma membrane is hyperpolarized and Mg^{2+} blocks NMDARs. Such silent synapses contain only NMDA receptors. However, AMPA receptors are recruited from the cytosol to the PSD to activate such silent synapses in LTP. The PSD is a multiprotein complex with many functions. From the perspective of glutamatergic neurotransmission it may be viewed as a signal transduction machine that converts the extracellular glutamate signal into various intracellular signals. Apart from glutamate receptors, the PSD contains ion channels, glycolytic enzymes, transporters (e.g., a lactate transporter), proteins of intracellular signaling pathways, cell adhesion molecules and scaffolding proteins that link the proteins of the PSD together. A major scaffolding protein of the PSD is PSD-95 (Kano et al 1997). This protein contains several domains that bind other proteins: three so-called PDZ domains (short for PSD-95/disc large/zona occludens-1), an Src homology (SH3) domain,

and a guanylate kinase (GK) domain. This family of proteins is called MAGUKs (membrane-associated guanylate kinases), although the guanylate kinase domain is catalytically inactive. PDZ domains are stretches of about 90 amino acids that bind C-termini of other proteins (Boeckers et al 1999, Kano et al 1997) (figure 8).

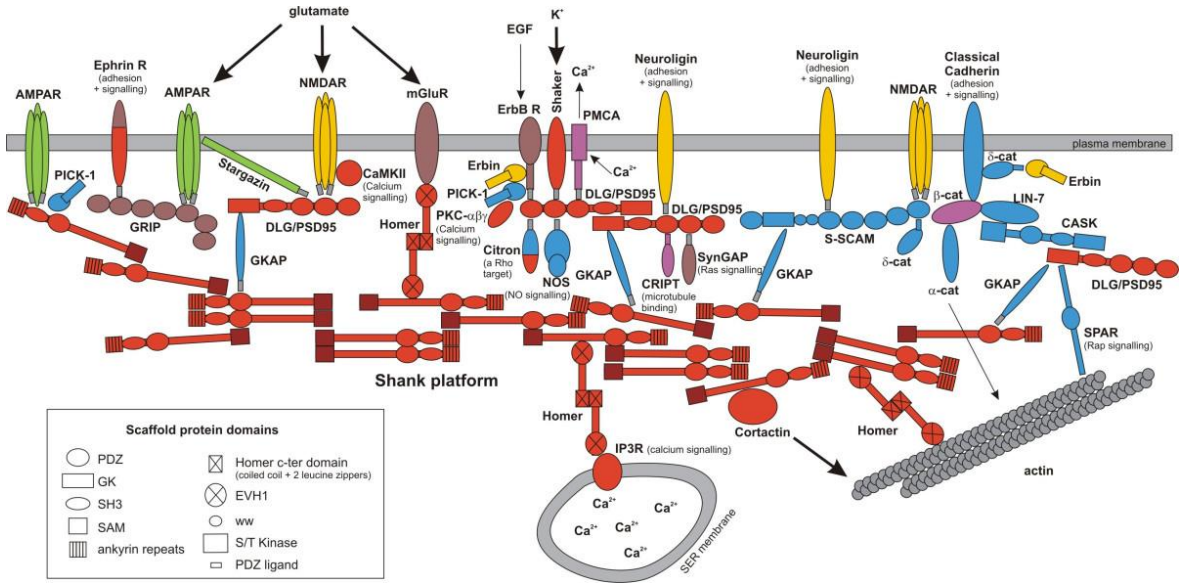

Figure 8 *Graphic representation of the mammalian post-synaptic density. As the major components of the postsynaptic density of excitatory neuronal synapses, PDZ-domain-containing scaffold proteins regulate the clustering of surface glutamate receptors, organize synaptic signalling complexes, participate in the dynamic trafficking of receptors and ion channels, and coordinate cytoskeletal dynamics. These scaffold proteins often contain multiple PDZ domains, with or without other protein-binding modules, and they usually lack intrinsic enzymatic activities. Recent biochemical and structural studies have shown that tandemly arranged PDZ domains often serve as structural and functional supramodules that could regulate the organization and dynamics of synaptic protein complexes, thus contributing to the broad range of neuronal activity*

Several proteins bind PSD-95. For instance, Neuroligin is a protein that binds to the PDZs of PSD-95. Neuroligin reaches into the synaptic cleft and interacts with β-neurexin, a protein that reaches into the synaptic cleft from the presynaptic side; β-neurexin is anchored presynaptically to the PDZ domain of another MAGUK, CASK. This arrangement connects the pre- and postsynaptic elements and stabilizes the synapse mechanically (Meyer et al 2004).

The GluN2 subunit of NMDAR binds to PDZ domains of PSD95 with its cytoplasmic C-terminus. PSD-95 also binds α-actinin, which again binds to filamentous actin (F-actin), a main cytoskeletal protein in dendritic spines. In this manner PSD-95 anchors the NMDAR to the cytoskeleton of the dendritic spine(Dunah et al 2000, Sheng & Pak 2000, Wyszynski et al 1997). PSD-95 also couples the NMDAR to intracellular signaling systems that mediate intracellular effects of NMDAR activation. Calcium ions that enter the postsynaptic cell through the NMDA receptor bind to calmodulin probably at all glutamatergic synapses. Calmodulin with bound Ca^{2+} activates a protein kinase, Ca^{2+}/calmodulin-dependent kinase II (CaM kinase II). CaM kinase II is one of the most abundant proteins at the PSD; it

connects to α-actinin via the scaffolding protein densin (Nakagawa et al 2004). Activated CaM kinase II can phosphorylate a host of other proteins. One such protein is the GluA1 subunit of the AMPA receptor, which is phosphorylated on a serine residue (ser 831). Phosphorylation of GluA1 by CaM kinase II increases the conductance of the AMPA receptor, which is one mechanism that contributes to potentiation of glutamatergic synapses (Lee et al 2000). Other target proteins of CaM kinase II are SAP97 (synapse-associated protein of 97 kDa) and PSD-95: in both cases the phosphorylation of the PDZ1 domain disrupts their interaction with the GluN2A subunit of NMDAR (Gardoni et al 2003)

The Ca^{2+}–calmodulin complex may also activate nitric oxide synthase (NOS), which binds to a PDZ domain of PSD-95 (Piazza et al 2012, Yan & Tso 2004). Activated NOS produces NO from arginine; NO, in turn, activates guanylate cyclase, the enzyme that catalyzes the conversion of GTP to the intracellular messenger cGMP, which activates protein kinase G (PKG) (Ko & Kelly 1999) AKAP (A-kinase anchor protein) is another scaffolding protein of the PSD (Colledge et al 2000, Gomez et al 2002). AKAP binds PKA (protein kinase A), PKC (protein kinase C), and the protein phosphatase calcineurin (PP2B) as well as PSD-95 (at its SH3 and GK domains). This arrangement ensures a close proximity of NMDARs to PKA. Calcium influx through the NMDAR causes Ca^{2+}-calmodulin activation of adenylate cyclase and formation of cAMP. cAMP activates PKA, which, among other things, phosphorylates GluA1 on serine 845; this phosphorylation is necessary for recruitment of AMPA receptors to the plasma membrane of the dendritic spine (Oh et al 2006). In fact, AMPA receptors are to a variable degree located intracellularly in recycling endosomes, whence they may be recruited to the postsynaptic membrane to strengthen the synapse during induction of LTP. PKC in the PSD has an important role in phosphorylating other serines on GluA1 (S816 and S818). Once phosphorylated here, GluA1 can bind to an actin-binding protein (Protein 4.1N), and travel along actin filaments to the plasma membrane driven by the motor protein myosin V (Correia et al 2008, Lin et al 2010). Long-term depression of glutamatergic synapses, which is also mediated by NMDARs activation, involves Ca^{2+}-dependent activation of the phosphatase calcineurin, which causes the dephosphorylation of GluA1 on serine 845 (Collingridge et al 2010). The result of this dephosphorylation is the relocation of AMPA receptors from the plasma membrane to the cytosol.

AMPARs do not appear to bind directly to PSD-95, but may do so indirectly through other proteins, such as TARPs (trans-membrane AMPA-R regulatory proteins), and this interaction appears necessary for the recruitment of AMPARs from the intracellular pool to the PSD (Kato et al., 2010). The C termini of AMPARs bind directly to other PSD proteins with PDZ domains: GRIP (glutamate receptor-interacting protein), PICK1 (protein interacting with C kinase 1), ABP (AMPA receptor-binding protein) and SAP97. GRIP is another protein that is palmitoylated and therefore has an affinity for lipid rafts (Hering et al 2003).

Metabotropic glutamate receptors are anchored to the periphery of the PSD by the scaffolding proteins homer and shank. Homer is a cytoplasmic protein that may multimerize and link proteins that have homer-binding motifs, such as mGlu receptors and shank. Shank binds to the GK domain of PSD-95 and thus links mGlu receptors to PSD-95. Through homer, mGlu receptors also connect to the IP3 receptor (1,4,5-trisphosphate receptors) (Correia et al 2008); the activation of the IP3 receptor by IP3 causes the release of Ca^{2+} from the smooth endoplasmic reticulum. The proximity of mGlu receptors and IP3 receptors ensures that the IP3 that is formed upon stimulation of type I mGlu receptors reaches the IP3 receptor. Similar arrangements occur presynaptically, where mGlu7a binds to the PDZ domain of PICK1.

4 TRAFFICKING IN NEURONAL CELLS

Neurons are highly polarized cells with a single long axon and several dendrites. The axon can extend over long distances and delivers the information to other neurons, while dendrites form a complex branched structure that receive information from other neurons. The activity of the neurons is guaranteed by a correct trafficking of different proteins within the cells, and due to the different nature and functionality of the axons and dendrites, the transport of the proteins requires different sets of specific blocks of cellular organelles (Chia et al 2013, Kapitein & Hoogenraad 2011). Transport within the neurons is dependent on molecular motors that move cargo along cytoskeleton: long-distance communication is mediated by microtubules-based transport, while local-trafficking is mediated by actin-based transport (Chevalier-Larsen & Holzbaur 2006). Regarding the long-distance communication, the transport can be divided, accordingly to the rate, in fast and slow transport. Fast transport is bidirectional and many proteins that are distributed in anterograde transport are returned in retrograde direction. On the contrary, the proteins transported at slow rates are degraded when they reach their destination (Brady et al 1980, Tytell et al 1981). Fast anterograde axonal transport represents the movement of membrane-bounded organelle along microtubules away from the cell body at rate ranging from 2-10 µm/second (brandy 1991). This process provides newly synthesized components essential for neuronal membrane function and maintenance; these materials include small vesicles, tubulovesicular structures, mitochondria and dense core vesicles (Smith 1980, Tsukita & Ishikawa 1980). The membrane-bounded organelles moving in retrograde transport are heterogeneous and larger than the structures observed in anterograde transport (Smith 1980, Tsukita & Ishikawa 1980). Uptake of exogenous materials by endocytosis in distal regions of the axon results in the return of trophic substances and growth factors to the cell body (Kristensson 1978). Once the

transported material reaches the cell body, the cargo can be delivered to the lysosomal system for degradation, to nuclear compartments for regulation of gene expression, or to the Golgi network for repackaging.

Neuronal microtubules form a polarized network from the cell body to the projections. The core structure is a polymer of tubulin subunit, which can be α-tubulin or β-tubulin. Heterodimers of α- and β-tubulin align end to end to form the protofilaments. The dimers bind two GTPs protein and exhibit GTPase activity needed for assembly and disassembly of microtubules (Amos & Schlieper 2005, Desai & Mitchison 1997). In microtubules, the heterodimers are oriented in the same direction, with β-tubulin subunit exposed to the "plus" end that represents the preferred end to incorporate new dimers (Amos & Schlieper 2005, Wade 2007). In the axons, microtubules can be more than 100 μm and they have the same orientation, with the plus end distal from the cell body, while in the dendrites, microtubules are shorter with a mixed polarity (Kapitein & Hoogenraad 2011). The composition of the neuronal microtubules can differ according to the localization (axon or dendrite), thus suggesting that microtubules are specialized structures that perform specific tasks in neuronal cells.

The actin microfilaments represent the oldest family elements of the cytoskeleton and are composed by two filaments of monomers of actin, intertwined like a pearls necklace. A variety of proteins can interact with actin microfilaments, from myosin motors to cross-linkers, from bundling proteins to anchoring proteins and small GTPase regulatory proteins (dos Remedios et al 2003, Letourneau 2009). The microfilaments are particularly enriched in the presynaptic terminals, dendritic spines and growth cones and play an important role in the Golgi complex morphology and localization (Valderrama et al 1998). As described above, microfilaments can be associated to several proteins and among them spectrin and ankyrin have been extensively characterized. Spectrin is a flexible rod-shaped molecule composed of α- and β-subunits, whose heterodimers can be aligned end to end to form tetramers cross-linked by actin microfilaments. This complex is tightly associated to the plasma membrane through a direct binding with membrane proteins mediated by ankyrin, which has a specific binding site for the β-subunit of spectrin and for at least 12 integral membrane proteins (Beck & Nelson 1996). This linkage is essential for the maintenance of the integrity of the plasma membrane, and for anchoring ion channels, exchangers and transporters to the plasma membrane.

The polarized cells require a highly specialized sorting mechanism to ensure the correct localization of the components in the specific cellular domains; all the components of the postsynaptic density must be guided to dendrites, while all the presynaptic proteins and vesicles membrane must be driven to the axon. The dynamic nature of the cytoskeleton allows this differential segregation. (Conde & Caceres 2009, Mandell & Banker 1995). During differentiation, neurons initially extend and retract a number of neuritic processes comparable for length and growth rate, with microtubules oriented with

plus end distal from cell body, associated with MAP2 and tau proteins. Among these nascent processes, one neurite outgrows the others and becomes the axon. This differentiation is not stochastic, in fact that neurite starts to lose MAP2 and to be enriched of tau that is differentially phosphorylated (Dehmelt & Halpain 2005). At the same time, the other neurites are stabilized and begin to form the elaborate dendrites branching in which MAP2 becomes enriched (Dehmelt & Halpain 2005). The expression of specific microtubules associated proteins (MAPs) and the timing of the expression are essential events that define an axon-to-be or a dendrite-to-be. The inhibition of the expression of tau, before or after the commitment to axonal outgrowth, causes respectively no formation or retraction of the axon. Similarly, the inhibition of MAP2 expression leads to a defect of dendrites formation (Caceres & Kosik 1990).

Microtubules and actin-filaments represent the rails for the motor proteins that move unidirectionally all the cargos. Kinesins drive anterograde fast transport that is necessary to supply the distal axon with newly synthesized components for synaptic vesicle assembly and release (Hirokawa & Takemura 2005). The protein is a heterotetramer comprising two heavy chains and two light chains, with two globular heads connected to a fanlike tail by a long stalk (Hirokawa et al 1989). The heavy chain heads comprise the motor domain, containing both ATP and microtubules binding motifs. On the contrary, the retrograde transport is mediated by dynein, a multi-subunit protein complex with a motor domain within the dynein heavy chain. This transport is required for the cellular maintenance because the misfolded and aggregated proteins are driven back to the cell body for the degradation through lysosomal or autophagic (Jordens et al 2001, Ravikumar et al 2005). Moreover, the retrograde transport is important for the signal transduction cascades such as the neutotrophic factor signaling and the injury response (Heerssen et al 2004, Perlson et al 2005). For the actin-based transport, the myosin superfamily represents the group of proteins specialized in short-distance transport at dendritic spines or axon terminals (Langford 2002).

The differential structure of the motor components of the cytoskeleton is essential for intracellular trafficking. The presence of specialized organelles with unique protein and lipid composition allows the neurons to perform two essential functions through (Derby & Gleeson 2007, van Vliet et al 2003):

- the biosynthetic secretory pathway;
- the endocytic pathway.

The biosynthetic secretory pathway is responsible to sort and deliver proteins necessary for cell-cell communications. This process starts from the endoplasmic reticulum (ER) and finishes at the plasma membrane or into specific organelles. On the other hand, the endocytic pathway allows neurons to internalize macromolecules from the extracellular space through the endosome formation (figure 9).

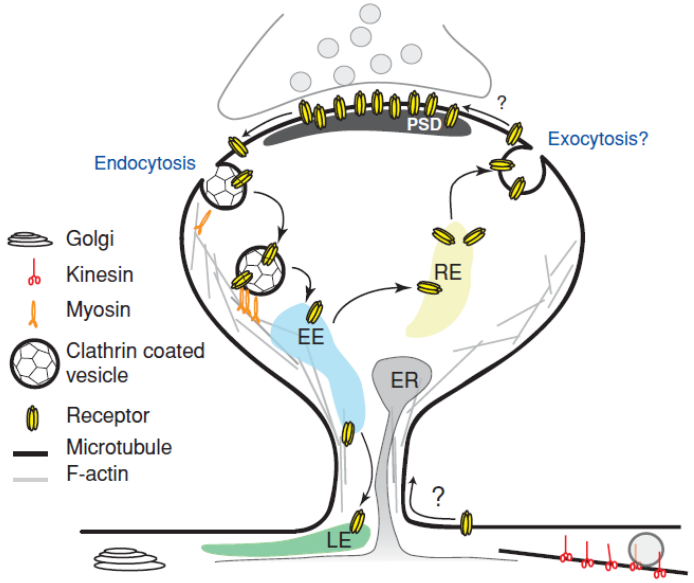

Figure 9 *Model for local postsynaptic trafficking. Components of the synapse either diffuse from the synapse or are actively transported to endocytic zones surrounding the PSD, where they are internalized and trafficked to early endosomes (EE) and sorted either to late endosomes (LE) for degradation or to recycling endosomes (RE) for return to the spine surface. Cargo destined for the synapse is exocytosed to the cell surface at an unknown location, perhaps at the plasma membrane of the spine head. Alternatively,synaptic components could be exocytosed to the surface of the dendritic shaft and diffused through the spine neck to the synapse*

Endosomes represent intermediate intracellular organelles necessary for the receptor-signaling pathway or to deliver the macromolecules to other specialized compartments such as lysosomes. Intracellular trafficking requires a number of ordered and regulated molecular events, such as coat formation, vesicle budding and fusion, which allows the correct protein segregation (Derby & Gleeson 2007, van Vliet et al 2003).

The first step of the vesicle transport is the coat formation, which is necessary to define the portion of the donor organelle that will serve for the formation of the transport vesicle, and to concentrate in that region the proteins ready to be transported (Kreis et al 1995). The nature of the coat proteins ensures the different transport and destiny of the vesicles. Up to date, there are three well-established coat-protein subunits:

1. the clathrin-coated vesicles, that mediate the transport from the Golgi apparatus (GA) to endosome or from the plasma membrane to endosome (Schmid 1997). This process requires multi subunit protein with a main actor, clathrin, and several adaptor proteins (AP) specific for Golgi complex assembly (AP1) and for plasma membrane assembly (AP2);
2. the COPI-coated vesicles, that mediate intra-Golgi transport and Golgi-to-ER retrograde transport (Hsu & Yang 2009). The protein composition of this coated vesicle is complex and presents small GTP-binding proteins, ADP-ribosylation factor 1 (Arf1) and subunits with a sequence similar to the clathrin adaptor;

3. the COPII-coated vesicles, that mediate the anterograde transport in the early secretory pathway from the ER (Barlowe 2002, Gurkan et al 2006). The coated-vesicles are composed of four individual subunits, with a small GTP-binding protein (Sar1), very similar to Arf1. COPII-coated vesicle budding starts from the ER and finishes to the Golgi. These vesicles exit the ER from a specific region known as "ER exit site" (ERES), start to lose their coat and form the ER-Golgi intermediate compartments (ERGICs) (Appenzeller-Herzog & Hauri 2006).

The coat protein assembly is controlled by the recruitment of the GTPase, specialized proteins that can switch from an active state to an inactive state by exchange GTP with GDP and vice versa (Stenmark 2009). The modulation of the active or inactive state is mediated by guanine-nucleotide exchange factors (GEFs) that promote the exchange of GDP with GTP, and GTPase-activating proteins (GAPs) that promote GTP to GDP exchange. In neuronal cells, the clathrin, COPI and COPII coats need to be removed to permit the active translocation by molecular motors (kreis et al 1995).

The recognition of specific target membranes is under the control of two different subsets of proteins: Rabs and SNAREs. Rabs represent a family of monomeric GTPase, which normally are localized on the cytosolic face (Pfeffer & Aivazian 2004). The variable carboxyl terminus of these proteins ensures their right targeting and represents the domain responsible for the interaction with membrane proteins of a specific organelle (Zerial & McBride 2001). The soluble N-ethylmaleimide sulfhydryl factor attachment protein receptors (SNAREs) are transmembrane proteins with a cytoplasmic helical domain, that provides specificity to a target membrane, and are involved in the fusion process (Pelham 2001). SNAREs can be further divided in two different subsets, v-SNAREs and t-SNAREs, which are segregated, in a complementary manner, respectively in the transport vesicles and target membranes. When a v-SNARE vesicle meets the complementary t-SNARE expressing-membrane, their cytoplasmic helical domains establish a coiled-coil interaction, that results in the formation of a stable complex known as *trans*-SNARE pair (Brocker et al 2010). After fusion, this complex becomes *cis*-SNARE who can be disassembled by the soluble ATPase N-ethylmaleimide-sensitive fusion protein (NFS), which acts as a chaperon promoting the unfolding of the coiled-coil interaction (Brocker et al 2010).

The GA is particularly enriched in neuronal cells due to the high rate of synthesis and processing of membrane proteins, and its localization depends on the presence of intact microtubules and on the activity of microtubule-based molecular motors. The GA usually consists of three to eight cisternae and can be morphological divided in *cis*-, medial- and *trans*-Golgi (Glick & Nakano 2009). The *cis*- and *trans*-faces can be associated with interconnected tubular or vesicular structures, known as *cis*-Golgi network (CGN) and *trans*-Golgi network (TGN). The processing of proteins that include sorting and glycosylation of membrane proteins and secretory proteins occurs in this Golgi complex.

4.1 Local Trafficking

The complex geometry of the dendrites allows the spatial segregation and integration of diverse signals (Ehlers 2013). The functional properties of dendrites are highly compartmentalized, and individual dendritic segments possess distinct molecular composition, synaptic inputs and electrophysiological properties (Losonczy & Magee 2006, Losonczy et al 2008, Spruston 2008). This segmentation requires the control of receptors and ion channels distribution by cargo transport to and from the dendritic membrane.

The neuronal ER is extended throughout dendrites and soma, and can function both as an intracellular store of Ca^{2+} and as membrane protein and lipid synthesis compartment (Borgese et al 2006, Cui-Wang et al 2012, Rose & Konnerth 2001, Torre & Steward 1996). In distal dendrites both smooth-ER and rough-ER can be found and such compartments can drive the dendrites local synthesis of membrane proteins, which can mediate the spatially delimited modification (Mameli et al 2007, Sutton et al 2006). This local synthesis, and the subsequently secretory processing, can require local components of the secretory organelles such as ERES (ER exit site), ERGIC (ER-Golgi intermediate compartment) and Golgi compartments. In the neurons, GA consists of both classical perinuclear Golgi cisternae and discrete structures termed Golgi outposts (GOs) that are dispersed in selected dendrites (Gardiol et al 1999, Horton & Ehlers 2003, Lowenstein et al 1994, Torre & Steward 1996). Not all dendrites contain morphological and/or molecular markers for GA and, in this case, the early secretory cargoes can be trafficked in a long-range manner to the soma, where they will be processed to reach the plasma membrane (Horton & Ehlers 2003). Alternatively, the nascent secretory cargo can bypass the classical Golgi utilizing distinct post-ER carriers (Cutrona et al 2013, Jeyifous et al 2009), or can use ERGIC (figure 10). Which are the mechanisms that control the faith of early secretory cargoes for the long-range or local trafficking? It is still unknown, but the possibility to bypass the GA can diversify the properties of neurotransmitters receptors and voltage-gated ion channels since the Golgi-associated glycosylation of ion channels has a strong impact on their distribution, stability and biophysical properties (Schwetz et al 2011, Storey et al 2011, Watanabe et al 2004).

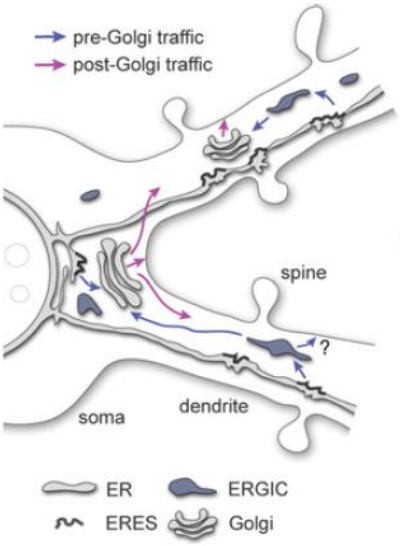

Figure 10 *Dendrites contain coremachinery for early secretory trafficking including ER, ERESs, ERGICs and GOs.Whereas ER, ERESs andERGICs are distributed throughout the somatodendritic compartment and in all dendrites, GOs localize to a subset of dendrites.As a consequence, post-ER carriers originating in dendrites lacking GOs must either be transported long distances back to thesomatic Golgi or bypass the GA by utilizing ERGICs for subsequent processing and sorting.*

The ER also exists as a continuous anastomosing network in dendrites (Cooney et al 2002, Terasaki et al 1994) and, for numerous synaptic receptors, the ER export is the rate-limiting step for the plasma membrane delivery, and multisubunit channels or receptors can remain in the ER for several hours (Gorrie et al 1997, Herpers & Rabouille 2004, Merlie & Lindstrom 1983). The lateral diffusion within ER determines the location of the ER exit and newly synthesized membrane proteins rapidly diffuse within the continuous network of the dendritic ER (Cui-Wang et al 2012). The distance and the length scales of cargo diffusion are determined by the topological complexity of the ER, which is greatest at the dendritic branch points and subjacent to large dendritic spines (Cui-Wang et al 2012). The complex geometry of dendritic ER is controlled by the interaction of the ER-resident protein CLIMP63 with microtubules (Cui-Wang et al 2012) and this interaction promotes the elongation of ER tubules to the cell periphery along microtubules tracts (Klopfenstein et al 1998, Schweizer et al 1993). Such interaction is in turn disrupted by PKC phosphorylation of CLIMP63, whose activaty is stimulated upon activation of mGluRs type 1 (Klopfenstein et al 1998, Vedrenne et al 2005) (figure 11) . The activation of this pathway leads to the ER uncoupling from the microtubules, bunching up and adoption of a more complex topology that can trap nascent membrane proteins within smaller domains.

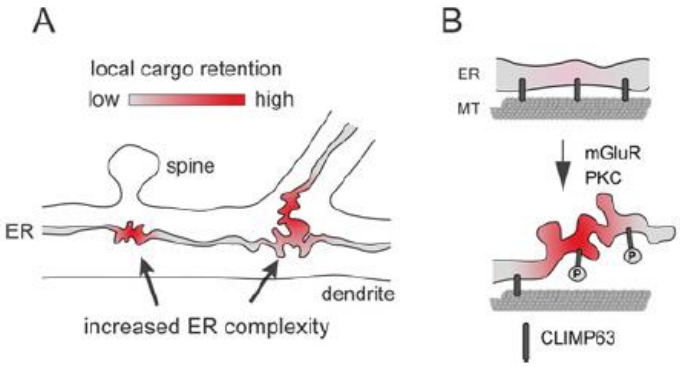

Figure 11 *The ER exists as a continuous anastomosing network of tubules and sheets throughout dendrites. Nascent integral membrane secretory cargo diffuses laterally and rapidly within the lipid bilayer of the dendritic ER. The distance and length scales over which cargo diffuses is determined by the topological complexity of the ER, which is greatest at dendritic branch points and subjacent to large dendritic spines. (B) Geometric complexity of the dendritic ER is controlled by interaction of the ER-resident protein CLIMP63 with microtubules (MT) and this interaction is in turn disrupted by PKC phosphorylation of CLIMP63 stimulated upon activation of mGluRs. Upon activation of the mGluR/PKC/CLIMP63 pathway, the ER uncouples from microtubules, bunches up and adopts a more complex topology, thereby confining cargo to smaller length scales of effective diffusion in the dendrite*

The increase of ER complexity promotes AMPARs surface expression and increases synaptic strength by directing a higher proportion of newly synthesized receptors to local forward trafficking (Cui-Wang et al 2012). The secretory trafficking is essential for dendrites growth and maintenance; in cortical and hippocampal pyramidal neurons the somatic Golgi is oriented towards the large apical dendrite, and post-Golgi cargo flux is strongly biased towards the large apical dendrites (Horton & Ruban 2005). Moreover, the polarity and morphology of Golgi precede and predict the dendrite formation and polarization (Horton et al 2006, Horton & Ruban 2005). The translocation of the GA into developing apical dendrites is mediated by the reelin, a secreted factor that requires an LKB1/Skt25/GM130 signalling pathway and the Cdc42/Rac1 guanine-nucleotide-exchange factor αPIX/Arhgef6 (Meseke et al 2013).

All the organelles of the secretory pathway are concentrate at dendritic branch points and GOs are stably positioned at a subset of branch points and can receive and transmit secretory cargos (Horton & Ruban 2005). At the dendrite level, the ER complexity can promote dendritic branching, thus the local post-ER trafficking directs membrane cargos relevant to dendrite formation and growth. Together with GOs, this biosynthetic machinery allows neurons to locally regulate dendritic morphology and molecular composition.

4.1.1 Exocytosis

After the processing, all the intracellular cargo must be exocytosed to reach the surface of dendrites. The fusion of intracellular membranes with the plasma membrane controls the cell-surface composition and the release of soluble factors. Many forms of exocytosis are regulated by molecular

or electrical stimuli such as depolarization of the pre-synaptic compartment that induces neurotransmitter release (Jahn & Fasshauer 2012). This process has been fully studied and, up to date, it is known that the presynaptic exocytosis depends on the number and positioning of Ca^{2+} channels (Rettig et al 1997), the activity of SNARE (Sudhof & Rothman 2009) and Ca^{2+} sensing synaptotagmins (Chapman 2008). On the other hand, little is known about the exocytosis from the postsynaptic compartment, but specific forms of exocytosis regulate synapse function, plasticity and neuronal morphology. Several studies indicate that different neurons can present vesicles containing glutamate, GABA, dopamine and neuropeptides (Famiglietti 1970, Price & Powell 1970, Shanks & Powell 1981). Like the presynaptic machinery, the postsynaptic exocytosis can require intracellular Ca^{2+}, activation of ionotropic receptors such as NMDARs and SNARE activity (Adler et al 1991, Bergquist et al 2002, Halabisky et al 2000, Isaacson 2001).

The main function of the dendritic exocytosis is the retrograde signaling to the presynaptic terminals. For example, the brain-derived neurotrophic factor BDNF, that controls synaptic transmission, synapse differentiation, plasticity and gene transcription through the TrkB receptor activation (Lohof et al 1993, Tanaka et al 2008, Yoshii & Constantine-Paton 2010), is a well know presynaptic neurotrophin, but it has recently been demonstrate that it can be released from dendrites in an activity dependent manner (Dean et al 2009, Hartmann et al 2001). The exocytosis from dendritic terminals requires CaMKIIα activity (Kolarow et al 2007), influx of Ca^{2+} and synaptotagmin IV that regulates activity-dependent release of BDNF (Dean et al 2009).

Another important role of the exocytosis is the morphogenesis of dendritic arbors that controls the morphological plasticity. Initially, the neuron is a spherical cell and subsequently increases the membrane area: this process requires a huge amount of new membrane synthesis that can be directed to the axon or dendrites. As described above, the ER export indicates the site of new dendritic branch formation and dendritic exocytosis (Cui-Wang et al 2012), but the link between the spatial positioning of these compartments and the exocytic machinery is still unclear. Many forms of synaptic plasticity require exocytosis at the postsynaptic membrane and several studies demonstrate that disruption of SNARE-mediated membrane fusion blocks LTP (Lledo et al 1998). Other studies show that, at dendritic terminals, there are AMPARs containing vesicles that are fused with plasma membrane after LTP induction; this event increases the number of surface AMPARs with a subsequent potentiation of synaptic strength (Anggono & Huganir 2012, Shepherd & Huganir 2007). Moreover, the LTP induction increases ~2 fold the volume of dendritic spines (Matsuzaki et al 2004), confirming the concept that dendritic exocytosis is necessary for plasticity. To confirm these results, different researchers performed several manipulations preventing SNARE-mediated membrane fusion, thus demonstrating

that the lack of such process prevents the LTP-induced spine growth (Kopec et al 2007, Park et al 2006, Yang et al 2008).

The second important players in controllling synaptic plasticity are the recycling endosomes (REs) in dendrites and dendritic spines (Cooney et al 2002, Park et al 2006). In response to the LTP induction, the endocytosed AMPARs are reinserted at the plasma membrane (Ehlers 2000, Luscher et al 1999); blocking the RE transport, using syntaxin 13 dominant-negative and Eps15 homology domain protein Rme1/EHD1, prevents LTP induction, proving how AMPARs exocytosis through REs is crucial for synaptic plasticity (Ehlers 2000). The AMPARs exocytosis occurs within spines, immediately adjacent to the PSD, at microdomains enriched for syntaxin 4 that forms part of the core SNARE machinery (Kennedy et al 2010) together with SNAP-23 (Suh et al 2010). Just before the membrane fusion, the REs are mobilized into spines by the actin-based motor protein myosin Vb (MyoVb) whose structure conformation is Ca^{2+} sensitive (Li et al 2006, Wang et al 2008). At low concentrations of intracellular Ca^{2+}, MyoVb adopts a close conformation that binds actin, while at high Ca^{2+} concentrations, MyoVb adopts a more extended conformation that facilitates the interaction with the endosomal adaptor protein Rab11-FIP2 (Hales et al 2001, Lapierre et al 2001, Li et al 2006). The activation of the NMDARs, that leads to Ca^{2+} influx, promotes the recruitment of MyoVb to the REs with their subsequent mobilization towards actin-rich spines where the syntaxin 4 positive exocytic domains are present.

4.1.2 Endocytosis

The PSD is a highly dynamic compartment in which the composition of surface receptors changes in response to specific stimuli. As described above, the exocytosis governs the expression of surface receptors and other constituents, while the mechanism that controls the removal of dendritic membrane cargos relies on endocytosis. As for exocytosis, endocytosis of glutamate receptors controls diverse forms of synaptic plasticity and the endocytic machinery interacts with PSD protein complexes at the excitatory glutamatergic synapse. For example, the GluA2 subunit of AMPARs and GluN2B subunit of NMDARs interact with the AP2 clathrin adaptor complex (Lavezzari et al 2003, Roche et al 2001) and the PSD adaptor protein Homer binds the dynamin-3 that mediates vesicles fission (Campelo & Malhotra 2012, Gray et al 2003). The endocytosis mechanism is tightly regulated and involves different proteins. The NMDAR-dependent LTD that causes the endocytosis of AMPARs is mediated by the Ca^{2+} sensor hippocalcin that binds the beta2-adaptin subunit of AP2 complex along with GluA2; this interaction governs the AMPARs endocytosis in a Ca^{2+} sensitive manner (Palmer et al 2005). On the contrary, the interaction of GluN2B with the AP2 complex is negatively regulated by the binding of PSD-95 to another domain of the subunit and by the phosphorylation of GluN2B mediated by Fyn

(Prybylowski et al 2005, Roche et al 2001). The phosphorylation itsself is very important for the endocytosis of GluN2B, in fact the dephosphorylation of tyrosine mediated by STEP promotes the NMDA subunit removal from membrane surface (Snyder et al 2005).

In dendritic spines the clathrin puncta are found adjacent to PSD where coats repeatedly assemble and disassemble during endocytosis (Blanpied et al 2002). This highly dynamic process finely tunes the glutamate receptors levels in a spine. Several studies showed that dynamin-3 is enriched at the PSD and it is the only dynamin isoform that directly binds the adaptor protein Homer (Brakeman et al 1997, Gray et al 2005, Xiao et al 1998). Homer proteins assemble as tetramers and form a complex network with members of the Shank family (Hayashi et al 2006, Hayashi et al 2009); the complexity of this system controls the spatial localization of the endocytic zone that ensures the spine-localized endocytic cycling and serves as a trap to recapture and maintain the extrasynaptic pool of AMPARs (Lu et al 2007). The dendritic endocytosis is regulated also by the activity of the early gene product Arc/Arg3.1 (Bramham et al 2008, Lyford et al 1995). The up-regulation of the local translation of the Arc mRNA is neuronal activity dependent and, after translation, Arc binds the endocytic adaptor endophilin-2, which stimulates the endocytosis of AMPARs and other postsynaptic cargo (Chowdhury et al 2006, Wu et al 2011). After endocytosis, postsynaptic cargo such as AMPARs and NMDARs are sorted in endosomes for recycling or lysosomal degradation (Ehlers 2000). The endosomal sorting of AMPARs corresponds to the phosphorylation state of GluA1 subunit; dephosphorylation of Ser^{845} of GluA1 occuring during LTD leads to a lysosomal degradation (Ehlers 2000, Lee et al 1998), while the phosphorylation promotes the reinsertion at the dendritic membrane (Ehlers 2000, Esteban et al 2003). The LTD induces also the Ca^{2+} dependent activation of Rab5 that regulates the endocytosis and the early endosome transport of GluA1 (Brown et al 2005). Unlike AMPA receptors, synaptic NMDARs are stable components of the PSD. The endocytosis of NMDARs is more robust early in development and declines during synaptic development. GluN2A and GluN2B subunits have distinct endocytic motifs encoded in their distal C terminal domains, which interact with clathrin adaptor complexes with differing affinities (Lavezzari et al 2003). Moreover, GluN2A and GluN2B sort into different intracellular pathways after endocytosis, with GluN2B preferentially trafficking through recycling endosomes. In mature cultures, GluN2B undergoes more robust endocytosis than GluN2A, consistent with other studies showing that GluN2A is more highly expressed at stable synaptic sites (Lavezzari et al 2003, Scott et al 2004).

In dendrites, internal membrane compartments, resembling endosomes and including coated and uncoated vesicles, tubules and multivesicular bodies (MVBs), can be observed (Cooney et al 2002, Park et al 2006). The 70% of endosome-like structures are localized within or at the base of dendritic spines and one-third of the CA1 hippocampal spines are associated with endosomes, suggesting an organelles

sharing among spines (Cooney et al 2002). On the other hand, degradative compartments, MVBs and lysosomes are more sparse (Cooney et al 2002, Von Bartheld & Altick 2011) and in particular the MVBs are present in association with postsynaptic sites, while lysosomes are generally concentrated in the soma and proximal dendrites of neurons (Chicurel & Harris 1992, Cooney et al 2002, Gorenstein et al 1985, Gorenstein & Ribak 1985, Rind et al 2005).

4.2 Trafficking of App Metabolism Players

APP and the secretases are all integral transmembrane proteins, and so they are dynamically sorted in neurons. Therefore, neuronal sorting mechanisms responsible for APP and the secretases colocalization in the same membranous compartment play important roles in the regulation of Aβ production (Musardo et al 2013).

4.2.1 APP Trafficking

Like other integral membrane proteins, APP is synthesized in the ER and transported to the cell surface via the secretory pathway, and is subject to N- and O-glycosylation within its extracellular/luminal domain. The N-glycosylated form of APP is localized to the ER and early Golgi. Then the N-glycosylated APP is further trafficked within the Golgi and subjected to O-glycosylation. During the late secretory pathway, APP is subjected to consecutive cleavage events in the primary extracellular/luminal juxtamembrane region by the secretases (Small & Gandy 2006). In neuronal cells, APP undergoes rapid anterograde transport and is targeted to the presynaptic terminals (Zheng & Koo 2006). APP can also be delivered to the somatodendritic compartments, colocalizes with PSD95 (Hoe et al 2009) and is a component of the PSD (Marcello et al 2007). Other studies showed that, after initial delivery to axons, APP is transported to dendrites via transcytosis (Simons et al 1995).

The neuronal sorting protein-related receptor SorLA/LR11 regulates processing and trafficking of APP and its processing. SorLA is a retromer-associated protein, a category of proteins that have been implicated in the sorting of endosomal cargo to the TGN (Bonifacino & Hurley 2008, Seaman 2004). Retromers form heteropentameric protein complexes composed of mainly two components: the structural part made of a dimer of sorting nexins and, the other, which is the cargo-recognition complex, composed of a vacuolar protein sorting (VPS26/29/35) trimer (Bonifacino & Hurley 2008, McGough & Cullen 2011). Loss of retromerassociated proteins, such as SorLA, has been shown to affect APP transport from early endosomes to the TGN, to increase Aβ levels and, consequently, affect the risk for AD (Andersen et al 2005, Small et al 2005). Retromer malfunction may also affect the

endosomal transport of BACE-1, leading to an increased release of Aβ (Okada et al 2010). Indeed, SorLA/LR11 is also genetically associated with AD and its steady-state levels are markedly reduced in the brains of AD patients, supporting the implication of this sorting molecule in the physiological regulation of APP metabolism (Andersen et al 2005, Rogaeva et al 2007).

4.2.2 BACE-1 Trafficking

BACE-1 cleaves APP at the expected sites on its extracellular domain at positions D1 and E11. In addition, the Swedish mutation APP670NL that replaces KM on the N-terminal side of D1 is readily cleaved *in vivo* to generate higher levels of CTF99 and Aβ and is also a much better BACE-1 substrate *in vitro* (Sinha et al 1991, Sinha & Lieberburg 1999, Vassar et al 1999). Several evidences suggested that BACE-1 is localized in the ER, Golgi network, cell surface and endosomes (Capell et al 2000, Huse et al 2000). BACE-1 is enriched in neuronal Golgi membranes (Yan et al 2001) and the phosphorylation of a serine residue at the BACE-1 C-terminal region may regulate its intracellular trafficking (Walter et al 2001). BACE-1, like all the other aspartic proteases, is initially synthesized as a zymogen (containing a short prodomain) in the ER. After synthesis, BACE-1 is transported to the cell surface via the ER and Golgi. When it is translocated into the ER, four Asn residues are N-glycosylated and disulfide bonds are formed between the Cys residues (Haniu et al 2000). In the ER, ProBACE-1 is also subjected to transient acetylation on seven Arg residues. ProBACE-1 does not spontaneously convert to mature BACE-1 like some aspartic protease zymogens, but requires other proteases to eliminate the pro-peptide and to rapidly mature. The efficient exit of the enzyme from the ER is determined by the prodomain (Benjannet et al 2001). The enzyme is then transported to the Golgi apparatus; then furin or furin-like proteases remove the prodomain (Benjannet et al 2001, Bennett et al 2000, Creemers et al 2001). This process is not required for BACE-1 activation in fact ProBACE-1 can cleave APP (Creemers et al 2001). However, the removal of its prodomain increases BACE-1 activity by approximately two-fold (Shi et al 2001). The mature enzyme is trafficked to the cell surface where it is internalized into early endosomal compartments which can either recycle directly back to the cell surface, fuse with the TGN or move to the late endosomal/lysosomal compartments (Huse et al 2000, Walter et al 2001, Yan et al 2001). Early endosomes are the main compartment of Aβ generation (Rossner et al 2005).

4.2.3 γ-Secretase Complex Trafficking

The γ-secretase is not a single polypeptide; the proteolytic activity resides in a complex that mediates a unique process of regulated intramembrane proteolysis (RIP) that entails cleavage of a peptide bond within the hydrophobic environment of a lipid bilayer (Brown et al 2000). γ-Secretase is a promiscuous aspartyl protease responsible for the final intramembrane cleavage of various type I transmembrane proteins after their large ectodomains are shed. Its substrates are involved in several mechanisms such as cell fate decisions, adhesion, neurite outgrowth and synapse formation, highlighting the important role of γ-secretase in development and neurogenesis (Iwatsubo 2004a, Iwatsubo 2004b, Selkoe & Kopan 2003). Genetic studies conducted on the link between early-onset familial AD and mutations in the genes coding for presenilin 1 and presenilin 2 on chromosomes 1 and 14 gave the first indication of the proteins responsible for the γ-secretase activity (Levy-Lahad et al 1995, Rogaev et al 1995, Sherrington et al 1995). The active complex consists of at least four protein: presenilin 1 or 2 (PS1-2) at the catalytic core, nicastrin (NCT), anterior pharynx-defective phenotype 1 (APH-1) and PS-enhancer 2 (PEN-2) (De Strooper 2003, Edbauer et al 2003, Wolfe et al 1999).

γ-Secretase components assemble into the γ-secretase complex in the ER in two possible ways: (A) APH-1 binds NCT, this heterodimer binds FL-PS1, after this step PEN-2 is incorporated in the complex and this interaction mediates the endoproteolysis of FL-PS; (B) FL-PS1 might first bind to PEN-2, which leads to endoproteolysis and binding to the pre-existing NCT/APH-1 subcomplex. γ-Secretase complex is then converted to the active form in the Golgi/TGN compartment (Musardo et al 2013).

4.2.4 ADAM10 Trafficking

A key mechanism responsible for ADAM10 activity regulation in neurons is related to its intracellular trafficking. ADAM10 is a component of the PSD and its synaptic localization influences its activity towards the substrates. For example the interaction with the scaffolding protein and synapse-organizer SAP97 positively influences ADAM10 activity (Marcello et al 2007, Musardo et al 2013). SAP97 SH3 domain binds to the proline-rich sequences in the cytosolic domain of ADAM10, thereby driving the protease to the postsynaptic membrane and increasing APP α-secretase cleavage. In addition, this mechanism is fostered by short-term activation of the NMDA receptor in primary neurons (Marcello et al 2007). However, NMDA receptor can also affect ADAM10 expression, because its activation leads to upregulation of the genes encoding ADAM10 and β-catenin proteins. Inhibitors of Wnt/β-catenin signaling abolished the ADAM10 upregulation, while the activation of the Wnt/ β-catenin signaling pathway by recombinant Wnt3a stimulated ADAM10 expression. Moreover, ERK

inhibitors blocked both the NMDA receptor and Wnt3A-induced ADAM10 upregulation. These data suggest that the NMDA receptors control ADAM10 expression via a Wnt/MAPK signaling pathway (Wan et al 2012). ADAM10 trafficking mechanism and ADAM10/SAP97 association are involved in AD pathogenesis. Indeed, ADAM10 synaptic levels and ADAM10/SAP97 association are reduced in the hippocampus of AD patients at an early stage of disease (Marcello et al 2012b) and interfering with the ADAM10/SAP97 complex for 2 weeks by means of a cell-permeable peptide strategy in mice is sufficient to increase amyloid levels and leads to the reproduction of initial phases of sporadic AD (Epis et al 2010). In addition to the SAP97 binding domain, ADAM10 cytoplasmic tail contains other sequences regulating its intracellular localization, such as an ER retention motif. Sequential deletion/mutagenesis analyses showed that an arginine-rich sequence was responsible for the retention of ADAM10 in the ER and its inefficient surface trafficking (Marcello et al 2010). On the contrary, recently we demonstrate that ADAM10 removal from the synaptic membrane is mediated by clathrin-dependent endocytosis. The clathrin adaptor AP2, a heterotetrameric assembly that initiates the endocytosis process, directly interacts with ADAM10 C-terminal domain. ADAM10/AP2 association has pathological relevance, in fact parallel to a defect in ADAM10 binding to SAP97 (Marcello et al 2012b), we report the concomitant increase in ADAM10 association to the clathrin adaptor AP2 in the hippocampus of AD patients (Marcello et al 2013). Our results suggest that in early stages of the disease, the reduction of α-secretase synaptic localization and activity (Marcello et al 2012b) could be ascribed to a defect in ADAM10 exocytosis/endocytosis processes rather than to an alteration of its expression.

The structural determinants of ADAM10/AP2 interaction have been defined in minute details using several approaches. In particular, we have identified an atypical AP2-binding motif (RQR) in ADAM10 C-teminal, which is necessary for AP2 binding and ADAM10 internalization (Marcello et al 2013). The lack of AP2 interaction significantly affects ADAM10 synaptic membrane levels, underlying the relevance of clathrin-mediated endocytosis in the modulation of ADAM10 surface expression. Thus both SAP97 and clathrin adaptor AP2 directly bind the C-terminal tail of the enzyme but in a non-overlapping mode. Moreover, activity dependent forms of plasticity affect either SAP97 or AP2 binding to ADAM10. In particular we found that LTD boost ADAM10 membrane insertion by fostering its SAP97-mediated forward trafficking to synaptic membrane, whereas LTP reduces the enzyme membrane levels by inducing AP2-mediated endocytosis (Marcello et al 2013). Regulated interaction of ADAM10 with SAP97 and AP2 discloses a physiological mechanism of ADAM10 activity regulation at the synapses. This phenomenon produces a situation whereby synaptically regulated ADAM10 activity is positioned to modulate synaptic functioning. The balance between these two partners association is impaired in AD patients hippocampus at early stages of disease, leading to a reduction of ADAM10

levels at the postsynaptic compartment (Marcello et al 2012a). In light of the role of ADAM10 in Aβ production and synapse function, this loss of balance could affect both APP processing and activity-dependent synaptic plasticity in AD.

4.3 Synapse to Nucleus Communication

The communication among neurons consists in synaptic contacts and signaling events that ensure the long-term responses to specific stimuli. This adaptation requires changes in gene expression at the nucleus and the length of neuronal processes pose a significant challenge for the intracellular communication. Membrane depolarization and calcium influx represent two mechanisms responsible for transferring the information in neurons, and for many years this electrophysiological encoding process has been considered as the major route for communication of synaptic activity to the nucleus (Adams & Dudek 2005, Bading 2013). The calcium wave generated after the activation the receptor-gated calcium channels is propagated to the soma, and can promote the activation of calcium-dependent pathways connected to gene transcription (Saha & Dudek 2013). During NMDARs-dependent LTP the calcium transients generated after synaptic activation are spatially restricted in spines with low diffusion to dendritic shaft (Hagenston & Bading 2011, Yuste et al 2000). This is due to the uptake and clearance systems that depress calcium signals, but regenerative wave mechanisms may cover the gap between the synapse and the nucleus. The synaptic activation of voltage-gated ion channels or the activation of mGluRs lead to an initial calcium signal that can be amplified and propagated by a mechanism of calcium-induced calcium release (CICR). The latter is mediated by the activation of IP3 and ryanodine receptors (RyRs) located to the ER that represents the most important intracellular store of calcium (Berridge 2009, Jaffe & Brown 1994). The theory of calcium regenerative waves can represent a plausible mechanism to elucidate the communication between synapse and nucleus, but a recent study demonstrates that the nucleus itself can generate autonomous calcium transients through the BK-type calcium-sensitive potassium channels that reside on the nuclear envelope (Li et al 2014). In particular, the blockage of nuclear BK channels (nBK channels) induces nuclear envelope-derived Ca^{2+} release, nucleoplasmic Ca^{2+} elevation and cyclic AMP response element binding protein (CREB)-dependent transcription. More importantly, blockade of nBK channels regulates nuclear Ca^{2+}-sensitive gene expression and promotes dendritic arborization in a nuclear Ca^{2+}-dependent manner (Li et al 2014). These results suggest that the nBK channel functions as a molecular link between neuronal activity and nuclear Ca^{2+} to convey signals from the synapse to the nucleus.
A second mechanism for the synapse-to-nucleus communication is based on a slower process that depends on the nuclear import of proteins released from synapse. This process can couple local

synaptic activity to specific gene expression programs (Jordan & Kreutz 2009, Karpova et al 2012). The complex network of proteins linked to the NMDARs (Emes et al 2008, Trinidad et al 2008) can regulate the activity-dependent gene expression. This multi-proteins complex represents a potential source for long-distance protein messengers. Among them, the mitogen-activated protein kinase (MAPK) cascade plays an important role in transducing synaptic signals to the nucleus, and the MAPK extracellular signal-regulated kinase (ERK) regulates gene transcription in learning and memory (Carasatorre & Ramirez-Amaya 2013). Using advanced imaging, Zhai and colleagues demonstrated that after LTP the propagation to the nucleus of ERK signaling occurs after stimulation of three or more spines, moreover the signals can be spatially and temporally integrated from multiple branches (Zhai et al 2013). The physical transportation of macromolecules to the nucleus is necessary for the nucleus to discriminate the signals that derive from synaptic or extrasynaptic NMDARs activation that have different roles in synaptic plasticity (Hardingham et al 2002, Ivanov et al 2006). The synaptic activation of NMDARs governs the cell survival and plasticity gene expression, while the extrasynaptic NMDARs activation induces the expression of genes that are involved in cell death pathways (Hardingham et al 2002, Karpova et al 2013). Recently, Karpova and colleagues identified the synaptic protein Jacob as the messenger that encodes the origin of synaptic versus extrasynaptic NMDAR signals and their delivery to the nucleus (Karpova et al 2013). Moreover, ERK activity was found to be required for nuclear translocation, in particular the activation of synaptic NMDARs leads to the phosphorylation of Jacob at serine-180 by ERK, while the activation of extrasynaptic NMDAR doesn't require ERK activity to induce Jacob nuclear accumulation (Karpova et al 2013). During translocation, the phosphorylation state of Jacob is protected from phosphatases by the interaction with the intermediate filament α-internexin and ERK. Upon the arrival to the nucleus, the phosphorylation state of Jacob determines cell death or promotes cell survival and enhances synaptic plasticity (Karpova et al 2013).

Interestingly, Ronicke and colleagues (Ronicke et al 2011) demonstrate that Aβ oligomer administration to primary neuronal cell culture and hippocampal slices, cause nuclear accumulation of Jacob that can be blocked by a simultaneous application of ifenprodil, a selective antagonist of GluN2B. The authors conclude that Aβ oligomers induce early neuronal dysfunction mainly by activation of GluN2B-containing NMDA-receptors, and a subsequent nuclear translocation of Jacob which might be involved in an Aβ-mediated shift to neuronal silencing (Ronicke et al 2011).

Another protein capable of translocating from the synapse to the nucleus in an activity-dependent manner is the proline-rich synapse-associated protein 2 (proSAP2)/SH3 and Ankyrin repeat domains 3 (Shank3) (Grabrucker et al 2014). Hippocampal neurons were stimulated for 1 min with 50 µM NMDA at DIV 14 and fixed after 1 h followed by immunocytochemistry labeling ProSAP2/Shank3, Abi-1 and nuclei. The authors found, compared to non-stimulated control neurons, a clear enrichment of

ProSAP2/Shank3 and Abi-1 within the nucleus of cells treated with NMDA. ProSAP/Shank proteins are a family of scaffolding molecules found at excitatory glutamatergic synapses. At the PSD, these proteins are capable of interacting with structural elements as well as ligand gated ion channels, cell adhesion molecules such as neuroligins, and proteins regulating the dynamic assembly of F-actin (Kreienkamp 2008). Grabrucker and colleagues found that hippocampal neurons, with mutations in ProSAP2/Shank3, show altered E/I ratio (ratio of excitatory to inhibitory synapses) and reduced dendritic branching (Grabrucker et al 2014). Synaptogenesis and synaptic plasticity crucially depend on the dynamic and locally specific regulation of the actin cytoskeleton. An important component for controlled actin assembly is abelson interacting protein-1 (Abi-1), a binding partner of ProSAP2/Shank3 (Proepper et al 2007). During early neuronal development, Abi-1 is localized in neurites and growth cones; at later stages, the protein is enriched in dendritic spines and PSDs, as component of a trimeric complex consisting of Abi-1, Eps8 and Sos-1 (Proepper et al 2007). Upon NMDA application, Abi-1 translocates from the PSDs to the nuclei where enhances E-box-regulated gene transcription (figure 12).

On the same waves, Jordan and colleagues identified AIDA-1d as a new component of the PSD that can regulate global protein synthesis by altering nucleolar numbers (Jordan et al 2007). AIDA-1d binds to the first two PDZ domains of the scaffolding protein PSD-95 via its C-terminal three amino acids. Stimulation of NMDARs, which are also bound to PSD-95, results in a Ca^{2+}-independent translocation of AIDA-1d to the nucleus, where it couples to Cajal bodies and induces Cajal body–nucleolar association. Cajal bodies are nuclear structures originally identified by Santiago Ramon y Cajal as circular nucleolar-associated bodies (Cajal 1903). They are enriched with small nucleolar ribonucleoproteins (snoRNPs) and other factors involved in pre-mRNA and pre-rRNA processing (Cioce & Lamond 2005, Dolmetsch et al 2001, Gall 2003, Zhao et al 2005). Cajal bodies are thought to participate to the maturation of RNPs and modifications of snRNAs, especially pseudouridylation (Cioce & Lamond 2005).

Another shuttling protein is LAPSER1 (Schmeisser et al 2009). This protein is highly expressed in the brain, localizes at the postsynaptic compartment and interacts with the PDZ domain of ProSAP2/Shank3. Upon NMDA receptor activation, LAPSER1 alters its spatial localization and binding properties and rapidly shuttles with β-catenin to the nucleus. The translocation is followed by the expression of β-catenin target genes including c-Myc and TcfE2a (Schmeisser et al 2009).

Active nucleocytoplasmic transport of macromolecules across the double lipid bilayer of the nuclear membrane occurs through channels formed by nuclear pore complexes (NPC). This process involves the specific recognition of cargoes by soluble transport carriers of the importin/karyopherin superfamily. These carriers bind nuclear localization signals (NLS) in cargoes either directly or through

an adaptor protein and escort them through the NPC (Cook et al 2007, Stewart 2007, Wente 2000). In classical nuclear import pathway, an importin-α binds the NLS within the cargo protein directly. Its affinity for NLS is increased by interaction with an importin-β, which then facilitates transport of the complex through the nuclear pore. Formation and dissociation of the importin-α/β complex is regulated by the small GTPase Ran, which controls the directionality of transport (4,5). Importins α and β1 are expressed in a wide range of mammalian tissues and cell lines, with expression levels of individual α isoforms changing during cell differentiation (Kohler et al 2002). Kawata and colleagues have recently performed in situ hybridization analyses to examine the mRNA expression patterns of importin α isoforms and importin β1 in the mouse CNS at adult and early postnatal stages (Hosokawa et al 2008). They found moderate to high expression levels of importins α3, α5, α7 and β1 throughout the brain and spinal cord. Importin α4 revealed a more restricted pattern of expression, while importin α1 was found at low expression levels throughout the brain and spinal cord, and at moderate expression levels in the olfactory bulb and reticular system.

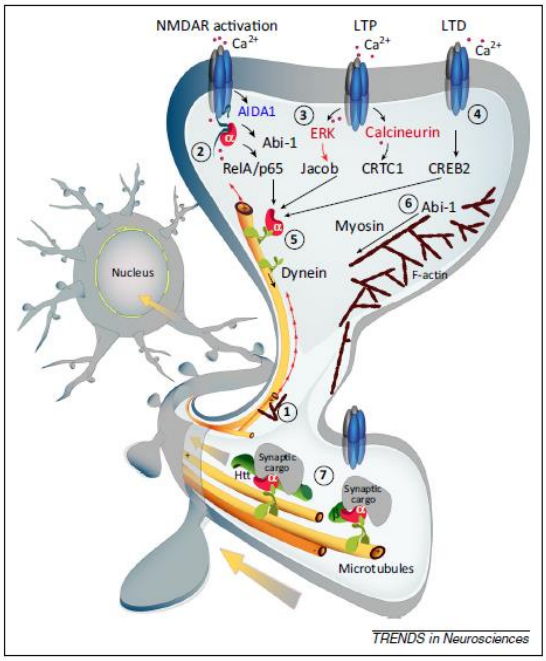

Figure 12 *Long-distance transport from synapse to nucleus. (1) Dynamic microtubules can transiently invade a subset of spine synapses following NMDAR activation in a strictly Ca2+-dependent manner. (2) Neuronal importins can associate with several synapto-nuclear messengers at synaptic sites but it is currently unclear how this interaction might be regulated. (3,4) Signaling downstream of NMDAR that eventually elicits nuclear transport might also encode that type of NMDAR activation. (3) Ca2+-dependent (Jacob and CRTC1) and independent (AIDA1, blue) dissociation of protein messengers from NMDAR has been reported and local phosphorylation via ERK in the case of Jacob or dephosphorylation via calcineurin in the case of CRTC1 is required to exit the synapse. (4) Interestingly, NMDAR-dependent LTP but not LTD induces nuclear translocation of Jacob, while the reverse occurs for CREB2. (5) For many proteins binding to a dynein motor, likely via association with an importin α, is a prerequisite for long-distance transport. Whether this transport requires microtubule invasion of dendritic spines is presently unclear. (6) Alternatively, proteins like Abi-1 might leave the synapse utilizing a myosin motor. (7) At present it is also unknown whether the macromolecular transport complex is assembled in spines or in the dendritic shaft below the synapse.*

In the adult, importin α and β1 mRNAs were predominantly expressed in neuronal cells of the hippocampus and in the cerebral cortex, while their expression levels in glial cells were relatively low (Hosokawa et al 2008). Martin and colleagues investigated the role of importins in this process using two models of learning-related synaptic plasticity: long-term facilitation (LTF) of Aplysia sensory–motor synapses and long-term potentiation of mouse hippocampal synapses. They found that importins were present in distal synaptic compartments, and that stimuli known to induce transcription triggered their translocation to the nucleus (Thompson et al 2004). Specifically, importins accumulated in the Aplysia sensory neuron nucleus in response to stimuli producing transcription-dependent LTF, but not in response to stimuli producing transcription-independent short-term facilitation. In cultured hippocampal neurons, it was found that activation NMDARs triggered an accumulation of importins in the nucleus, which was accompanied by a decrease in importin immunoreactivity in distal dendrites. Chemical induction of transcription-dependent, late-phase LTP in acutely prepared hippocampal slices produced an accumulation of importins α and β in the nuclei of CA1 pyramidal neurons (Thompson et al 2004). The importance of nucleocytoplasmic transport in long distance cytoplasmic transport in neurons and the requirement for importins imply that their perturbation could lead to disease. Ogawa et al. reported aberrant localization of nuclear proteins in neurons from AD patients (Ogawa et al 2003). Zhu and colleagues then compared the localization of importin α1 within neurons of AD and non-affected brains and found that importin α1 abnormally accumulated in Hirano bodies in vulnerable hippocampal neurons in AD (Lee et al 2006). Hirano bodies are rod-shaped cytoplasmic inclusions consisting mostly of F-actin and actin associated proteins (Galloway et al 1987, Izumiyama et al 1991) and are found in a variety of neurodegenerative diseases and also in conditions that present persistent injury or stress, such as in diabetes and alcoholism. Abnormal distributions of importins might also be implicated in some types of motor neuron degeneration. Zhang et al. examined the subcellular localization of nucleocytoplasmic transport proteins in the lumbar spinal cord in the mutant SOD1 (G93A) transgenic mouse model of Amyotrophic Lateral Sclerosis (Zhang et al 2006). They found that nucleocytoplasmic partition of importin immunoreactivities were changed in a subset of the surviving anterior horn cells in these transgenic mice, although it is not clear at this stage if this observation reflects disease causation or outcome (Zhang et al 2006).

AIM

As described in the introduction, AD is placing a considerable and increasing burden on society. Diagnosis is difficult and largely dependent on cognitive and functional assessments. Emerging evidences suggest that AD is a slowly evolving disorder in which pathophysiological abnormalities precede overt clinical symptoms by many years to decades (Jack et al 2013). Up to date there is no cure for AD. The current treatment options are considered to be symptomatic and are only moderately effective in stabilizing or improving cognitive and functional symptoms for 6-12 months.

The lack of a detailed understanding of the molecular basis of the disease process represents the limiting factor to develop effective treatments of disease-modifying therapies. Currently, the state-of-the art of AD knowledge is stuck to the amyloid hypothesis, which posits that Aβ has an early and vital role in AD pathogenesis since it triggers a cascade of events leading to synaptic dysfunction, tau pathology and neuronal loss (Hardy 2002). Indeed, in the last few years, the biological steps leading to Aβ generation have been described in details. The concerted action of BACE1 and γ-secretase on APP leads to the production of the toxic peptides, while the activity of ADAM10 prevents Aβ generation (Kuhn et al 2010, Selkoe 2001). The research on Aβ has proven that its accumulation in brain areas serving memory and cognition contributes strongly to the development of AD. *In vivo* and *in vitro* studies have demonstrated that high levels of Aβ, particularly in oligomeric forms, alter glutamatergic synaptic transmission and cause synapse loss (Mucke et al 2000, Shankar et al 2007, Walsh et al 2002c). The main protagonist of the glutamatergic transmission is the NMDAR whose activation can induce LTP or LTD, depending on the extent of the resultant intracellular Ca^{2+} rise in the dendritic spines and the downstream activation of specific intracellular cascades (Kullmann & Lamsa 2007). LTP induction promotes recruitment of AMPA receptors (AMPAR) and growth of dendritic spines, whereas LTD induces spine shrinkage and synaptic loss (Kullmann & Lamsa 2007).

Pathological Aβ levels and Aβ oligomers may indirectly cause a partial block of NMDAR and shift the activation of NMDAR-dependent signalling cascades toward pathways involved in the induction of LTD and synaptic loss (Hsieh et al 2006, Kamenetz et al 2003, Shankar et al 2007). Remarkably, Aβ oligomers (but not monomers) impair LTP and enhance LTD (Li et al 2009, Shankar et al 2008). On the other hand, the production of Aβ and its secretion into the extracellular space are regulated in part by neuronal activity *in vitro* and *in vivo* (Cirrito et al 2005). In particular, neuronal activity enhances Aβ generation while blocking neuronal activity has the opposite effect (Kamenetz et al 2003).

The study of the mechanisms underlying the cross-talk between Aβ and synaptic function is fundamental because synapse loss has a central role in AD pathogenesis. Synaptic dysfunction drives the cognitive decline in AD and it is not just a consequence of cell death (Walsh & Selkoe 2004). Although many studies have suggested different pathways through which elevated extracellular Aβ

levels can alter synaptic transmission (Mucke et al 2000), how Aβ oligomers initially affect synaptic structure and function remains to be determined.

In this frame, the aim of this thesis was to understand whether Aβ could affect two pathways relevant to neuronal signalling and function: local and long-distance trafficking. Neurons communicate at synaptic contacts by signalling events. The local trafficking and the synapse-to-nucleus communication play a key role in the regulation of short-term and long-term structural modifications and may be mechanisms required for the integration of multiple signalling pathways (Jordan & Kreutz 2009, Karpova et al 2012, Mucke et al 2000).

In particular, specific aims were:

1. to assess whether ADAM10 local trafficking could represent a target of Aβ oligomers and to design specific tools able to rescue such synaptic defect. Indeed, we have previously demonstrated that ADAM10 local trafficking can be regulated by activity-dependent synaptic plasticity. Moreover, we have previously shown in AD patients' hippocampi there is a decrease of the association between ADAM10 and SAP97, which control the forward trafficking (Marcello et al 2012b), and a concomitant increase of the association with AP2 (Marcello et al 2013). In early stages of AD, an imbalance of ADAM10 local trafficking could lead to the observed reduction of α-secretase activity.

2. to understand how Aβ can influence the synapse to nucleus communication in order to promote the long lasting changes in gene expression. We have recently identified a novel GluN2A binding partner that can translocate from the synapse to the nucleus upon NMDAR activation, thus modulating specific sets of genes involved in synaptic morphology and AD pathogenesis.

MATERIAL & METHODS

1. HUMAN TISSUE

The hippocampus (Hp) from late onset/sporadic AD patients (AD; *n*=6) and healthy controls (HC; *n*=6) were obtained from the Netherlands Brain Bank. Stringent criteria were used in the case selection of human brain tissues employed in this study. HC have no history of psychiatric or neurological disease and no evidence of significant age-related neurodegeneration.

2. ANIMALS

Animals used in this project were male C57/BL6 mice of 6-8 weeks, 3xTg AD animal model, male Sprague-Dawley rats of 6 weeks, E18 embryos from Sprague-Dawley rats for primary hippocampal neuron cultures. Animal handling and surgical procedures were carried out with care taken to minimize discomfort and pain, in accordance with ethical regulations and guidelines of the European Communities Council (Directive of 14 November 1986, 86/609/EEC).

3. CELL CULTURES

3.1 COS7 Cell Line

COS7 cells were grown on 100 mm dishes and maintained in Dulbecco's Modified Eagle's Medium containing Glutamax (DMEM + Glutamax, GIBCO) supplemented with 10% Fetal Bovine Serum and penicillin-streptomycin (GIBCO). Cells were allowed to grow till confluence before passaging every 3-4 days using trypsin. The day before transfection, COS-7 cells were placed in a 12 wells multiwell, then cells were transfected with 250-500 ng of plasmid DNA (Tac-ADAM10-RAR) using the lipofectamine method. After 36 hours COS-7 cells were lysed or fixed for antibody unptake assay.

3.2 7PA2 Cell Line

CHO cells stable transfected with $hAPP^{swe}$ (Walsh et al 2002) were grown on 100 mm dishes and maintained in Dulbecco's Modified Eagle's Medium containing Glutamax (DMEM + Glutamax, GIBCO) supplemented with 10% Fetal Bovine Serum, penicillin-streptomycin and neomicin (GIBCO). Cells were allowed to grow till confluence before passaging every 3-4 days using trypsin.

3.3 Primary Hippocampal Neurons

Hippocampal neuronal primary cultures were prepared from embryonic day 18-19 (E18-E19) rat hippocampi as previously described (Piccoli et al., 2007). Neurons were transfected at DIV9 with 2-4 μg of plasmid DNA for shRNF10, pGIZ-ShScramble, hRNF10-flag, using calcium-phosphate method. Neurons were treated at DIV15, lysed or fixed and then immunostained.

4. CELL-PERMEABLE PEPTIDES TREATMENTS

The cell-permeable peptides were created by fusing the peptides with the HIV Tat-derived peptide, which is a small basic peptide that has been successfully shown to deliver a large variety of cargoes, from small particles to proteins, peptides and nucleic acids. The domain conveying the cell penetrating properties appears to be confined to a small (11 amino acids) stretch of basic amino acids, with the sequence YGRKKRRQRRR (Ruben et al 1989). On the basis of the interaction domain between ADAM10 and AP2 we developed four different active peptides and the corresponding inactive peptides.

For acute hippocampal slices all peptides were diluted at concentration of 10 μM in Krebs' buffer containing NaCl (124 mM), KCl (5mM), $MgSO_4*7H_2O$ (1,3mM), $NaHCO_3$ (26mM), D(+)glucose (10mM), $CaCl_2$ (2mM) pH 7.5. Treatments were performed for 30 minutes and then the samples were immediately frozen.

Neurons from primary cultures were treated, after 14 days of growth at 37° and O_2 95%-CO_2 5% (v/v), with active or inactive peptides at 1 μM or 10 μM concentrations in complete medium. Treatments were performed at 37° for 30 minutes and then neurons were lysed and processed for the immunoblotting.

Adult male mice were treated with active or the respective inactive peptides at different concentration (1nmol/g or 3nmol/g) diluted in sterile saline or treated with vehicle alone. Peptides were administered with intraperitoneal or subcutaneous injections for different time. After treatment, animals were sacrificed and the brain was rapidly dissected, divided in two part and frozen at -80°C or formalin fixed paraffin embedded.

5. PRIMARY HIPPOCAMPAL NEURONS TREATMENTS

For induction of Bicuculline treatment, hippocampal neurons *(DIV14)* were incubated with Bicuculline (50µM; Tocris) and 2,5mM 4-Aminopyridine (4-AP;Tocris) in Neurobasal medium supplemented with B27 in presence or absence of 10µM MK-801.

The following drugs, and relative concentration, were used in the experiments with Abeta:

- 2-amino-5-phosphonopentanoic acid (APV) 100 µM, 15 minutes of pre-incubation;
- ethylene glycol tetraacetic acid (EGTA) 250 µM;
- 1,2-bis(o-aminophenoxy)ethane-N,N,N',N'-tetraacetic acid (BAPTA) 5µM;
- 2-Aminoethoxydiphenyl borate (2APB) 50 µM, 1h of pre-incubation.

For induction of calcium release from internal store, hippocampal neurons *(DIV14)* were incubated with caffeine 10mM with or without APV 100uM for 30min in ACSF after 45 minutes of resting.

6. Aβ OLIGOMERS PREPARATION AND PURIFICATION FROM 7PA2 CELLS

Synthetic Aβ peptide (and scramble sequence) was purchased from Bachem. The lyophilized was dissolved in 1,1,1,3,3,3-Hexafluoro-2-Propanol (HFIP, Sigma-Aldrich) at 1 mM final concentration. The solution was aliquoted (10µL) in sterile tubes and left over-night under hood for HFIP evaporation. The day after the tubes were centrifuged in a Speedvac to remove any remaining traces of HFIP or moisture. The resulting peptide was stocked at -20°C. For oligomers preparation, the peptides were allowed to reach room temperature and then resuspended in DMSO at 5mM final concentration, vortexed for 30 seconds, sonicated for 10 minutes and diluted with cold Neurobasal medium to obtain a final concentration of 100 µM. The resulting solution was vortexed for 15 seconds and transferred to 4°C for 24hrs.

Natural secreted Aβ was purified from 7PA2 cells. Cells were allowed to grow till 80% of confluence, then were starved for 16hrs with DMEM + Glutamax. The medium was collected and centrifuged at 1.000 for 10 minutes for remove any presence of cells. Protease inhibitors were added and the medium was concentrated ~10-fold using a Centriprep Ultracel YM-3 filter.

7. HIPPOCAMPAL ACUTE SLICES

Acute hippocampal slices were prepared removing brains from sacrificed rats and placing into chilled (4°C) oxygenated Krebs' buffer. After removal of meninges, hippocampal slices were prepared quickly with a McIlwain tissue chopper and placed in custom-made chambers equilibrated continuously with O_2 95%-CO_2 5% (v/v). Slices were then equilibrated at room temperature for 45 minutes. After the equilibration period, slices were treated with peptides. After treatments, slices were quickly frozen at -80°C or processed.

8. BS^3-CROSS LINK ASSAY

Bissulfosuccinimidyl suberate (BS^3) was dissolved in ACSF (NaCl 120mM,KCl 2.5 mM, $NaHCO_3$ 26mM, $NaHPO_4$ 1.25mM, $CaCl_2$ 2mM, $MgSO_4$ 2mM and D-Glucose 10mM) at final concentration of 2mM. After treatment with peptides, hippocampal acute slices were incubated in ACSF-BS^3 solution at 4°C in a shaking plate. After 30 minutes glycine (100mM) was added to quench the BS^3 action and samples were left at 4°C for 10 minutes. Tissue and medium were then centrifuged at 13.000g for 2 minutes and the resulting pellet was resuspended in NaCl 500mM, HEPES 25mM, EDTA 2mM, DTT 1mM, PMSF 1mM NaF 20mM and NP-40 0,1%. Samples were then sonicate at 20Hz for 5 seconds and centrifuged at 13.000g. The supernatant (cytosolic pool) were then analyzed by WB.

9. PURIFICATION OF POST-SYNAPTIC DENSITIES, TRITON INSOLUBLE POSTSYNAPTIC FRACTIONS AND CRUDE NUCLEAR FRACTIONS

To isolate Post-Synaptic Densities (PSDs) rat hippocampus (from 15 animals) were rapidly dissected and pooled. Animals were killed, and hippocampi were dissected within 2 min. Homogenization was carried out by 10 strokes in a Teflon-glass homogenizer (700 rpm) in 4 ml/g of cold 0.32M sucrose containing 1mM HEPES, 1mM $MgCl_2$, 1mM $NaHCO_2$, and 0.1mM phenylmethylsulfonyl fluoride (PMSF) (pH 7.4). The homogenized tissue was centrifuged at 1,000g for 10min. The resulting supernatant was centrifuged at 13,000g for 15min to obtain a fraction containing mitochondria and synaptosomes. The pellet was resuspended in 2.4ml/g of 0.32M sucrose containing 1mM HEPES, 1mM $NaHCO_3$, and 0.1mM PMSF, overlaid on a sucrose gradient (0.85-1.0-1.2 M), and centrifuged at 82,500g for 2h. The

fraction between 1.0 and 1.2M sucrose was removed, diluted with an equal volume of 1% Triton X-l00 in 0.32M sucrose containing 1mM HEPES, 15min. This solution was spun down at 82,500g for 45 min. The pellet (triton insoluble postsynaptic fraction, PSD1) was resuspended, layered on a sucrose gradient (1.0-1.5-2.1M), and centrifuged at 100,000g at 4°C for 2h. The fraction between 1.5 and 2.1M was removed and diluted with an equal volume of 1% Triton X-l00 and 150mM KCl. PSD2 were finally collected by centrifugation at 100,000g at 4°C for 45min and stored at -80°C until processing.

Triton Insoluble Fraction (TIF), a fraction highly enriched in all categories of postsynaptic density proteins (i.e., receptor, signaling, scaffolding, and cytoskeletal elements) absent of presynaptic markers, was isolated from mouse half brain. To obtain the TIF fractions, samples were homogenized at 4°C in an ice-cold buffer with protease inhibitors (*Complete™,* GE Healthcare, Mannheim, Germany), phosphatase inhibitors (*PhosSTOP™,* Roche Diagnostics GmbH, Mannheim, Germany*),* 0.32 M Sucrose, 1 mM Hepes, 1 mM NaF, 0.1 mM PMSF, 1 mM $MgCl_2$ using a hand held glass-teflon. An aliquot of homogenate (Homo) was kept for Western Blot (WB) analysis. Homo were then centrifuged at 1,000 g for 5 min at 4°C, to remove nuclear contamination and white matter. The supernatant was collected and centrifuged at 13,000 g for 15 min at 4°C. The resulting pellet (crude membrane) was resuspended in hypotonic buffer (1 mM Hepes with protease inhibitors (*Complete™,* GE Healthcare)) and then centrifuged at 100,000 g for 1 h at 4°C. Triton-X-100 extraction of the resulting pellet was carried out at 4°C for 15 min in an extraction buffer (1% Triton-X-100, 75 mM KCl and protease inhibitors (*Complete™,* GE Healthcare)). After extraction, the samples were centrifuged at 100,000 g for 1 h at 4°C and the TIFs obtained were resuspended using glass-glass homogenizer in 20 mM HEPES with protease inhibitors (*Complete™,* GE Healthcare).

To obtain TIF and nuclear fraction from cells, primary hippocampal neurons were lysed and scraped in ice-cold buffer containing 0.32 M sucrose, 1 mM Hepes, 1 mM $MgCl_2$, 1 mM $NaHCO_3$, 1 mM NaF, 0.1 mM PMSF pH 7.4. To obtain nuclear fraction, cell lysates were spun at 1000 g for 7 min at 4°C and the pellet (nuclear fraction) was finally resuspended in 1 mM Hepes buffer containing *Complete™*. Instead, to purify the postsynaptic Triton-insoluble fraction (TIF), cell lysates were centrifuged at 13000 g for 15 min at 4°C. The resulting pellet was resuspended in 150mM KCl, 0.5% Triton and spun at 100000 g for 1 h at 4°C. The final pellet (TIF) was homogenized with a glass-glass potter in 20mM Hepes buffer containing *Complete™*. All purifications were performed in presence of complete sets of protease and phosphatase inhibitors (Roche Diagnostics). Protein content of the samples has been quantified by using Bio-Rad (Hercules, CA, USA) protein assay.

10. sAPPα PURIFICATION

To obtain the soluble fraction S2, used for measure the release of APP ectodomain generated by α-secretase, half mouse brain was initially homogenized with a lysis buffer containing EDTA (2mM), EGTA (1mM), PMSF (0,1mM), Hepes (25mM), protease inhibitors Complete (1X) and phosphatase inhibitors Phospho stop (1X) using a teflon-glass potter in cold room at 4°C.
The samples of homogenate were centrifuged for 10 minutes at 10.000g at 4°C, and the supernatant (S1) was further centrifuged for 1 hour at 100.000g at 4°C to obtain the soluble fraction (S2). The pellet thus obtain can be resuspended in 1mM Hepes and protease inhibitors.
The proteins concentration were quantified with the method described by Bradford (Bradford, 1976). For the calibration line were used appropriate diluitions of a solution of BSA (Bovine-Serum-Albumin) at a concentration of 1 mg / 1ml.

11. GENE EXPRESSION AND MICROARRAY

Real time-quantitative PCR (qPCR) was performed as described in (De Fabiani et al 2003). The following gene expression assay kits from Life Technologies have been used: Rn01409258_g1 for S100a11; Rn01504461_g1 for Rac2; Rn01526492_m1 for Apbb1ip; Rn01422083_m1 for Il18; Rn01430875_g1 for Timp1; Mm00623991_m1 for Itgb8; Rn01513693_m1 for Thbs1; Rn00580728_m1 for Cd36; Rn00579162_m1 for Mmp9. For microarray experiments, RNA was analyzed by the Genopolis Consortium using an Affimetrix platform (GEO accession number GSE69267). Data was primarily analyzed using the TAC and Partek Genomic suite softwares. The Robust Multichip Average (RMA) method was employed to calculate probe set intensity (Irizarry et al 2003). Differentially-expressed genes whose fold change was higher or equal than 1.75 (up-regulated genes) and lower or equal to 0.65 (down-regulated genes) with a p value lower than 0.05 were selected as significantly modulated. The expression value of each probe is divided by the mean value of the scramble controls and the log2 of this ratio has been reported.

12. COS7 ANTIBODY UPTAKE ASSAY

COS7 cells were grown on glass coverslip in a 12 wells dishes. TAC-Adam10-RAR was transfected using Lipofectamine method, and the day after cells were treated. After treatment COS7 cells were incubated at 4°C (cold room) in primary antibody (anti-TAC 7G7) in cold COS7 medium for 1 hour, to prelabel surface receptors. After surface protein labeling, cells were washed in cold medium or cold D-PBS to remove excess antibody. Cells were bring back at 37°C (in incubator) for 10 minutes to restore the physiological cellular processes. Cells were then washed 1x with cold D-PBS to arrest trafficking and fixed with 4% paraformaldehyde + 4% sucrose in PBS for 10 minutes. Then were blocked in PBS plus 5%BSA, 4% Nserum for 30 minute and incubated with Alexa 488-conjugated secondary antibody for 1 hour. Cells were washed 3 times in PBS1x and permeabilized with PBS, 5%BSA, 4% NSerum, 0.2% Saponin. After 30 minutes, cells were incubated with pAb anti-ADAM10 (Abcam) overnight at 4°C to label internalized proteins, followed by incubation with Alexa 555-conjugated secondary antibody. The nuclei were stained with DAPI and after wash, cells were mounted on slides.

13. CO-IMMUNOPRECIPITATION ASSAYS (co-IP)

Aliquots of proteins were incubated overnight at 4°C in RIA buffer containing 50mM Tris HCl (pH 7.2), 150mM NaCl, 1% NP-40, 0.5% deoxycholic acid, 0.1% sodium dodecyl sulphate in a final volume of 150µl with the antibody. As a control, one sample was incubated in the absence of the antibody (No IgG lane) and another sample in presence of an irrelevant antibody. Protein A/G-sepharose beads (Santa-Cruz) were added and incubation was continued for 2h, at room temperature, with shaking. Beads were collected by centrifugation and washed three times with RIPA buffer before adding sample buffer for SDS-PAGE and boiling for 5min. Beads were collected by centrifugation, all supernatants were applied onto 7% - 12% SDS-PAGE and revealed by western blotting.

14. WESTERN BLOTTING

The electrophoretically separated proteins on 7% or 12% SDS-PAGE were transferred onto a nitrocellulose membrane. The transfer was performed in a 'blotting buffer' containing 20% Methanol and 1X Blotting buffer (Tris 0,025 M, glicina 0,192 M, MeOH 20%, pH 8.3) for two hours at 240mA.

After transfer membranes were blocked with iBlock-TBS (Invitrogen, T2015) for at least 45 minand subsequently exposed to primary antibody overnight at 4°C in iBlock-TBS. The next day, membranes were washed in Tris-buffered saline/Tween 20 (TBST) three times for at least 10 min at room temperature, then incubated with horseradish peroxidase (HRP)-coupled secondary antibody (Bio-Rad Laboratories) for 1 h at room temperature and washed again as before. For detection, Clarity™ Western ECL Substrates (Bio-Rad Laboratories) were used, and chemiluminescence was exposed to trans-UV (302nm) with Chemidoc MP System (Bio-Rad Laboratories).

15. CONFOCAL STUDIES

For co-localization and morphological studies, treated hippocampal neurons were fixed 7 minutes in 4% paraformaldehyde plus 4% sucrose in PBS at room temperature; then extensively washed with PBS supplemented with $CaCl_2$ and $MgCl_2$ (PBS-C.M), permeabilized with 0.2% Triton-X100 in PSB-C.M and blocked for 2h at room temperature with 5% BSA in PBS-C.M. Primary and secondary antibodies were applied in 5% BSA in PBS-C.M. Cells were chosen randomly for quantification from different coverslips. Fluorescence images were acquired by using Zeiss Confocal LSM510 Meta system with a sequential acquisition setting at 1024x1024 pixels resolution; for each image two up to four 0.5µm sections were acquired and a z projection was obtained (Malinverno et al., 2010).

The SP5 CLSM system (Leica-Microsystems, Mannheim, Germany) equipped with Diode (405nm), Argon (488nm) and Diode Pumped Solid State (561nm) lasers was used for time-lapse imaging of RNF10 fused to tdEOS. Images were taken with HCX APO L20x/1.00W objective (Leica, Germany). Along the z-axis at list 10 optical sections with focus depth of 300-400 nm were taken in order to cover the complete volume of imaged neurons.

16. DIL LABELING FOR SPINE MORPHOLOGY

Carbocyanine dye DiI (invitrogen) was used to label neurons as it is a lipophilic fluorescent molecule. Protocol used for labeling has been previously described (B. G. Kim, Dai, McAtee, Vicini, & Bregman, 2007). DiI crystals were applied using a thin needle by delicately touching region of interested on both sides of 3 mm hippocampal slices prepared with cardiac perfusion of 1.5% PFA in PB 0.1 M. DiI was left to diffuse for 1 day in the dark at room temperature, then slices were fixed with 4% PFA in PB 0.1 M for 45min at 4ºC. 80 µm hippocampal slices were then obtain using a vibratome.

The first slice was discarded. Slices were then mounted on glass slides with Fluoromount (Sigma) for confocal imaging.

17. PERFUSION WITH PARAFORMALDEYDE (PFA) AND FREE-FLOATING FLUORESCENT IMMUNOHISTOCHEMISTRY (F-IHC)

Anesthetized mice were persufed with 4% PFA (prepared in PBS 1X, pH 7.2- 7.6, on ice) through the right atrium for about 10 minutes. At this time brain, was taken and was placed in PFA for one hour and half, and, after washes in 1X PBS were placed in 30% sucrose O/N. Brain was washed again in PBS 1X and sections of 50µm were cut on vibratome and free-floating fluorescent immunohistochemistry was carried out. Sections were treated for antigen retrieval to increase the antibody detection: a solution of citrate buffer (10mM citric acid and 0.05% Tween, pH 6) was boiled in a microwave and the sections were transferred into boiled solution and let cool to room temperature (RT). After this, sections were carefully washed three time with TBS 1x, blocked for 1 hr at RT with 4% normal goat serum in TBS plus 0.1% Triton-X 100 and incubated with primary antibody diluted in TBS 1x plus 0.1% Triton-X 100 O/N at 4°C. Sections were than washed three times with TBS 1x and incubated with secondary antibody conjugated with different fluorophores for 2 hr at RT. After the labelling the sections were incubated for 5 minutes with DAPI for the nuclear staining and immediately mounted onto SuperFrost Plus slides with flouromount media and covered with coverslip. Fluorescence images were acquired by using Zeiss Confocal LSM510 Meta system with 63x objective and a sequential acquisition setting at 1024x1024 pixels resolution.

18. TISSUE FIXATION AND PARAFFIN INCLUSION

After sacrificed, a piece of liver and half brain were fixed in 10% formalin solution for 48h. After fixation, sample were embedded in paraffin following this method:

1. 70% ethanol for 1 hour;
2. 95% ethanol (95% ethanol/5% methanol) for 1 hour;
3. First absolute ethanol for 1 hour;
4. Second absolute ethanol 90 minutes;
5. Third absolute ethanol 90 minutes;
6. Fourth absolute ethanol 2 hours;
7. First clearing agent (Xylene or substitute) 1 hour;

8. Second First clearing agent (Xylene or substitute) 1 hour;
9. First wax (Paraplast X-tra) at 58°C for 1 hour;
10. Second wax (Paraplast X-tra) at 58°C 1 hour.

Samples were then transferred into a cassette containing wax, orientated properly and then left to solidify at room temperature. from each sample a longitudinal section were obtained dehydrated, clarified in xylene and then embedded in paraffin was. From each paraffin block, five six-micrometer thick serial sections were obtained. Sections were stained with Hematoxylin and Eosin or processed for immunohistochemistry.

19. IMMUNOHISTOCHEMISTRY

Immunohistochemistry was performed with the avidin–biotin–peroxidase (ABC) method (Hsu et al 1981) using a commercial immunoperoxidase kit (Vectastain Standard Elite; Vector Laboratories, Burlingame, CA, USA). Following deparaffinization, sections were incubated for 20 min with 0.5% hydrogen peroxide in methanol to quench endogenous peroxidase activity, and then rehydrated. Section were then immersed in TRIS buffer pH 7.6 and then incubated at room temperature with normal goat serum 1:60 diluted in 0.1 M TRIS buffer (pH 7.6) for 20 min in a humid chamber. Sections, covered with the primary antibodies (anti-GFAP Dako, anti-Iba1 Wako Chemicals) and placed in a humid chamber, were incubated overnight at 4°C. After three washes in TRIS buffer, the sections were incubated with goat anti-rabbit biotinylated immunoglobulin (Vector Laboratories) for 30 min at a 1:200 dilution in TRIS buffer. Afterwards, the sections were incubated with 1:100 ABC complex (Vectastain Elite, Vector Laboratories) for 30 min at room temperature and then developed in red stain with aminoethyl carbazole. The sections were counterstained with Mayer's hematoxylin. Negative control slides were incubated with secondary antibody only, replacing the primary antibodies with normal goat serum. Immunohistochemical labeling for each antibody were quantitatively assessed in the hippocampus by using Image-Pro plus image analysis software. Images of five fields at 400X were acquired, and positive cells in each field were then counted.

20. HEMATOLOGY

The blood has been analysed with a laser-based counter (ADVIA120, Siemens) using mouse-specific software. A blood smear was prepared from each sample. Leukocyte differential, morphology of blood cells, and platelet estimate were determined on May Grünwald-Giemsa stained smears.
After the automated cell count and smear preparation, all the samples were centrifuged and plasma was transferred in separate tubes. The amount of plasma was variable as specified in the clinical chemistry sections of the results, and had a slight degree of hemolysis. Clinical chemistry was immediately performed on plasma samples with an automated spectrophotometer (ILAB-300, Instrumentation Laboratory). All the results were compared with those provided by Charles River for mice of the same strain and age

21. ANTIBODIES

The following antibodies were used : polyclonal antibody (pAb) anti-ADAM10 (rabbit), pAb anti-GABA-A Receptor β-3, monoclonal antibody (mAB) anti-TAT, mAb anti-2072 and mAb anti-Meox2 were purchased from Abcam; anti-ADAM10 (rat), was purchased from R&D; mAb anti- α-adaptin, mAb anti-β-adaptin, mAb anti-μ2, mAb anti-p21, mAb N-Cadherin (c-termial) and mAb anti-importin α1 were purchased from BD Science; pAb anti- APP C-term, mAb anti-tubulin, pAb anti-actin, and pAb anti-BACE1, pAb anti-GluN2A and mAb anti-Flag were purchased from Sigma; mAb anti-Notch1 was purchased from Cell Signaling; mAb anti-SAP97 was purchased from StressGene; mAb anti-GluR1, mAb anti GluN2B, mAb anti-GluN1, mAb anti-GFP and mAb anti-PSD-95 were purchased from Neuromab (Davis, CA, USA); mAb anti-MAP2 and mAb anti-GFAP were purchased from Immunological Sciences; mAb anti-6E10 and mAb anti-22C11 were purchase from Millipore; pAb anti-histone H3 and pAb anti-RNF10 were purchased from Proteintech (Chicago, USA). Peroxidase-conjugated secondary anti-mouse Ab was purchased from Pierce, peroxidase-conjugated secondary anti-rabbit Ab was purchased from Bio-Rad, while peroxidase-conjugated secondary anti-rat Ab was purchased from Abcam. AlexaFluor secondary Abs were purchased from Invitrogen (Carlsbad, CA).

22. NOVEL OBJECT RECOGNITION TEST

The novel object recognition test (NORT) evaluates the rodents' ability to recognize a novel object in the environment. Basically, in the NOR task, there are no positive or negative reinforcers, and this methodology assesses the natural preference for novel objects displayed by rodents. The task procedure consists of three phases: habituation, familiarization, and test phase. In the habituation phase, each animal is allowed freely exploring the open-field arena in the absence of objects. The animal is then removed from the arena and placed in its holding cage. During the familiarization phase, a single animal is placed in the open-field arena containing two identical sample objects, for 5 minutes. The day after, during the test phase, the animal is returned to the open-field arena with two objects, one is identical to the sample and the other is novel. During both the familiarization and the test phase, objects are located in opposite and symmetrical corners of the arena. The entire exploration process of mice is recorded using camera and stored in computer. Exploration time of novel and familiar objects were taken in consideration.

23. QUANTIFICATION AND STATISTICAL ANALYSIS

Quantification of WB analysis was performed by means of computer-assisted imaging (ImageLab, Biorad). The levels of the proteins were expressed as relative optical density (OD) measurements and normalized on actin or tubulin. Levels and values were expressed as mean ± standard error of the mean (SEM). Colocalization analysis was performed using Zeiss AIM 4.2 software. Statistical evaluations were performed by Student *t* test or, as appropriate, by one-way ANOVA followed by Bonferroni's as a *post hoc* test.

RESULT

Aβ AFFECTS ADAM10 LOCAL TRAFFICKING: DEVELOPMENT OF CELL PERMEABLE PEPTIDES TARGETING ADAM10/AP2 INTERACTION

1. LOCAL TRAFFICKING IN SPINES: DETERMINATION OF Aβ TARGETS

Aβ can be considered a key determinant in AD pathogenesis. *In vivo* and *in vitro* studies have demonstrated that high levels of Aβ oligomeric forms modify glutamatergic synaptic transmission causing an impairment of LTP (Shankar et al 2008, Walsh et al 2002b) and enhancement of LTD (Hsieh et al 2006, Li et al 2009). Moreover, the production of Aβ and its secretion into the extracellular space are regulated by neuronal activity *in vitro* (Kamenetz et al 2003) and *in vivo* (Cirrito et al 2005). Increased neuronal activity enhances Aβ generation and blocking neuronal activity has the opposite effect (Kamenetz et al 2003). Indeed, we have recently demonstrated that LTP and LTD can control the synaptic localization and activity of ADAM10 and, thereby, can affect the APP processing and Aβ generation (Marcello et al 2013).

Starting from this consideration, we analyzed the effects of Aβ oligomers on ADAM10 local trafficking. Aβ oligomers obtained from synthetic Aβ42 and prepared according to (Stine et al 2003), loaded onto a non-denaturing gel and analyzed by Western Blot (WB) with 6E10 in antibody to verify that they consist exclusively of small oligomers and monomers. As shown in figure 1A, the immunoblot shows the presence of small oligomers and monomers (from 4 kDa up to 16 kDa (figure 1A). Once assessed the quality of Aβ42 oligomers preparation, we tested their toxicity. We exposed primary hippocampal neurons at *DIV14* with Aβ42 oligomers, or with scrAβ (a peptide with Aβ42 inverted sequence used as control), at different concentrations (200pM, 500nM, 1μM, 5 μM and 10 μM) and, after 24h, we performed the MTT test to evaluate the cells viability. As shown in figure 1B the decrease of viability is proportional to the concentration of Aβ42 used. In particular, the 200pM and 500nM concentrations do not significantly affect cell viability, while higher concentrations (1μM, 5 μM and 10 μM) dramatically increase the mortality by 40%. In light of these results, we decide to use Aβ42 oligomers at a concentration able to affect synapse structure (500 nM, (Lacor et al 2004)) but that not induce mortality. Moreover, as shown in figure 1C the treatment with Aβ42 500nM induce a dephosphorylation of serine 845 of AMPA containing GluA1 subunit, confirming that this concentration induce synaptic depression (He et al 2011).

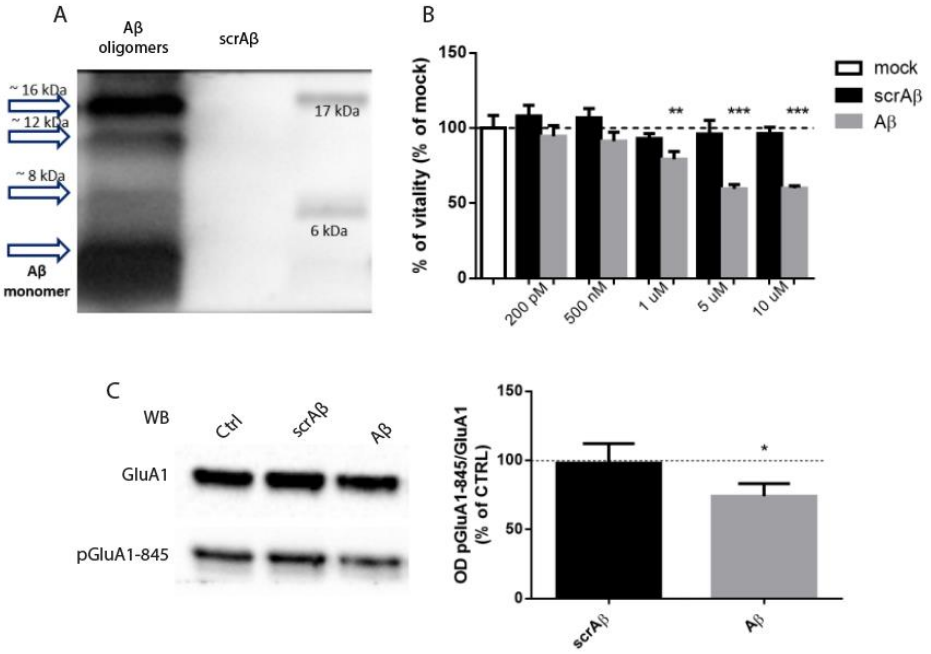

Figure 1 *(A) Aβ42 preparation was resolved onto a non-denaturing gel and immunoblotted with 6E10 antibody. The antibody recognized Aβ oligomers up to 16kDa. (B) MTT test performed on DIV14 primary hippocampal neurons after 24h of Aβ42 treatment at different concentration (200pM, 500nM, 1µM, 5 µM, 10 µM, 24 hr), shows an increase of cell mortality starting from 1 µM (**p<0.01, ***p<0.001). (C) Western blot analysis of GluA1 phosphorylation at serine-845 residue. The Aβ treatment induce a decrease of phosphorylation state of AMPAR (scrAβ 98.09%±7.059%, Aβ 74.01%±4.56% *p<0.05)*

To study the effects of toxic peptides on ADAM10 local trafficking, we exposed primary hippocampal neurons to Aβ42 (500nM) and after 30 minutes the Triton-Insoluble fraction (TIF), which is enriched in postsynaptic proteins, was purified and analyzed by WB to assess ADAM10 postsynaptic levels.

As shown in figure 2A and 2B the treatment with Aβ42 leads to a significant increase of ADAM10 in TIF fraction compared to scrAβ treated or untreated cells. To determine the cellular mechanism underlying Aβ-induced increase in ADAM10 synaptic localization, we analyzed the two mechanisms that control ADAM10 local trafficking at the synapse. In particular, with co-ip experiments we checked the binding with AP2 complex or with SAP97, which control the endocytosis and the exocytosis respectively. As shown in figure 2C and 2D, the Aβ42 treatment does not alter the interaction with SAP97, while significantly decreases the interaction with β2-adaptin, one of the subunits of AP2 complex. These results demonstrate that acute exposure to Aβ42, affects ADAM10 synaptic localization because of a decrease of endocytosis rather than to an increase of forward trafficking.

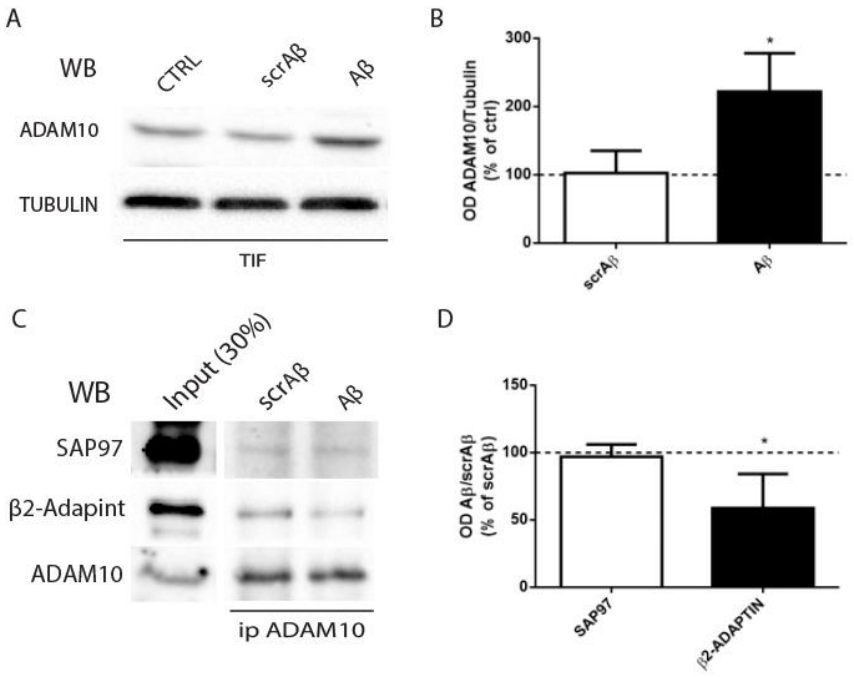

Figure 2 *Aβ alters ADAM10 local trafficking. (A) Western blot analysis of ADAM10 performed on synaptic fraction (TIF) of primary hippocampal neurons treated with either Aβ or scr Aβ (500nM, 30 min). (B) Quantification analysis shows an increase of ADAM10 synaptic availability after treatment with Aβ (scr Aβ 102.7%±18.90, Aβ 222%±32.46% *p<0.05). (C) co-ip assay performed on cell lysate of primary hippocampal neurons after treatment with Aβ (500nM, 30 min). (D) Quantification analysis show Aβ treatment does not change the interaction between ADAM10 and SAP97, while decrease the interaction with β2-Adaptin, a subunit of AP2 complex (SAP97 -3.05%±5.263%; β2-Adaptin -41.13%±12.68%, *p<0.05)*

Interestingly, an alteration in ADAM10/AP2 binding is detectable also in AD patients and AD transgenic mice models, thus demonstrating that it takes part to the pathogenesis of the disease. Remarkably, in chronic pathological conditions, represented by AD patients and animal models, we detect an increase and not a reduction in ADAM10/AP2 interaction. In fact, we have already demonstrated that in AD patients hippocampi there is a reduction of ADAM10 interaction with SAP97, with a concomitant increase in the binding with AP2. Such alterations in ADAM10 local trafficking lead to a decrease of ADAM10 synaptic levels (Marcello et al 2012b, Marcello et al 2013). Moreover, we found the same trend in a transgenic AD animal model: in the brain of 13 month-old 3xTg mice (APP^{swe}, Tau P301L, PS1M146V) (Oddo et al 2003) we measured a decrease in ADAM10 synaptic levels due to an increase of its interaction with AP2 complex (figure 3).

All together these results clearly demonstrate the two faces of the coin of Aβ synaptic toxicity.

In acute treatment Aβ oligomers, at a concentration capable of inducing LTD, can foster ADAM10 synaptic localization, suggesting that Aβ oligomers can initially trigger a negative feedback mechanism. On the other hand, in chronic pathological conditions such as AD, Aβ accumulation drives the activation of complex cascade of molecular events that leads to a reduction in ADAM10 synaptic localization.

The unbalance between ADAM10 exo- and endocytosis can be considered a synaptic feature of AD and one of the mechanisms involved in AD pathogenesis, therefore the rescue of such alteration could represent a potential therapeutic intervention.

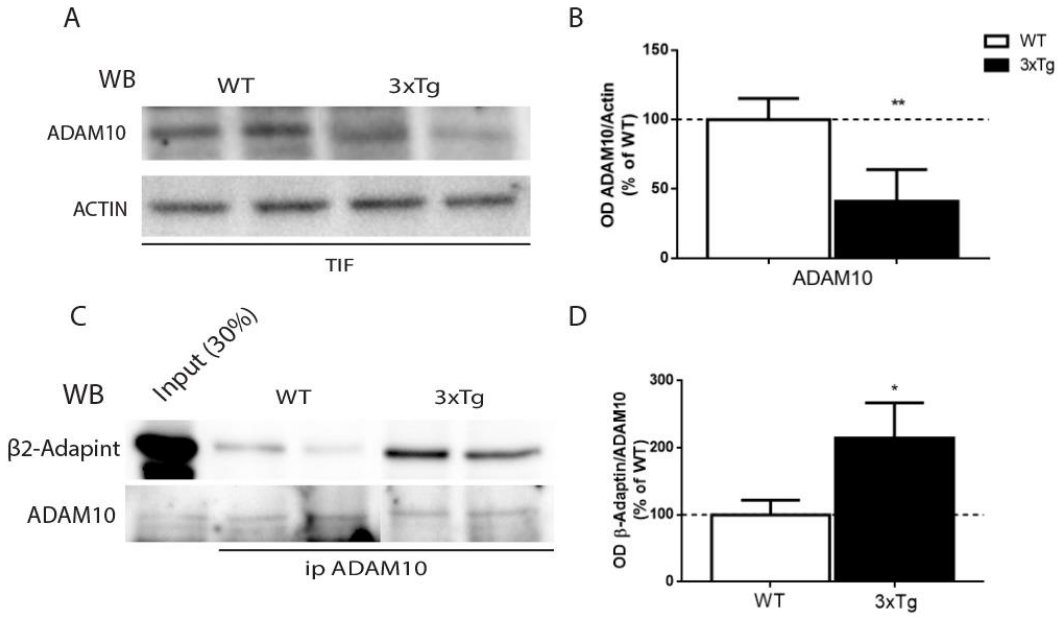

Figure 3 *(A) Western blot analysis of ADAM10 performed on synaptic fraction (TIF) of wildtype animal (WT) and a transgenic animal model of AD (3xTg). (B) Quantification analysis shows an decrease in ADAM10 synaptic availability in 3xTg animals compared to WT animals (WT 100%±7.581, 3xTg 41.11%±11.44% **p<0.01). (C) co-ip assay performed on brain homogenate of WT and 3xTg animals. (D) Quantification analysis show that in 3xTg animals there is an increase of the interaction between ADAM10 and β2-Adaptin (WT 100%±22.17%; 3xTg 214.6%%±26.22%, *p<0.05)*

2. DEVELOPMENT OF CELL PERMEABLE PEPTIDES TARGETING ADAM10/AP2 INTERACTION

As reported Marcello et al. 2012, we demonstrated that the AP2-binding region of ADAM10 contains 2 positively charged residues, R735 and R737, and a hydrophilic amino acid, Q736. The two R residues are crucial for the binding, since the double mutation to A completely abolished the interaction (Marcello et al 2013). To better characterize the interaction between ADAM10 and AP2 complex we performed a biocomputational analysis in collaboration with Dr. Di Marino and we found out that the residues P733, P734, Q736, and R737, of ADAM10 interact with residues F469, G472, and E471 of β2-subunit of AP2. Moreover, the residue D437 of the β2 subunit is properly positioned to establish an electrostatic interaction with R735 of ADAM10.

In light of these results and in order to interfere with ADAM10/AP2 interaction to increase ADAM10 synaptic localization/activity, Dr. Di Marino designed four active cell permeable peptides (CPPs) (PEP1, PEP2, PEP3 or PEP4) and four corresponding inactive CPPs (inPEP1, inPEP2, inPEP3 or inPEP4), used as control in each experiment. These CPPs are constituted by the sequence of the HIV-trans activating

protein (TAT - YGRKKRRQRRR), which confers the capability to cross the biological membranes, and the sequence of ADAM10 C-tail responsible for the interaction with AP2 complex. The peptide is competes with ADAM10 binding to AP2.

3. UNCOUPLING ADAM10/AP2 INTERACTION *in vitro*

3.1 Testing CPPs efficacy and specificity

Since we developed four different CPPs, we first evaluated the efficacy of the CPPs in uncoupling ADAM10/AP2 complex. To address this issue, we treated acute rat hippocampal slices with either the active CPPs or the related inactive CPPs at the concentration of 10 μM for 30 minutes. The slices were lysated and the homogenates were used to evaluate the interaction between ADAM10 and AP2 complex. Co-immunoprecipitation (co-IP) experiments using an anti-ADAM10 antibody showed that two of the four CPPs (PEP2 and PEP3) are able to disrupt the interaction between ADAM10 and α-adaptin, one of the AP2 complex subunits (fig. 4A). In particular the quantitative analysis (fig. 4B) showed that PEP2 significantly reduced the interaction by 58,4%, while PEP3 caused a 62.6% reduction of the ADAM10/AP2 complex levels (ratio PEP2/inPEP2 vs CTRL p=0.0054, PEP3/inPEP3 vs CTRL p=0.003).

After this first screening, we confirmed these results in another biological model and using lower concentrations of PEP2 and PEP3. We treated primary hippocampal neurons at DIV14 with either PEP2 or PEP3 or the corresponding inactive peptides, at the concentration of 1 μM. After 30 minutes, the cells were homogenized and the lysates were used for the co-IP assay. As showed in figure 4C, the treatment with both active peptides reduced the interaction between ADAM10 and two subunits of AP2 complex, i.e. α-adaptin and μ2. The quantitative analysis (fig. 4D) shows that the treatment with PEP2 and PEP3 decreased the levels of the ADAM10/AP2 complex interaction respectively by 66% and 89% for α-adaptin subunit (ratio PEP2/inPEP2 vs CTRL p=0.0019, PEP3/inPEP3 vs CTRL p=0.0013), and by 48% and 78% for μ2-subunit (ratio PEP2/inPEP2 vs CTRL p=0.002, PEP3/inPEP3 vs CTRL p=<0.0001).

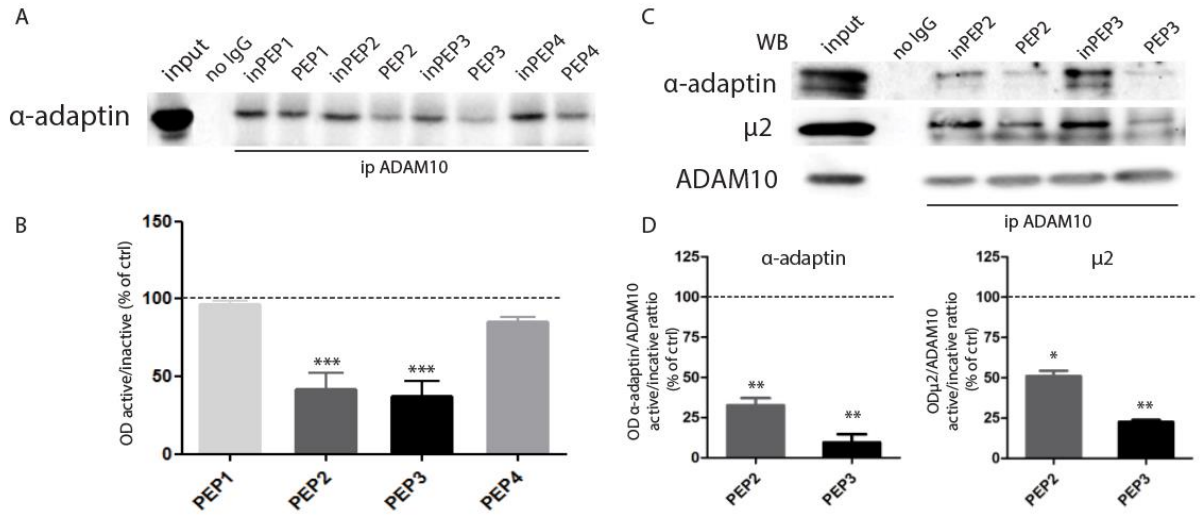

Figure 4 *ADAM10/AP2 association is reduced after treatment with PEP2 and PEP3. (A) Homogenates from hippocampal acute slices treated with either the active or inactive CPPs (10μM, 30 min) were immunoprecipitated with anti-ADAM10 antibody and α-adaptin precipitation was evaluated. (B) Quantification of experiments in A. Optical density (OD) analysis of PEP/inPEP ratio shows that PEP2 and PEP3 significantly reduce ADAM10/AP2 co-precipitation (PEP2/inPEP2 41.6±23.86 ** p=0.0054, PEP3/inPEP3 37.4±21.76 ** p=0.003). (C) Primary hippocampal neurons were treated with either PEP2 or PEP3 (1μM, 30 min) and their corresponding control, and total homogenates were immunoprecipitated with anti-ADAM10 antibody and α-adaptin, μ2 and ADAM10 precipitation was evaluated. (D) quantification of experiments in C. OD analysis shows that the active PEP2 and PEP3 significantly decrease ADAM10/AP2 complex co-precipitation (α-adaptin PEP2/inPEP2 33.92±5.001 ** p=0.0019, PEP3/inPEP3 10.84±5.616 ** p=0.0013; μ2 PEP2/inPEP2 52.01±3.765 ** p=0.002, PEP3/inPEP3 22.43±1.247 *** p<0.0001).*

Since the clathrin-mediated endocytosis is a common mechanism used to remove proteins from plasma membrane, we verified that CPPs did not affect the binding of AP2 to other endocytic partners. To address this issue, we focused on three synaptic proteins, which have been shown to be internalized through AP2-dependent endocytosis: APP (Carroll et al 1999, Nordstedt et al 1993), the GluA1 subunit of AMPA receptor (Carroll RC et al., 1999) and the β3 subunit of GABA-A receptor (Smith et al 2012). Remarkably, GABA-A receptor β3-subunit harbours a novel AP2 binding motif containing three R residues (405 RRR 407) (Smith et al 2012), that is very similar to the AP2-binding domain in ADAM10 c-tail (Marcello et al 2012b). Samples obtained from acute rat hippocampal slices treated with both PEP2 and PEP3 (10μM) or with their related control, were co-immunoprecipitated using an anti-APP C-term antibody for detecting APP, an anti-GluA1 antibody, an anti-GABAA-β3 antibody. The WB analysis using an anti-α-adaptin antibody showed no significant changes in the interaction between AP2 complex and all the analysed target proteins, after the treatment with both active peptides (figure 5). These results underline the specificity of CPPs to hamper specifically the interaction between ADAM10 and AP2 complex.

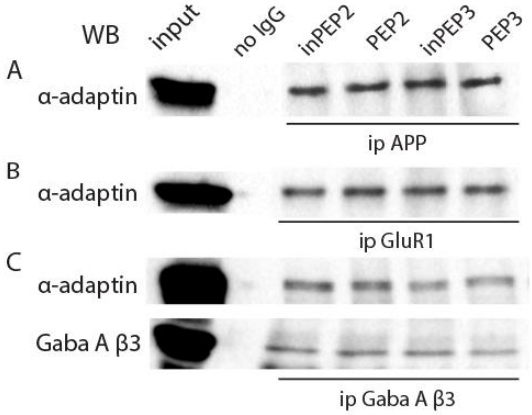

Figure 5 *PEP2 and PEP3 peptides do not alter AP2 binding to other target proteins. Total homogenates of either PEP2 or PEP3 treated hippocampal slices were immunoprecipitated with an antibody recognizing APP (A) or AMPA receptor subunit GluR1 (B) or the β3 subunit of GABA A receptor (C) and α-adaptin co-precipitation was evaluated. As shown in the representative WB, both peptides do not interfere with AP2 interaction with APP, GluR1 and the the β3 subunit of GABA A receptor.*

3.2 CPPs modulate ADAM10 internalization and synaptic localization

Since the clathrin-adaptor protein complex AP2 is responsible for ADAM10 internalization, to evaluate the functional significance of CPPs activity, we carried out different assays to determine the efficacy of the CPPs in interfering with ADAM10 endocytosis and in determining an increase in ADAM10 membrane and synaptic levels

First of all, we performed a fluorescence-based "antibody uptake" assay to assess ADAM10 internalization in COS7 cells. We transfected TacADAM10-RAR, a chimera of the surface reporter protein Tac (human IL-2 receptor α-subunit) (Bonifacino & Hurley 2008) with a modified version of the ADAM10 C-terminal tail that harbours a mutation in the ER retention motif. This mutation allowed ADAM10 ER exit and permitted delivery to the surface (Marcello et al 2010). TacADAM10-RAR-transfected COS7 cells were treated with either PEP2 or PEP3 and their related control peptides at the concentration of 1μM for 30 minutes. Surface TacADAM10- RAR chimeras were first "pulse labeled" in live cells, at 4°C to block membrane trafficking by incubation with anti-Tac antibody. Subsequently, cells were either returned to 37°C to resume endocytosis or kept at 4°C as control. The accumulation of antibody-bound TacADAM10-RAR chimeras in intracellular compartments and the amount of antibody-bound TacADAM10-RAR chimeras remaining on the surface were tracked by quantitative immunofluorescence staining under permeabilizing versus nonpermeabilizing conditions. The ratio of intracellular fluorescence/surface fluorescence (internalization index) was used to control for the variable expression levels of TacADAM10-RAR chimeras in different cells.

We found that the internalization index of cells treated with PEP3 was significantly lower compared with inPEP3-exposed cells (figure 6, A and B; internalization index, TacADAM10-RAR PEP3 = –12.85% ±

1.605%, TacADAM10-RAR inPEP3 = +1.3% ± 2.815% p=0.0489). However, PEP2 treatment didn't significantly affect TacADAM10-RAR internalization index (figure 6, A and B; internalization index, TacADAM10-RAR PEP2 =-10.95% ± 15.82% p>0.05, TacADAM10-RAR inPEP2 = -1.84% ± 13.92% p > 0.05). This assay demonstrates the capability of PEP3 of altering the internalization process of ADAM10, while the data obtained with PEP2 reveal a reduction in ADAM10 endocytosis even if not significant.

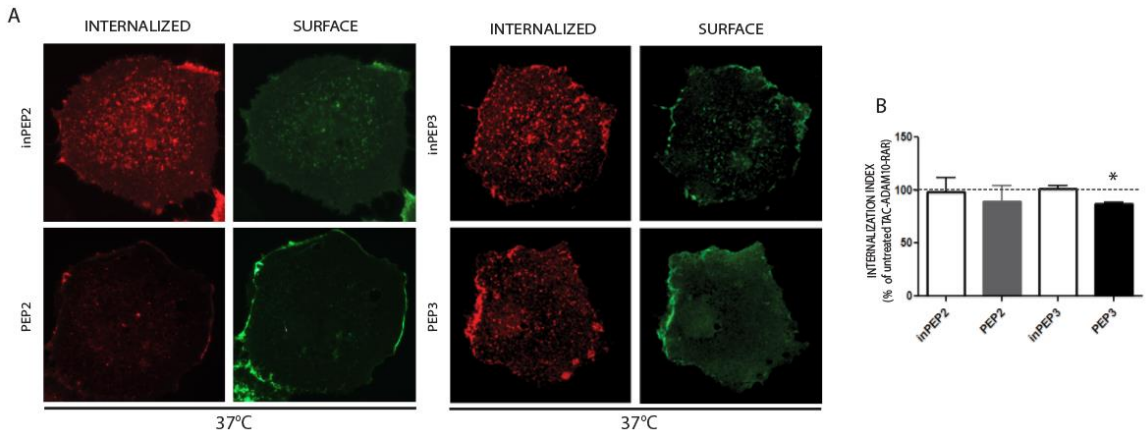

Figure 6 *ADAM10 endocytosis is alterated after treatment with CPPs. (A) Antibody uptake assays were performed on COS7 cells transfected with TacADAM10-RAR, and internalization was analyzed after treatment with either PEP2 or PEP3 active or inactive peptides (1µM, 30 min). Representative images of cells returned to 37°C to allow endocytosis. A decrease in the number of internalization puncta of TacADAM10-RAR after treatment with active peptides is detected. (B) Quantification of the internalization index of experiments in A. Treatment with PEP3 causes a significant decrease in the internalization index while PEP2 treatment doesn't affect the endocytosis (TacADAM10-RAR PEP2 =-10.95% ± 15.82%, TacADAM10-RAR inPEP2 = -1.84% ± 13.92%; TacADAM10-RAR PEP3 = –12.85% ± 1.605%, TacADAM10-RAR inPEP3 = +1.3% ± 2.815% * p=0.0489).*

To better assess the effect of both CPPs on ADAM10 membrane levels, acute rat hippocampal slices were treated either with PEP2 or PEP3 (or their related control) at the concentration of 10µM for 30 minutes and Bis(sulfosuccinimidyl)suberate (BS^3) cross-linking assay was carried out. BS^3 is a membrane-impermeable compound able to covalently cross-link the cell surface–expressed proteins. BS^3 treatment generates high-molecular weight aggregates of membrane proteins, which barely enter the gel. Since intracellular proteins are not modified, the amount of intracellular proteins can be measured by WB and reflects the levels of membrane-inserted proteins (Amy et al 2012). After CPPs treatment in presence or in absence of BS^3, the rat hippocampal slices were processed and the intracellular pool of ADAM10 was evaluated. As demonstrated in figure 7A and 7B, the immunoblot shows a substantial reduction of intracellular levels of ADAM10 when the slices are exposed to either PEP2 or PEP3 in presence of BS^3. In particular, the quantitative analysis demonstrates that ADAM10 intracellular levels are significantly reduced after the treatment with PEP2 and PEP3 when compared with control samples (figure7 C-D, PEP2 74.22% ± 3.83% * p=0.009; inPEP2 102.9% ± 4.671% p>0.05; PEP3 37.52% ± 3.378% * p=0.0032; inPEP3 102.7% ± 9.734% p>0.05). As internal control of the

experiment, we evaluated the levels of GluA1, the AMPA receptor subunit, which is enriched in the synaptic membrane. As shown in figure 7A and 7B, in presence of BS^3 the subunit GluA1 of AMPAR is barely detectable in the intracellular pool and its intracellular levels are not affected by the treatment, thus demonstrating that the CPPs specifically interfere with the synaptic localization of ADAM10. These results demonstrate that both CPPs not only interfere with the ADAM10/AP2 complex formation but also increase ADAM10 surface expression.

Then, we checked ADAM10 synaptic localization, since we have demonstrated that the enzyme is an integral component of the PSD (Marcello et al 2007). Primary hippocampal neurons at DIV14 were treated with either PEP2 or PEP3 and their related inactive peptides at the concentration of 1 μM for 30 minutes. After treatment, cells were lysate and TIF was purified. As shown by the immunoblot in figure 8A and by the quantitative analysis in figure 8B, the treatment with both PEP2 and PEP3 increased the synaptic availability of ADAM10 when compared with their related control peptides (PEP2 +65.75% ± 3.185% ** $p<0.01$ PEP2 vs inPEP2, PEP3 +114.9% ± 17.89% *** $p<0.001$, PEP3 vs inPEP3).

All together these results from *in vitro* experiments demonstrate that CPPs are able to interfere with ADAM10/AP2 complex formation, increasing ADAM10 surface expression and synaptic localization. In particular, PEP3 seems to be more effective in interfering with ADAM10 endocytosis and in increasing its synaptic availability.

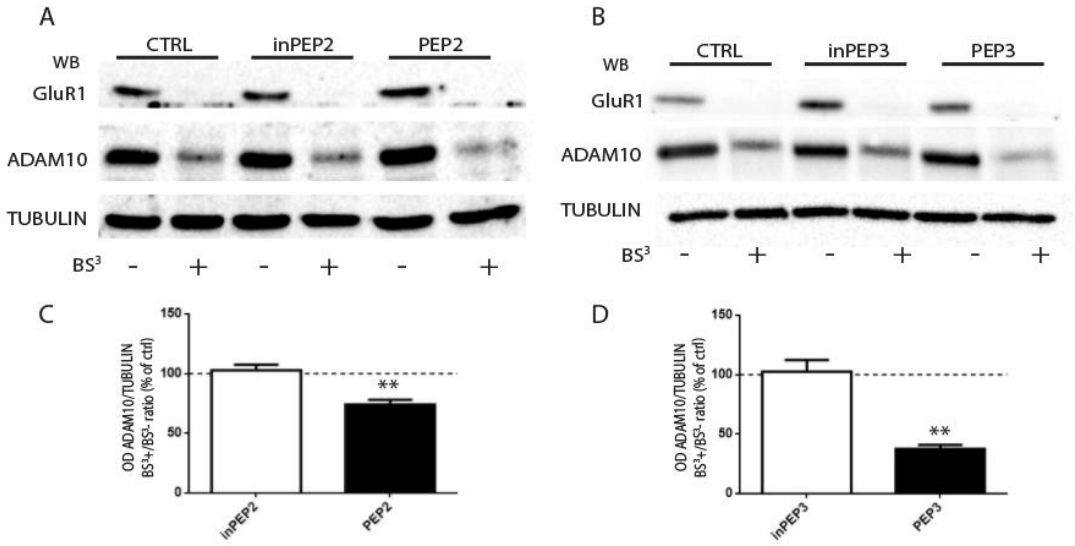

Figure 7 *Modulation of ADAM10 membrane localization after treatment with CPPs. Immunoblot of ADAM10, GluR1, and tubulin from rat hippocampal acute slices treated with PEP2 (A) or PEP3 (B) either exposed or not exposed to the crosslinker BS^3. Both peptides lead to a significant decrease in ADAM10 intracellular pool, which mirrors an augment in ADAM10 surface expression. (C) Quantification experiment in A (PEP2 74.22% ± 3.83% * p=0.009; inPEP2 102.9% ± 4.671% p>0.05). (D) Quantification experiment in B ((PEP3 37.52% ± 3.378% * p=0.0032; inPEP3 102.7% ± 9.734% p>0.05).*

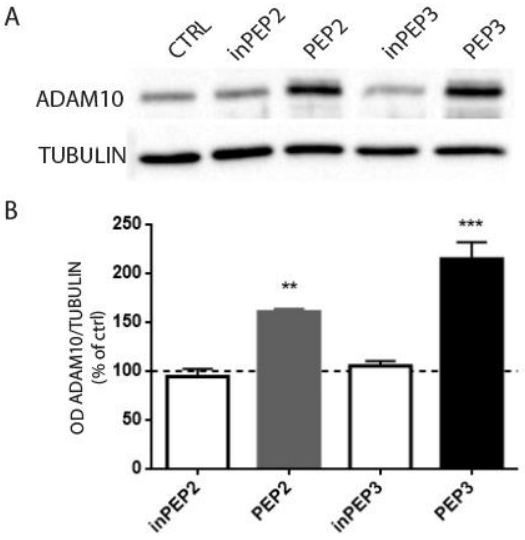

Figure 8 *Modulation of ADAM10 synaptic avalaibility after treatment with CPP. (A) Western blot analysis of ADAM10 performed on synaptic fraction of primary hippocampal neurons treated with either PEP2 or PEP3 peptides or their corresponding inactive peptides. (B) Quantification experiment in (A). Both active peptides treatment increase ADAM10 synaptic localization (PEP2 +65.75% ± 3.185%, inPEP2 -5.55% ± 7.718% ** p<0.01 PEP2 vs inPEP2, PEP3 +114.9% ± 17.89%, inPEP3 +5.3% ± 4.934% *** p<0.001, PEP3 vs inPEP3)*

4. UNCOUPLING ADAM10/AP2 INTERACTION *in vivo* : ACUTE TREATMENT

4.1 Testing CPPs ability to cross the blood-brain barrier

After the positive results obtained from *in vitro* experiments, we decided to test the CPPs *in vivo*.

The brain of the mammalian is protected by the blood-brain barrier (BBB), a highly selective permeability barrier that separates the circulating blood from the brain extracellular fluid. The BBB is formed by brain endothelial cells connected by tight junctions and allows the passage of water, some gases, and lipid-soluble molecules by passive diffusion, as well as the selective transport of molecules such as glucose and amino acids that are crucial to neural function.

First of all, we checked the capability of CPPs to cross the BBB. To assess this issue, PEP2 or PEP3 or their corresponding control CPPs were administered by intraperitoneal injection to C57BL/6 adult mice at a dose of 3nmol/g. After 24 hours, the animals were anesthetized and perfused with 4% PFA., 50 µm brain coronal sections were prepared for the immunofluorescence labeling, to assess the capability of the CPPs to cross the BBB.

The immunofluorescence labelling was performed using the neuronal marker MAP2 (green) and an antibody against the TAT sequence of the CPPs (red). As shown in figure 9, the TAT protein is detectable only in the animal treated with CPPs, in particular the red signal is confined in neuronal cells with a

perinuclear and dendritic distribution (figure 9B and C). Conversely, in the brain of animals treated only with saline solution (figure 9A) no red signal corresponding to TAT is detectable, indicating the specificity of the antibody used for the detection of the CPPs.

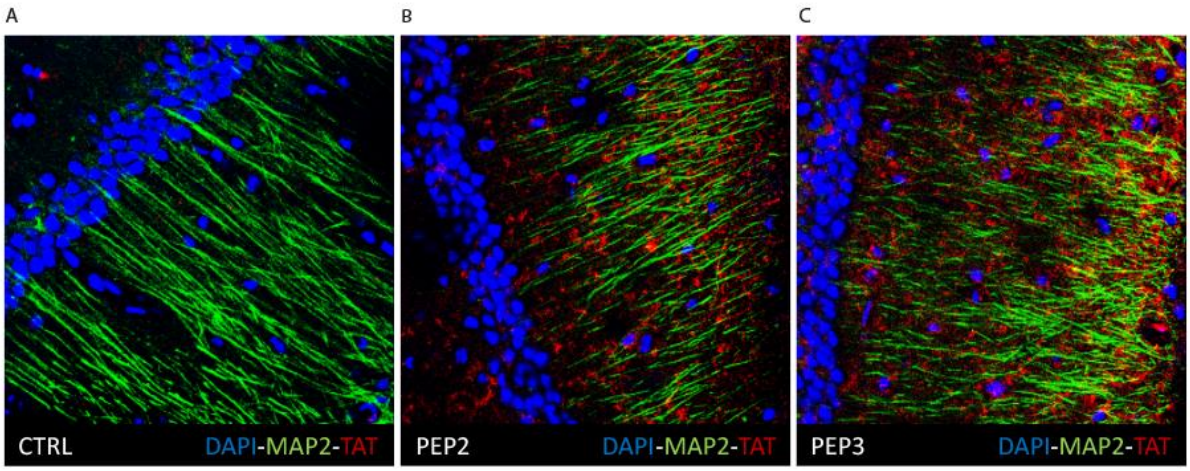

Figure 9 *CPPs are able to cross the BBB. Six weeks old C57BL/6 mice were intraperitoneally injected with either PEP2 or PEP3 (3nmoles/g) or saline solution (control mice) and after 24h were perfused with PFA. Brain coronal sections of control mice (A) and mice treated with PEP2 (B) or PEP3 (C) were immunostained with the nuclear marker DAPI (blue), the neuronal marker MAP2 (green) and an antibody against N-terminus of TAT domainBoth PEP2 and PEP3 are able to cross the BBB and to penetrate into neuronal cells, while control mice treated with saline are not immunopositive for TAT antibody.*

4.2 Testing CPPs efficacy in uncoupling ADAM10/AP2 complex in vivo

After having verified the capability of CPPs to cross the BBB, we evaluated the efficacy in uncoupling ADAM10/AP2 complex formation. Six weeks old C57BL/6 mice were treated by intraperitoneal injection with PEP2 or PEP3 at the dose of 3nmol/g and after 24 hours the animals were sacrificed by dislocation and the forebrain was rapidly dissected.

Total homogenate was used to analyze the levels of the interaction between ADAM10 and the different subunits of AP2 complex. The samples were immunoprecipitated using an anti-ADAM10 antibody and then the presence of α-adaptin, β2-adaptin and μ2 was evaluated. The immunoblot in figure 10A and the quantitative analysis in figure 10B showed that both CPPs significantly interfere with the interaction between ADAM10 and AP2 subunits (PEP2 α-adaptin -62.82% ± 12.78% ** p< 0.01, β2-adaptin -73.36% ± 4.233% *** p<0.001, μ2 -54.39% ± 7.882% ** p<0.01; PEP3 α-adaptin -64.96% ± 9.8113 ** p< 0.01, β-adaptin -92.45% ± 4.023% *** p<0.001, μ2 -61.06% ± 11.63% ** p<0.01). These results demonstrate the capability of CPPs to interfere with ADAM10/AP2 complex formation *in vivo*.

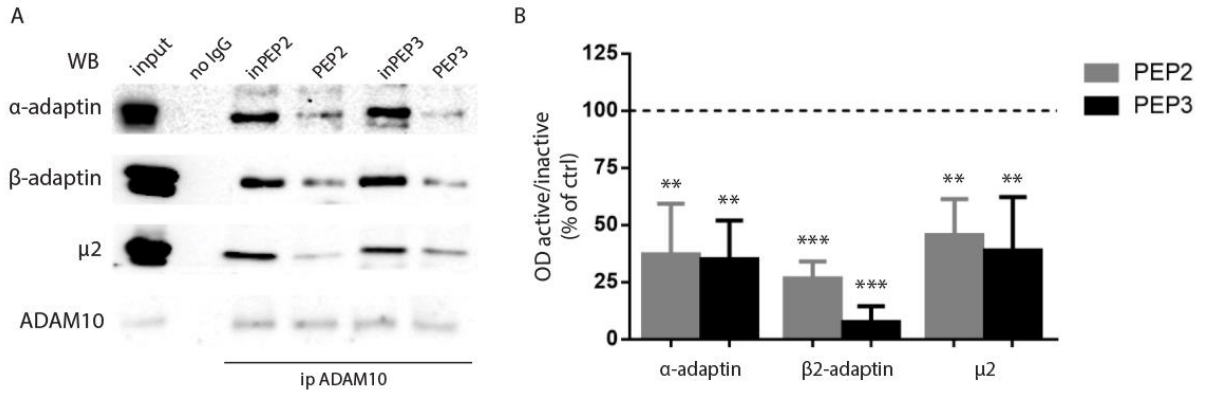

Figure 10 *ADAM10/AP2 association is reduced after treatment with PEP2 and PEP3 in vivo. (A) Brain homogenates from control and treated mice were immunoprecipitated with rabbit anti-ADAM10 antibody and α-adaptin, β-adaptin and μ2 co-precipitation was evaluated. Immunoprecipitated ADAM10 was detected by WB with a rat anti-ADAM10 antibody. (B) Quantification of experiments in A. Both PEP2 and PEP3 significantly reduced ADAM10/AP2 subunits co-precipitation (PEP2 α-adaptin -62.82% ± 12.78% ** p< 0.01, β2-adaptin -73.36% ± 4.233% *** p<0.001, μ2 -54.39% ± 7.882% ** p<0.01; PEP3 α-adaptin -64.96% ± 9.8113 ** p< 0.01, β2-adaptin -92.45% ± 4.023% *** p<0.001, μ2 -61.06% ± 11.63% ** p<0.01).*

4.3 CPPs increase ADAM10 synaptic availability and activity in vivo

To verify the efficacy of CPPs *in vivo*, we analyzed ADAM10 synaptic availability and activity towards APP after the treatment with active CPPs. To this aim, we purified TIF fraction from one brain hemisphere to determine ADAM10 synaptic levels, while form the other hemisphere we isolated the soluble fraction to measure the levels of soluble APP alpha (sAPPα), the main released product of ADAM10 activity on APP. As shown in figure 11, A and C, WB analysis demonstrated that the levels of ADAM10 in total homogenate are not affected by the treatment with both active peptides (inPEP2 102%±5.24%, PEP2 98.48%±11.02% p>0.05, inPEP3 97.53%±10.85%, PEP3 100%±11.62% p>0.05), while we observed a dramatic increase in ADAM10 levels in the TIF fraction (figure 11B). In particular the quantitative analysis (figure 8D) demonstrated that both active CPPs increase by 50% the synaptic localization of ADAM10 compared to inactive peptides (PEP2 151.7%±9.768% * p<0.05, PEP3 147.5%±7.093% * p<0.05). These results clearly demonstrate that, since the levels in the homogenate do not change after treatment, the increase of synaptic levels of ADAM10 are due to a modification of its trafficking rather than to an increase of the protein synthesis.

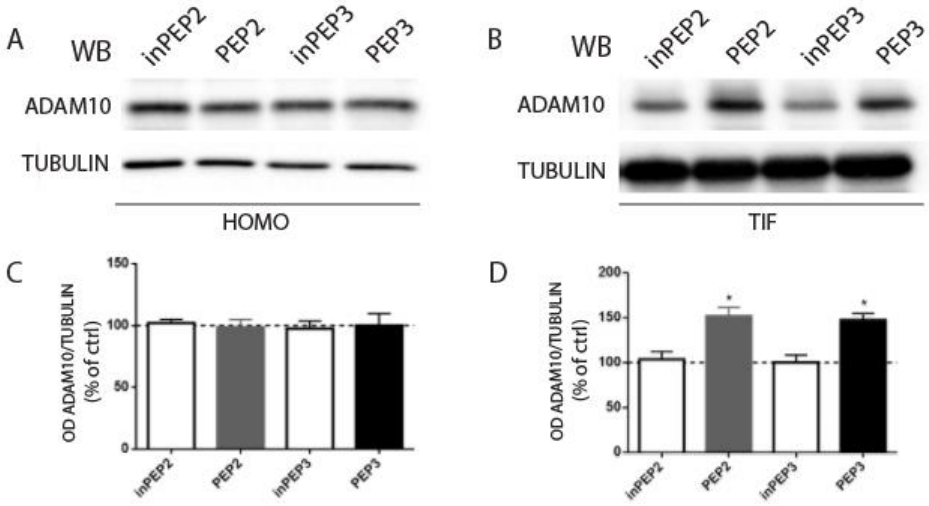

Figure 11 *Modulation of ADAM10 synaptic availability after treatment with CPPs in vivo. C57BL/6 mice were treated with either PEP2 and PEP3 and 24h later WB analysis of ADAM10 was performed on total brain homogenate (A) and TIF fraction (B). (C) Quantification of experiment in A, ADAM10/tubulin OD ratio. Treatment with CPPs does not alter ADAM10 levels in total brain homogenates (inPEP2 102%±5.24%, PEP2 98.48%±11.02% p>0.05, inPEP3 97.53%±10.85%, PEP3 100%±11.62% p>0.05). (D) Quantification of experiments in B, ADAM10/tubulin OD ratio. Both active peptides increase ADAM10 synaptic localization (inPEP2 103.6%±8.689%, PEP2 151.7%±9.768% * p<0.05, inPEP3 100.2%±8.22%, PEP3 147.5%±7.093% * p<0.05)*

As far as concern sAPPα levels, the treatment with both active peptides stimulates sAPPα release, indicating a shift of APP metabolism towards the non-amyloidogenic pathway (Fig. 12, inPEP2 130.8% ± 34.66%, PEP2 271.4%±36.9% * p<0.05, inPEP3 98.41% ± 9.689%, PEP3 155.5%±15.05% p<0.05). These outcomes revealed that a single dose of 3nmol/g CPPs is able to uncouple ADAM10/AP2 complex and to enhance ADAM10 synaptic levels and activity activity towards APP 24 hours after the intraperitoneal injection.

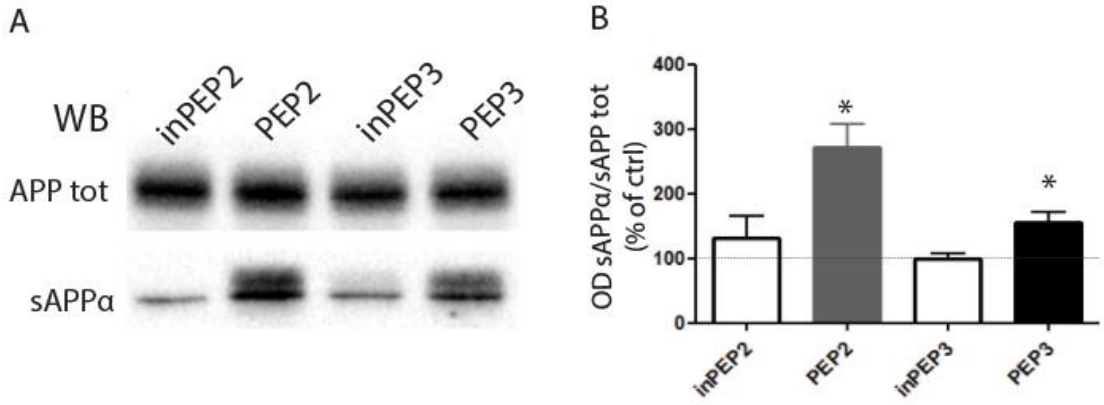

Figure 12 *Active peptides treatment positively modulates ADAM10 activity in vivo. WB analysis was performed on the brain soluble fraction of mice treated with either PEP2 or PEP3. (B) Quantification of experiments in (A). sAPPα/sAPPtot ratio is increased in mice treated with both PEP2 and PEP3 active peptides (inPEP2 130.8% ± 34.66%, PEP2 271.4%±36.9% * p<0.05, inPEP3 98.41% ± 9.689%, PEP3 155.5%±15.05% p<0.05)*

5. 14-DAYS CPPs ADMINISTRATION: SETTING UP THE EXPERIMENTAL CONDITIONS

To assess the efficacy and toxicity of CPPs treatment, we focused on PEP3, since it was more effective in altering ADAM10 endocytosis and in modulating its synaptic availability.

To set up the conditions for a 14 days treatment, we tested two doses (either 1 nmol/g or 3nmol), different routes of administration, i.e. either subcutaneous or intraperitoneal injection, and we checked the stability of PEP3 effect 24h and 48h after the administration.

Adult C57BL/6 mice were treated by either intraperitoneal or subcutaneous injection with either PEP3 or inPEP3 at the dose of either 3nmol/g or 1nmol/g. After 24h or 48h the animals were sacrificed, the brain was dissected and TIF and soluble fraction were purified. For each experimental group, the interaction between ADAM10 and AP2 complex, ADAM10 synaptic availability and activity were evaluated.

Co-immunoprecipitation experiments performed in total brain homogenate of animals treated by intraperitoneal injection (figure 13A), showed that PEP3 is able to disrupt ADAM10/AP2 interaction only at the higher dose (3nmol/g) and its effect is stable only for 24 hours, since at 48 hours no alteration of ADAM10/AP2 complex levels is observed. In fact, the quantitative analysis showed in figure 13B revealed a reduction of ADAM10/AP2 levels only in the brain of animals treated with a dose of 3nmol/g and sacrificed after 24 hour (PEP3/inPEP3 -35.74% ± 7.795% $p<0.05$).

We then evaluated the levels of ADAM10 in the synaptic TIF fraction of animals treated by intraperitoneal injection.

The immunoblot in figure 13C and the quantitative analysis in figure 13D, show that only a dose of 3nmol/g of PEP3 leads to a significant increase in ADAM10 synaptic levels 24h after the injection, but not after 48h (PEP3 113.7% ± 2.827% $p<0.05$). PEP3 is ineffective at a lower dose (1nmol/g). According to these results, the immunoblot and the quantitative analysis of the sAPPα levels in the brain soluble fraction (figure 13E,F) demonstrate that PEP3 positively modulates ADAM10 activity only in mice treated with a dose of 3nmol/g and sacrificed after 24 hours (PEP3 151.6% ± 12.22% $p<0.05$). Neither the 1nmol/g dose nor the 48h time point led to significant modifications of sAPPα release.

These results indicate that PEP3 is effective only when it is intraperitoneally administered at a dose of 3nmol/g and its effect is stable only for 24 hours. The next step was to evaluate a different route of administration, thus the same analyses were performed in mice treated by subcutaneous injection with a dose of either 3nmol/g or 1nmol/g and sacrificed either 24 or 48 hours after the injection.

Co-IP experiments showed that PEP3 is ineffective in interfering with ADAM10/AP2 interaction in all experimental groups (figure 14 A and B). Moreover, the subcutaneous injection of PEP3 does not

change the ADAM10 synaptic availability as demonstrate by the immunoblot performed in TIF fraction (figure 14 C andD). As expected, also the activity of ADAM10 is not affected: the immunoblot performed on the brain soluble fraction (figure 14 E) and the quantitative analysis (figure 14 F), demonstrated that there are no significant changes in the levels of sAPPα release in mice treated with PEP3 compared with animals treated with inPEP3.

All these results demonstrate that the subcutaneous injection is not a valid administration route and that only intraperitoneal injection with a dose of 3nmol/g is the best condition to guarantee the efficacy of PEP3 in the modulation of ADAM10/AP2 complex formation, and thereby of ADAM10 activity.

Then, we decided to assess the stability and efficacy of PEP3 at different time points.

Adult C57BL/6 mice were treated with PEP3 and inPEP3 by intraperitoneal injection with a dose of 3nmol/g, and after 8, 12, 24 or 36 hours animals were sacrificed, the brain was dissected to purify TIF and soluble fraction. We evaluated the ADAM10/AP2 interaction, ADAM10 synaptic availability and activity. Total brain homogenates were immunoprecipitated with an ADAM10 antibody, and α-adaptin co-IP was used to evaluate the interaction between ADAM10 and AP2 complex. As shown in figure 15A and demonstrated by quantitative analysis in figure 15B, PEP3 reduces, as expected, by 31% the interaction between ADAM10 and α-adaptin 24 hours after the injection (PEP3/inPEP3 24h -31% ± 6.124% $p<0.05$). 36 hours after the injection, we measured a 20% reduction, but it was not statistically significant (PEP3/inPEP3 36h -19.69% ± 16.86% $p>0.05$). As shown in figure 15C and confirmed by quantitative analysis in figure 15D, PEP3 increases the synaptic availability of ADAM10 24 hours after the administration (PEP3 24h 137.4% ± 6.324% $p<0.05$). 12h and 36 hours after the injection a slight but not statistically significant increase in ADAM10 synaptic levels can be observed.

As a consequence, the ADAM10 activity shows the same trend. Brain soluble fraction was used to evaluate the sAPPα and PEP3 increases sAPPα levels by around 30% 24 hours after the injection (PEP3 24h 126.3% ± 6.225% $p<0.05$). A slight increase in sAPPα levels can be detected 12h and 36h after the administration, but this change is not statistically significant (PEP3 12h 112.7% ± 5.616% $p>0.05$; PEP3 36h 120% ± 5.703%).

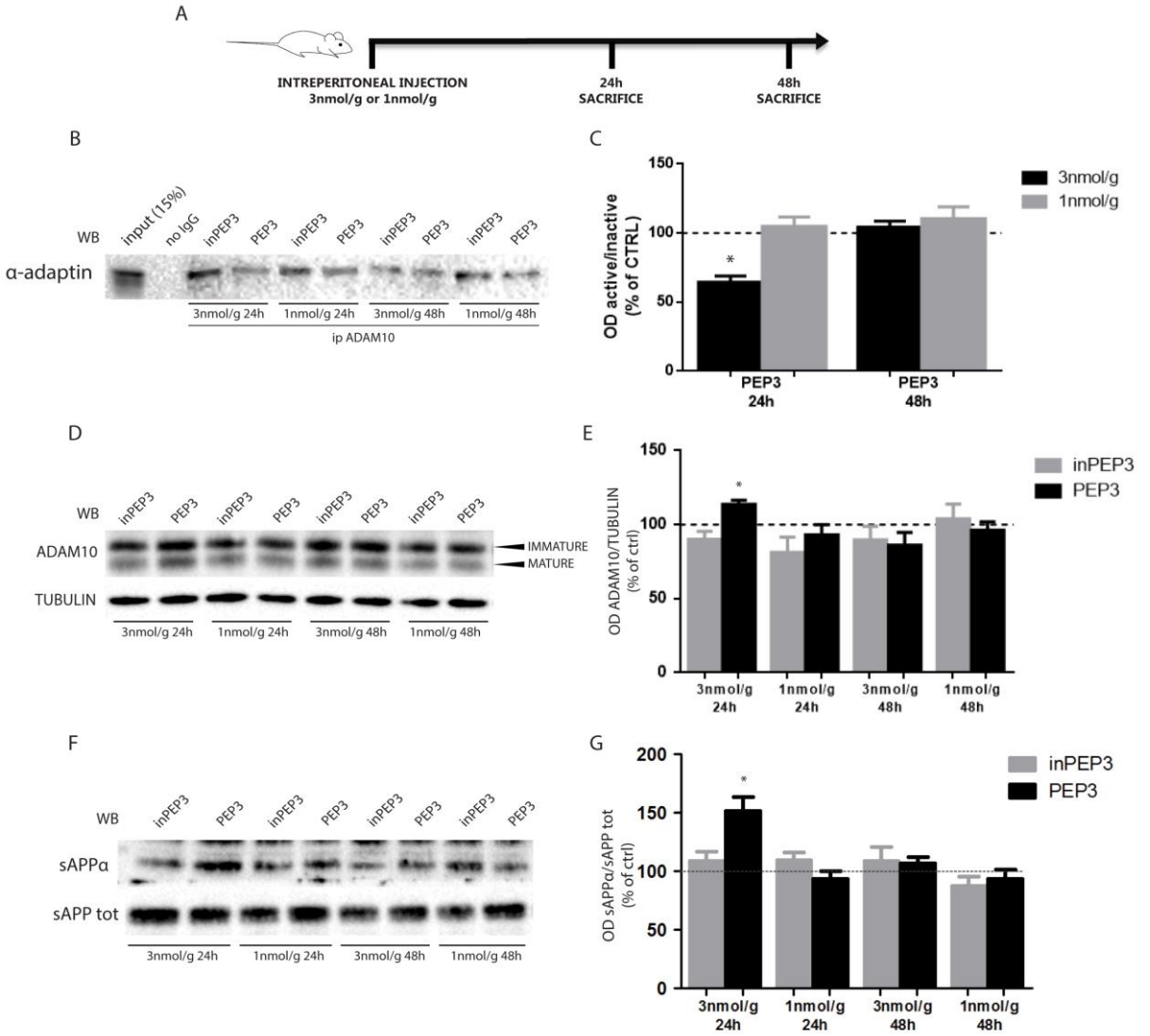

Figure 13 *Testing time and dose efficacy of intraperitoneal injection. (A) Experimetal paradigm. (B) Brain homogenates from control and mice treated with either 1nmol/g or 3nmol/g, and sacrificed after either 24 or 48 hours were immunoprecipitated with anti-ADAM10 antibody and α-adaptin co-precipitation was evaluated. (C) OD PEP3/inPEP3 quantification of experiments in B. PEP3 significantly reduces ADAM10/AP2 co-precipitation only with a dose of 3nmol/g and the effect is stable only for 24h (inPEP3/PEP3 -35.74% ± 7.795%, * p<0.05) (D) TIF fraction obtained from mice treated with either 1nmol/g or either 3nmol/g PEP3 or inPEP3, and sacrificed after 24 or 48 hours. TIF fraction was used to evaluate ADAM10 synaptic levels. (E) Quantification of experiments in D, ADAM10/tubulin OD ratio. Only the mice treated with a dose of 3nmol/g and sacrificed 24 hours after the injection, show a significant increase of ADAM10 synaptic levels (inPEP3 90.2% ± 5.385%, PEP3 113.7% ± 2.827% * p<0.05. (F) Western blot analyses were performed on brain soluble fraction of mice treated with PEP3 at either 1nmol/g or 3nmol/g and sacrificed 24 or 48 hours after the injection. Representative immunoblots performed using APPα and APP tot antibody show an increase of the release of sAPPα only in the animals treated with PEP3 3nmol and analysed 24h after the injection. (G) Quantification of experiments in F. OD of sAPPα/sAPP tot ratio was measured for each group (3nmol/g-24 hours inPEP3 108.7% ± 8.004%, PEP3 151.6% ± 12.22% * p<0.05).*

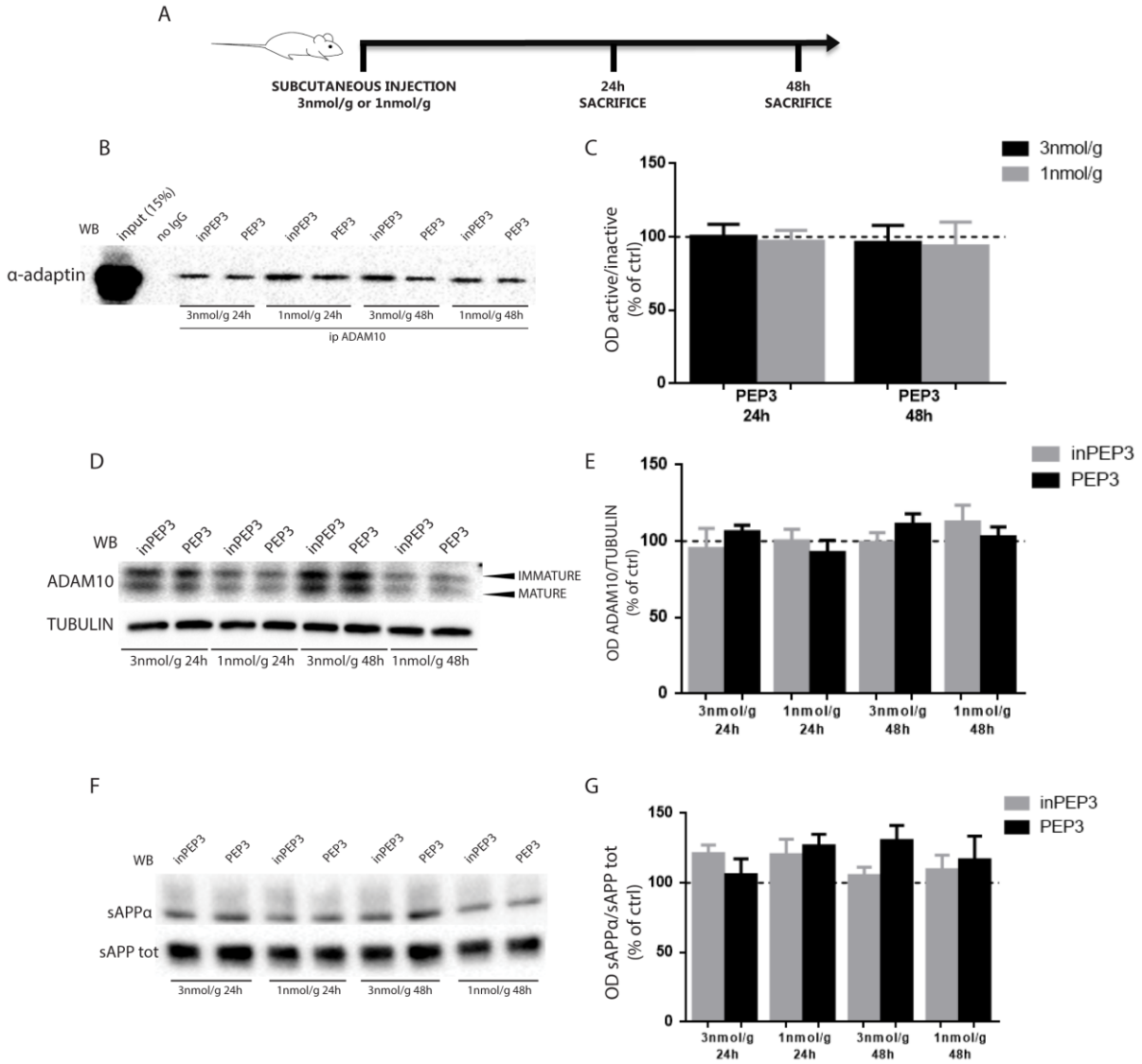

Figure 14 *Testing subcutaneous injection efficacy. (A) Experimental paradigm. (B) Brain homogenates from mice treated by subcutaneous injection with a dose of either 1nmol/g or 3nmol/g, and sacrificed 24 or 48 hours after the injection, were immunoprecipitated with an anti-ADAM10 antibody and α-adaptin co-precipitation was evaluated. (C) PEP3/inPEP3 OD quantification of experiments in B. The subcutaneous injection does not change the interaction between ADAM10 and AP2 complex. (D) Representative immunoblot of ADAM10 WB analysis of TIF. (E) Quantification of experiments in D, ADAM10/tubulin OD ratio. The subcutaneous injection of PEP3 does not change the synaptic availability of ADAM10. (F) WB analyses were performed on brain soluble fraction to measure sAPPα release. (G) Quantification of experiments in F. sAPPα/sAPP tot OD ratio was measured for each group; subcutaneous injection of PEP3 does not change the release of sAPPα.*

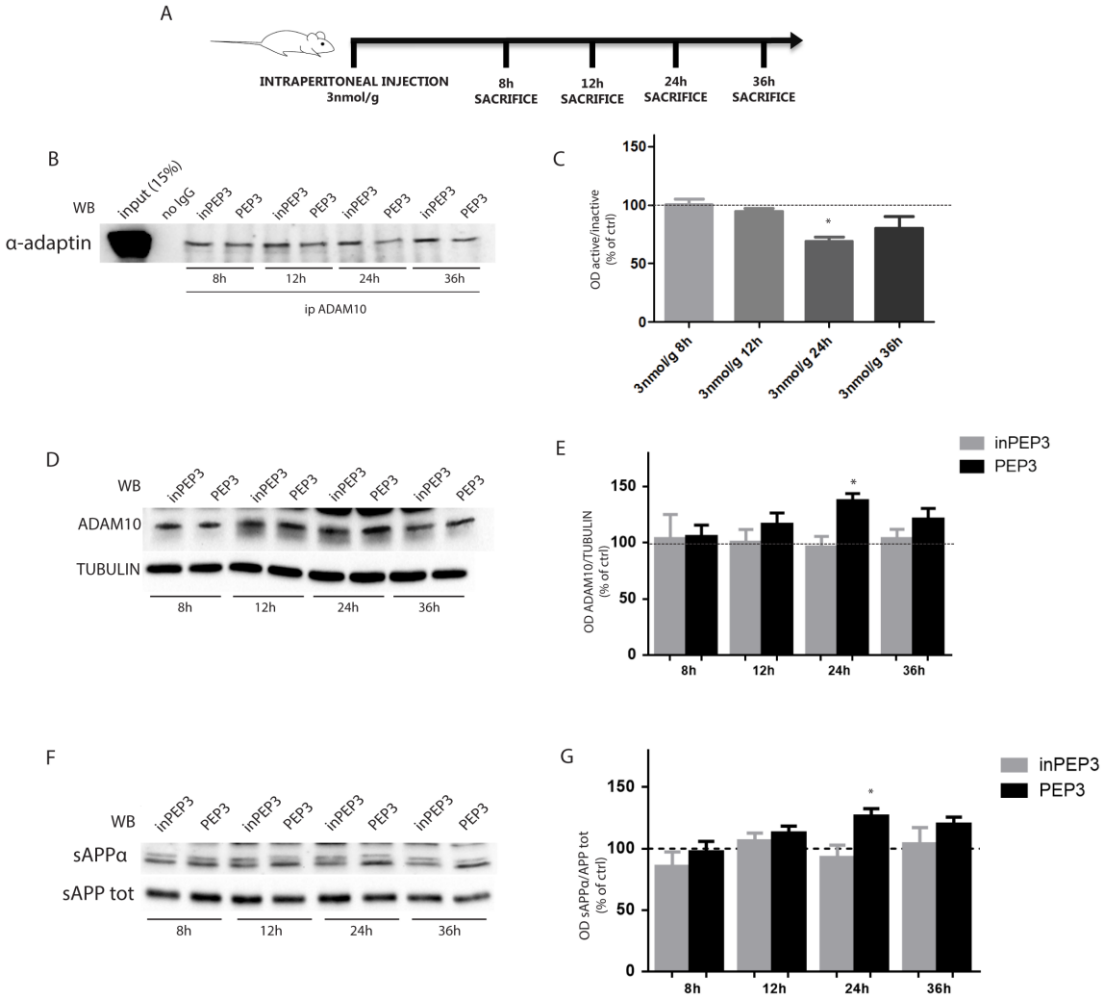

Figure 15 *Testing time-dependent efficacy of PEP3. (A)Experimental paradigm. (B) Brain homogenates from mice treated by intraperitoneal injection of PEP3 (3 nmol/g), and sacrificed after 8, 12, 24 or 36 hours, were immunoprecipitated with anti-ADAM10 antibody and α-adaptin co-precipitation was evaluated. (C) inPEP3/PEP3 OD quantification of experiments in B. PEP3 significantly reduces ADAM10/AP2 co-precipitation only 24 hours after the administration (PEP3/inPEP3 -31% ± 6.129%, * p<0.05). A slight but not significant reduction of ADAM10/α-adaptin interaction can be observed 36 hours after the injection (PEP3/inPEP3 -19.69% ± 16.86%). (D) Representative immunoblot of ADAM10 WB analysis. (E) Quantification of experiments in D, ADAM10/tubulin OD ratio. Only the animals sacrificed after 24 hours showed a significant increase in ADAM10 synaptic levels. (inPEP3 6.43% ± 9.229%, PEP3 137.4% ± 6.324% * p<0.05). (F) Representative immunoblot performed using sAPPα and sAPP tot antibody show an increase in the release of sAPPα only in mice sacrificed after 24 hours. (G) Quantification of experiments in F, sAPPα/sAPP tot OD ratio (24 hours, inPEP3 92.84% ± 10.05% PEP3 126.3% ± 6.225% * p<0.05).*

6. 14 DAYS-TREATMENT: TESTING EFFICACY AND TOXICITY

All the results obtained from *in vivo* treatment demonstrate that PEP3 is effective 24h after the injection and that the best route of administration is intraperitoneal injection. In light of these results, we decided to perform a 14-days treatment to test the safety and efficacy of CPPs. To address this issue, we treated 2-month-old C57BL/6 mice with either PEP3 or inPEP3 with a 3nmol/g dose every 24h for 14 days. We weight the mice and we measured the food intake everyday. 24 hours after the last injection, mice were anesthetized, blood was collected through cardiac puncture and brain and liver were rapidly dissected.

6.1 Hematology and histology analyses

6.1.1 Erythrograms and platelet counts

In all the groups mean and median data of erythroid parameters, as well as individual results, were within the reference intervals, except for MCV (mean corpuscular volume) value that was higher than the reference interval in some mice, and MCH (mean corpuscular hemoglobin) and MCHC (mean corpuscular hemoglobin concentration) values that were lower than the reference intervals in all the mice, suggesting that this difference may depend on analytical or pre-analytical factors compared with instruments/methods (not known) employed to determine the reference interval (table 1).
Statistical analysis (figure 16) did not reveal any differences in Ht (hematocrit), Hb (hemoglobin), MCV, MCH, MCHC values, but showed a significantly higher RBC (red blood cell) number in mice treated with the inactive peptide compared with the other groups. This may be consistent with a moderate dehydration but it is not particularly relevant from a biological point of view, since all the results remain within the reference intervals. Platelet counts were very low in most mice but the morphological analysis of blood smears revealed that platelets were always present in adequate amounts and were often clumped. This means that the low platelet counts depends on an analytical artifact (clumps does not enter in the counting chamber of the analyzer) and that none of these mice is actually thrombocytopenic.

SAMPLE	RBC x10^6/µL	Hb (g/dL)	Ht (%)	MCV (fL)	MCH (pg)	MCHC (%)	PLT x10^3/µL	RDW (%)	Plt Estimate /clumps
saline	8,84	12,1	46,6	52,7	13,7	26,0	1199	19,6	A/+++
	8,67	11,7	45,7	52,7	13,5	25,6	382	19,6	A/+++
	9,00	12,0	45,9	51,0	13,3	26,1	345	19,6	A/+++
	8,58	11,4	42,7	49,8	13,3	26,7	1327	21,0	A/+++
	9,11	12,1	46,7	51,3	13,3	25,9	737	21,2	A/+++
	8,93	12,1	47,8	53,5	13,5	25,3	657	20,1	A/+++
Mean ± SD (Median)	**8,86**	**11,9**	**45,9**	**51,8**	**13,4**	**25,9**	**775**	**20,2**	
	± 0,20	**± 0,3**	**± 1,7**	**± 1,4**	**± 0,2**	**± 0,5**	**± 410**	**± 0,7**	
	(8,89)	**(12,1)**	**(46,3)**	**(52,0)**	**(13,4)**	**(26,0)**	**(697)**	**(19,9)**	
inPEP3	9,36	12,6	50,1	53,5	13,5	25,1	522	20,4	A/+++
	9,34	12,6	49,5	53,0	13,5	25,5	661	20,6	A/+++
	9,01	12,0	47,8	53,1	13,3	25,1	656	21,4	A/+++
	9,21	12,4	48,7	52,9	13,5	25,5	341	21,8	A/+++
	9,04	12,1	48,0	53,1	13,4	25,2	998	19,6	A/+++
	8,97	12,0	47,3	52,7	13,4	25,4	790	20,1	A/+++
Mean ± SD (Median)	**9,16**	**12,3**	**48,6**	**53,1**	**13,4**	**25,3**	**661**	**20,7**	
	± 0,17	**± 0,3**	**± 1,1**	**± 0,3**	**± 0,1**	**± 0,2**	**± 224**	**± 0,8**	
	(9,13)	**(12,3)**	**(48,4)**	**(53,1)**	**(13,5)**	**(25,3)**	**(659)**	**(20,5)**	
PEP3	8,14	10,9	41,5	51,0	13,4	26,3	861	18,7	A/+++
	8,75	11,7	47,4	54,2	13,4	24,7	711	19,3	A/+++
	9,04	12,5	48,5	53,7	13,8	25,8	1333	19,9	A/+++
	8,94	11,9	48,0	53,7	13,3	24,8	391	19,9	A/+++
	8,84	11,9	46,3	52,4	13,5	25,7	1302	19,7	A/+++
	8,72	11,9	45,7	52,4	13,6	26,0	1394	19,7	A/+++
Mean ± SD (Median)	**8,74**	**11,8**	**46,2**	**52,9**	**13,5**	**25,6**	**999**	**19,5**	
	± 0,32	**± 0,5**	**± 2,5**	**± 1,2**	**± 0,2**	**± 0,7**	**± 408**	**± 0,5**	
	(8,80)	**(11,9)**	**(46,9)**	**(53,1)**	**(13,5)**	**(25,8)**	**(1082)**	**(19,7)**	
ref. interval	9.51±1.25	14.3±2.6	47.0±7.3	49.4±3.9	14.9±1.1	30.3±3.0	N/A	1350±338	

Table 1 *Results regarding erythrograms and platelet counts. Reference intervals provided by Charles River for C57BL mice, 56-70 days old bled by cardiac puncture after euthanasia. A = platelet estimate adequate; +, ++, +++ subjective evaluation of the amount of platelet clumps on smears.*

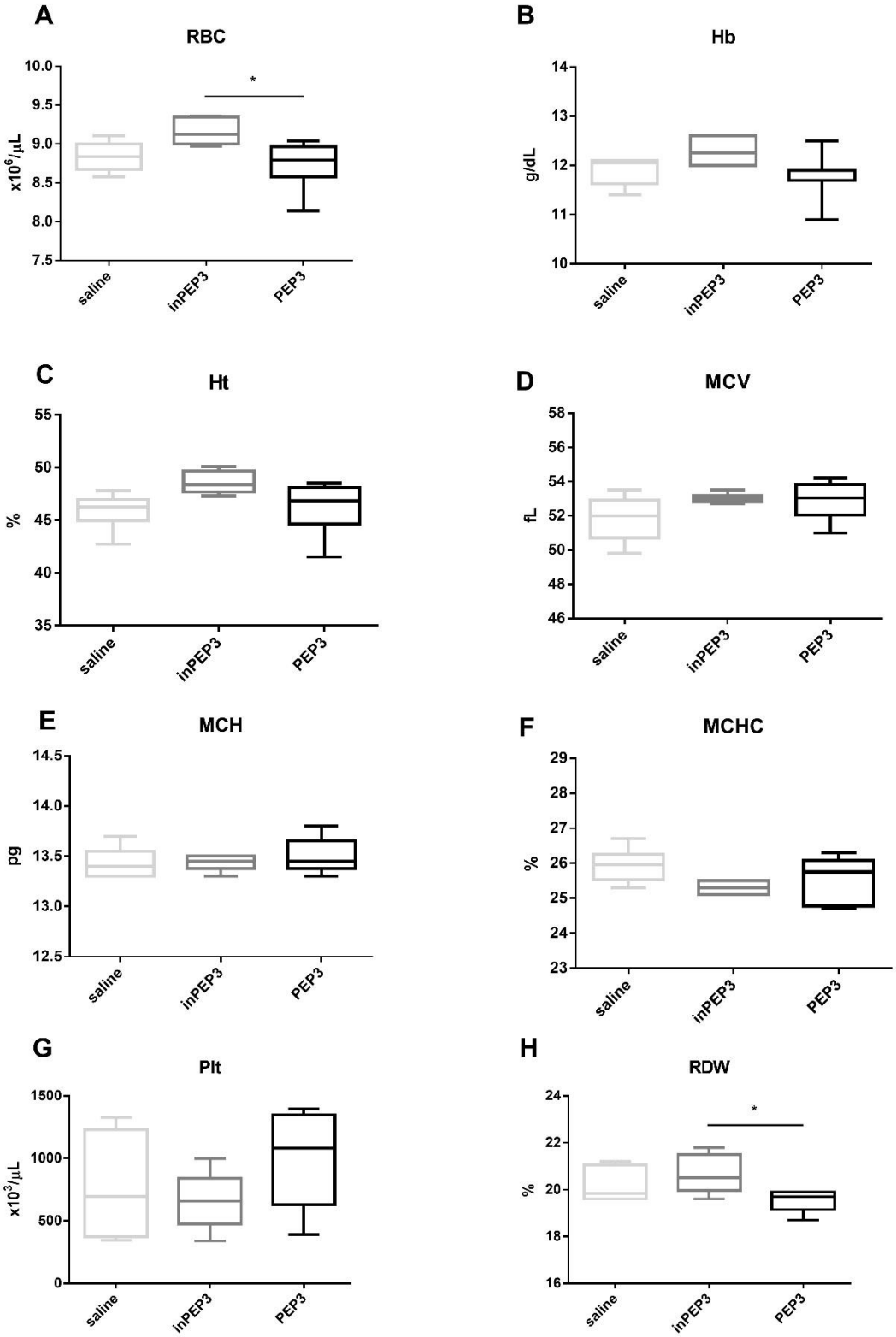

Figure 16 *Distribution of data regarding erythrogram (table 1) and corresponding statistical analysis. For all the markers taken into account, except for MCH, the mean of the measure falls in the reference interval without significant changes. Only the number of red blood cell (RBC) (A) and the red cells distribution width (RDW) of animal treated with inPEP3 (H) is higher respect the other groups, but this difference has not a biological relevance. RBC, red blood cells; Hb, hemoglobin; Ht, hematocrit; MCV, mean corpuscular volume; MCH, mean corpuscular hemoglobin; MCHC, mean corpuscular hemoglobin concentration; RDW, red cell distribution width.*

6.1.2 Leucograms

Total and differential WBC (white blood cells) counts are lower than the reference interval in all mice, except for basophils and eosinophils. However, the reference intervals reported by Charles River are particularly high compared with reference intervals reported in control groups of other articles analyzing the same strains (Schnell M.A. et al.,2002; Mazzaccara C., et al 2008). Therefore, this difference seems to be related to preanalytical factors affecting the Charles River reference interval (e.g. methodology, sampling, etc). However, both the analysis of individual data and the analysis of mean and median results in the different groups indicates some differences in mice treated with the active peptide compared with controls or with the other groups (table 2).

SAMPLE	WBC x10³/µL	neutrophils x10³/µL	lymphocytes x10³/µL	monocytes x10³/µL	eosinophil x10³/µL	basophils x10³/µL	Plt Estimate/clumps
SALINE	2,2000	0,73	1,30	0,11	0,04	0,02	A/+++
	2,1100	0,44	1,54	0,08	0,04	0,00	A/+++
	3,9000	0,47	3,24	0,12	0,08	0,00	A/+++
	4,0700	1,10	2,69	0,20	0,08	0,00	A/+++
	2,4700	0,25	2,07	0,10	0,02	0,02	A/+++
	1,7600	0,16	1,48	0,07	0,04	0,02	A/+++
Mean ± SD (Median)	**2,7517**	**0,52**	**2,05**	**0,11**	**0,05**	**0,01**	
	0,9834	**± 0,34**	**± 0,77**	**± 0,05**	**± 0,02**	**± 0,01**	
	2,3350	**(0,46)**	**(1,81)**	**(0,10)**	**(0,04)**	**(0,01)**	
inPEP3	2,6100	0,2610	2,2185	0,1044	0,0261	0,0000	A/+++
	1,5500	0,2325	1,2710	0,0155	0,0310	0,0000	A/+++
	4,4800	2,2848	1,9712	0,1792	0,0448	0,0000	A/+++
	6,2000	2,7900	2,9760	0,3720	0,0620	0,0000	A/+++
	1,8000	0,2160	1,4760	0,0720	0,0360	0,0000	A/+++
	1,9800	0,1584	1,7028	0,0792	0,0396	0,0000	A/+++
Mean ± SD (Median)	**3,1033**	**0,9905**	**1,9359**	**0,1371**	**0,0399**	**0,0000**	
	1,8494	**1,2093**	**0,6117**	**0,1268**	**0,0126**	**0,0000**	
	2,2950	**0,2468**	**1,8370**	**0,0918**	**0,0378**	**0,0000**	
PEP3	6,8300	0,68	5,74	0,27	0,14	0,00	A/+++
	3,1200	0,34	2,65	0,06	0,06	0,00	A/+++
	4,5500	0,46	3,82	0,18	0,09	0,00	A/+++
	4,3800	0,44	3,72	0,13	0,04	0,04	A/+++
	5,8700	0,65	4,81	0,29	0,12	0,00	A/+++
	6,9900	0,63	6,01	0,28	0,07	0,00	A/+++
Mean ± SD (Median)	**5,2900**	**0,53**	**4,46**	**0,20**	**0,09**	**0,01**	
	1,5286	**± 0,14**	**± 1,29**	**± 0,09**	**± 0,04**	**± 0,02**	
	5,2100	**(0,54)**	**(4,32)**	**(0,23)**	**(0,08)**	**(0,00)**	
ref. interval	8.91±2.50	1.45±1.01	6.85±1.97	0.43±0.24	0.14±0.12	0.03±0.03	

Table 2 *Leucograms results. Reference intervals provided by Charles River for C57BL mice, 56-70 days old bled by cardiac puncture*

Specifically, as demonstrated by statistical analysis (figure 17), mice treated with the active peptide had a higher

1) total WBC count (compared with controls),

2) a higher lymphocyte count (compared with both controls and mice treated with the inactive peptide) suggesting a subacute-chronic activation of the immune responses,

3) a higher eosinophil count (compared with mice treated with inPEP3) indicating an allergic/hyperergic condition (although this finding may be statistically significant but not biologically relevant, since all the groups had values falling within the reference intervals).

However, none of the mice included in this study had morphological abnormalities detectable on blood smears.

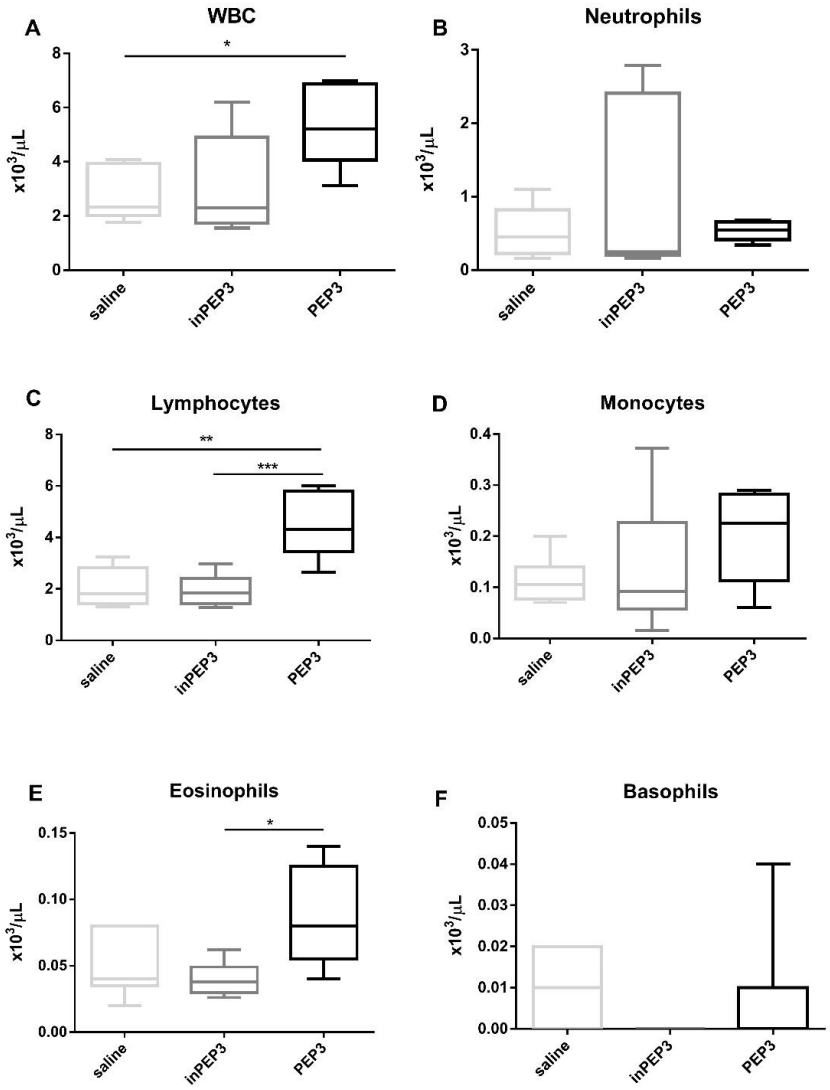

Figure 17 *Distribution of leukograms data (table 2) and corresponding statistical analysis. Total and differential white blood cells are in all mice lower than the reference interval, except for eosinophils and basophils. Mice treated with PEP3 had a significant change in total WBC (A), lymphocytes (C) and eosinophils (E) compared to saline or inPEP3 treated mice. * p<0.05, ** p<0.01, *** p<0.001.*

6.1.3 Clinical chemistry

The concentration of urea, creatinine and ALT (alanine aminotransferase) measured in control mice were within the reference intervals (table 3). Total protein, total globulin and, to a lesser extent, albumin, were lower than the reference intervals in the large majority of controls and in treated mice. Also the concentration of triglycerides was lower than the reference interval in controls and in treated mice.

SAMPLE	Creatinine (mg/dL)	Urea (mg/dL)	Total protein (g/dL)	Albumin (g/dL)	Globulin (g/dL)	A/G Ratio	Triglycerides (mg/dL)	ALT (U/L)	GLDH (U/L)
SALINE	0,61	59	4,47	2,80	1,67	1,68	71	32	17,30
	0,43	40	4,49	2,72	1,77	1,54	50	23	14,70
	0,37	70	4,82	2,91	1,91	1,52	83	22	19,20
	0,36	56	5,46	2,81	2,65	1,06	97	41	26,60
	0,39	73	5,22	2,78	2,44	1,14	140	28	13,00
	0,38	53	4,14	2,52	1,62	1,56	61	24	21,10
Mean ± SD (Median)	**0,42**	**59**	**4,77**	**2,76**	**2,01**	**1,42**	**84**	**28**	**18,65**
	± 0,09	**± 12**	**± 0,50**	**± 0,13**	**± 0,43**	**± 0,25**	**± 32**	**± 7**	**± 4,88**
	(0,39)	**(58)**	**(4,66)**	**(2,79)**	**(1,84)**	**(1,53)**	**(77)**	**(26)**	**(18,25)**
inPEP3	0,38	60	4,89	3,01	1,88	1,60	87	24	12,60
	0,47	57	4,71	2,83	1,88	1,51	76	30	22,70
	0,46	67	4,78	2,73	2,05	1,33	70	45	36,20
	0,44	67	4,55	2,78	1,77	1,57	80	62	27,00
	0,46	55	4,67	2,85	1,82	1,57	75	29	17,10
	0,37	56	4,53	2,86	1,67	1,71	59	16	11,60
Mean ± SD (Median)	**0,43**	**60**	**4,69**	**2,84**	**1,85**	**1,55**	**75**	**34**	**21,20**
	± 0,04	**± 5**	**± 0,14**	**± 0,10**	**± 0,13**	**± 0,13**	**± 9**	**± 17**	**± 9,42**
	(0,45)	**(59)**	**(4,69)**	**(2,84)**	**(1,85)**	**(1,57)**	**(76)**	**(30)**	**(19,90)**
PEP3	0,28	nd	4,60	2,29	2,31	0,99	26	nd	10,10
	0,45	58	4,46	2,72	1,74	1,56	81	42	27,20
	0,43	60	4,88	2,80	2,08	1,35	86	32	12,40
	0,47	63	4,68	2,85	1,83	1,56	76	33	15,00
	0,34	55	4,59	2,83	1,76	1,61	82	17	11,90
	0,34	65	4,65	2,82	1,83	1,54	80	37	13,40
Mean ± SD (Median)	**0,39**	**60**	**4,64**	**2,72**	**1,93**	**1,43**	**72**	**32**	**15,00**
	± 0,08	**± 4**	**± 0,14**	**± 0,21**	**± 0,22**	**± 0,24**	**± 23**	**± 9**	**± 6,19**
	(0,39)	**(60)**	**(4,63)**	**(2,81)**	**(1,83)**	**(1,55)**	**(81)**	**(33)**	**(12,90)**
ref. Interval	0,33 ± 0,12	31 ± 11**	5,67 ± 0,76	3,24 ± 0,46	3,33 ± 0,87	N/A	153 ± 56	66 ± 184	N/A

Table 3 *Clinical chemistry results. Reference intervals provided by Charles River for C57BL mice, 56-70 days old bled by cardiac puncture after euthanasia.*
*** expressed as blood urea*

Based on the lack of signs consistent with liver insufficiency, the low albumin and triglyceride concentration and to some extent the lower concentration of globulin, may depend on dietary factors or on peculiar features of the group of mice. Reference intervals for GLDH (glutamate dehydrogenase) were not available, but results of control mice were on line with reference intervals of other murine strains (Henninger et al 2012).

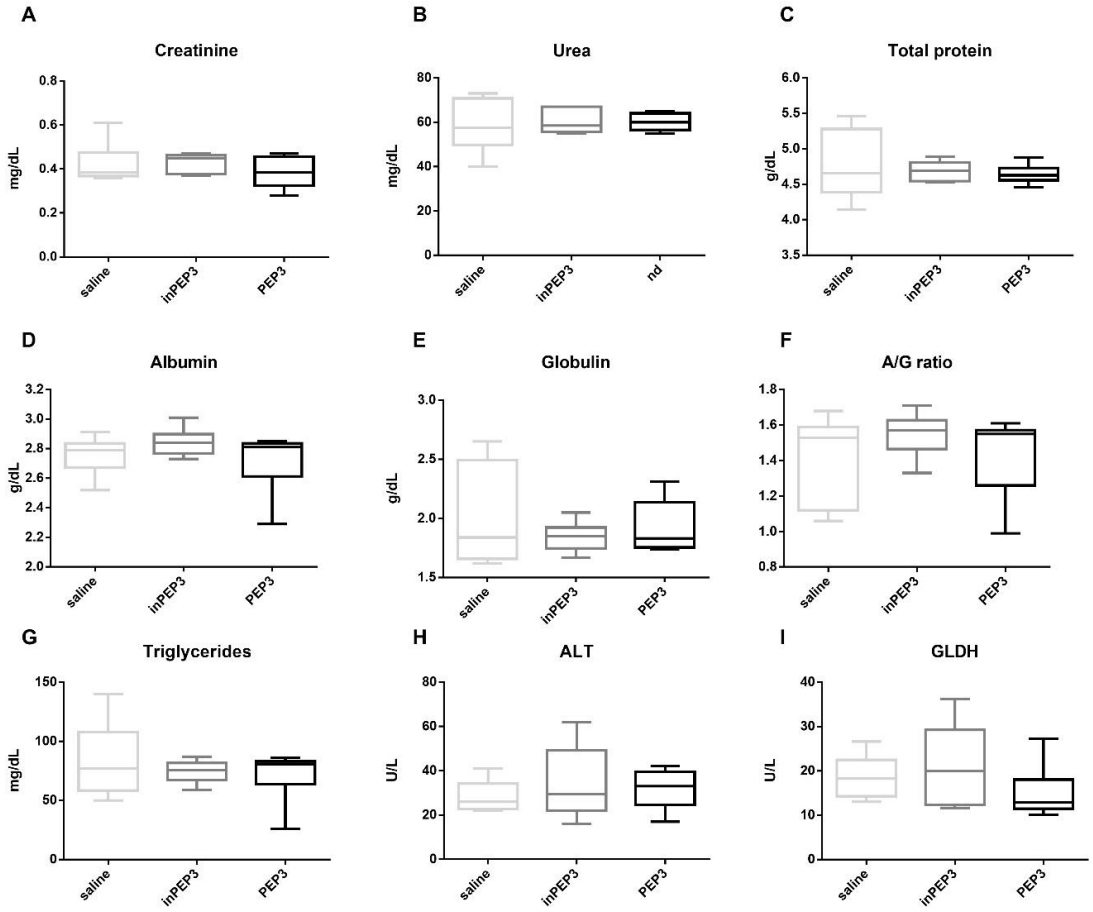

Figure 18 *Distribution of clinical chemistry data (table 2). The statistical analysis didn't show any significant changes among the different groups, suggesting that treatment doesn't induce dysmetabolism.*

Mean and median values of treated mice, as well as individual values of treated mice, did not visually differ from those of the two controls and often showed a particularly wide distribution, consistent with a moderately high individual variability. This visual impression is confirmed by the results of statistical analysis (figure 18) that did not reveal significant differences among groups for none of the analytes included in this study. This suggests that treatment did not functionally affect the main systems or organs and did not induce significant systemic dysmetabolism.

In conclusion, the combined analysis of hematological and biochemical results suggests that the administration of PEP3 induces a stimulation of specific immunity, and possibly an allergic/hyperergic

reaction. However, neither the active or inactive peptide seems to induce systemic or organ-specific damages or hematological changes regarding the erythrogram.

6.1.4 Liver and brain histology after PEP3 14-days treatment

Liver and one hemisphere of every animal were fixed in formalin, embedded in paraffin and processed for histology. From each paraffin block, 4 µm-thick serial sections were obtained and stained with Hematoxylin-Eosin or with Periodic Acid-Shiff (PAS) staining. In the liver of all examined subject, we detected a mild to moderate diffuse presence of poorly defined vacuoles in the cytoplasm of hepatocytes. Vacuoles did not displace the nucleus to the periphery of the cells and were PAS-positive (figure 19A-B). These features are characteristic of glycogen accumulation. The degree of glycogen accumulation was similar in all subject examined. Because rodents typically feed at night, the degree of glycogen accumulation within hepatocytes is typically highest in the early morning hours and wanes throughout the day; consequently, comparisons among animals should take the time of necropsy into consideration.

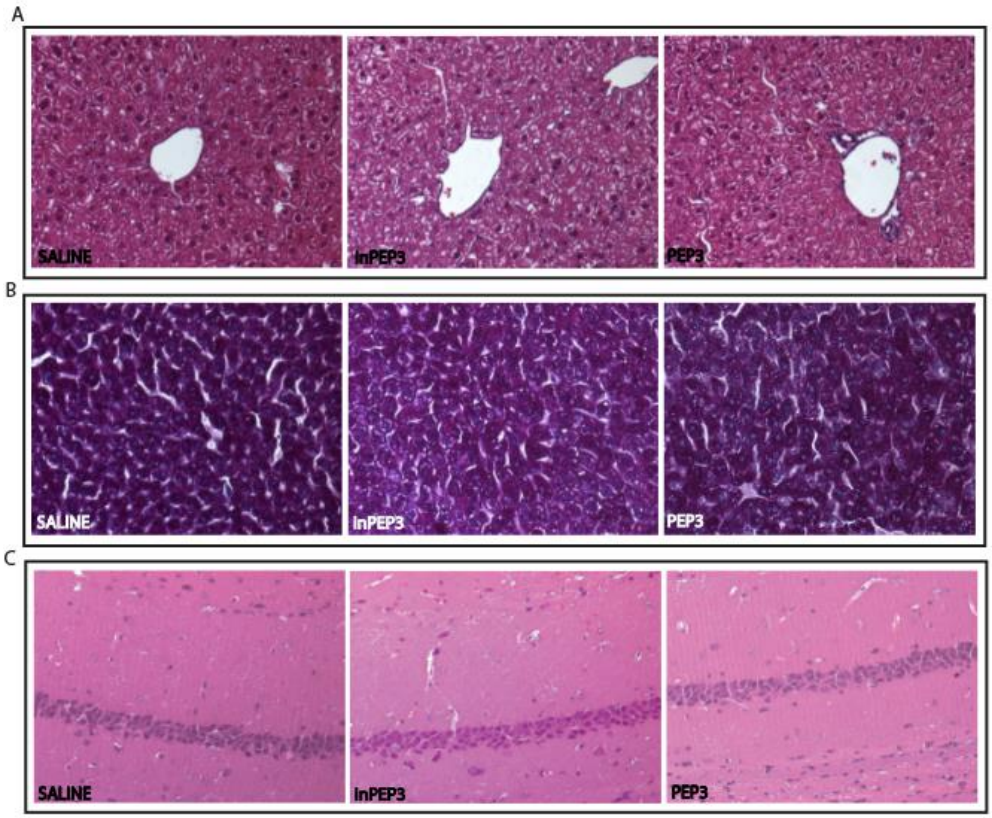

Figure 19 *For all treated mice, liver and brain were fixed in formalin and embedded in paraffin. The hematoxylin-eosin staining shows no structure alterations or lesion in CA1 region of hippocampus (C), and liver (A). In particular mild to moderate, diffuse presence of poorly defined vacuoles in the cytoplasm of hepatocytes was observed. Vacuoles did not displace the nucleus to the periphery of the cells and were PAS-positive (B).*

Lesions were absent in all mice, as shown by Hematoxylin-Eosin staining both in liver (figure 19A) and CA1 region of hippocampus (figure 19C). Moreover, the number of GFAP and Iba-1 positive cells were counted in 5 different fields of the hippocampus in order the evaluate neuroinflammation. The semi-quantitative analysis didn't revealed difference in the number of positive cells among each group, suggesting that CPPs do not induce activation of neuroinflammation (GFAP: inPEP3 31.67±1.116, PEP3 37.17±3.544; Iba-1: inPEP3 8.5±0.4282, PEP3 7.33±1.63). In conclusion the CPPs treatment does not induce evident morphological changes in all samples taken into consideration.

6.2 Effect of PEP3 14 days treatment on body weight and food intake

We measured average daily food intake and body weight. As shown in panel A (figure 20) the treatment with active or inactive peptides doesn't affect weight gain, moreover the food intake of treated animal is comparable with food intake of saline treated animal (figure 20B). These results are in line with data obtained with clinical chemistry analysis, and clearly demonstrate that the treatment with CPPs doesn't affect the metabolism.

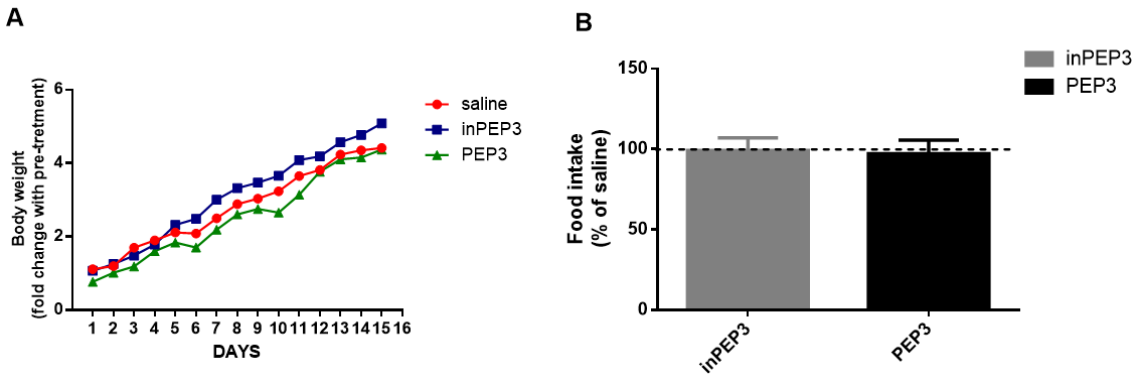

Figure 20 *Body weight and food intake during CPPs treatment. (A Body weight was measured every day with a precision scale and the average value of each group was calculated. As shown in the graph, the treatment with CPPs does not affect the increase of body weight. (B) For each animal cage, the food pellet was weighted every day and we calculated the ratio between the every day food intake and the average of body weight. As demonstrated by the histogram, animasl treated with active or inactive peptides don't show alterations in food intake (inPEP3 99.03±2.031, PEP3 97.09±2.178)*

6.3 PEP3 effect on ADAM10/AP2 interaction, ADAM10 synaptic availability and activity

To determine the efficacy of a 14-days treatment on our target, we evaluated the interaction between ADAM10 and AP2 complex, ADAM10 synaptic availability and activity.

Co-immunoprecipitation experiments performed in total brain homogenate (figure 21A) showed that, after 14 days of treatment, PEP3 is able to disrupt ADAM10/AP2 complex formation. In particular, the

quantitative analysis (figure 21B) shows that PEP3 significantly decreases the interaction with all subunits of AP2 (α-adaptin PEP3 -21.49% ± 5.205% p<0.05; β2-adaptin PEP3 -30.77% ± 7.34% p<0.05; μ2 PEP3 -23.26% ± 6.998% p<0.05).

We then assessed the levels of ADAM10 in the synaptic TIF fraction, and the immunoblot in figure 21C and the quantitative analysis in figure 21D, show a significant increase of ADAM10 synaptic levels in animals treated with PEP3 (PEP3 125.6% ± 14.10% p<0.05).

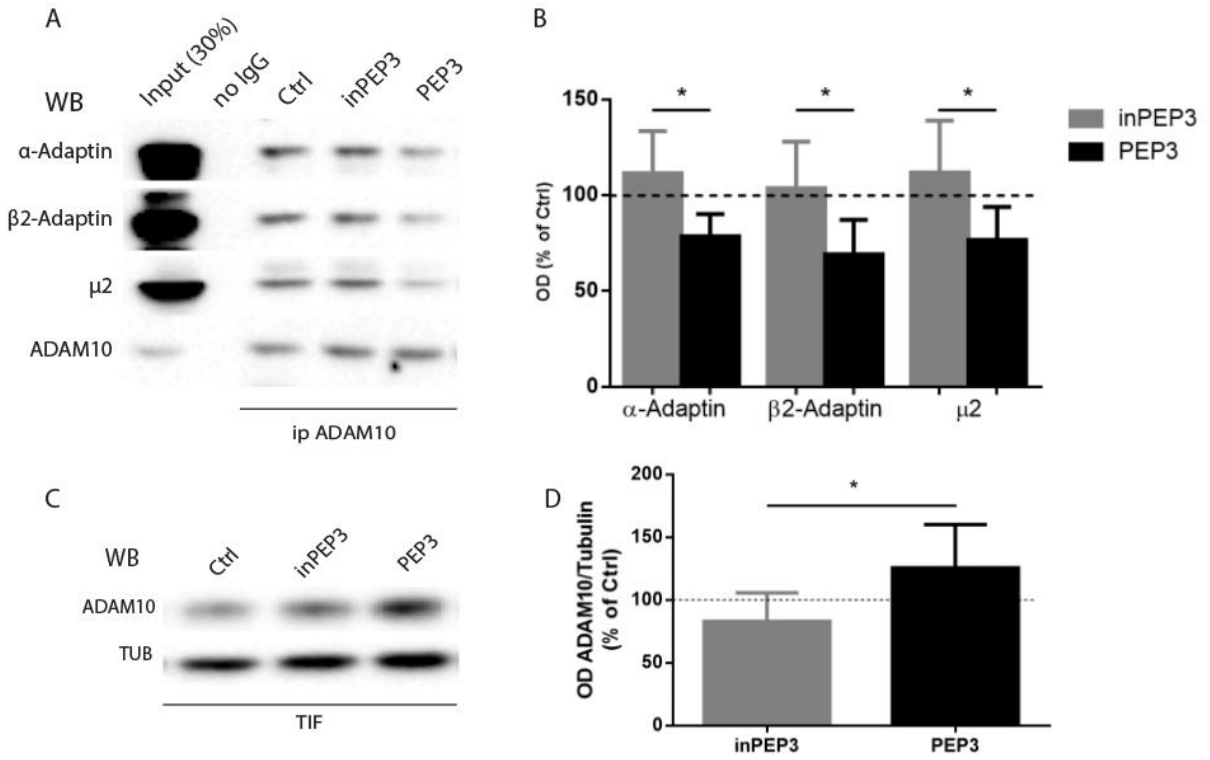

Figure 21 *ADAM10/AP2 interaction and ADAM10 synaptic availability after 14-days PEP3 treatment. (A) Brain homogenates were immunoprecipitated with anti-ADAM10 antibody and α-adaptin, β2-adaptin and μ2 co-precipitation were evaluated. (B) OD quantification of experiments in A. PEP3 significantly reduces ADAM10 interaction with all AP2 subunits (α-adaptin PEP3 -21.49%±5.203% inPEP3 +11.4%±9.857%; β-adaptin PEP3 -30.77%±7.34% inPEP3 +3.7%±10.81%; μ2 PEP3 -23.6%±6.998% inPEP3 +11.8%±12.18%; * p<0.05). (C) Representative immunoblot of ADAM10 WB analysis in TIF fraction. (D) Quantification of experiments in C, ADAM10/tubulin OD ratio revealed a significant increase in ADAM10 synaptic levels in animals treated with active peptide (inPEP3 82.973% ± 10.18%, PEP3 125.6% ± 14.1% * p<0.05).*

The results obtained with co-IP assay and WB analysis demonstrate that the PEP3 reduces the interaction between ADAM10 and AP2 complex inducing a concomitant increase in ADAM10 synaptic availability.

We then evaluated the effect of active peptide on ADAM10 activity. First of all, we measured the release of sAPPα using an ELISA kit. As shown in figure 22A, in total brain homogenate of PEP-3-treated mice, the sAPPα levels are significantly augmented, thus demonstrating an increase of enzyme activity (inPEP3 94.935±5.620, PEP3 121.5%±5.990% **<0.01).

Then, we evaluated the metabolism of two other substrates of ADAM10: N-CADHERIN and NOTCH-1 (Malinverno et al 2010, Reiss et al 2005, Hartmann et al 2002). We measured the levels of the fragments of these two proteins resulting from ADAM10 cleavage. As expected, the representative immunoblot in figure 22B and D and the quantitative analysis in figure 22C and E, clearly showed that the treatment with PEP3 significantly increased the levels of N-CADHERIN CTF (inPEP3 90.22%±11.73%, PEP3 124%±5.415%, *p<0.05) and NOTCH-1 fragment (inPEP3 101.7%±9.453%, PEP3 207.6%±23.58%, **p<0.01).

All together, these results demonstrate that the treatment with the active peptide interferes with ADAM10 local trafficking and significantly increases the activity of ADAM10 towards its substrates.

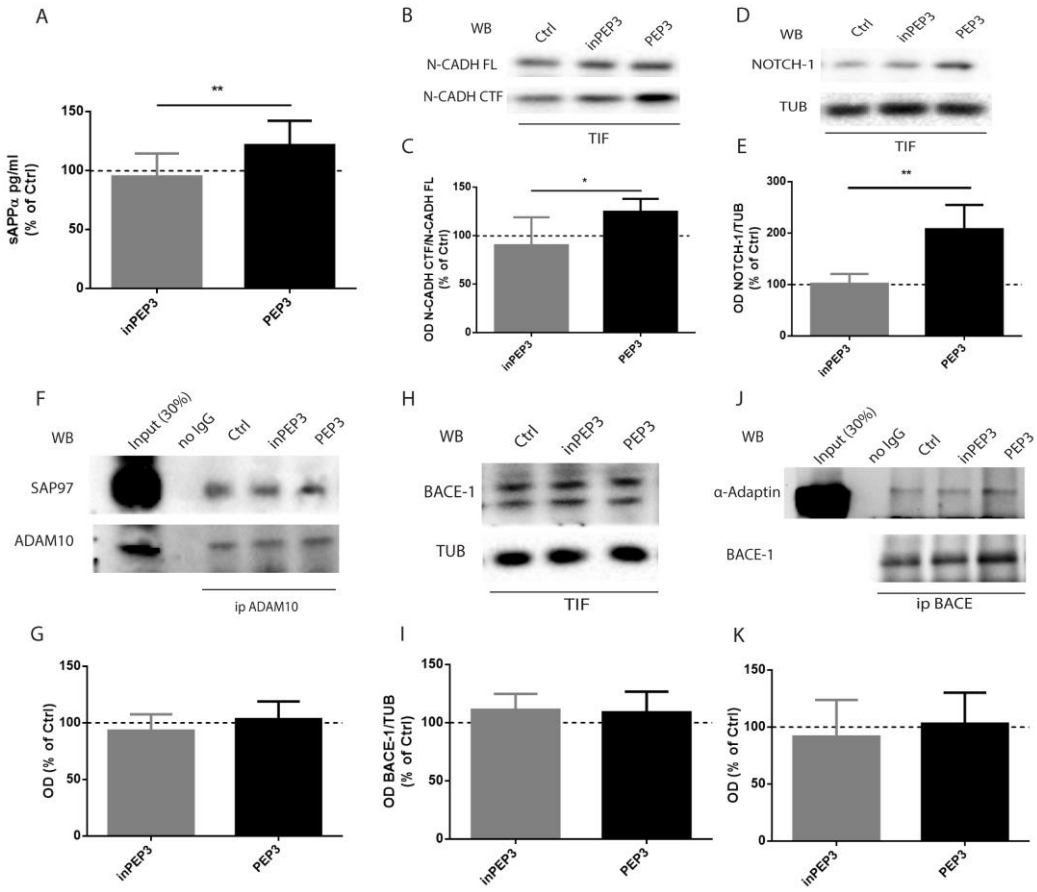

Figure 22 *PEP3 increases ADAM10 activity after subchronic treatment. (A) ELISA analysis on brain homogenates show an increase in sAPPα release after treatment with active peptide (inPEP3 94.935±5.620, PEP3 121.5%±5.990% **<0.01). (B) Representative immunoblot of N-Cadherin CTF analysis. An anti-N-Cadherin c-terminal antibody was used to reveal N-Cadherin full length (FL) protein and N-Cadherin CTF fragment. The quantification in C show a significant increase of N-Cadherin cleavage after treatment with PEP3 (inPEP3 90.22%±11.73%, PEP3 124%±5.415%, *p<0.05). Similarly, the immunoblot in D and the quantification in E show an increase of NOTCH-1 fragment in PEP3-treated mice (inPEP3 101.7%±9.453%, PEP3 207.6%±23.58%, **p<0.01). (F) co-IP assay performed on total brain homogenate using an anti-ADAM10 antibody. The immunoblot and the quantification in (G) show that the PEP3 treatment doesn't change the interaction between ADAM10 and SAP97 (inPEP3 -6.8%±5.863%, PEP3 +3.3%±6.403%). Similarly the immunoblot in (H) and (J) and the quantification in (I) and (K) show that PEP3 treatment doesn't alterate BACE localization (inPEP3 111%±5.621%, PEP3 108.9%±7.241%) or interaction with AP2 complex (inPEP3 -8.33%±13.13%, PEP3 +2.9%±11.16%).*

6.4 PEP3 specifically interfere with ADAM10/AP2 complex formation

To demonstrate the specificity of PEP3 on ADAM10/AP2 interaction, we evaluated the interaction of ADAM10 with other partners, i.e. SAP97, that has been shown to be involved in ADAM10 forward trafficking (Marcello et al 2007), The co-IP assay performed in brain total homogenate of treated animal shows that the active peptide does not alter the interaction between SAP97 and ADAM10 (figure 22F and G). Thus the increase in ADAM10 synaptic availability reported in figure 21C, can be ascribed specifically to the impairment of ADAM10 endocytosis rather than to an increase in its forward trafficking.

Since several proteins bind AP2, we performed co-IP assay between AP2 and other endocytic target proteins. First of all, we assessed the binding of AP2 to the GABA A β3 subunit, whose endocytic sequence is similar to the AP2 binding motif in ADAM10 cytoplasmic tail. Total brain homogenates were immunoprecipitated using an anti-GABA A β3 subunit antibody and the presence of α-adaptin was evaluated. As expected, the immunoblot showed in figure 23A, demonstrates that the active peptide doesn't alter the interaction between α-adaptin and GABA A β3 subunit (figure 23A).

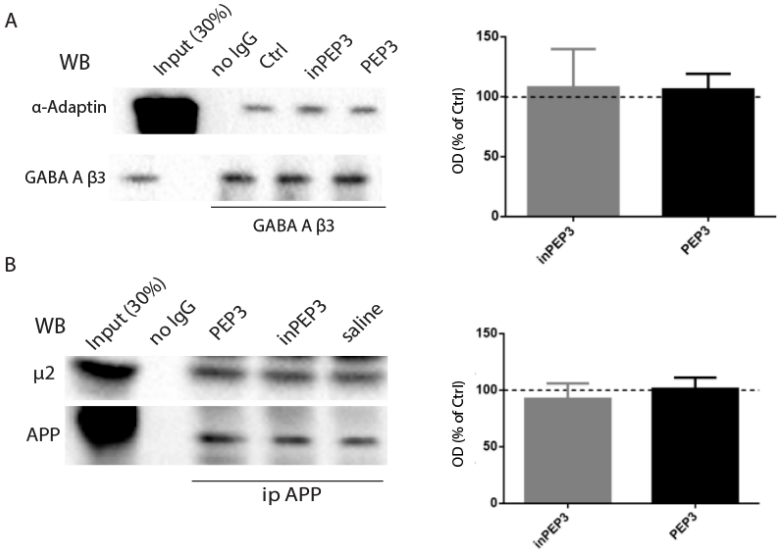

Figure 23 *PEP3 specifically interferes with ADAM10/AP2 complex. (A) brain homogenates were immunoprecipitated with anti-GABA A β3 antibody and the presence of α-adaptin was evaluated. As shown in the histogram (right panel) the CPPs treatment doesn't interfere with GABA A β3 complex formation (inPEP3 +7.8%±13.08%, PEP3 +6%±5.361%). Similarly, co-IP assay using anti-APP antibody (B) shows that PEP3 doesn't alter the interaction between APP and AP2 complex.*

Then, we analysed two players of the amyloid cascade that are able to bind AP2: APP and BACE-1, the enzyme involved in the APP amyloidogenic pathway (Tian et al 2013, Chia et al 2013).

The treatment with PEP3 does not interfere with the interaction between between APP and μ2 (figure 23B) and with the binding of BACE1 with α-adaptin (figure 22J-K). Moreover, we analyzed the

localization of BACE-1. The immunoblot of reported in figure 22H and the related quantification in figure 22I show that the active peptide doesn't interfere with synaptic localization of BACE-1.
In conclusion, these results demonstrate the specificity of PEP3 and strengthen the idea that the increase of ADAM10 activity towards APP is specifically due to the alteration of ADAM10 endocytosis rather than to a decrease of BACE-1 protein localization.

6.5 EFFECT OF PEP3 ON GLUTAMATE RECEPTORS LOCALIZATION AND ON SPINE MORPHOLOGY

After having demonstrated that PEP3 alters ADAM10 synaptic localization and increase its activity, we decided to evaluate the synaptic composition and the spine morphology. Immunoblots of GluN1, GluN2B, GluN2A and GluA1 were performed on all samples. As shown in the representative blot in figure 24A and in the quantitative analysis in figure 24B the treatment with active peptide doesn't affect the glutamate receptor composition of the synapse.

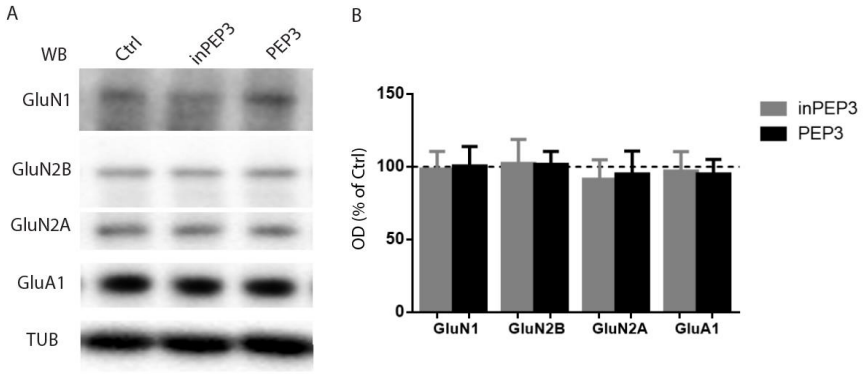

Figure 24 *PEP3 doesn't alter receptor composition of the synapse. (A) WB analysis using anti-GluN1, anti-GluN2B, anti-GluN2A and anti-GluA1 antibody were performed for each samples. The quantification analysis in (B) shows that the treatment with active peptides doesn't alter the synaptic receptor composition*

Since ADAM10 activity is relevant for spine remodelling (Malinverno et al 2010), we focused our attention on dendritic spine morphology. Since the first description by Ramon y Cajal at the end of the 19th century, dendritic spines have been proposed as important sites of neuronal contacts and it has been suggested that changes in the activity of neurons directly affect spine morphology. Spines can be divided into three categories based on their morphology: thin, stubby (without a well-defined neck) and mushroom (spines with a large bulbous head) (Bourne & Harris 2008). To evaluate the effect of PEP3 on spine morphology, two animals for each group were perfused after 14-days treatment and

brain was dissected, post-fixed in PFA and cut with vibrotome. To stain dendritic spines (see method), we used the lipophilic-tracer DilDye on brain coronal section. Confocal images were acquired and the number, the length and the head width of hippocampal dendritic spines were measured.

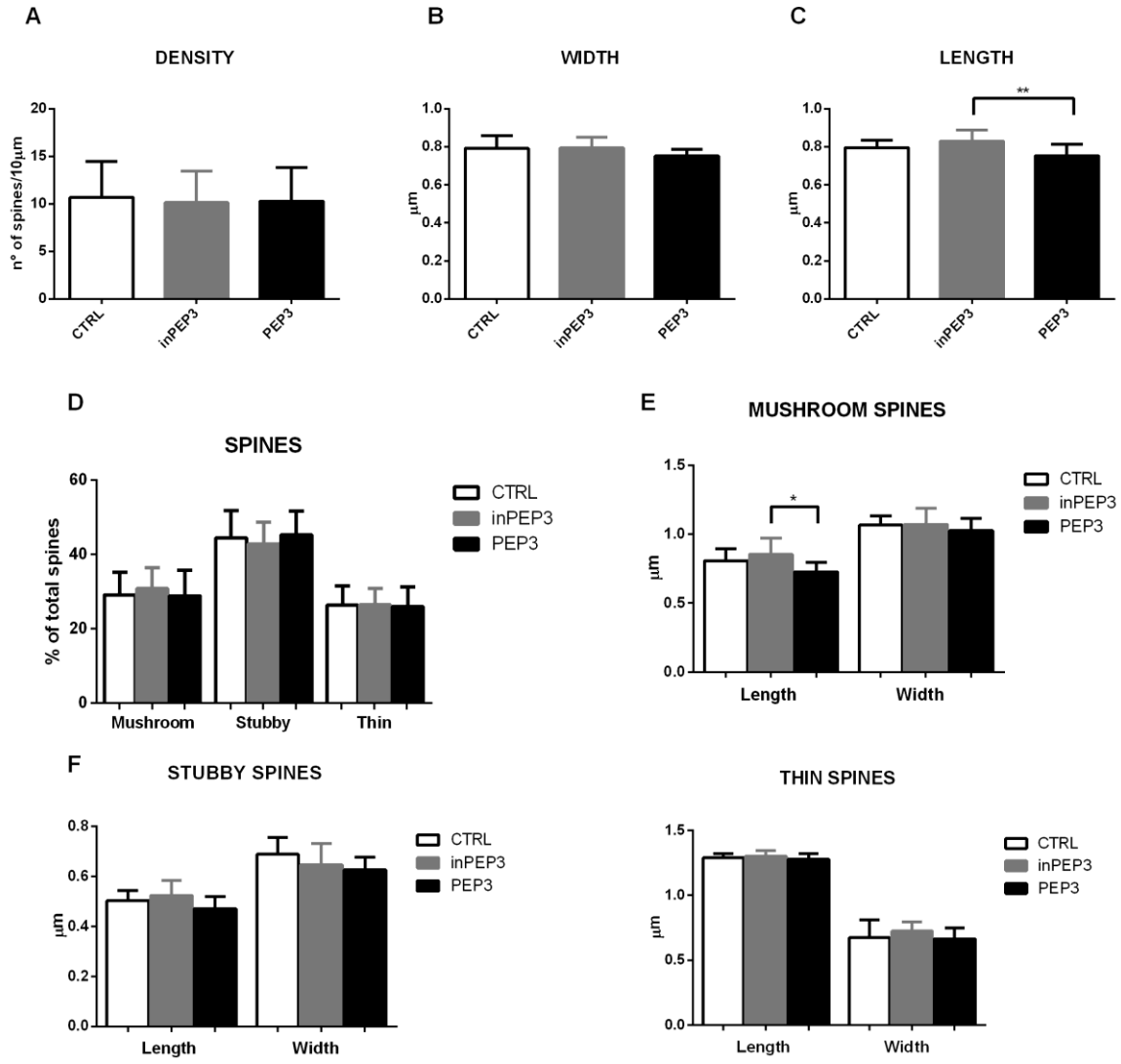

Figure 25 *Spines density and morphology analysis after 14-days treatment. For each groups the number of hippocampal dendritic spines was counted. The graph in A shows that PEP3 treatment doesn't change the density of dendritic spines (saline 10.68±1.192, inPEP3 10.15±1.049, PEP3 10.30±1.113). As reported in the graph B there is no change in spines width after PEP3 treatment (saline 0.7929±0.012, inPEP3 0.7952±0.01802, PEP3 0.7521±0.011), while the length decreases in PEP3-treated mice (C) (saline 0.7965±0.012, inPEP3 0.8341±0.018, PEP3 0.7535±0.01917 **p<0.01). There is no alteration in the percentage of mushroom, stubby and thin spines in each group (D) (mushroom: saline 29.14±1.907%, inPEP3 30.81±1.776%, PEP3 28.83±2.18%; stubby: saline 44.49±2.28%, inPEP3 42.78±1.86%, PEP3 45.25±2.025; thin: saline 26.37±1.63%, inPEP3 26.41±1.42%, PEP3 25.92±1.68%). In each group no changes in length and width were detected (E-F-G), with the exception of the decrease in mushroom spines length in PEP3-treated mice (saline 0.8±0.027, inPEP3 0.854±0.037, PEP3 0.7275±0.0215 *p<0.05).*

The quantitative analysis in figure 25 shows that the PEP3 treatment doesn't induce significant changes in spines density, spines head width and in the distribution of spines in the different categories. Only the total length, and in particular the length of mushroom spines, is significantly decreased after treatment with active PEP3. However, even if we assessed a decrease of mushroom spines length, we didn't measure significant changes in mushroom spines width. Moreover, as reported in figure 25, the synaptic receptor composition doesn't change after treatment with active peptide, suggesting that PEP3 treatment doesn't significantly affect synapse function.

To strenghten of these results, we performed a behavioural test to evaluate the cognitive function. Animals were subjected at two days of training followed by novel object recognition test (see material and methods). The graph in figure 26 shows that there are no significant differences in the time spent exploring the novel object when we compare animals treated with PEP3 to mice administered with inPEP3 or saline.

Thus, we can conclude that CPPs treatment doesn't induce any functional difference at the synaptic level and does not alter the cognitive function of the animals.

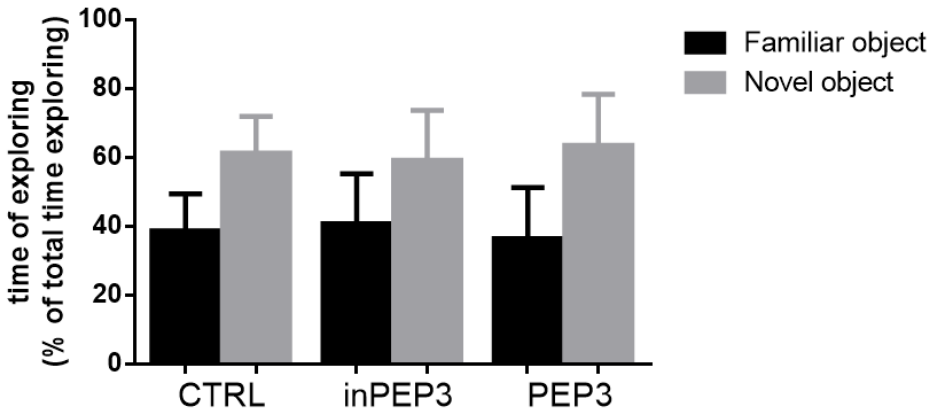

Figure 26 *Novel object recognition was performed on animal treated with either active or inactive PEP3. The graph shows that the treatment with PEP3 or inPEP3 does not change the novel object exploring time compared to saline treated animals (saline 61.26%±3.569%, inPEP3 59.24%±4.582%, PEP3 63.52%±4.691%).*

LONG DISTANCE SPINE TO NUCLEUS SIGNALLING: RNF10 PATHWAY AS A NOVEL Aβ TARGET

1. RING FINGER PROTEIN 10 AS A NEW BINDING PARTNER OF GluN2A

Several pathways have been shown to be affected by Aβ soluble oligomers and to be implicated in Aβ-induced impairment of synaptic transmission (Mucke et al 2000). However, how Aβ oligomers can initially affect synaptic structure and function remains to be determined.

Neurons communicate at synaptic contacts by signalling events, yet their long-term responses to such stimuli require changes in gene expression at the nucleus. Indeed, synapse-to-nucleus communication plays a key role in the regulation of the long-term structural modifications (Karpova et al 2012) and may be a mechanism required for the integration of multiple signalling pathways (Jordan & Kreutz 2009). The prevailing point of view in the literature is that calcium signals are the major route for communication of synaptic activity to the nucleus (Bading 2013). Calcium signals can act locally near the site of calcium entry into the cytoplasm but are also often transmitted over long distances and can reach the cell nucleus (Hagenston & Bading 2011). In addition to calcium, recent studies demonstrated that macromolecules and synaptonuclear protein messengers play key roles in connecting synapses and nucleus thus enabling bidirectional transfer of information (Karpova et al 2012). Synapses contain several nuclear localization signals (NLS)-containing cargo proteins and different components of the nuclear import machinery, like importin-α and importin-β, which have been shown to translocate to the nucleus in an activity-dependent manner (Thompson et al 2004). Notably the activation of NMDAR can regulate gene transcription (Dieterich et al 2008), thus affecting global protein synthesis and, thereby memory formation. Such effect of NMDAR activation requires the long-distance trafficking of synapto-nuclear proteins.

In this framework, the results obtained carrying out a yeast two-hybrid screening using the C-terminal domain of GluN2A (aa 839-1461, without the aa 1462-1464 PDZ-binding sequence) as bait, revealed the Ring Finger protein 10 (RNF10) as a new binding partner of GluN2A (Dinamarca et al., under revision). RNF10 is a protein implicated in the transcriptional regulation of myelin formation in Schwann cells (Hoshikawa et al 2008). However, very little is known about the neuronal function of this protein (Hoshikawa et al 2008, Lin et al 2005, Malik et al 2013, Seki et al 2000). RNF10 protein contains a binding sequence for the transcription factor Mesenchyme Homeobox 2 (Meox2; Meox2 Binding Domain, MBD, aa 101-185; (Lin et al 2005)), a Ringer Finger Domain (RFD, aa 225-270) and two putative NLS (NLS1, aa 591-599 and NLS2, aa 784-791). The presence of two different NLS motifs (figure

27A) and its interaction with GluN2A and Meox2 (Lin et al 2005) suggest that RNF10 could be a novel synapto-nuclear protein messenger.

Analysis of endogenous RNF10 in *DIV14* primary hippocampal neurons showed clustered RNF10 immunolabeling along dendrites and most puncta co-localized with GluN2A (figure 23B, left panels), PSD-95 (figure 27B, right panels). Moreover, PSDs were purified from the rat hippocampus to confirm the subcellular distribution of RNF10 by a biochemical approach. Subcellular fractionation demonstrated that RNF10 is associated with particulate fractions and that it is prominently present in the PSD fractions (figure 27C). To substantiate the yeast two-hybrid data and to confirm the interaction between RNF10 and GluN2A, co-IP studies from hippocampal protein extracts were performed. The immunoblot in figure 27D indicated a specific interaction of RNF10 with GluN2A but not with GluN2B subunit of the NMDARs. No signal for GluN2A or GluN2B was obtained by using anti-synaptophysin as an irrelevant antibody or in the absence of the antibody in the co-i.p. assay (figure 27D).

2. NEURONAL ACTIVITY AFFECTS RNF10 TRANSLOCATION TO THE NUCLEUS REGULATES THE EXPRESSION OF SPECIFIC TARGET GENES

The presence of two different NLS motifs (figure 27A) and its interaction with GluN2A and Meox2 (Lin et al 2005) suggest that RNF10 could be a novel synapto-nuclear protein messenger. To validate this hypothesis, we assessed whether the modulation of neuronal activity affects the subcellular localization of RNF10 and its association with interacting proteins. We first enhanced synaptic excitatory activity with the GABA-A receptor antagonist Bicuculline (50 μM) in the presence of the K^+ channel blocker 4-AP (2.5 mM; (Hardingham et al 2002)). Enhanced excitatory activity significantly increases RNF10 nuclear staining as shown in figure 23E. This effect is significantly reduced by the co-incubation with the NMDAR blocker MK801. The import of proteins from the cytosol into the nucleus through the nuclear pore complex depends on the binding of importins to a specific NLS (Jordan & Kreutz 2009, Karpova et al 2012, Thompson et al 2004). According to this scheme, importins function as adapter molecules by binding NLS-bearing proteins. Components of the classical nuclear import machinery are present at synapses in association with NMDARs and importins translocate to the nucleus in response to NMDAR stimulation (Ch'ng et al 2012, Jeffrey et al 2009, Marfori et al 2011). Based on these results, we next evaluated a possible RNF10 interaction with importins in hippocampal neurons. Immunoprecipitation experiments performed with hippocampal neuronal extracts revealed that RNF10 interacts with importin α1 in neuronal cells and that Bicuccullin treatment significantly increased RNF10/importin α1 association (figure 27F). Interestingly, also the RNF10 interaction with the transcription factor Meox2 was significantly increased by Bicucullin treatment. On the contrary,

the treatment significantly decreased RNF10/GluN2A interaction compared to control neurons (figure 27G). We next questioned whether RNF10 translocation from dendritic spines to the nucleus produced a modulation of the protein level of Meox2/RNF10 target genes. We analyzed the expression of p21WAF1/cip1, a known Meox2 target gene (Lin et al 2005, Malik et al 2013). Bicuculline treatment increased p21WAF1/cip1 levels as evaluated by immunofluorescence and the up-regulation was significantly attenuated by co-treatment with the NMDAR blocker MK801 (figure 28).

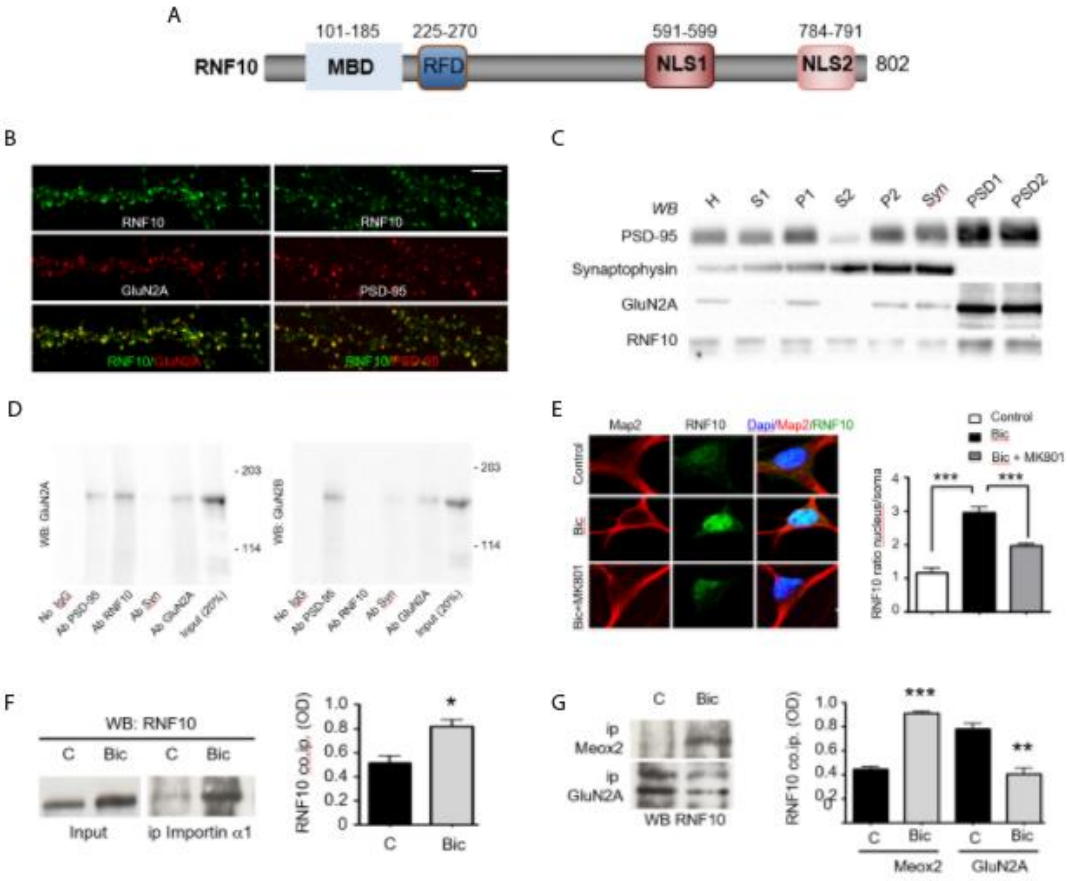

Figure 27 *RNF10 is a new GluN2A interacting binding protein. (A) RNF10 protein contains a binding sequence for the transcription factor Meox2 (Meox2 Binding Domain, MBD, aa 101-185), a Ringer Finger Domain (RFD, aa 225-270) and two putative nuclear localization sequences (NLS1, aa 591-599 and NLS2, aa 784-791). (B) High magnification confocal images of neuronal dendrites (DIV14) immunolabeled for RNF10 (green) and GluN2A (red; left panels) or PSD-95 (red; right panels). (C) RNF10 and markers of the presynaptic (synaptophysin) and postsynaptic compartment (PSD-95, GluN2A) were analyzed by WB in various subcellular compartments. (H: Homogenate fraction; S1: supernatant 1; P1: nuclear fraction; S2: cytosolic fraction 2; P2: crude membrane fraction 2; Syn: synaptosomal fraction; PSD1: Triton Insoluble postsynaptic fraction; PSD2: postsynaptic density fraction). (D) Co-immunoprecipitation (co-i.p.) assay performed in hippocampal extracts by using antibodies against PSD-95, RNF10, synaptophysin (Syn) and GluN2A. WB analysis shows the levels of GluN2A (left panel) and GluN2B (right panel) in the co-immunoprecipitated material. No IgG line: control lane in absence of antibodies during the co-i.p. assay. (E) Confocal images of hippocampal neurons (DIV14) treated with Bic in presence or absence of the NMDAR blocker MK801 and immunolabeled for Map2 (red), RNF10 (green) and stained with Dapi (blue). The histogram shows the quantification of RNF10 signal (ratio nucleus/soma) (***P<0.001 Bic vs control and Bic+MK801 vs Bic). (F)Co-i.p. assay performed by using an importin α1 antibody from cell homogenates of control neurons or treated with Bic. WB analysis was performed with RNF10 antibody. The histogram shows the quantification of RNF10/importin α1 interaction (*P<0.05). (G) Representative co-i.p. assay from cell homogenates of control neurons or treated with Bic. WB analysis was performed with RNF10 antibody. The histogram shows the quantification of RNF10 interaction with GluN2A and Meox2 (***P<0.001, Meox2, Bic vs control; **P<0.01, GluN2A, Bic vs control).*

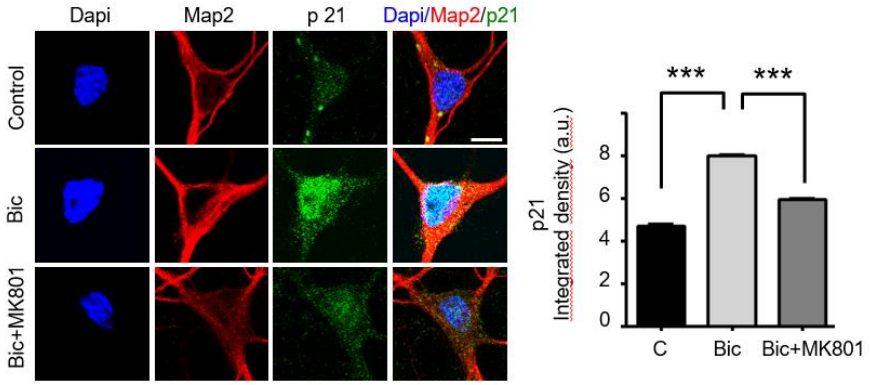

Figure 28. *RNF10 nuclear trafficking regulates the expression level of specific target genes. Hippocampal neurons (DIV14) were treated with Bic in the presence or absence of MK801, immunolabeled for Map2 (red), p21$^{WAF1/cip1}$ (green) and stained with Dapi (blue). Histogram shows the quantification of p21$^{WAF1/cip1}$ signal in the nucleus following treatment with Bic (***P<0.001 Bic vs control and Bic+MK801 vs Bic).*

3. RNF10 SILENCING INDUCES MORPHOLOGICAL MODIFICATIONS OF THE GLUTAMATERGIC SYNAPSE

To understand the role of RNF10 in neurons, we silenced RNF10 expression by using a short hairpin (sh) RNF10 knock-down or scrambled sequence (as a control) in primary hippocampal cultures. Confocal imaging of hippocampal neurons transfected with shRNF10 or scramble plasmids demonstrated a significant effect of RNF10 knock down on dendritic spine density (figure 29A-D). RNF10 silencing produced a significant reduction of dendritic spine density that is fully rescued by co-expressing a wild-type human variant of RNF10 resistant to shRNA (figure 29B). On the contrary, the length and the width of spines remain unaffected (figure 29C-D)

To learn more about the effect of RNF10 knock-down on gene expression we performed a microarray analysis from organotypic hippocampal slices virally infected with pLKO-shRNF10 lentivirus in order to identify RNF10 target genes. Interestingly, heat map (figure 29F) of differentially expressed genes, and real-time PCR validation (figure 29E) showed that RNF10 silencing modulated the expression of both genes involved in AD pathogenesis (e.g. TREM2, MMP-9, TIMP1, a Fe65 binding protein) and key regulators of spine morphology (e.g. OphN1, αPIX/Arhgef6 and ArhGap4 (Michaluk et al 2011, Ramakers et al 2012, Vogt et al 2007), indicating that RNF10 can be implicated in AD-synaptic dysfunction.

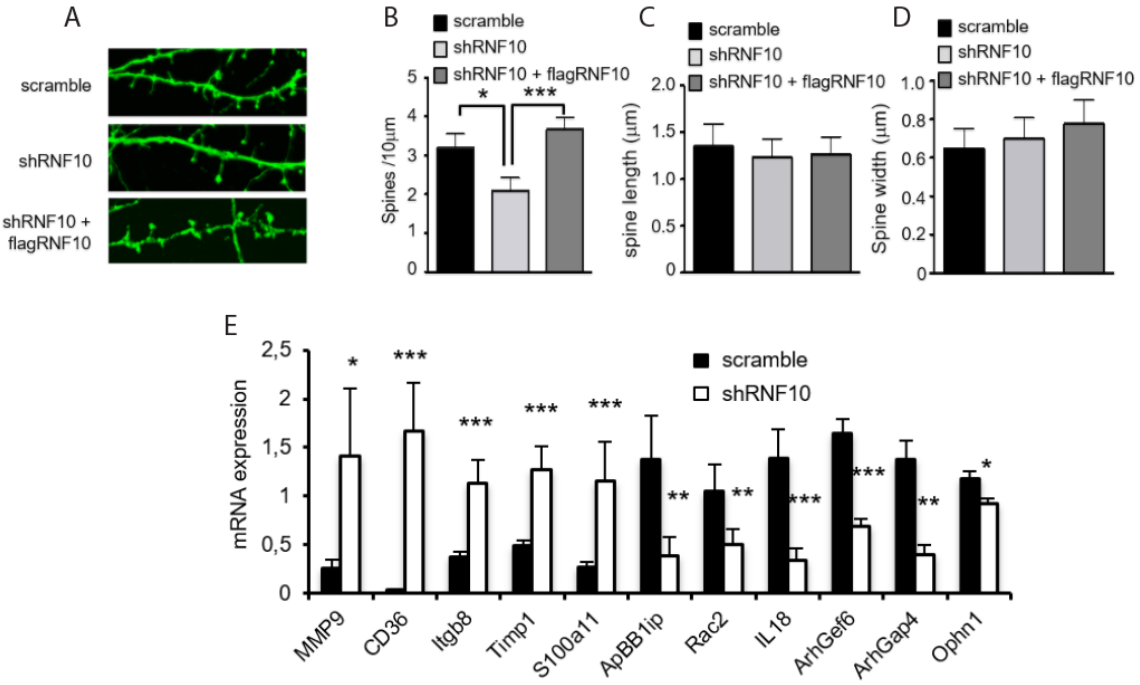

Figure 29. *RNF10 silencing induces morphological modifications of the glutamatergic synapse. (A) Confocal images of primary hippocampal neurons (DIV14) transfected at DIV7 with pGIPZ-scramble, shRNF10 and shRNF10 plus flagRNF10 and immunolabeled for GFP (green). (B-D) Histograms show the quantification of dendritic spine density (B) (*P<0.05, scramble vs shRNF10; ***P<0.001, shRNF10 vs shRNF10 + flagRNF10), dendritic spine length (C), dendritic spine head width (D). (E) mRNA expression levels of genes associated with synaptic transmission or dendritic spine morphology by real-time PCR from DIV14 organotypic hippocampal slices lentivirally infected (DIV4) with pGIPZ-scramble sequence (scramble) as control or with pLKO-shRNF10 (shRNF10) (***P<0.001; **P<0.01; *P<0.05). (F) Heat map of differentially expressed genes. Expression data are reported as log2 and blue color indicates high expression values and red color low expression value. Sc represents the different scramble control while Sh represents the shRNA against RNF10.*

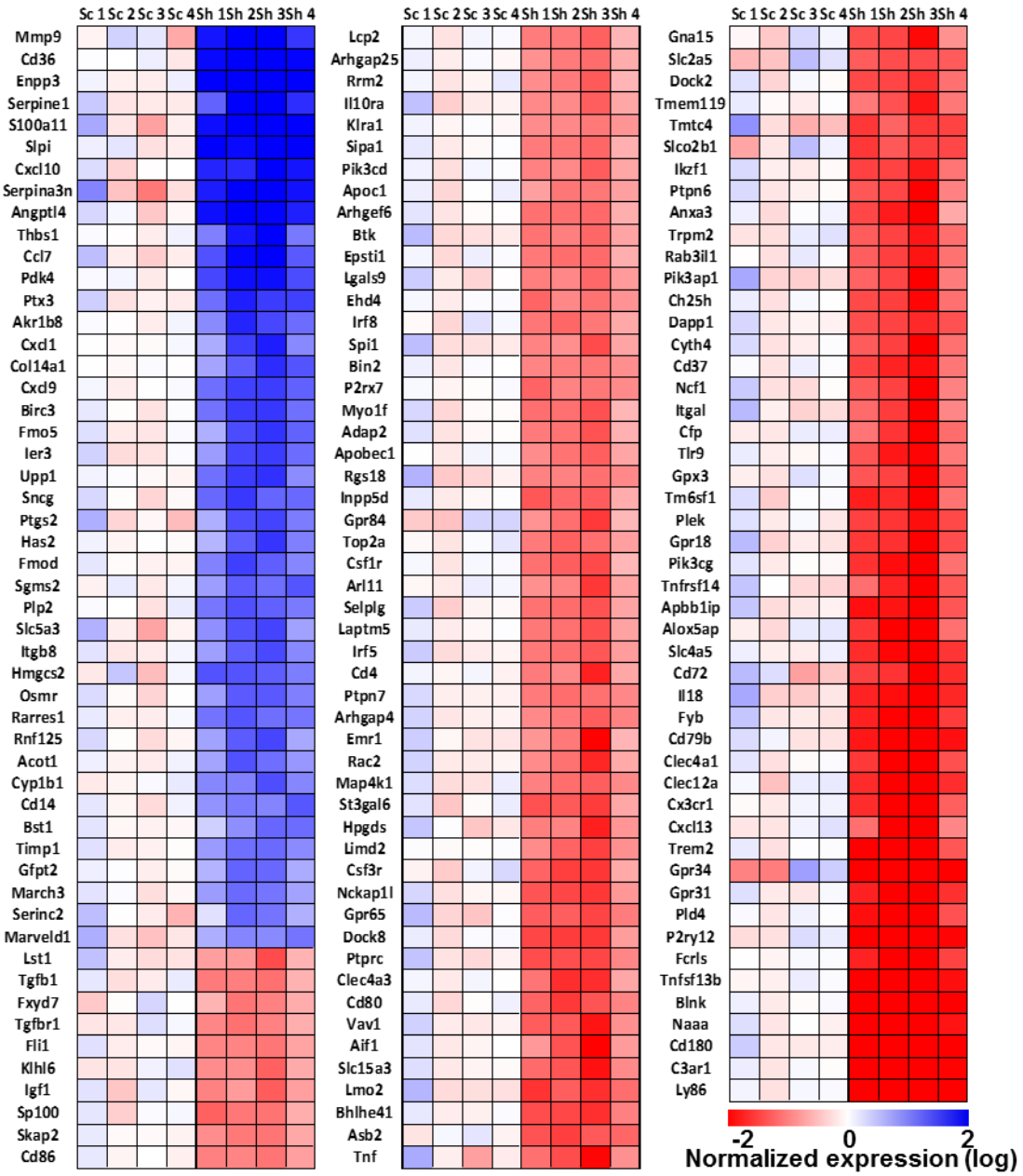

Figure 29 F *Heat map of differentially expressed genes. Expression data are reported as log2 and blue color indicates high expression values and red color low expression value. Sc represents the different scramble control while Sh represents the shRNA against RNF10.*

4. Aβ MODULATES RNF10 NUCLEAR LOCALIZATION

To understand whether Aβ can directly trigger RNF10-mediated signalling pathway, we decided to perform different *in vitro* assay exposing primary hippocampal neurons with Aβ oligomers.

To set up a reliable *in vitro* model, we used two different sources of Aβ oligomers: (i) Aβ oligomers obtained from synthetic Aβ42 and prepared according to Lambert et al., 2001 (see figure 1) and (ii) Aβ oligomers collected and prepared from the conditioned medium of the APP V717F-expressing CHO cells (called 7PA2 cells), according to Walsh et al., 2002, named $A\beta^{7PA2}$. After the preparation, synthetic Aβ42 oligomers (see figure 1) and $A\beta^{7PA2}$ (figure 30A) were loaded onto a non-denaturing gel and analyzed by Western Blot (WB) with 6E10 in antibody to verify that they consist exclusively of small oligomers and monomers. As shown in figure 1 and figure 30A, the immunoblot shows the presence of small oligomers and monomers (from 4 kDa up to 16 kDa) in both preparations.

We carried out WB analysis and immunofluorescence assays to evaluate the nuclear localization of RNF10 after exposing *DIV14* primary hippocampal neurons to Aβ42 or scrAβ 500 nM for 30min or 2h. The immunostaining (figure 30A) shows that Aβ42 induces RNF10 nuclear translocation after both 30min or 2h of treatment (figure 30B). These results were confirmed by WB analysis performed on nuclear fraction purified from *DIV14* primary hippocampal neurons treated with Aβ42 or scrAβ (500 nM, 30 min or 2h). As expected, the immunoblot in figure 30D and the related quantitative analysis show that Aβ42 treatment increases the nuclear localization of RNF10 after both 30min and 2h of treatment. Interestingly, RNF10 nuclear translocation seems to be concentration dependent, in fact the treatment with a lower concentration of Aβ42 (200pM) doesn't affect RNF10 localization, as shown in figure 30E.

To strengthen the results obtained with synthetic Aβ42, we decided to treat *DIV14* primary hippocampal neurons with $A\beta^{7PA2}$. Immunofluorescence performed on neurons treated with $A\beta^{7PA2}$ shows an increase of RNF10 nuclear localization compared with untreated cells (figure 32F).

Since in hippocampal cultures are present both neuronal and glial cells, and considering that RNF10 is express in both cell types, we evaluated the RNF10 nuclear localization in glial cells after Aβ42 exposure. Immunostaining assays reveal that in astrocytes Aβ42 treatment doesn't change RNF10 nuclear localization compared with scrAβor untreated cells (figure 30G). These results confirm that the RNF10 pathway is specifically modulated by Aβ in neuronal cells.

As demonstrated in figure 28, RNF10 translocation induces the transcription of its target gene p21waf1/cip1. Therefore, we analyzed the expression of this protein after Aβ42 treatment. The WB analysis performed on cell lysate of Aβ-treated *DIV14* primary hippocampal neurons shows that Aβ42 induces the expression of p21waf1/cip1 only 2h after the treatment (figure 30H).

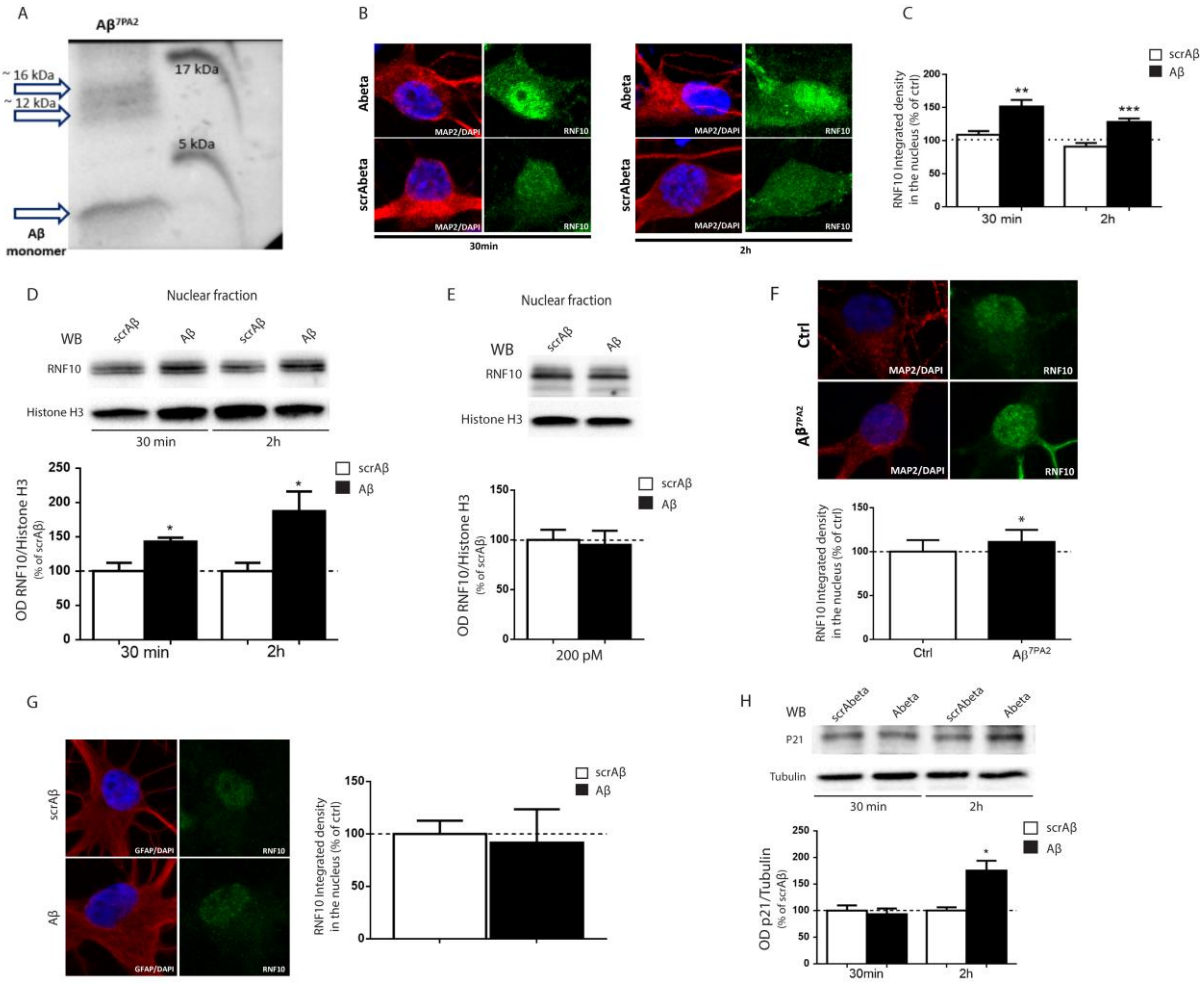

Figure 30 *Aβ treatment affects RNF10 localization. (A) Aβ7PA2 preparation was resolved onto a non-denaturing gel and immunoblotted with 6E10 antibody. The antibody recognized Aβ oligomers up to 16kDa. (B) Confocal imaging of DIV14 neurons treated for 30min or 2h with Aβ42 (or scrAβ), immunolabeled with Map2 (red) and RNF10 (green). (C) Quantitative analysis of RNF10 integrated density in the nucleus shows that Aβ42 fosters RNF10 nuclear localization after both 30 min (Aβ +51.9%±10.02% **p<0.01) and 2h of treatment (Aβ +28.5% ±5.364% ***p<0.001). (D) Immunoblot of nuclear fraction obtained from Aβ42 treated neurons. The histogram shows an increase of RNF10 nuclear localization after both 30min (scrAβ 100±11.88%, Aβ 142.8±5.873% *p<0.05) and 2h from treatment (scrAβ 100±11.90%, Aβ 187.01±28.95% *p<0.05). (E) Immunoblot and quantification of RNF10 nuclear localization after treatment with 200pM Aβ42, the treatment with lower concentration of Aβ does not affect RNF10 nuclear translocation. (F) Confocal imaging of DIV14 neurons treated with Aβ7PA2, immunolabeled with Map2 (red) and RNF10 (green). Quantitative analysis shows that Aβ7PA2 treatment leads to a slight but significant increase in RNF10 nuclear localization compared to untreated cells (Aβ7PA2 +11%±3.750% *p<0.05). (G) Confocal images of hippocampal cultures immunolabeled with a glial marker (GFAP, red) and RNF10 (red) after 2h of Aβ42 treatment. Aβ42 does not affect RNF10 nuclear localization in glial cells. (H) Immunoblot of cell lysates obtained from DIV14 hippocampal neurons treated with Aβ42. The histogram shows an increase of p21waf1/cip1 expression after 2h of treatment (scrAβ 100±6.130%, Aβ 175.2±18.73 *p<0.05).*

To further confirm that RNF10 accumulates in the nucleus because of long-distance protein transport we performed time-lapse confocal imaging of RNF10 tagged with the photoconvertible tdEOS (RNF10-tdEos). We photoconverted RNF10-tdEOS in distal dendrites from green-to-red emission using 405 nm irradiation immediately after Aβ42 or scrAβ treatment and tracked the red fluorescence signal over 45 minutes. Aβ treatment induces a significant increase in RNF10-tdEOS photoconverted fluorescence intensity in the nucleus compared with scrAβ treated or untreated neurons. Notably this increase is accompanied by a decline of emission in distal dendrites (figure 31).

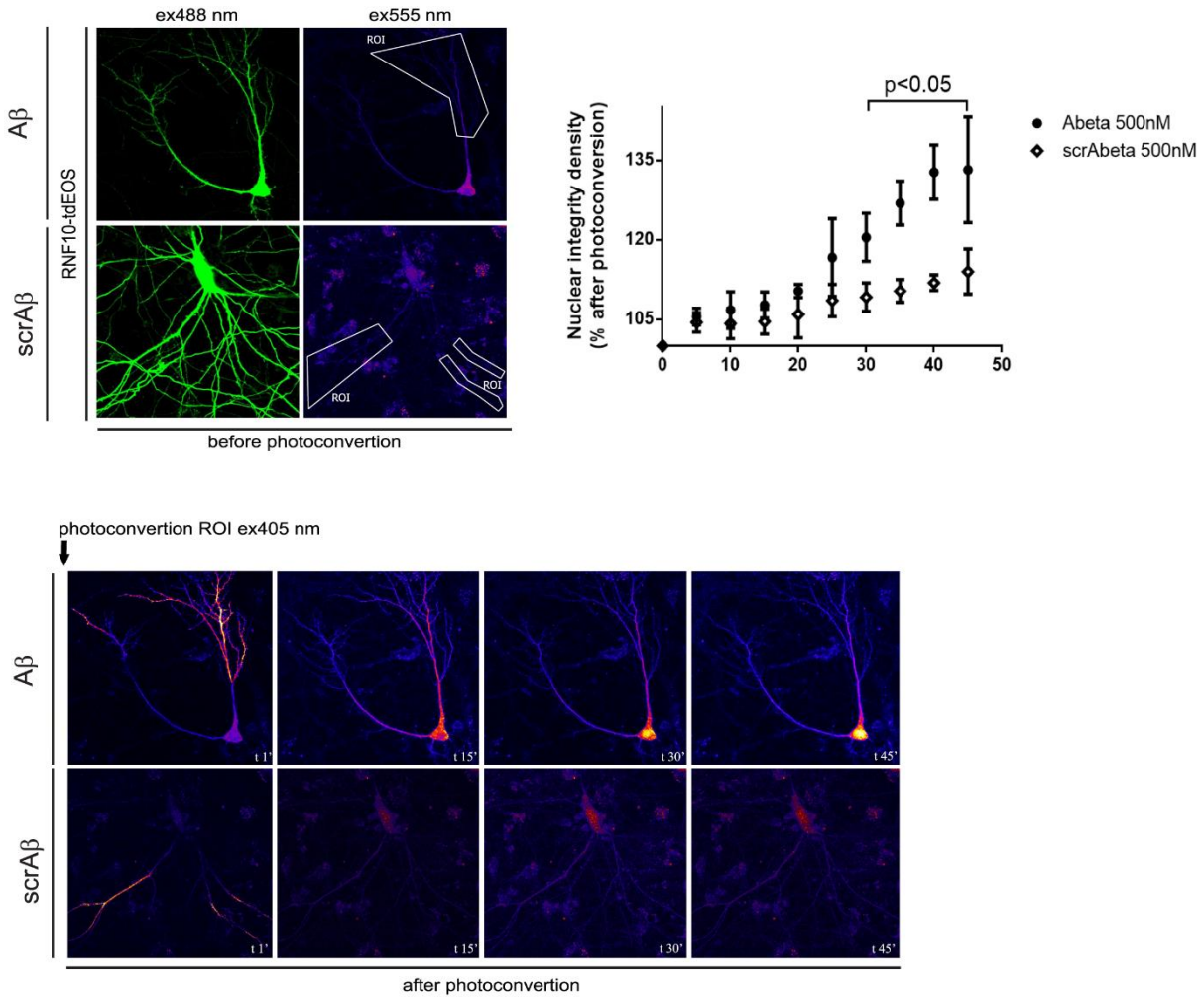

Figure 31. *Aβ42 treatment induces RNF10-tdEOS translocation from distal dendrites to the nucleus in hippocampal neurons. Upper-left panels: Baseline confocal image of RNF10-tdEOS expressing hippocampal neuron illuminated sequentially with 488nm and 555nm laser excitation wavelengths showing no emitted signal in the red spectra (ex555nm; left panels). Distal dendrite (ROI) selected for photoconversion was illuminated with UV laser (405nm wavelengths) repetitively through the image z-stack. Bottom- panels: confocal max intensity projection images at respective time points in control after Aβ42 (or scrAβ) treatment neurons. The histogram (upper-left panel) shows a significant increase in RNF10-tdEOS photoconverted fluorescent intensities in the nucleus following Aβ42 treatment (*p<0.05 Aβ42 vs. scrAβ, from 30' to 45').*

Based on these results, we next evaluated if importins machinery was involved in RNF10 synapto-nuclear translocation. Immunoprecipitation experiments performed with cell lysates of hippocampal neurons revealed that Aβ42, but not scrAβ, significantly increases RNF10/importin α1 association. Interestingly, the treatment significantly decreases RNF10/GluN2A interaction compared to scrAβ treated neurons (figure 32 A-C).

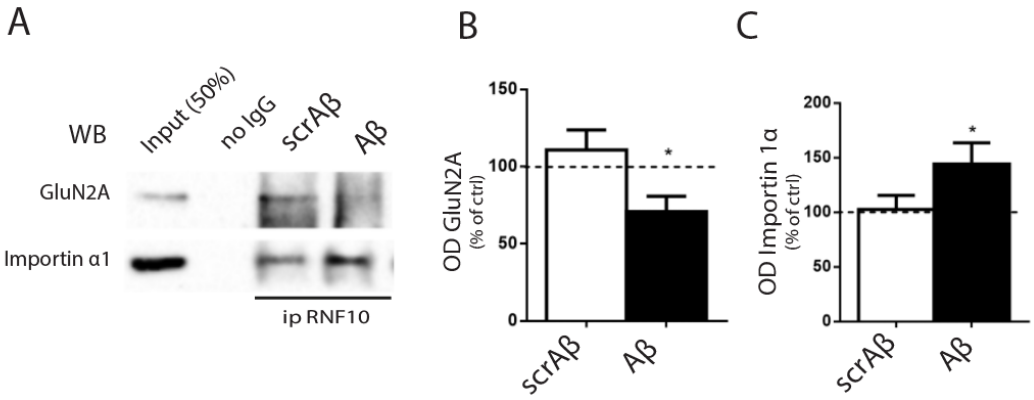

Figure 32 *Aβ42 treatment affects RNF10/GluN2A and RNF10/importin 1α interactions. (A) Representative co-i.p. assays showing the interaction between RNF10/GluN2A and importin α1 in cell lysate of Aβ42 treated neurons. WB analysis was performed with RNF10, GluN2A, importin 1α antibody. (B-C) quantitative analysis shows that Aβ42 treatment decreases the RNF10/GluN2A interaction (-29.16% ±5.735% *p<0.05), while increases RNF10/importin 1α interaction (+44.3%±11.16 *p<0.05).*

5. Aβ MEDIATED RNF10 NUCLEAR TRANSLOCATION IS CALCIUM DEPENDENT

After demonstrating that Aβ42 treatment triggers RNF10 nuclear translocation, we focused our attention on the mechanism underlying this synapto-nuclear communication. It is well established that Aβ42 can directly activate NMDARs (Texido et al 2011, Wang et al 2013), and since we found out that RNF10 is a binding partner of GluN2A, we dissected the role of NMDAR activation taking advantage of pharmacological approaches. We treated DIV14 primary hippocampal neurons with Aβ42 (500nM) for 2hrs with or without APV, a selective NMDAR antagonist that competitively inhibits the glutamate binding site of NMDAR. The immunostaining in Figure 33A shows that the presence of APV completely prevents the Aβ-induced RNF10 translocation. This result demonstrates that NMDAR activation is re in Aβ-triggered RNF10 nuclear translocation. In physiological conditions, the neurotransmitter glutamate binds NMDAR and leads to an influx of calcium. Therefore, we hypothesized that Calcium entry through NMDAR could be involved in RNF10 synapto-nuclear translocation. To address this issue, we decided to chelate extracellular calcium using two different molecules. First, we used EGTA, a general chelating

agent for divalent ions. We treated DIV14 primary hippocampal neurons with Aβ42 (500nM) for 2hrs in presence, or absence, of EGTA. The WB analysis performed on nuclear fraction samples (figure 33B), showed that the presence of EGTA significantly reduced the translocation of RNF10. To strengthe this result we used BAPTA, a more selective calcium-chelating agent that decreases the number of free calcium ion in the medium. As expected, BAPTA completely prevented the RNF10 translocation in Aβ2 treated neurons (figure 33C). These results clearly demonstrate that extracellular calcium influx through NMDAR, is necessary for RNF10 translocation in Aβ42-treated neurons.

Emptage et al., hypothesized that calcium entry through NMDAR can trigger calcium release from intracellular stores (Emptage et al 1999). Indeed, calcium stored within the endoplasmic reticulum of neurons represents an important source of calcium that is released upon activation of either the InsP3Rs (inositol 1,4,5-triphosphate receptor) or the ryanodine-sensitive Ca^{2+} release channel (RyR) (Henzi & MacDermott 1992, Kostyuk & Verkhratsky 1994, Simpson et al 1995). RyRs play a central role in calcium-induced calcium release (CICR), a mechanism by which local elevations of intracellular calcium are amplified by calcium release from ryanodine-sensitive Ca^{2+} stores. Similarly, InsP3Rs, whose activation is mainly due to inositol 1,4,5-triphosphate leading to inositol-induced calcium release (IICR), in certain circumstances can be opened by an increase of calcium, turning thus IICR to CICR (Iino & Tsukioka 1994).

To determine whether calcium influx through NMDA channels triggers calcium release from the intracellular stores, we pharmacologically modulated the intracellular calcium, to better understand its involvement on RNF10 synapto-nuclear communication. To address this issue, we exposed DIV14 Aβ42-treated neurons to 2-Aminoethoxydiphenyl borate (2-APB), a chemical agent that acts to inhibit InsP3Rs. The immunoblot performed on nuclear fraction of treated neurons and the related quantitative analysis showed that 2-APB completely blocks RNF10 translocation (figure 34A). Interestingly, 2APB treatment blocks also the Aβ42-induced expression of the RNF10 gene target p21waf1/cip1 (figure 30B). Moreover, the co-IP experiment (figure 34C) demonstrate that the exposure to 2-APB decrease the interaction of RNF10 with importin 1α (figure 34E) while increase the interaction with GluN2A (figure 34D), compared to neurons treated only with Aβ42. These results demonstrate that Aβ42 directly modulates RNF10 pathway through a CICR mechanism that requires the activation of InsP3Rs.

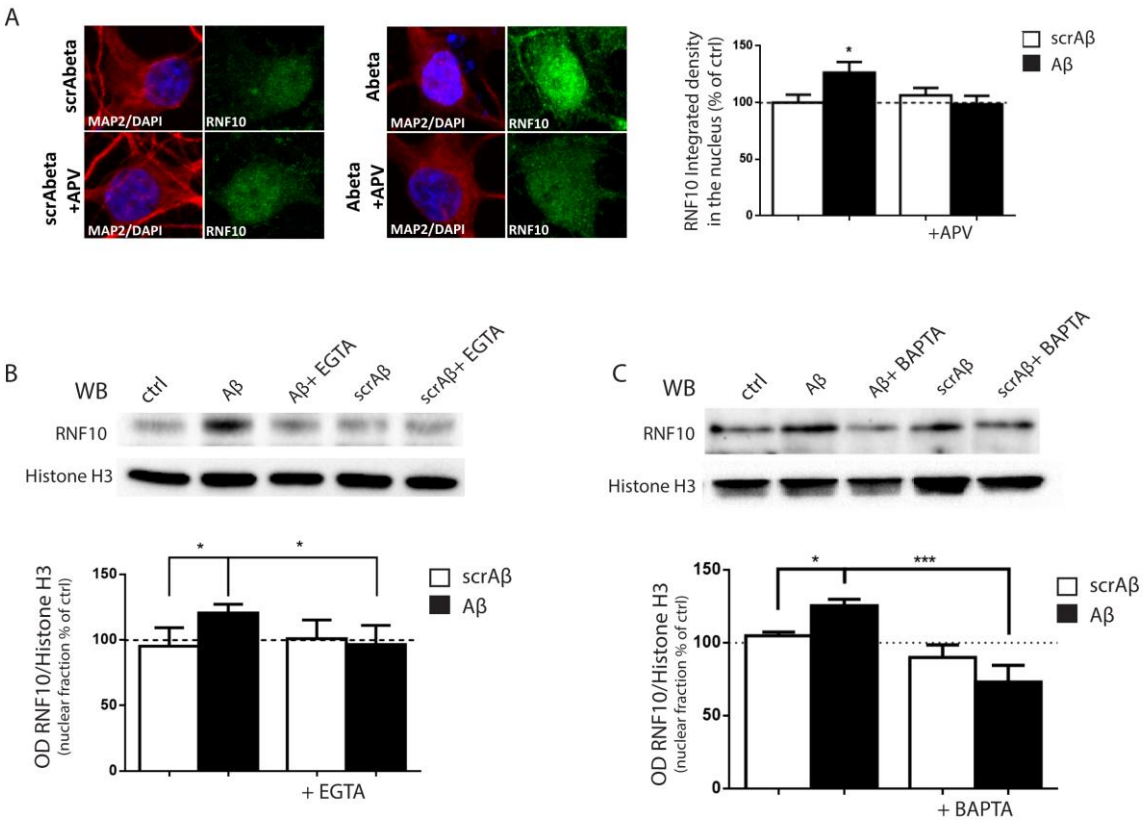

Figure 33 *Aβ42-mediated RNF10 nuclear translocation needs NMDARs activation and calcium entry. (A) Confocal images of DIV14 neurons treated with Aβ42 (or scrAβ) in presence or absence of APV, and immunolabeled for RNF10 (green) and Map2 (red). The histogram shows the quantification of RNF10 signal in nucleus 2h after Aβ42 treatment. The presence of APV completely blocks RNF10 nuclear translocation compared to cell treated only with Aβ42 (B-C) Representative immunoblot from cell nuclear fraction of neurons treated with Aβ42 (or scrAβ) in presence of EGTA (B) or BAPTA (C). WB analysis was performed with RNF10 antibody. The histogram shows that both EGTA and BAPTA inhibit Aβ42-mediated RNF10 nuclear translocation (EGTA *p<0.05; BAPTA *p<0.05, ***p<0.001).*

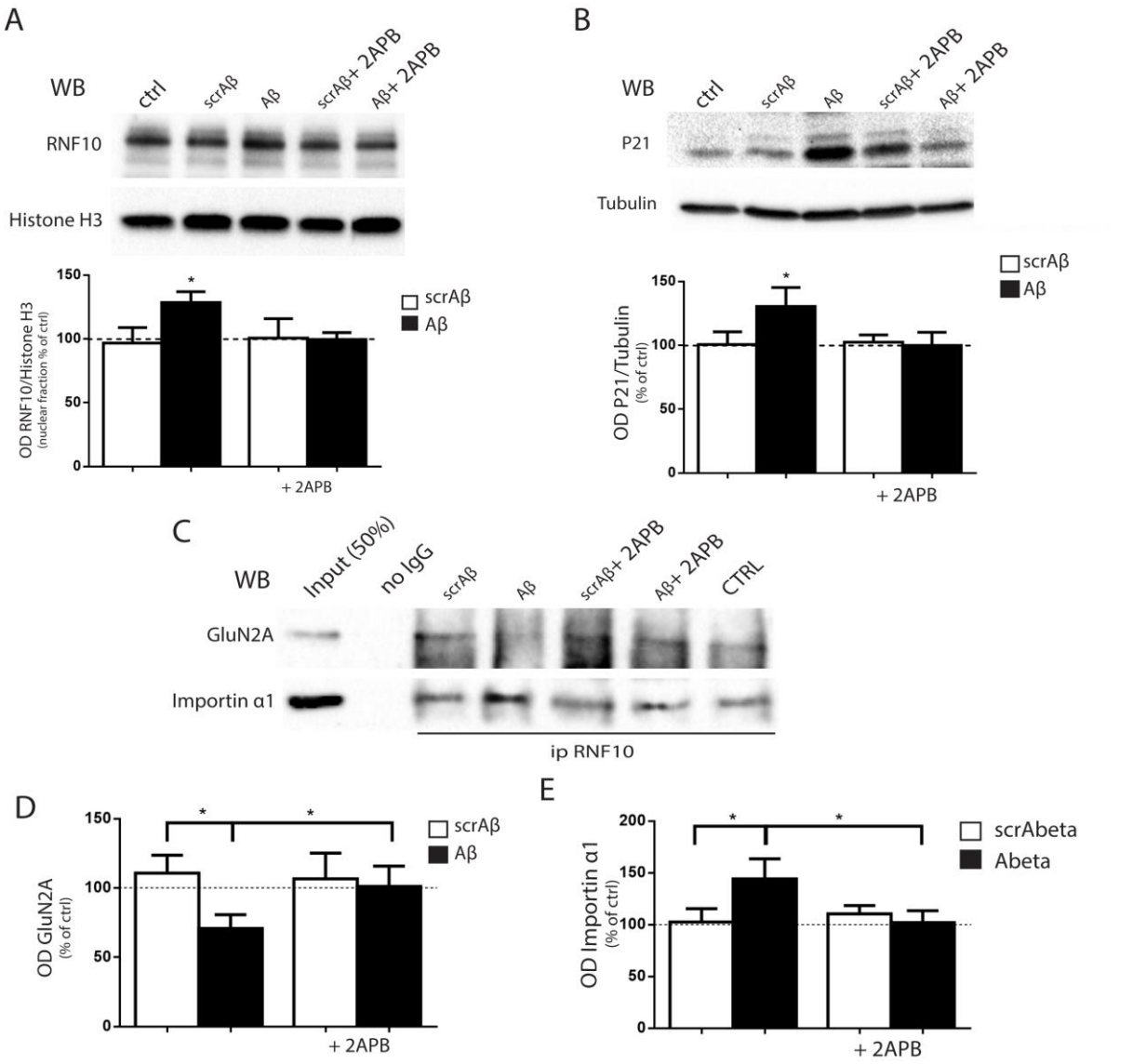

Figure 34 *Calcium-induced calcium-released (CICR) is involved in Aβ42-driven RNF10 nuclear translocation. (A) Representative immunoblot of cell nuclear fraction of neurons treated with Aβ42 (or scrAβ) in presence of 2APB. WB analysis was performed with RNF10 antibody. The histogram shows that 2APB inhibits Aβ42-mediated RNF10 nuclear translocation (*p<0.05). (B) Representative immunoblot of cell lysate of treated neurons. WB analysis was performed with p21$^{waf1/cip1}$ antibody. The quantitative analysis shows that the exposure to 2APB completely inhibits the Aβ42-induced p21$^{waf1/cip1}$ expression (*p<0.05). (C) Representative co-i.p. assay from cell lysate of neurons treated with Aβ42 (or scrAβ42) in presence or absence of 2APB. WB analysis was performed with RNF10, GluN2A and importin α1 antibody. The histograms show the quantification of RNF10 interaction with GluN2A (D) and importin α1 (E). (*p<0.05).*

6. RNF10 SILENCING DECREASE SPINE DENSITY IN Aβ42 TREATED NEURONS

One of the earliest events of AD pathogenesis is the Aβ induced spine loss, even if the mechanism through which this occurs is still unknown (Hsie, sato et al 2006; Shankar et al 2007). We identified a new synapto-nuclear messenger, which regulates the expression of several genes involved in spine morphology (see paragraph 3). Moreover, the silencing of RNF10 leads to a decrease of spine density. Thus, we decide to study the effect of Aβ42 treatment on spine morphology, in primary hippocampal neurons lacking RNF10. GFP-transfected hippocampal neurons either transfected or non-transfected with shRNF10/scrRNF10 were exposed to Aβ42 for 24h. Afterwards we carried out an immunofluorescence assay to measure the density of PSD-95 clusters.

First, we confirmed that, as expected, in our experimental conditions that Aβ42 treatment leads to a significant decrease in PSD-95 clusters density compared to control or scrAβ treated neurons (ctrl 4.578±0.183 spines, scrAβ 4,1.55±0.1208 spines, Aβ 3.360±0.187 spines) (figure 35A). In neurons lacking of RNF10 Aβ42 treatment led to significant reduction of the PSD-95 clusters density to a greater extent as that of the neurons transfected with scramble plasmid (scrRNF10 scrAβ 4.559±0.299 spines, scrRNF10 Aβ 3.679±0.2021 spines, shRNF10 scrAβ 3.525±0.1389, shRNF10 Aβ 2.748±0.2080 spines) (figure 35B).

This result demonstrates that the lack of RNF10 and Aβ42 treatment have a synergistic effect on the loss of spines, suggesting that they act on a common pathway.

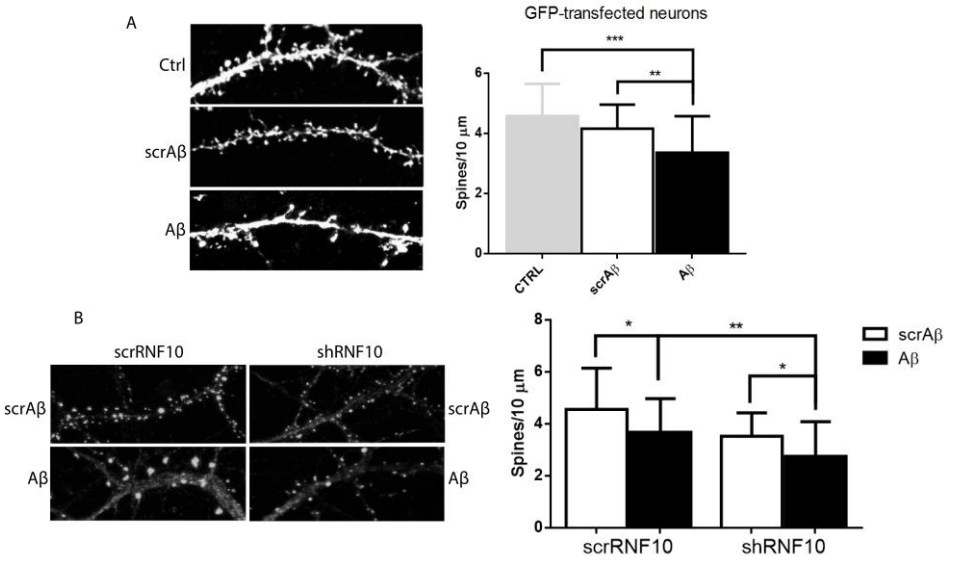

Figure 35 *Silencing of RNF10 decrease Aβ42-mediated dendritic spine density. (A) Representative confocal images and histogram of GFP-transfected neurons treated for 24h with Aβ42 or scrAβ. The quantitative analysis shows that Aβ42 treatment decrease the number of dendritic spines (**p<0.01, ***p<0.001). (B) Representative confocal images and histogram of DIV14 neurons transfected with shRNF10 or pGIZ-scramble (scrRNF10) plasmid and treated for 24h with Aβ42 or scrAβ. The silencing of RNF10 decreases to a greater extent as that of the neurons transfected with scramble plasmid in Aβ42 treated neurons (*p<0.05, **p<0.01)*

7. RNF10 IN ALZHEIMER'S DISEASE

Noteworthy, alterations of the proteins involved in such synapse-to-nucleus pathway have been described in AD patients. In particular it has been shown a decreased expression of Meox-2 in AD patients (Wu et al 2005), suggesting a role of this pathway in the pathology. To assess the involvement of RNF10 pathway in AD, we analyzed RNF10 levels in AD patients' hippocampi provided by the Netherlands Brain Bank. We took advantage of autoptic specimens of hippocampi obtained from 6 AD patients, fulfilling Braak 4 and 5 stage, and 6 aged-matched healthy control subjects. As shown in figure 36, in both total homogenate and nuclear fraction RNF10 protein levels are significantly reduced in AD patients when compared to control subjects (total homogenate -30%, nuclear fraction -56%), indicating the alteration of such protein in AD pathogenic cascade.

Interestingly, as reported for ADAM10 local trafficking, during acute treatment Aβ oligomers can foster RNF10 synapse-to-nucleus trafficking. On the other hand, in chronic pathological conditions such as AD, Aβ accumulation drives the activation of complex cascade of molecular events that leads to a reduction in RNF10 translocation to the nucleus.

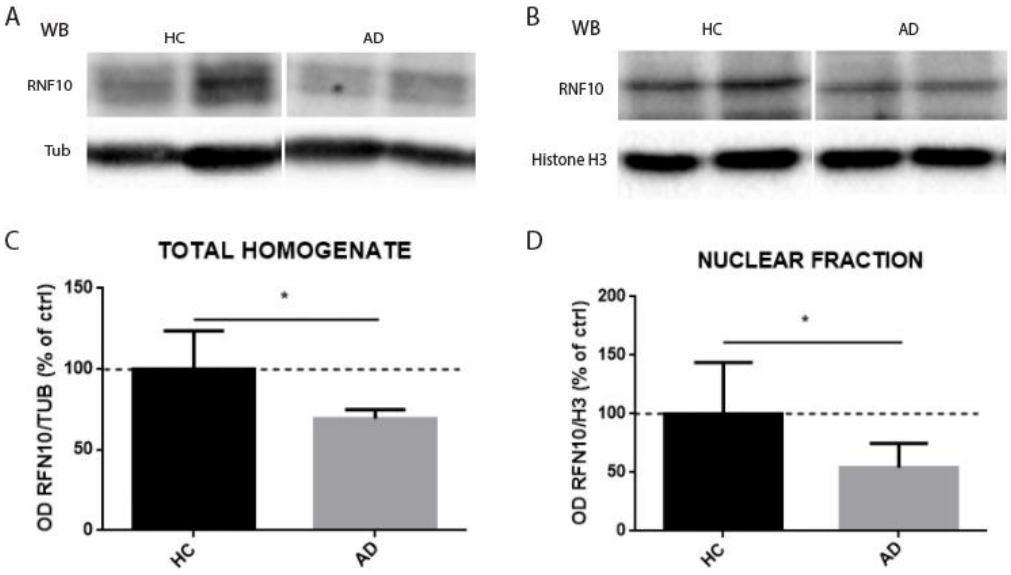

***Figure 36**. RNF10 expression and localization are affected in AD patients. (A-B) Representative immunoblot of total homogenate and nuclear fraction of autoptic specimens of hippocampi obtained from 6 AD patients, fulfilling Braak 4 and 5 stage, and 6 aged-matched healthy control (HC). (C-D) Quantitative analysis reveals that in AD patients there is a significant decrease of RNF10 expression (C, HC 100%±9.664%, AD 69.32%±2.265% *p<0.05) and a significant decrease of nuclear localization (D, HC 100%±17.87, AD 54.11%±8.505% *p<0.05).*

DISCUSSION

The molecular pathogenesis of AD is still controversial, although genetic and cell biology findings indicate accumulation of β-amyloid, especially in soluble oligomeric conformation, as the driving force of synaptic dysfunction with concomitant activation of complex cascade of molecular events leading to dementia (Marcello et al 2012a, Walsh et al 2002b). *In vivo* and *in vitro* studies have demonstrated that high levels of Aβ, particularly in oligomeric forms, alter glutamatergic synaptic transmission and cause synapse loss (Kamenetz et al 2003, Li et al 2009, Li et al 2011, Mucke et al 2000, Shankar et al 2007). The excitatory synapse is characterized by a complex network of protein-protein interaction linking surface receptors, such as ionotropic glutamate receptors, to downstream signalling through a number of scaffold elements.

The number of surface molecules of the PSD, for example glutamate receptors, which control the response of post-synaptic neuron to specific stimuli, is dynamically adjusted by local trafficking namely exo- and endocytosis. Moreover, long-term responses to such stimuli require changes in gene expression at the nucleus. Indeed, the local trafficking and the synapse-to-nucleus communication play a key role in the regulation of the short-term and long-term structural modifications and may be mechanisms required for the integration of multiple signalling pathways.

In the last few years, several studies aimed at understanding how Aβ accumulation and assembly compromise synaptic structure and function of excitatory synapses. In this study, we evaluated how Aβ can affect the local and the long-distance trafficking, since the alteration of these mechanisms could represent a key determinant for synaptic dysfunction.

The first aim of this study was to investigate whether Aβ can affect the synaptic localization of the α-secretase ADAM10. ADAM10 synaptic localization in dynamically governed by the interaction with SAP97 and AP2 complex, which control respectively the exocytosis (Marcello et al 2007) and the endocytosis (Marcello et al 2013) of the enzyme. Moreover, the balance between these two mechanisms is finely tuned by activity-dependent synaptic plasticity: LTP triggers ADAM10 endocytosis while LTD fosters ADAM10 forward trafficking (Marcello et al 2013).

Here we found Aβ42 (500nM, 30 min) exposure results in an increase of ADAM10 synaptic availability. In particular, Aβ42 treatment leads to a decrease in the association between ADAM10 and AP2 complex, suggesting that the augment in ADAM10 synaptic localization is due to a decrease of the endocytosis rather than to an increase of forward trafficking. Several studies demonstrate that Aβ42 induces a LTD-like response (Hsieh et al 2006, Li et al 2009, Li et al 2011, Shankar et al 2008), and in our model we found that Aβ42 decreases the phosphorylation of GluA1 serine-845 site, that is related to LTD (Hsieh et al 2006, Lee et al 1998, Li et al 2009, Li et al 2011, Shankar et al 2008). Therefore, the increase of ADAM10 synaptic availability after Aβ42 treatment can be ascribed to the activation of a LTD-related signaling pathway (Marcello et al 2013). In physiological condition, LTD fosters ADAM10

delivery to the postsynaptic compartment stimulating its association to SAP97. On the other hand we observed that the Aβ42-driven LTD-like response affects the interaction with AP2, thus suggesting that physiological and pathological conditions can differentially regulate ADAM10 local trafficking. Moreover, the ADAM10 increased synaptic availability can represent a negative feedback mechanism through which Aβ42 toxic concentration of can down-regulate Aβ generation.

Interestingly, this mechanism is completely lost in the context of AD. In the early stage of the disease, we found a decrease in the interaction between ADAM10 and SAP97, with a concomitant augmented association with AP2 complex; the unbalance between the exocytosis and the endocytosis underlies the decrease in ADAM10 synaptic localization and activity towards APP (Marcello et al 2012b, Marcello et al 2013). Furthermore, here we demonstrate that this phenomenon occurs also in 3xTg AD mice, suggesting that the increase in ADAM10 endocytosis, and thus the reduction of its activity towards APP, could be a synaptic mechanism of AD pathogenesis.

Developing a drug that can interfere with the primary mechanism of the disease could be a potential disease-modifying strategy capable of modifying the progression of the disease and rescuing the pathological phenotype. Since the use of CPPs has been already exploited in clinical studies for acute neurological disorder (Hill et al., 2012), we developed CPPs able to interfere with ADAM10 clathrin-mediated endocytosis and to restore the unbalance between exo- and endocytosis.

We took advantage of biocomputational study modeling the interaction between the cytoplasmic tail of ADAM10 and AP2 complex (Marcello et al 2013) and we designed four different CPPs that could interfere with ADAM10/AP2 association. We develop also four inactive CPPs that were used as control in each experiment.

First of all, we checked the efficacy and specificity of CPPs using different *in vitro* approaches. We used hippocampal acute slices as a model to screen the efficacy of the four CPPs to affect ADAM10/AP2 association. Co-IP experiments showed that two of the four CPPs, i.e. PEP2 and PEP3, were able to significantly disrupt the interaction.

Once identified the functional CPPs, we used a different *in vitro* models to confirm their activity. In primary hippocampal neurons, we confirmed that PEP2 and PEP3 were also able to disrupt the ADAM10/AP2 interaction at a lower concentration (1μM). Afterwards, we demonstrated that CPPs specifically interfere only with ADAM10/AP2 association; in fact the interactions between AP2 complex and other target proteins, such as APP, GluA1 and GABA A β3 subunits, were not affected by the CPPs. Noteworthy, GABA A β3 subunits represents is an importan control protein because harbours an AP2 binding motif containing three R residues (405 RRR 407) (Smith et al 2012), that is very similar to the AP2-binding domain in ADAM10 c-tail (Marcello et al 2013).

Then, we carried out different assays to determine the efficacy of the CPPs in interfering with ADAM10 endocytosis and in determining an increase in ADAM10 membrane and synaptic levels.

In a heterologous system (COS7 cells) we analysed the internalization rate of ADAM10, and we found that the treatment with one of the active CPPs, i.e. PEP3, significantly reduced the internalization index of the enzyme. On the other hand, PEP2 caused a reduction of the internalization index that was not statistically significant. We also evaluated if CPPs were capable of affecting ADAM10 synaptic localization and surface expression. To address this issue, we performed a BS^3-crosslink assay on hippocampal acute slices and we found that both active CPPs reduced the intracellular pool of ADAM10, indicating an increase of surface expression. Moreover, when we purified the TIF fraction, which is enriched with synaptic proteins, we found an increase in ADAM10 synaptic after the treatment with both PEP2 and PEP3.

All together these results demonstrate that CPPs are able not only to interfere with the interaction between ADAM10 and AP2 complex, but also to modify ADAM10 synaptic localization and surface expression. These promising *in vitro* results led us to set up a series of *in vivo* experiments, with the final aim of rescuing AD phenotype in AD transgenic mouse models.

In light of above, we treated adult C57BL/6 mice with either PEP2 or PEP3, and first we checked if CPPs were able to cross the BBB. It turned out that 24 hours after the intraperitoneal injection, CPPs were distributed in the soma and dendrites of neuronal cells, confirming the capability of CPPs to cross biological membranes. Afterwards, we verified CPPs efficacy analyzing three main parameters: i) the interaction between ADAM10 and AP2 complex, ii) ADAM10 synaptic availability and iii) ADAM10 activity. A first set of animals were treated with both PEP2 and PEP3 with a dose of 3nmol/g. Twenty-four hours after the injection, co-IP experiments showed that CPPs were able to interfere with ADAM10/AP2 association and to increase ADAM10 synaptic availability. Since the ADAM10 is active only when is properly inserted at the synaptic membrane, the increase of ADAM10 synaptic localization should lead to an increase in ADAM10 activity. To address this issue, we purified the brain soluble fraction of treated animals and we evaluated the release of sAPPα as an index of ADAM10 activity. We found out that both PEP2 and PEP3 treatments significantly increases sAPPα release, indicating a shift of APP metabolism towards the non-amyloidogenic pathway. All together these outcomes revealed that a single dose of 3nmol/g CPPs is able to uncouple ADAM10/AP2 complex and to enhance ADAM10 synaptic levels and activity towards APP in 24 hours after the intraperitoneal injection.

In light of the results obtained *in vitro* and *in vivo*, we decide to select PEP3 for the following studies, because PEP3 gave positive results in all the tests carried out.

In order to determine the best conditions for a chronic administration of PEP3, we evaluated the stability, an alternative administration route (subcutaneous injection) and a different dose of PEP3 (1 nmol/g). Mice were treated with PEP3 (1 nmol/g or 3 nmol/g) by intraperitoneal injection and 24 or 48 hours after the administration the ADAM10/AP2 interaction, ADAM10 synaptic availability and activity were evaluated. The results showed that only the dose of 3nmol/g is able to affect ADAM10 endocytosis pathway while the lower dose is not effective. Moreover, 48 hours after the injection the effect on ADAM10 endocytosis, localization and activity is not detectable anymore.

Another set of animals was treated by subcutaneous injection with the same paradigm described above. It turned out that PEP3 doesn't produce any alteration of ADAM10/AP2 association, thus suggesting that such route of administration is not suitable for our treatment.

Finally, we performed a time-course experiment to better understand the stability and availability of PEP3. We treated the mice with PEP3 or inPEP3 and 8, 12, 24 and 36 hours after the intraperitoneal injection we evaluated the capability of PEP3 of uncoupling ADAM10/AP2 interaction, ADAM10 synaptic availability and activity towards APP. Even if we measured a modification of the interaction between ADAM10 and AP2 complex, an alteration of ADAM10 synaptic availability and activity 12 and 36 hours after the injection, these changes were not statistically significant.

Taken together these results demonstrate that, in our experimental conditions, the best dose, administration route and time to detect an effect on ADAM10/AP2 interaction, ADAM10 synaptic localization and activity are 24 hours after an intraperitoneal injection of a dose of 3nmol/g CPPs.

In light of these results, we carried out a 14-days treatment administering either the PEP3 or the inactive inPEP3 or saline solution by intraperitoneal injection every day and we performed a full characterization of efficacy.

The toxicity was assessed on the basis of mortality, changes in physical appearance, body's weight and serum biochemistry profile. The treatment with PEP3 did not cause mortality or changes in physical appearance. No significant alterations in body weight or food intake were detected in the mice treated with PEP3 when compared to mice receiving inPEP3 or saline solution. Afterwards, we evaluated the peripheral system and the combined analysis of hematological and biochemistry results suggests that the administration of PEP3 induces a stimulation of specific immunity, and possibly an allergic/hyperergic reaction. Mice treated with PEP3 had a higher total white blood cells count (compared with controls), a higher lymphocyte count (compared with both controls and mice treated with inPEP3) suggesting a subacute-chronic activation of the immune responses. Moreover, a higher eosinophil count (compared with mice treated with inPEP3) suggested an allergic/hyperergic condition. However, although these findings may be statistically significant, they are not biologically relevant, since all the groups had values within the reference intervals. Furthermore, neither PEP3 nor

inPEP3 induced systemic or organ-specific damage or hematological changes regarding the erythrogram. The results revealed a moderately high globulin concentration in treated mice of the 3 groups, likely depending on the production of acute phase proteins. Lymphocytes and GLDH were occasionally high in individual mice but not in others, suggesting that these are non-specific changes.

To further assess toxicity we performed histological analysis on liver and brain; two pathologists blindly evaluated stained sections. In the liver of all examined animals mild to moderate, diffuse presence of poorly defined vacuoles in the cytoplasm of hepatocytes was observed. These features are characteristic of glycogen accumulation. However, glycogen accumulation can be considered a background change since the degree of glycogen accumulation was similar in all examined subject and is a common feature in mice. No lesions were found in the liver and brain of all examined mice, moreover the PEP3 treatments doesn't induce neuroinflammation since the levels of glial cells or activated microglia is unaltered among the different groups.

With regard to PEP3 efficacy, we assessed the ADAM10/AP2 interaction, ADAM10 synaptic availability and activity. Biochemical analysis showed a significant decrease in ADAM10/AP2 association and a significant increase in ADAM10 synaptic levels in mice treated with PEP3 when compared to mice treated with the inPEP3 and the saline. To evaluate the effect of PEP3 on ADAM10 activity, we analyzed the metabolism of three different substrates, i.e. APP, N-Cadherin and Notch-1. The ELISA analysis measured an enhancement in sAPPα release in the brain of PEP3-treated mice when compared to mice receiving inPEP3 or saline. Accordingly, WB analysis revealed an increase in the N-Cadherin and Notch-1 products generated by ADAM10-mediated cleavage. Notch signaling promotes proliferative signaling during neurogenesis and was found to be critical mainly for neural progenitor cell (NPC) maintenance and self-renewal as well as cell fate specification (Bolos et al 2007). Since we found that treatment with active PEP3 increase Notch-1 cleavage, we can speculate that CPPs could affect neurogenesis. However, further and detailed studies are necessary to demonstrate this hypothesis.

To demonstrate the specificity of PEP3 we evaluated the interaction between ADAM10 and another protein partner, i.e. SAP97, which is involved in ADAM10 forward trafficking (Marcello et al 2007). Co-IP experiment revealed that active peptide doesn't affect ADAM10/SAP97 association, thus demonstrating that the increase in ADAM10 synaptic availability and activity is specifically due to the impairment of endocytosis. Furthermore, we assessed the binding of AP2 with other proteins that undergo clathrin-dependent endocytosis, such as APP, BACE1 and the β3 subunit of the GABA A receptor. We found that PEP3 administration for 2 weeks does not affect the binding of the β3 subunit of the GABA A receptor to AP2, thus demonstrating the specificity of PEP3.

Noteworthy, also APP/AP2 interaction and AP2/BACE-1 association and BACE-1 localization are not affected by PEP3 treatment. These results demonstrate that the PEP3-induced increase in sAPPα

release is due specifically to an increase of ADAM10 activity rather than to an alteration of BACE1 localization and interaction with AP2 complex.

Since ADAM10 is implicated in the complex sequence of events through which N-cadherin affects spine maturation and controls structure and function of glutamatergic synapses (Malinverno et al 2010), and we found that PEP3 increase ADAM10-mediated N-Cadherin cleavage, we evaluated synaptic composition and spine morphology in mice receiving either inPEP3 or PEP3.

We found that active PEP3 doesn't affect synaptic localization of NMDARs or AMPARs subunits. Moreover, PEP3 doesn't change the density of hippocampal dendritic spines. Furthermore, the analysis of spines morphology revealed that PEP3 doesn't change the head width of the spines, while decrease the length, specifically of mushroom types spines. In conclusion, even if PEP3 affects spines length, this effect doesn't alter synaptic composition, suggesting that no alteration of synaptic function occur. To prove this hypothesis, we performed a NOR task to evaluate the working memory of wild-type animals after treatment with either PEP3 or inPEP3, and we found out that active PEP3 has no effect on cognitive function.

In conclusion, we demonstrated that the administration of PEP3 interferes with AP2/ADAM10 complex formation, can increase the synaptic availability of ADAM10 and also its activity towards APP. The increase in sAPPα level suggested a shift of metabolism towards the non-amyloidogenic pathway, precluding the formation of the amyloidogenic fragments. Therefore, the use of PEP3 can be considered a potential disease-modifying tool since it can affect the primary mechanism of AD pathogenesis at the synapse, and could interfere with disease progression.

Another aim of the thesis project was to identify novel Aβ targets in long-distance trafficking in neurons that can be related to long-term modifications of synaptic activity. Indeed, in physiological conditions, the activation of NMDARs can regulate gene transcription (Dieterich et al 2008), thus affecting global protein synthesis and, thereby memory formation. Such effect of NMDAR activation requires the long-distance trafficking of synapto-nuclear proteins.

Here we describe a novel synapse-to-nucleus signaling pathway, involving the RNF10 protein, that specifically links activation of synaptic GluN2A-containing NMDARs to nuclear gene expression. We demonstrate that RNF10 is highly expressed in the nucleus as well as at synapses, where it is part of the NMDAR complex and interacts directly with GluN2A subunit of NMDARs. RNF10 dissociates from the NMDAR complex in an activity-dependent manner and we provide compelling evidence for importin-dependent long-distance transport from synapto-dendritic compartments to the nucleus. Taken together, these findings suggest that synaptonuclear trafficking of RNF10 is involved in the control of gene expression, which is necessary for synaptic plasticity in hippocampal neurons.

Very few studies are available addressing the role of RNF10 in the central nervous system, and they mainly address its association with the transcription factor Meox2, which regulates cell proliferation and differentiation (Hoshikawa et al 2008, Malik et al 2013, Seki et al 2000). A very recent study performed in P19 carcinoma cell line and in mouse cerebellar granule cells suggests that RNF10 acts as a positive regulator of neuronal differentiation, as its knockdown reduced the number of cells expressing early and late neuronal markers (Malik et al 2013). Notably, microarray and subsequent real-time PCR and western blotting analysis allowed us to find, among others, novel RNF10 target genes known to be involved in the regulation of the excitatory synapse function and morphology (Bagni et al 2012, Michaluk et al 2011, Pavlowsky et al 2012, Ramakers et al 2012, Vogt et al 2007) RNF10 silencing induced a dramatic up-regulation of MMP9 expression and a concomitant reduction of Arhgef6, ArhGap4 and Ophn1 levels. Intriguingly, all these genes are mutated or dysregulated in intellectual disability syndromes in humans and/or in the corresponding mouse models (Michaluk et al 2011, Ramakers et al 2012, Vogt et al 2007), which are characterized by various alterations in dendritic spines, thus suggesting a key role in synaptic effects observed following RNF10 silencing.

In this framework, modulation of RNF10 expression in hippocampal neurons is relevant in regulating dendritic spine morphology under resting conditions as well as following activity-dependent plasticity. RNF10 silencing leads to a significant decrease in spine density that is fully rescued by co-transfection of a sh-resistant RNF10 construct.

The present study indicates that NMDAR complex is likely a very rich source of protein messengers that are capable of trafficking to the nucleus. A very recent study showed that the protein messenger Jacob, following long-distance transport and nuclear import, can encode and transduce the synaptic and extrasynaptic origin of GluN2B NMDAR signals to the nucleus and might dock a NMDA-receptor derived signalosome to nuclear target sites in a stimulus-dependent manner (Karpova et al 2013). Interestingly, Aβ oligomer administration to primary neuronal cell culture and hippocampal slices, causes nuclear accumulation of Jacob, that can be blocked by a simultaneous application of ifenprodil, a selective antagonist of GluN2B. This suggest that Aβ oligomers induce early neuronal dysfunction mainly by activation of NR2B-containing NMDA-receptors, and a subsequent nuclear translocation of Jacob (Ronicke et al 2011).

Starting from this consideration, we evaluated if Aβ oligomers could affect RNF10 nuclear translocation. We found that Aβ oligomers foster RNF10 nuclear translocation in a concentration dependent manner, in particular Aβ 500nM increases RNF10 nuclear localization after 30 minutes of treatment, while Aβ 200pM has no effect. Moreover, it turned out that importin-dependent long-distance transport from synapto-dendritic compartments to the nucleus is implicated in this process. To better demonstrate the synapse-to-nucleus translocation we performed an *in vivo* time-lapse using

a RNF10 photoconvertable construct. The live acquisition shows that accumulation of nuclear RNF10 is due to a specific translocation of RNF10 from distal dendrites after application of Aβ. To reinforce the concept that the synapto-nuclear translocation is mediated by Aβ application, we exposed neurons to another source of Aβ. We found that also naturally secreted Aβ oligomers, purified from 7PA2 cells, trigger the nuclear translocation of RNF10. Moreover, this effect is neuron specific since glial cells didn't show RNF10 nuclear accumulation after Aβ treatment.

Since we found that activation of NMDARs leads to a RNF10 translocation, we wondered if the same mechanisms is involved in Aβ-induced RNF10 translocation. To address this issue, we exposed primary hippocampal neurons to Aβ oligomers in presence of APV, an antagonist of GluN2A containing NMDARs. The presence of the drug completely prevented the translocation of RNF10, suggesting that activation of NMDAR is necessary for RNF10 Aβ-mediated translocation.

Notably the activation of NMDAR induce an intracellular influx of Ca^{2+}, thus we hypothesized that calcium can be involved in RNF10 nuclear translocation. To address this issue, we exposed primary hippocampal neurons to Aβ in presence of two different chelating agents, i.e. EGTA and BAPTA. In both cases we found that the chelation of extracellular calcium revert the Aβ-mediated RNF10 nuclear translocation, demonstrating that the activation of NMDAR without the influx of calcium is insufficient to mediate the process.

Calcium plays an important role in regulating a great variety of neuronal processes. The transient changes of cytoplasmic calcium concentration are important element of intracellular signaling. Moreover, the calcium stored within the endoplasmic reticulum of neurons represents an important source of signal Ca^{2+} that is released upon activation of either the InsP3Rs or the RYRs leading to CICR. To evaluate the involvement of this mechanism in RNF10 nuclear translocation, we exposed primary hippocampal neurons to Aβ in presence of a strong InsP3Rs inhibitor, i.e. 2-APB. We demonstrated that the block of calcium release from intracellular store reverts the Aβ-mediated RNF10 nuclear translocation and impairs importin-dependent long-distance transport from synapto-dendritic compartments. Taken together, these results demonstrate that Aβ-driven RNF10 synapse-to-nucleus trafficking is dependent on calcium influx through NMDAR and on a CICR mechanism.

A hallmark of AD is the Aβ-induced spine loss, even if the mechanism through which it occurs is still unknown (Hsieh et al 2006, Shankar et al 2007). The silencing of RNF10 leads to a decrease of spine morphology. Thus we decide to study the effect of Aβ42 on spine morphology in primary hippocampal neurons transfected with shRNF10. It turned out that the lack of RNF10 leads has a synergistic effect with Aβ-induced spine loss, thus suggesting that they share a common pathway

Taken together, these results demonstrate the identification of a novel synaptonuclear protein messenger responsible for long-lasting re-shaping of dendritic spines. Notably, the acute exposure to

Aβ stimulates this synapse-nucleus communication in a calcium-dependent manner. Noteworthy, alterations of the proteins involved in such synapse-to-nucleus pathway have been described in AD patients. In particular it has been shown a decreased expression of Meox-2 in AD patients (Wu et al 2005), suggesting a role of this pathway in the pathology. To evaluate a possible alteration of RNF10 translocation in AD, we evaluated nuclear fraction obtained from AD patients hippocampus specimens and we found that AD patients show a decrease of RNF10 nuclear localization, suggesting that RNF10 could be involved in AD pathogenesis.

In conclusion, we demonstrate that Aβ can affect RNF10 long-distance trafficking. During acute exposure, Aβ induces RNF10 translocation while in a chronic AD pathological context we found a reduction of the translocation. To explain this paradoxical effect, we should take into consideration that Aβ oligomers may enhance LTD by blocking neuronal glutamate uptake at synapses, leading to increased glutamate levels at the synaptic cleft (Li et al 2009). A resultant rise in glutamate levels would initially activate synaptic NMDARs followed by desensitization of the receptors and, ultimately, synaptic depression. Thus, Aβ-induced synaptic depression may result from an initial increase in synaptic activation of NMDARs by glutamate (inducing RNF10 translocation), followed by synaptic NMDAR desensitization and NMDAR/AMPAR internalization.

The study of the mechanisms underlying the cross-talk between Aβ and synaptic function is fundamental because synapse loss has a central role in AD pathogenesis. Synaptic dysfunction drives the cognitive decline in AD and it is not just a consequence of cell death. Synapse-to-nucleus signalling is an uncharted pathway in AD pathogenesis and such mechanism, and the related synaptonuclear protein messengers, can have a central role in the crosstalk between Aβ and synaptic function, being involved in the Aβ-induced synaptic failure. The understanding of the molecular effectors and pathways underlying Aβ-driven synaptic dysfunction is mandatory for the development of successful therapies targeting the disease biology directly and can be exploited for the identification of novel biomarkers of synaptic failure in AD.

REFERENCES

Adams JP, Dudek SM. 2005. Late-phase long-term potentiation: getting to the nucleus. *Nat Rev Neurosci* 6: 737-43

Adler EM, Augustine GJ, Duffy SN, Charlton MP. 1991. Alien intracellular calcium chelators attenuate neurotransmitter release at the squid giant synapse. *J Neurosci* 11: 1496-507

Almeida CG, Tampellini D, Takahashi RH, Greengard P, Lin MT, et al. 2005. Beta-amyloid accumulation in APP mutant neurons reduces PSD-95 and GluR1 in synapses. *Neurobiol Dis* 20: 187-98

Amos LA, Schlieper D. 2005. Microtubules and maps. *Adv Protein Chem* 71: 257-98

Amy C, Zagorski B, Chan V, Parsons D, Vander Laan R, Colantonio A. 2012. Acute care alternate-level-of-care days due to delayed discharge for traumatic and non-traumatic brain injuries. *Healthc Policy* 7: 41-55

Anders A, Gilbert S, Garten W, Postina R, Fahrenholz F. 2001. Regulation of the alpha-secretase ADAM10 by its prodomain and proprotein convertases. *FASEB J* 15: 1837-9

Andersen OM, Reiche J, Schmidt V, Gotthardt M, Spoelgen R, et al. 2005. Neuronal sorting protein-related receptor sorLA/LR11 regulates processing of the amyloid precursor protein. *Proc Natl Acad Sci U S A* 102: 13461-6

Andlin-Sobocki P, Jonsson B, Wittchen HU, Olesen J. 2005. Cost of disorders of the brain in Europe. *Eur J Neurol* 12 Suppl 1: 1-27

Anggono V, Huganir RL. 2012. Regulation of AMPA receptor trafficking and synaptic plasticity. *Curr Opin Neurobiol* 22: 461-9

Appenzeller-Herzog C, Hauri HP. 2006. The ER-Golgi intermediate compartment (ERGIC): in search of its identity and function. *J Cell Sci* 119: 2173-83

Bading H. 2013. Nuclear calcium signalling in the regulation of brain function. *Nat Rev Neurosci* 14: 593-608

Bagni C, Tassone F, Neri G, Hagerman R. 2012. Fragile X syndrome: causes, diagnosis, mechanisms, and therapeutics. *J Clin Invest* 122: 4314-22

Barlowe C. 2002. COPII-dependent transport from the endoplasmic reticulum. *Curr Opin Cell Biol* 14: 417-22

Baron M. 2006. Readers' responses and authors' reply to "medical marijuana: politics trumps science at the FDA". *MedGenMed* 8: 79; author reply 79

Barria A, Muller D, Derkach V, Griffith LC, Soderling TR. 1997. Regulatory phosphorylation of AMPA-type glutamate receptors by CaM-KII during long-term potentiation. *Science* 276: 2042-5

Baude A, Nusser Z, Roberts JD, Mulvihill E, McIlhinney RA, Somogyi P. 1993. The metabotropic glutamate receptor (mGluR1 alpha) is concentrated at perisynaptic membrane of neuronal subpopulations as detected by immunogold reaction. *Neuron* 11: 771-87

Beck KA, Nelson WJ. 1996. The spectrin-based membrane skeleton as a membrane protein-sorting machine. *Am J Physiol* 270: C1263-70

Benjannet S, Elagoz A, Wickham L, Mamarbachi M, Munzer JS, et al. 2001. Post-translational processing of beta-secretase (beta-amyloid-converting enzyme) and its ectodomain shedding. The pro- and transmembrane/cytosolic domains affect its cellular activity and amyloid-beta production. *J Biol Chem* 276: 10879-87

Bennett BD, Denis P, Haniu M, Teplow DB, Kahn S, et al. 2000. A furin-like convertase mediates propeptide cleavage of BACE, the Alzheimer's beta -secretase. *J Biol Chem* 275: 37712-7

Bergquist F, Niazi HS, Nissbrandt H. 2002. Evidence for different exocytosis pathways in dendritic and terminal dopamine release *in vivo*. *Brain Res* 950: 245-53

Berridge MJ. 2009. Inositol trisphosphate and calcium signalling mechanisms. *Biochim Biophys Acta* 1793: 933-40

Bertoni-Freddari C, Fattoretti P, Casoli T, Caselli U, Meier-Ruge W. 1996. Deterioration threshold of synaptic morphology in aging and senile dementia of Alzheimer's type. *Anal Quant Cytol Histol* 18: 209-13

Blackstone C, Murphy TH, Moss SJ, Baraban JM, Huganir RL. 1994. Cyclic AMP and synaptic activity-dependent phosphorylation of AMPA-preferring glutamate receptors. *J Neurosci* 14: 7585-93

Blanpied TA, Scott DB, Ehlers MD. 2002. Dynamics and regulation of clathrin coats at specialized endocytic zones of dendrites and spines. *Neuron* 36: 435-49

Boeckers TM, Winter C, Smalla KH, Kreutz MR, Bockmann J, et al. 1999. Proline-rich synapse-associated proteins ProSAP1 and ProSAP2 interact with synaptic proteins of the SAPAP/GKAP family. *Biochem Biophys Res Commun* 264: 247-52

Bolos V, Grego-Bessa J, de la Pompa JL. 2007. Notch signaling in development and cancer. *Endocr Rev* 28: 339-63

Bonifacino JS, Hurley JH. 2008. Retromer. *Curr Opin Cell Biol* 20: 427-36

Borchelt DR, Thinakaran G, Eckman CB, Lee MK, Davenport F, et al. 1996. Familial Alzheimer's disease-linked presenilin 1 variants elevate Abeta1-42/1-40 ratio in vitro and in vivo. *Neuron* 17: 1005-13

Borgese N, Francolini M, Snapp E. 2006. Endoplasmic reticulum architecture: structures in flux. *Curr Opin Cell Biol* 18: 358-64

Boulter J, Hollmann M, O'Shea-Greenfield A, Hartley M, Deneris E, et al. 1990. Molecular cloning and functional expression of glutamate receptor subunit genes. *Science* 249: 1033-7

Bourne JN, Harris KM. 2008. Balancing structure and function at hippocampal dendritic spines. *Annu Rev Neurosci* 31: 47-67

Brady ST, Crothers SD, Nosal C, McClure WO. 1980. Fast axonal transport in the presence of high Ca2+: evidence that microtubules are not required. *Proc Natl Acad Sci U S A* 77: 5909-13

Brakeman PR, Lanahan AA, O'Brien R, Roche K, Barnes CA, et al. 1997. Homer: a protein that selectively binds metabotropic glutamate receptors. *Nature* 386: 284-8

Bramham CR, Worley PF, Moore MJ, Guzowski JF. 2008. The immediate early gene arc/arg3.1: regulation, mechanisms, and function. *J Neurosci* 28: 11760-7

Brocker C, Engelbrecht-Vandre S, Ungermann C. 2010. Multisubunit tethering complexes and their role in membrane fusion. *Curr Biol* 20: R943-52

Brown MS, Ye J, Rawson RB, Goldstein JL. 2000. Regulated intramembrane proteolysis: a control mechanism conserved from bacteria to humans. *Cell* 100: 391-8

Brown TC, Tran IC, Backos DS, Esteban JA. 2005. NMDA receptor-dependent activation of the small GTPase Rab5 drives the removal of synaptic AMPA receptors during hippocampal LTD. *Neuron* 45: 81-94

Burke JR, Roses AD. 1991. Genetics of Alzheimer's disease. *Int J Neurol* 25-26: 41-51

Burnashev N, Monyer H, Seeburg PH, Sakmann B. 1992. Divalent ion permeability of AMPA receptor channels is dominated by the edited form of a single subunit. *Neuron* 8: 189-98

Caceres A, Kosik KS. 1990. Inhibition of neurite polarity by tau antisense oligonucleotides in primary cerebellar neurons. *Nature* 343: 461-3

Cai XD, Golde TE, Younkin SG. 1993. Release of excess amyloid beta protein from a mutant amyloid beta protein precursor. *Science* 259: 514-6

Cajal SR. 1903. Un sencillo método de coloración selectiva del retículo protoplásmico

y sus efectos en los diversos órganos nerviosos de vertebrados e invertebrados.

. *Tra. Lab. Invest. Biol. 2:129–221.*

Campelo F, Malhotra V. 2012. Membrane fission: the biogenesis of transport carriers. *Annu Rev Biochem* 81: 407-27

Capell A, Steiner H, Willem M, Kaiser H, Meyer C, et al. 2000. Maturation and pro-peptide cleavage of beta-secretase. *J Biol Chem* 275: 30849-54

Carasatorre M, Ramirez-Amaya V. 2013. Network, cellular, and molecular mechanisms underlying long-term memory formation. *Curr Top Behav Neurosci* 15: 73-115

Carroll RC, Beattie EC, Xia H, Luscher C, Altschuler Y, et al. 1999. Dynamin-dependent endocytosis of ionotropic glutamate receptors. *Proc Natl Acad Sci U S A* 96: 14112-7

Ch'ng TH, Uzgil B, Lin P, Avliyakulov NK, O'Dell TJ, Martin KC. 2012. Activity-dependent transport of the transcriptional coactivator CRTC1 from synapse to nucleus. *Cell* 150: 207-21

Chakravarthy B, Gaudet C, Menard M, Atkinson T, Brown L, et al. 2010. Amyloid-beta peptides stimulate the expression of the p75(NTR) neurotrophin receptor in SHSY5Y human neuroblastoma cells and AD transgenic mice. *J Alzheimers Dis* 19: 915-25

Chakravarthy B, Menard M, Ito S, Gaudet C, Dal Pra I, et al. 2012. Hippocampal membrane-associated p75NTR levels are increased in Alzheimer's disease. *J Alzheimers Dis* 30: 675-84

Chapman ER. 2008. How does synaptotagmin trigger neurotransmitter release? *Annu Rev Biochem* 77: 615-41

Chen BS, Roche KW. 2007. Regulation of NMDA receptors by phosphorylation. *Neuropharmacology* 53: 362-8

Cheng D, Hoogenraad CC, Rush J, Ramm E, Schlager MA, et al. 2006. Relative and absolute quantification of postsynaptic density proteome isolated from rat forebrain and cerebellum. *Mol Cell Proteomics* 5: 1158-70

Chevalier-Larsen E, Holzbaur EL. 2006. Axonal transport and neurodegenerative disease. *Biochim Biophys Acta* 1762: 1094-108

Chia PZ, Gunn P, Gleeson PA. 2013. Cargo trafficking between endosomes and the trans-Golgi network. *Histochem Cell Biol* 140: 307-15

Chicurel ME, Harris KM. 1992. Three-dimensional analysis of the structure and composition of CA3 branched dendritic spines and their synaptic relationships with mossy fiber boutons in the rat hippocampus. *J Comp Neurol* 325: 169-82

Chowdhury S, Shepherd JD, Okuno H, Lyford G, Petralia RS, et al. 2006. Arc/Arg3.1 interacts with the endocytic machinery to regulate AMPA receptor trafficking. *Neuron* 52: 445-59

Chung HJ, Xia J, Scannevin RH, Zhang X, Huganir RL. 2000. Phosphorylation of the AMPA receptor subunit GluR2 differentially regulates its interaction with PDZ domain-containing proteins. *J Neurosci* 20: 7258-67

Cioce M, Lamond AI. 2005. Cajal bodies: a long history of discovery. *Annu Rev Cell Dev Biol* 21: 105-31

Cirrito JR, Yamada KA, Finn MB, Sloviter RS, Bales KR, et al. 2005. Synaptic activity regulates interstitial fluid amyloid-beta levels in vivo. *Neuron* 48: 913-22

Citron M, Oltersdorf T, Haass C, McConlogue L, Hung AY, et al. 1992. Mutation of the beta-amyloid precursor protein in familial Alzheimer's disease increases beta-protein production. *Nature* 360: 672-4

Citron M, Westaway D, Xia W, Carlson G, Diehl T, et al. 1997. Mutant presenilins of Alzheimer's disease increase production of 42-residue amyloid beta-protein in both transfected cells and transgenic mice. *Nat Med* 3: 67-72

Colledge M, Dean RA, Scott GK, Langeberg LK, Huganir RL, Scott JD. 2000. Targeting of PKA to glutamate receptors through a MAGUK-AKAP complex. *Neuron* 27: 107-19

Collingridge GL, Peineau S, Howland JG, Wang YT. 2010. Long-term depression in the CNS. *Nat Rev Neurosci* 11: 459-73

Conde C, Caceres A. 2009. Microtubule assembly, organization and dynamics in axons and dendrites. *Nat Rev Neurosci* 10: 319-32

Conn PJ. 2003. Physiological roles and therapeutic potential of metabotropic glutamate receptors. *Ann N Y Acad Sci* 1003: 12-21

Cook A, Bono F, Jinek M, Conti E. 2007. Structural biology of nucleocytoplasmic transport. *Annu Rev Biochem* 76: 647-71

Cooney JR, Hurlburt JL, Selig DK, Harris KM, Fiala JC. 2002. Endosomal compartments serve multiple hippocampal dendritic spines from a widespread rather than a local store of recycling membrane. *J Neurosci* 22: 2215-24

Correia SS, Bassani S, Brown TC, Lise MF, Backos DS, et al. 2008. Motor protein-dependent transport of AMPA receptors into spines during long-term potentiation. *Nat Neurosci* 11: 457-66

Costantini C, Scrable H, Puglielli L. 2006. An aging pathway controls the TrkA to p75NTR receptor switch and amyloid beta-peptide generation. *EMBO J* 25: 1997-2006

Costantini C, Weindruch R, Della Valle G, Puglielli L. 2005. A TrkA-to-p75NTR molecular switch activates amyloid beta-peptide generation during aging. *Biochem J* 391: 59-67

Creemers JW, Ines Dominguez D, Plets E, Serneels L, Taylor NA, et al. 2001. Processing of beta-secretase by furin and other members of the proprotein convertase family. *J Biol Chem* 276: 4211-7

Cui-Wang T, Hanus C, Cui T, Helton T, Bourne J, et al. 2012. Local zones of endoplasmic reticulum complexity confine cargo in neuronal dendrites. *Cell* 148: 309-21

Cutrona MB, Beznoussenko GV, Fusella A, Martella O, Moral P, Mironov AA. 2013. Silencing of mammalian Sar1 isoforms reveals COPII-independent protein sorting and transport. *Traffic* 14: 691-708

D'Amelio M, Cavallucci V, Middei S, Marchetti C, Pacioni S, et al. 2011. Caspase-3 triggers early synaptic dysfunction in a mouse model of Alzheimer's disease. *Nat Neurosci* 14: 69-76

Davies CA, Mann DM, Sumpter PQ, Yates PO. 1987. A quantitative morphometric analysis of the neuronal and synaptic content of the frontal and temporal cortex in patients with Alzheimer's disease. *J Neurol Sci* 78: 151-64

Daw MI, Chittajallu R, Bortolotto ZA, Dev KK, Duprat F, et al. 2000. PDZ proteins interacting with C-terminal GluR2/3 are involved in a PKC-dependent regulation of AMPA receptors at hippocampal synapses. *Neuron* 28: 873-86

De Fabiani E, Mitro N, Gilardi F, Caruso D, Galli G, Crestani M. 2003. Coordinated control of cholesterol catabolism to bile acids and of gluconeogenesis via a novel mechanism of transcription regulation linked to the fasted-to-fed cycle. *J Biol Chem* 278: 39124-32

de la Monte SM, Tong M, Nguyen V, Setshedi M, Longato L, Wands JR. 2010. Ceramide-mediated insulin resistance and impairment of cognitive-motor functions. *J Alzheimers Dis* 21: 967-84

De Strooper B. 2003. Aph-1, Pen-2, and Nicastrin with Presenilin generate an active gamma-Secretase complex. *Neuron* 38: 9-12

Dean C, Liu H, Dunning FM, Chang PY, Jackson MB, Chapman ER. 2009. Synaptotagmin-IV modulates synaptic function and long-term potentiation by regulating BDNF release. *Nat Neurosci* 12: 767-76

Dehmelt L, Halpain S. 2005. The MAP2/Tau family of microtubule-associated proteins. *Genome Biol* 6: 204

DeKosky ST, Scheff SW. 1990. Synapse loss in frontal cortex biopsies in Alzheimer's disease: correlation with cognitive severity. *Ann Neurol* 27: 457-64

Derby MC, Gleeson PA. 2007. New insights into membrane trafficking and protein sorting. *Int Rev Cytol* 261: 47-116

Derkach V, Barria A, Soderling TR. 1999. Ca2+/calmodulin-kinase II enhances channel conductance of alpha-amino-3-hydroxy-5-methyl-4-isoxazolepropionate type glutamate receptors. *Proc Natl Acad Sci U S A* 96: 3269-74

Desai A, Mitchison TJ. 1997. Microtubule polymerization dynamics. *Annu Rev Cell Dev Biol* 13: 83-117

Di Luca M, Baker M, Corradetti R, Kettenmann H, Mendlewicz J, et al. 2011. Consensus document on European brain research. *The European journal of neuroscience* 33: 768-818

Dickson DW, Crystal HA, Bevona C, Honer W, Vincent I, Davies P. 1995. Correlations of synaptic and pathological markers with cognition of the elderly. *Neurobiol Aging* 16: 285-98; discussion 98-304

Dieterich DC, Karpova A, Mikhaylova M, Zdobnova I, Konig I, et al. 2008. Caldendrin-Jacob: a protein liaison that couples NMDA receptor signalling to the nucleus. *PLoS Biol* 6: e34

Dingledine R, Borges K, Bowie D, Traynelis SF. 1999. The glutamate receptor ion channels. *Pharmacol Rev* 51: 7-61

Dolmetsch RE, Pajvani U, Fife K, Spotts JM, Greenberg ME. 2001. Signaling to the nucleus by an L-type calcium channel-calmodulin complex through the MAP kinase pathway. *Science* 294: 333-9

Dong H, O'Brien RJ, Fung ET, Lanahan AA, Worley PF, Huganir RL. 1997. GRIP: a synaptic PDZ domain-containing protein that interacts with AMPA receptors. *Nature* 386: 279-84

dos Remedios CG, Chhabra D, Kekic M, Dedova IV, Tsubakihara M, et al. 2003. Actin binding proteins: regulation of cytoskeletal microfilaments. *Physiol Rev* 83: 433-73

Duff K, Eckman C, Zehr C, Yu X, Prada CM, et al. 1996. Increased amyloid-beta42(43) in brains of mice expressing mutant presenilin 1. *Nature* 383: 710-3

Dunah AW, Wang Y, Yasuda RP, Kameyama K, Huganir RL, et al. 2000. Alterations in subunit expression, composition, and phosphorylation of striatal N-methyl-D-aspartate glutamate receptors in a rat 6-hydroxydopamine model of Parkinson's disease. *Mol Pharmacol* 57: 342-52

Edbauer D, Winkler E, Regula JT, Pesold B, Steiner H, Haass C. 2003. Reconstitution of gamma-secretase activity. *Nat Cell Biol* 5: 486-8

Ehlers MD. 2000. Reinsertion or degradation of AMPA receptors determined by activity-dependent endocytic sorting. *Neuron* 28: 511-25

Ehlers MD. 2013. Dendritic trafficking for neuronal growth and plasticity. *Biochem Soc Trans* 41: 1365-82

Ehlers MD, Zhang S, Bernhadt JP, Huganir RL. 1996. Inactivation of NMDA receptors by direct interaction of calmodulin with the NR1 subunit. *Cell* 84: 745-55

Emes RD, Pocklington AJ, Anderson CN, Bayes A, Collins MO, et al. 2008. Evolutionary expansion and anatomical specialization of synapse proteome complexity. *Nat Neurosci* 11: 799-806

Emptage N, Bliss TV, Fine A. 1999. Single synaptic events evoke NMDA receptor-mediated release of calcium from internal stores in hippocampal dendritic spines. *Neuron* 22: 115-24

Epis R, Marcello E, Gardoni F, Vastagh C, Malinverno M, et al. 2010. Blocking ADAM10 synaptic trafficking generates a model of sporadic Alzheimer's disease. *Brain* 133: 3323-35

Esteban JA, Shi SH, Wilson C, Nuriya M, Huganir RL, Malinow R. 2003. PKA phosphorylation of AMPA receptor subunits controls synaptic trafficking underlying plasticity. *Nat Neurosci* 6: 136-43

Fahrenholz F, Gilbert S, Kojro E, Lammich S, Postina R. 2000. Alpha-secretase activity of the disintegrin metalloprotease ADAM 10. Influences of domain structure. *Ann N Y Acad Sci* 920: 215-22

Famiglietti EV, Jr. 1970. Dendro-dendritic synapses in the lateral geniculate nucleus of the cat. *Brain Res* 20: 181-91

Fein JA, Sokolow S, Miller CA, Vinters HV, Yang F, et al. 2008. Co-localization of amyloid beta and tau pathology in Alzheimer's disease synaptosomes. *Am J Pathol* 172: 1683-92

Fu WY, Chen Y, Sahin M, Zhao XS, Shi L, et al. 2007. Cdk5 regulates EphA4-mediated dendritic spine retraction through an ephexin1-dependent mechanism. *Nat Neurosci* 10: 67-76

Gall JG. 2003. [A role for Cajal bodies in assembly of the nuclear transcription machinery]. *Tsitologiia* 45: 971-5

Galloway PG, Perry G, Gambetti P. 1987. Hirano body filaments contain actin and actin-associated proteins. *J Neuropathol Exp Neurol* 46: 185-99

Gardiol A, Racca C, Triller A. 1999. Dendritic and postsynaptic protein synthetic machinery. *J Neurosci* 19: 168-79

Gardoni F, Mauceri D, Fiorentini C, Bellone C, Missale C, et al. 2003. CaMKII-dependent phosphorylation regulates SAP97/NR2A interaction. *J Biol Chem* 278: 44745-52

Glabe CG. 2008. Structural classification of toxic amyloid oligomers. *J Biol Chem* 283: 29639-43

Glick BS, Nakano A. 2009. Membrane traffic within the Golgi apparatus. *Annu Rev Cell Dev Biol* 25: 113-32

Goate A, Chartier-Harlin MC, Mullan M, Brown J, Crawford F, et al. 1991. Segregation of a missense mutation in the amyloid precursor protein gene with familial Alzheimer's disease. *Nature* 349: 704-6

Gomez LL, Alam S, Smith KE, Horne E, Dell'Acqua ML. 2002. Regulation of A-kinase anchoring protein 79/150-cAMP-dependent protein kinase postsynaptic targeting by NMDA receptor activation of calcineurin and remodeling of dendritic actin. *J Neurosci* 22: 7027-44

Gorenstein C, Bundman MC, Lew PJ, Olds JL, Ribak CE. 1985. Dendritic transport. I. Colchicine stimulates the transport of lysosomal enzymes from cell bodies to dendrites. *J Neurosci* 5: 2009-17

Gorenstein C, Ribak CE. 1985. Dendritic transport. II. Somatofugal movement of neuronal lysosomes induced by colchicine: evidence for a novel transport system in dendrites. *J Neurosci* 5: 2018-27

Gorrie GH, Vallis Y, Stephenson A, Whitfield J, Browning B, et al. 1997. Assembly of GABAA receptors composed of alpha1 and beta2 subunits in both cultured neurons and fibroblasts. *J Neurosci* 17: 6587-96

Grabrucker S, Proepper C, Mangus K, Eckert M, Chhabra R, et al. 2014. The PSD protein ProSAP2/Shank3 displays synapto-nuclear shuttling which is deregulated in a schizophrenia-associated mutation. *Exp Neurol* 253: 126-37

Gray NW, Fourgeaud L, Huang B, Chen J, Cao H, et al. 2003. Dynamin 3 is a component of the postsynapse, where it interacts with mGluR5 and Homer. *Curr Biol* 13: 510-5

Gray NW, Kruchten AE, Chen J, McNiven MA. 2005. A dynamin-3 spliced variant modulates the actin/cortactin-dependent morphogenesis of dendritic spines. *J Cell Sci* 118: 1279-90

Gu Z, Liu W, Yan Z. 2009. {beta}-Amyloid impairs AMPA receptor trafficking and function by reducing Ca2+/calmodulin-dependent protein kinase II synaptic distribution. *J Biol Chem* 284: 10639-49

Gurkan C, Stagg SM, Lapointe P, Balch WE. 2006. The COPII cage: unifying principles of vesicle coat assembly. *Nat Rev Mol Cell Biol* 7: 727-38

Gylys KH, Fein JA, Yang F, Wiley DJ, Miller CA, Cole GM. 2004. Synaptic changes in Alzheimer's disease: increased amyloid-beta and gliosis in surviving terminals is accompanied by decreased PSD-95 fluorescence. *Am J Pathol* 165: 1809-17

Haass C, Schlossmacher MG, Hung AY, Vigo-Pelfrey C, Mellon A, et al. 1992. Amyloid beta-peptide is produced by cultured cells during normal metabolism. *Nature* 359: 322-5

Haass C, Selkoe DJ. 1993. Cellular processing of beta-amyloid precursor protein and the genesis of amyloid beta-peptide. *Cell* 75: 1039-42

Hagenston AM, Bading H. 2011. Calcium signaling in synapse-to-nucleus communication. *Cold Spring Harb Perspect Biol* 3: a004564

Halabisky B, Friedman D, Radojicic M, Strowbridge BW. 2000. Calcium influx through NMDA receptors directly evokes GABA release in olfactory bulb granule cells. *J Neurosci* 20: 5124-34

Hales CM, Griner R, Hobdy-Henderson KC, Dorn MC, Hardy D, et al. 2001. Identification and characterization of a family of Rab11-interacting proteins. *J Biol Chem* 276: 39067-75

Haniu M, Denis P, Young Y, Mendiaz EA, Fuller J, et al. 2000. Characterization of Alzheimer's beta -secretase protein BACE. A pepsin family member with unusual properties. *J Biol Chem* 275: 21099-106

Hardingham GE, Fukunaga Y, Bading H. 2002. Extrasynaptic NMDARs oppose synaptic NMDARs by triggering CREB shut-off and cell death pathways. *Nat Neurosci* 5: 405-14

Hardy J. 1992. Framing beta-amyloid. *Nat Genet* 1: 233-4

Hardy J. 2002. Testing times for the "amyloid cascade hypothesis". *Neurobiol Aging* 23: 1073-4

Hardy J, Allsop D. 1991. Amyloid deposition as the central event in the aetiology of Alzheimer's disease. *Trends Pharmacol Sci* 12: 383-8

Hardy J, Duff K, Hardy KG, Perez-Tur J, Hutton M. 1998. Genetic dissection of Alzheimer's disease and related dementias: amyloid and its relationship to tau. *Nat Neurosci* 1: 355-8

Hardy J, Selkoe DJ. 2002. The amyloid hypothesis of Alzheimer's disease: progress and problems on the road to therapeutics. *Science* 297: 353-6

Hardy JA, Higgins GA. 1992. Alzheimer's disease: the amyloid cascade hypothesis. *Science* 256: 184-5

Hartmann M, Heumann R, Lessmann V. 2001. Synaptic secretion of BDNF after high-frequency stimulation of glutamatergic synapses. *EMBO J* 20: 5887-97

Hayashi MK, Ames HM, Hayashi Y. 2006. Tetrameric hub structure of postsynaptic scaffolding protein homer. *J Neurosci* 26: 8492-501

Hayashi MK, Tang C, Verpelli C, Narayanan R, Stearns MH, et al. 2009. The postsynaptic density proteins Homer and Shank form a polymeric network structure. *Cell* 137: 159-71

He K, Lee A, Song L, Kanold PO, Lee HK. 2011. AMPA receptor subunit GluR1 (GluA1) serine-845 site is involved in synaptic depression but not in spine shrinkage associated with chemical long-term depression. *J Neurophysiol* 105: 1897-907

Heerssen HM, Pazyra MF, Segal RA. 2004. Dynein motors transport activated Trks to promote survival of target-dependent neurons. *Nat Neurosci* 7: 596-604

Hendriks L, van Duijn CM, Cras P, Cruts M, Van Hul W, et al. 1992. Presenile dementia and cerebral haemorrhage linked to a mutation at codon 692 of the beta-amyloid precursor protein gene. *Nat Genet* 1: 218-21

Henninger C, Huelsenbeck J, Huelsenbeck S, Grosch S, Schad A, et al. 2012. The lipid lowering drug lovastatin protects against doxorubicin-induced hepatotoxicity. *Toxicol Appl Pharmacol* 261: 66-73

Henzi V, MacDermott AB. 1992. Characteristics and function of Ca(2+)- and inositol 1,4,5-trisphosphate-releasable stores of Ca2+ in neurons. *Neuroscience* 46: 251-73

Hering H, Lin CC, Sheng M. 2003. Lipid rafts in the maintenance of synapses, dendritic spines, and surface AMPA receptor stability. *J Neurosci* 23: 3262-71

Herpers B, Rabouille C. 2004. mRNA localization and ER-based protein sorting mechanisms dictate the use of transitional endoplasmic reticulum-golgi units involved in gurken transport in Drosophila oocytes. *Mol Biol Cell* 15: 5306-17

Hirokawa N, Pfister KK, Yorifuji H, Wagner MC, Brady ST, Bloom GS. 1989. Submolecular domains of bovine brain kinesin identified by electron microscopy and monoclonal antibody decoration. *Cell* 56: 867-78

Hirokawa N, Takemura R. 2005. Molecular motors and mechanisms of directional transport in neurons. *Nat Rev Neurosci* 6: 201-14

Hoe HS, Fu Z, Makarova A, Lee JY, Lu C, et al. 2009. The effects of amyloid precursor protein on postsynaptic composition and activity. *J Biol Chem* 284: 8495-506

Holtmaat A, Svoboda K. 2009. Experience-dependent structural synaptic plasticity in the mammalian brain. *Nat Rev Neurosci* 10: 647-58

Honer WG, Dickson DW, Gleeson J, Davies P. 1992. Regional synaptic pathology in Alzheimer's disease. *Neurobiol Aging* 13: 375-82

Hoover BR, Reed MN, Su J, Penrod RD, Kotilinek LA, et al. 2010. Tau mislocalization to dendritic spines mediates synaptic dysfunction independently of neurodegeneration. *Neuron* 68: 1067-81

Horiuchi K, Le Gall S, Schulte M, Yamaguchi T, Reiss K, et al. 2007. Substrate selectivity of epidermal growth factor-receptor ligand sheddases and their regulation by phorbol esters and calcium influx. *Mol Biol Cell* 18: 176-88

Horton AC, Ehlers MD. 2003. Dual modes of endoplasmic reticulum-to-Golgi transport in dendrites revealed by live-cell imaging. *J Neurosci* 23: 6188-99

Horton AC, Yi JJ, Ehlers MD. 2006. Cell type-specific dendritic polarity in the absence of spatially organized external cues. *Brain Cell Biol* 35: 29-38

Horton P, Ruban A. 2005. Molecular design of the photosystem II light-harvesting antenna: photosynthesis and photoprotection. *J Exp Bot* 56: 365-73

Hoshikawa S, Ogata T, Fujiwara S, Nakamura K, Tanaka S. 2008. A novel function of RING finger protein 10 in transcriptional regulation of the myelin-associated glycoprotein gene and myelin formation in Schwann cells. *PLoS One* 3: e3464

Hosokawa K, Nishi M, Sakamoto H, Tanaka Y, Kawata M. 2008. Regional distribution of importin subtype mRNA expression in the nervous system: study of early postnatal and adult mouse. *Neuroscience* 157: 864-77

Hsiao KK, Borchelt DR, Olson K, Johannsdottir R, Kitt C, et al. 1995. Age-related CNS disorder and early death in transgenic FVB/N mice overexpressing Alzheimer amyloid precursor proteins. *Neuron* 15: 1203-18

Hsieh H, Boehm J, Sato C, Iwatsubo T, Tomita T, et al. 2006. AMPAR removal underlies Abeta-induced synaptic depression and dendritic spine loss. *Neuron* 52: 831-43

Hsu SM, Raine L, Fanger H. 1981. Use of avidin-biotin-peroxidase complex (ABC) in immunoperoxidase techniques: a comparison between ABC and unlabeled antibody (PAP) procedures. *J Histochem Cytochem* 29: 577-80

Hsu VW, Yang JS. 2009. Mechanisms of COPI vesicle formation. *FEBS Lett* 583: 3758-63

Huse JT, Pijak DS, Leslie GJ, Lee VM, Doms RW. 2000. Maturation and endosomal targeting of beta-site amyloid precursor protein-cleaving enzyme. The Alzheimer's disease beta-secretase. *J Biol Chem* 275: 33729-37

Hutton M, Lendon CL, Rizzu P, Baker M, Froelich S, et al. 1998. Association of missense and 5'-splice-site mutations in tau with the inherited dementia FTDP-17. *Nature* 393: 702-5

Iino M, Tsukioka M. 1994. Feedback control of inositol trisphosphate signalling bycalcium. *Mol Cell Endocrinol* 98: 141-6

Irizarry RA, Ooi SL, Wu Z, Boeke JD. 2003. Use of mixture models in a microarray-based screening procedure for detecting differentially represented yeast mutants. *Stat Appl Genet Mol Biol* 2: Article1

Isaacson JS. 2001. Mechanisms governing dendritic gamma-aminobutyric acid (GABA) release in the rat olfactory bulb. *Proc Natl Acad Sci U S A* 98: 337-42

Ittner LM, Ke YD, Delerue F, Bi M, Gladbach A, et al. 2010. Dendritic function of tau mediates amyloid-beta toxicity in Alzheimer's disease mouse models. *Cell* 142: 387-97

Ivanov A, Pellegrino C, Rama S, Dumalska I, Salyha Y, et al. 2006. Opposing role of synaptic and extrasynaptic NMDA receptors in regulation of the extracellular signal-regulated kinases (ERK) activity in cultured rat hippocampal neurons. *J Physiol* 572: 789-98

Iwatsubo T. 2004a. Assembly and activation of the gamma-secretase complex: roles of presenilin cofactors. *Mol Psychiatry* 9: 8-10

Iwatsubo T. 2004b. The gamma-secretase complex: machinery for intramembrane proteolysis. *Curr Opin Neurobiol* 14: 379-83

Izumiyama N, Ohtsubo K, Tachikawa T, Nakamura H. 1991. Elucidation of three-dimensional ultrastructure of Hirano bodies by the quick-freeze, deep-etch and replica method. *Acta Neuropathol* 81: 248-54

Jack CR, Jr., Knopman DS, Jagust WJ, Petersen RC, Weiner MW, et al. 2013. Tracking pathophysiological processes in Alzheimer's disease: an updated hypothetical model of dynamic biomarkers. *Lancet Neurol* 12: 207-16

Jacob CP, Koutsilieri E, Bartl J, Neuen-Jacob E, Arzberger T, et al. 2007. Alterations in expression of glutamatergic transporters and receptors in sporadic Alzheimer's disease. *J Alzheimers Dis* 11: 97-116

Jaffe DB, Brown TH. 1994. Metabotropic glutamate receptor activation induces calcium waves within hippocampal dendrites. *J Neurophysiol* 72: 471-4

Jahn R, Fasshauer D. 2012. Molecular machines governing exocytosis of synaptic vesicles. *Nature* 490: 201-7

Jeffrey RA, Ch'ng TH, O'Dell TJ, Martin KC. 2009. Activity-dependent anchoring of importin alpha at the synapse involves regulated binding to the cytoplasmic tail of the NR1-1a subunit of the NMDA receptor. *J Neurosci* 29: 15613-20

Jeyifous O, Waites CL, Specht CG, Fujisawa S, Schubert M, et al. 2009. SAP97 and CASK mediate sorting of NMDA receptors through a previously unknown secretory pathway. *Nat Neurosci* 12: 1011-9

Jordan BA, Fernholz BD, Khatri L, Ziff EB. 2007. Activity-dependent AIDA-1 nuclear signaling regulates nucleolar numbers and protein synthesis in neurons. *Nat Neurosci* 10: 427-35

Jordan BA, Kreutz MR. 2009. Nucleocytoplasmic protein shuttling: the direct route in synapse-to-nucleus signaling. *Trends Neurosci* 32: 392-401

Jordens I, Fernandez-Borja M, Marsman M, Dusseljee S, Janssen L, et al. 2001. The Rab7 effector protein RILP controls lysosomal transport by inducing the recruitment of dynein-dynactin motors. *Curr Biol* 11: 1680-5

Jorissen E, Prox J, Bernreuther C, Weber S, Schwanbeck R, et al. 2010. The disintegrin/metalloproteinase ADAM10 is essential for the establishment of the brain cortex. *J Neurosci* 30: 4833-44

Kamenetz F, Tomita T, Hsieh H, Seabrook G, Borchelt D, et al. 2003. APP processing and synaptic function. *Neuron* 37: 925-37

Kano M, Hashimoto K, Kurihara H, Watanabe M, Inoue Y, et al. 1997. Persistent multiple climbing fiber innervation of cerebellar Purkinje cells in mice lacking mGluR1. *Neuron* 18: 71-9

Kapitein LC, Hoogenraad CC. 2011. Which way to go? Cytoskeletal organization and polarized transport in neurons. *Mol Cell Neurosci* 46: 9-20

Karpova A, Bar J, Kreutz MR. 2012. Long-distance signaling from synapse to nucleus via protein messengers. *Adv Exp Med Biol* 970: 355-76

Karpova A, Mikhaylova M, Bera S, Bar J, Reddy PP, et al. 2013. Encoding and transducing the synaptic or extrasynaptic origin of NMDA receptor signals to the nucleus. *Cell* 152: 1119-33

Keller BU, Hollmann M, Heinemann S, Konnerth A. 1992. Calcium influx through subunits GluR1/GluR3 of kainate/AMPA receptor channels is regulated by cAMP dependent protein kinase. *EMBO J* 11: 891-6

Kennedy MB, Beale HC, Carlisle HJ, Washburn LR. 2005. Integration of biochemical signalling in spines. *Nat Rev Neurosci* 6: 423-34

Kennedy MJ, Davison IG, Robinson CG, Ehlers MD. 2010. Syntaxin-4 defines a domain for activity-dependent exocytosis in dendritic spines. *Cell* 141: 524-35

Kim E, Sheng M. 2004. PDZ domain proteins of synapses. *Nat Rev Neurosci* 5: 771-81

Kim T, Vidal GS, Djurisic M, William CM, Birnbaum ME, et al. 2013. Human LilrB2 is a beta-amyloid receptor and its murine homolog PirB regulates synaptic plasticity in an Alzheimer's model. *Science* 341: 1399-404

Kleckner NW, Dingledine R. 1988. Requirement for glycine in activation of NMDA-receptors expressed in Xenopus oocytes. *Science* 241: 835-7

Klein WL, Krafft GA, Finch CE. 2001. Targeting small Abeta oligomers: the solution to an Alzheimer's disease conundrum? *Trends Neurosci* 24: 219-24

Klopfenstein DR, Kappeler F, Hauri HP. 1998. A novel direct interaction of endoplasmic reticulum with microtubules. *EMBO J* 17: 6168-77

Ko GY, Kelly PT. 1999. Nitric oxide acts as a postsynaptic signaling molecule in calcium/calmodulin-induced synaptic potentiation in hippocampal CA1 pyramidal neurons. *J Neurosci* 19: 6784-94

Kohler M, Fiebeler A, Hartwig M, Thiel S, Prehn S, et al. 2002. Differential expression of classical nuclear transport factors during cellular proliferation and differentiation. *Cell Physiol Biochem* 12: 335-44

Kolarow R, Brigadski T, Lessmann V. 2007. Postsynaptic secretion of BDNF and NT-3 from hippocampal neurons depends on calcium calmodulin kinase II signaling and proceeds via delayed fusion pore opening. *J Neurosci* 27: 10350-64

Kopec CD, Real E, Kessels HW, Malinow R. 2007. GluR1 links structural and functional plasticity at excitatory synapses. *J Neurosci* 27: 13706-18

Kostyuk P, Verkhratsky A. 1994. Calcium stores in neurons and glia. *Neuroscience* 63: 381-404

Kreienkamp HJ. 2008. Scaffolding proteins at the postsynaptic density: shank as the architectural framework. *Handb Exp Pharmacol*: 365-80

Kreis TE, Lowe M, Pepperkok R. 1995. COPs regulating membrane traffic. *Annu Rev Cell Dev Biol* 11: 677-706

Kristensson K. 1978. Retrograde transport of macromolecules in axons. *Annu Rev Pharmacol Toxicol* 18: 97-110

Kuhn PH, Wang H, Dislich B, Colombo A, Zeitschel U, et al. 2010. ADAM10 is the physiologically relevant, constitutive alpha-secretase of the amyloid precursor protein in primary neurons. *EMBO J* 29: 3020-32

Kullmann DM, Lamsa KP. 2007. Long-term synaptic plasticity in hippocampal interneurons. *Nat Rev Neurosci* 8: 687-99

Kurup P, Zhang Y, Xu J, Venkitaramani DV, Haroutunian V, et al. 2010. Abeta-mediated NMDA receptor endocytosis in Alzheimer's disease involves ubiquitination of the tyrosine phosphatase STEP61. *J Neurosci* 30: 5948-57

Lacor PN, Buniel MC, Chang L, Fernandez SJ, Gong Y, et al. 2004. Synaptic targeting by Alzheimer's-related amyloid beta oligomers. *J Neurosci* 24: 10191-200

Lammich S, Kojro E, Postina R, Gilbert S, Pfeiffer R, et al. 1999. Constitutive and regulated alpha-secretase cleavage of Alzheimer's amyloid precursor protein by a disintegrin metalloprotease. *Proc Natl Acad Sci U S A* 96: 3922-7

Langford GM. 2002. Myosin-V, a versatile motor for short-range vesicle transport. *Traffic* 3: 859-65

Lapierre LA, Kumar R, Hales CM, Navarre J, Bhartur SG, et al. 2001. Myosin vb is associated with plasma membrane recycling systems. *Mol Biol Cell* 12: 1843-57

Lau CG, Zukin RS. 2007. NMDA receptor trafficking in synaptic plasticity and neuropsychiatric disorders. *Nat Rev Neurosci* 8: 413-26

Lavezzari G, McCallum J, Lee R, Roche KW. 2003. Differential binding of the AP-2 adaptor complex and PSD-95 to the C-terminus of the NMDA receptor subunit NR2B regulates surface expression. *Neuropharmacology* 45: 729-37

Lee G, Rook SL. 1992. Expression of tau protein in non-neuronal cells: microtubule binding and stabilization. *J Cell Sci* 102 (Pt 2): 227-37

Lee HG, Ueda M, Miyamoto Y, Yoneda Y, Perry G, et al. 2006. Aberrant localization of importin alpha1 in hippocampal neurons in Alzheimer disease. *Brain Res* 1124: 1-4

Lee HK, Barbarosie M, Kameyama K, Bear MF, Huganir RL. 2000. Regulation of distinct AMPA receptor phosphorylation sites during bidirectional synaptic plasticity. *Nature* 405: 955-9

Lee HK, Kameyama K, Huganir RL, Bear MF. 1998. NMDA induces long-term synaptic depression and dephosphorylation of the GluR1 subunit of AMPA receptors in hippocampus. *Neuron* 21: 1151-62

Letourneau PC. 2009. Actin in axons: stable scaffolds and dynamic filaments. *Results Probl Cell Differ* 48: 65-90

Levy-Lahad E, Wijsman EM, Nemens E, Anderson L, Goddard KA, et al. 1995. A familial Alzheimer's disease locus on chromosome 1. *Science* 269: 970-3

Lewis J, Dickson DW, Lin WL, Chisholm L, Corral A, et al. 2001. Enhanced neurofibrillary degeneration in transgenic mice expressing mutant tau and APP. *Science* 293: 1487-91

Li B, Jie W, Huang L, Wei P, Li S, et al. 2014. Nuclear BK channels regulate gene expression via the control of nuclear calcium signaling. *Nat Neurosci* 17: 1055-63

Li S, Hong S, Shepardson NE, Walsh DM, Shankar GM, Selkoe D. 2009. Soluble oligomers of amyloid Beta protein facilitate hippocampal long-term depression by disrupting neuronal glutamate uptake. *Neuron* 62: 788-801

Li S, Jin M, Koeglsperger T, Shepardson NE, Shankar GM, Selkoe DJ. 2011. Soluble Abeta oligomers inhibit long-term potentiation through a mechanism involving excessive activation of extrasynaptic NR2B-containing NMDA receptors. *J Neurosci* 31: 6627-38

Li XD, Jung HS, Mabuchi K, Craig R, Ikebe M. 2006. The globular tail domain of myosin Va functions as an inhibitor of the myosin Va motor. *J Biol Chem* 281: 21789-98

Li Z, Jo J, Jia JM, Lo SC, Whitcomb DJ, et al. 2010. Caspase-3 activation via mitochondria is required for long-term depression and AMPA receptor internalization. *Cell* 141: 859-71

Liao FF, Xu H. 2009. Insulin signaling in sporadic Alzheimer's disease. *Sci Signal* 2: pe36

Lin A, Hokugo A, Choi J, Nishimura I. 2010. Small cytoskeleton-associated molecule, fibroblast growth factor receptor 1 oncogene partner 2/wound inducible transcript-3.0 (FGFR1OP2/wit3.0), facilitates fibroblast-driven wound closure. *Am J Pathol* 176: 108-21

Lin J, Friesen MT, Bocangel P, Cheung D, Rawszer K, Wigle JT. 2005. Characterization of Mesenchyme Homeobox 2 (MEOX2) transcription factor binding to RING finger protein 10. *Mol Cell Biochem* 275: 75-84

Lledo PM, Zhang X, Sudhof TC, Malenka RC, Nicoll RA. 1998. Postsynaptic membrane fusion and long-term potentiation. *Science* 279: 399-403

Loechel F, Gilpin BJ, Engvall E, Albrechtsen R, Wewer UM. 1998. Human ADAM 12 (meltrin alpha) is an active metalloprotease. *J Biol Chem* 273: 16993-7

Lohof AM, Ip NY, Poo MM. 1993. Potentiation of developing neuromuscular synapses by the neurotrophins NT-3 and BDNF. *Nature* 363: 350-3

Lorenzo A, Yankner BA. 1996. Amyloid fibril toxicity in Alzheimer's disease and diabetes. *Ann N Y Acad Sci* 777: 89-95

Losonczy A, Magee JC. 2006. Integrative properties of radial oblique dendrites in hippocampal CA1 pyramidal neurons. *Neuron* 50: 291-307

Losonczy A, Makara JK, Magee JC. 2008. Compartmentalized dendritic plasticity and input feature storage in neurons. *Nature* 452: 436-41

Louneva N, Cohen JW, Han LY, Talbot K, Wilson RS, et al. 2008. Caspase-3 is enriched in postsynaptic densities and increased in Alzheimer's disease. *Am J Pathol* 173: 1488-95

Lowenstein PR, Morrison EE, Bain D, Shering AF, Banting G, et al. 1994. Polarized distribution of the trans-Golgi network marker TGN38 during the in vitro development of neocortical neurons: effects of nocodazole and brefeldin A. *The European journal of neuroscience* 6: 1453-65

Lu J, Helton TD, Blanpied TA, Racz B, Newpher TM, et al. 2007. Postsynaptic positioning of endocytic zones and AMPA receptor cycling by physical coupling of dynamin-3 to Homer. *Neuron* 55: 874-89

Lum L, Reid MS, Blobel CP. 1998. Intracellular maturation of the mouse metalloprotease disintegrin MDC15. *J Biol Chem* 273: 26236-47

Luscher C, Xia H, Beattie EC, Carroll RC, von Zastrow M, et al. 1999. Role of AMPA receptor cycling in synaptic transmission and plasticity. *Neuron* 24: 649-58

Lyford GL, Yamagata K, Kaufmann WE, Barnes CA, Sanders LK, et al. 1995. Arc, a growth factor and activity-regulated gene, encodes a novel cytoskeleton-associated protein that is enriched in neuronal dendrites. *Neuron* 14: 433-45

Madden DR. 2002. The structure and function of glutamate receptor ion channels. *Nat Rev Neurosci* 3: 91-101

Malenka RC, Bear MF. 2004. LTP and LTD: an embarrassment of riches. *Neuron* 44: 5-21

Malik YS, Sheikh MA, Lai M, Cao R, Zhu X. 2013. RING finger protein 10 regulates retinoic acid-induced neuronal differentiation and the cell cycle exit of P19 embryonic carcinoma cells. *J Cell Biochem* 114: 2007-15

Malinverno M, Carta M, Epis R, Marcello E, Verpelli C, et al. 2010. Synaptic localization and activity of ADAM10 regulate excitatory synapses through N-cadherin cleavage. *J Neurosci* 30: 16343-55

Mameli M, Balland B, Lujan R, Luscher C. 2007. Rapid synthesis and synaptic insertion of GluR2 for mGluR-LTD in the ventral tegmental area. *Science* 317: 530-3

Manczak M, Reddy PH. 2013. Abnormal interaction of oligomeric amyloid-beta with phosphorylated tau: implications to synaptic dysfunction and neuronal damage. *J Alzheimers Dis* 36: 285-95

Mandell JW, Banker GA. 1995. The microtubule cytoskeleton and the development of neuronal polarity. *Neurobiol Aging* 16: 229-37; discussion 38

Marcello E, Epis R, Saraceno C, Di Luca M. 2012a. Synaptic dysfunction in Alzheimer's disease. *Adv Exp Med Biol* 970: 573-601

Marcello E, Epis R, Saraceno C, Gardoni F, Borroni B, et al. 2012b. SAP97-mediated local trafficking is altered in Alzheimer disease patients' hippocampus. *Neurobiol Aging* 33: 422 e1-10

Marcello E, Gardoni F, Di Luca M, Perez-Otano I. 2010. An arginine stretch limits ADAM10 exit from the endoplasmic reticulum. *J Biol Chem* 285: 10376-84

Marcello E, Gardoni F, Mauceri D, Romorini S, Jeromin A, et al. 2007. Synapse-associated protein-97 mediates alpha-secretase ADAM10 trafficking and promotes its activity. *J Neurosci* 27: 1682-91

Marcello E, Saraceno C, Musardo S, Vara H, de la Fuente AG, et al. 2013. Endocytosis of synaptic ADAM10 in neuronal plasticity and Alzheimer's disease. *J Clin Invest* 123: 2523-38

Marfori M, Mynott A, Ellis JJ, Mehdi AM, Saunders NF, et al. 2011. Molecular basis for specificity of nuclear import and prediction of nuclear localization. *Biochim Biophys Acta* 1813: 1562-77

Martin LJ, Blackstone CD, Levey AI, Huganir RL, Price DL. 1993. AMPA glutamate receptor subunits are differentially distributed in rat brain. *Neuroscience* 53: 327-58

Masliah E, Mallory M, Hansen L, DeTeresa R, Alford M, Terry R. 1994. Synaptic and neuritic alterations during the progression of Alzheimer's disease. *Neurosci Lett* 174: 67-72

Matsuda S, Mikawa S, Hirai H. 1999. Phosphorylation of serine-880 in GluR2 by protein kinase C prevents its C terminus from binding with glutamate receptor-interacting protein. *J Neurochem* 73: 1765-8

Matsuzaki M, Honkura N, Ellis-Davies GC, Kasai H. 2004. Structural basis of long-term potentiation in single dendritic spines. *Nature* 429: 761-6

Maurice T, Lockhart BP, Privat A. 1996. Amnesia induced in mice by centrally administered beta-amyloid peptides involves cholinergic dysfunction. *Brain Res* 706: 181-93

Mayer ML. 2006. Glutamate receptors at atomic resolution. *Nature* 440: 456-62

Mayer ML, Armstrong N. 2004. Structure and function of glutamate receptor ion channels. *Annu Rev Physiol* 66: 161-81

McDonald MP, Dahl EE, Overmier JB, Mantyh P, Cleary J. 1994. Effects of an exogenous beta-amyloid peptide on retention for spatial learning. *Behav Neural Biol* 62: 60-7

McGough IJ, Cullen PJ. 2011. Recent advances in retromer biology. *Traffic* 12: 963-71

Mehta A, Prabhakar M, Kumar P, Deshmukh R, Sharma PL. 2013. Excitotoxicity: bridge to various triggers in neurodegenerative disorders. *Eur J Pharmacol* 698: 6-18

Meldrum BS. 2000. Glutamate as a neurotransmitter in the brain: review of physiology and pathology. *J Nutr* 130: 1007S-15S

Merlie JP, Lindstrom J. 1983. Assembly in vivo of mouse muscle acetylcholine receptor: identification of an alpha subunit species that may be an assembly intermediate. *Cell* 34: 747-57

Meseke M, Rosenberger G, Forster E. 2013. Reelin and the Cdc42/Rac1 guanine nucleotide exchange factor alphaPIX/Arhgef6 promote dendritic Golgi translocation in hippocampal neurons. *The European journal of neuroscience* 37: 1404-12

Meyer G, Varoqueaux F, Neeb A, Oschlies M, Brose N. 2004. The complexity of PDZ domain-mediated interactions at glutamatergic synapses: a case study on neuroligin. *Neuropharmacology* 47: 724-33

Michaluk P, Wawrzyniak M, Alot P, Szczot M, Wyrembek P, et al. 2011. Influence of matrix metalloproteinase MMP-9 on dendritic spine morphology. *J Cell Sci* 124: 3369-80

Molokanova E, Akhtar MW, Sanz-Blasco S, Tu S, Pina-Crespo JC, et al. 2014. Differential effects of synaptic and extrasynaptic NMDA receptors on Abeta-induced nitric oxide production in cerebrocortical neurons. *J Neurosci* 34: 5023-8

Moss ML, Bomar M, Liu Q, Sage H, Dempsey P, et al. 2007. The ADAM10 prodomain is a specific inhibitor of ADAM10 proteolytic activity and inhibits cellular shedding events. *J Biol Chem* 282: 35712-21

Moss SJ, Blackstone CD, Huganir RL. 1993. Phosphorylation of recombinant non-NMDA glutamate receptors on serine and tyrosine residues. *Neurochem Res* 18: 105-10

Mucke L, Masliah E, Yu GQ, Mallory M, Rockenstein EM, et al. 2000. High-level neuronal expression of abeta 1-42 in wild-type human amyloid protein precursor transgenic mice: synaptotoxicity without plaque formation. *J Neurosci* 20: 4050-8

Mullan M, Crawford F, Axelman K, Houlden H, Lilius L, et al. 1992. A pathogenic mutation for probable Alzheimer's disease in the APP gene at the N-terminus of beta-amyloid. *Nat Genet* 1: 345-7

Musardo S, Saraceno C, Pelucchi S, Marcello E. 2013. Trafficking in neurons: searching for new targets for Alzheimer's disease future therapies. *Eur J Pharmacol* 719: 84-106

Nakagawa T, Engler JA, Sheng M. 2004. The dynamic turnover and functional roles of alpha-actinin in dendritic spines. *Neuropharmacology* 47: 734-45

Nakanishi N, Shneider NA, Axel R. 1990. A family of glutamate receptor genes: evidence for the formation of heteromultimeric receptors with distinct channel properties. *Neuron* 5: 569-81

Nitta A, Itoh A, Hasegawa T, Nabeshima T. 1994. beta-Amyloid protein-induced Alzheimer's disease animal model. *Neurosci Lett* 170: 63-6

Nordstedt C, Caporaso GL, Thyberg J, Gandy SE, Greengard P. 1993. Identification of the Alzheimer beta/A4 amyloid precursor protein in clathrin-coated vesicles purified from PC12 cells. *J Biol Chem* 268: 608-12

Nowak L, Bregestovski P, Ascher P, Herbet A, Prochiantz A. 1984. Magnesium gates glutamate-activated channels in mouse central neurones. *Nature* 307: 462-5

Oddo S, Caccamo A, Shepherd JD, Murphy MP, Golde TE, et al. 2003. Triple-transgenic model of Alzheimer's disease with plaques and tangles: intracellular Abeta and synaptic dysfunction. *Neuron* 39: 409-21

Ogawa O, Zhu X, Lee HG, Raina A, Obrenovich ME, et al. 2003. Ectopic localization of phosphorylated histone H3 in Alzheimer's disease: a mitotic catastrophe? *Acta Neuropathol* 105: 524-8

Oh MC, Derkach VA, Guire ES, Soderling TR. 2006. Extrasynaptic membrane trafficking regulated by GluR1 serine 845 phosphorylation primes AMPA receptors for long-term potentiation. *J Biol Chem* 281: 752-8

Okada H, Zhang W, Peterhoff C, Hwang JC, Nixon RA, et al. 2010. Proteomic identification of sorting nexin 6 as a negative regulator of BACE1-mediated APP processing. *FASEB J* 24: 2783-94

Okamoto S, Nakamura T, Cieplak P, Chan SF, Kalashnikova E, et al. 2014. S-nitrosylation-mediated redox transcriptional switch modulates neurogenesis and neuronal cell death. *Cell Rep* 8: 217-28

Palmer CL, Lim W, Hastie PG, Toward M, Korolchuk VI, et al. 2005. Hippocalcin functions as a calcium sensor in hippocampal LTD. *Neuron* 47: 487-94

Palop JJ, Jones B, Kekonius L, Chin J, Yu GQ, et al. 2003. Neuronal depletion of calcium-dependent proteins in the dentate gyrus is tightly linked to Alzheimer's disease-related cognitive deficits. *Proc Natl Acad Sci U S A* 100: 9572-7

Paoletti P, Bellone C, Zhou Q. 2013. NMDA receptor subunit diversity: impact on receptor properties, synaptic plasticity and disease. *Nat Rev Neurosci* 14: 383-400

Park M, Salgado JM, Ostroff L, Helton TD, Robinson CG, et al. 2006. Plasticity-induced growth of dendritic spines by exocytic trafficking from recycling endosomes. *Neuron* 52: 817-30

Passer B, Pellegrini L, Russo C, Siegel RM, Lenardo MJ, et al. 2000. Generation of an apoptotic intracellular peptide by gamma-secretase cleavage of Alzheimer's amyloid beta protein precursor. *J Alzheimers Dis* 2: 289-301

Pavlowsky A, Chelly J, Billuart P. 2012. Major synaptic signaling pathways involved in intellectual disability. *Mol Psychiatry* 17: 663

Pelham HR. 2001. SNAREs and the specificity of membrane fusion. *Trends Cell Biol* 11: 99-101

Perlson E, Hanz S, Ben-Yaakov K, Segal-Ruder Y, Seger R, Fainzilber M. 2005. Vimentin-dependent spatial translocation of an activated MAP kinase in injured nerve. *Neuron* 45: 715-26

Petralia RS, Wenthold RJ. 1992. Light and electron immunocytochemical localization of AMPA-selective glutamate receptors in the rat brain. *J Comp Neurol* 318: 329-54

Pfeffer S, Aivazian D. 2004. Targeting Rab GTPases to distinct membrane compartments. *Nat Rev Mol Cell Biol* 5: 886-96

Pham E, Crews L, Ubhi K, Hansen L, Adame A, et al. 2010. Progressive accumulation of amyloid-beta oligomers in Alzheimer's disease and in amyloid precursor protein transgenic mice is accompanied by selective alterations in synaptic scaffold proteins. *FEBS J* 277: 3051-67

Piazza M, Futrega K, Spratt DE, Dieckmann T, Guillemette JG. 2012. Structure and dynamics of calmodulin (CaM) bound to nitric oxide synthase peptides: effects of a phosphomimetic CaM mutation. *Biochemistry* 51: 3651-61

Poorkaj P, Bird TD, Wijsman E, Nemens E, Garruto RM, et al. 1998. Tau is a candidate gene for chromosome 17 frontotemporal dementia. *Ann Neurol* 43: 815-25

Postina R, Schroeder A, Dewachter I, Bohl J, Schmitt U, et al. 2004. A disintegrin-metalloproteinase prevents amyloid plaque formation and hippocampal defects in an Alzheimer disease mouse model. *J Clin Invest* 113: 1456-64

Potthoff MJ, Olson EN. 2007. MEF2: a central regulator of diverse developmental programs. *Development* 134: 4131-40

Price DL, Tanzi RE, Borchelt DR, Sisodia SS. 1998. Alzheimer's disease: genetic studies and transgenic models. *Annu Rev Genet* 32: 461-93

Price JL, Powell TP. 1970. The morphology of the granule cells of the olfactory bulb. *J Cell Sci* 7: 91-123

Proepper C, Johannsen S, Liebau S, Dahl J, Vaida B, et al. 2007. Abelson interacting protein 1 (Abi-1) is essential for dendrite morphogenesis and synapse formation. *EMBO J* 26: 1397-409

Prybylowski K, Chang K, Sans N, Kan L, Vicini S, Wenthold RJ. 2005. The synaptic localization of NR2B-containing NMDA receptors is controlled by interactions with PDZ proteins and AP-2. *Neuron* 47: 845-57

Puzzo D, Gulisano W, Arancio O, Palmeri A. 2015. The keystone of Alzheimer pathogenesis might be sought in Abeta physiology. *Neuroscience* 307: 26-36

Qu J, Nakamura T, Cao G, Holland EA, McKercher SR, Lipton SA. 2011. S-Nitrosylation activates Cdk5 and contributes to synaptic spine loss induced by beta-amyloid peptide. *Proc Natl Acad Sci U S A* 108: 14330-5

Racz B, Blanpied TA, Ehlers MD, Weinberg RJ. 2004. Lateral organization of endocytic machinery in dendritic spines. *Nat Neurosci* 7: 917-8

Ramakers GJ, Wolfer D, Rosenberger G, Kuchenbecker K, Kreienkamp HJ, et al. 2012. Dysregulation of Rho GTPases in the alphaPix/Arhgef6 mouse model of X-linked intellectual disability is paralleled by impaired structural and synaptic plasticity and cognitive deficits. *Hum Mol Genet* 21: 268-86

Rapoport M, Dawson HN, Binder LI, Vitek MP, Ferreira A. 2002. Tau is essential to beta -amyloid-induced neurotoxicity. *Proc Natl Acad Sci U S A* 99: 6364-9

Ravikumar B, Acevedo-Arozena A, Imarisio S, Berger Z, Vacher C, et al. 2005. Dynein mutations impair autophagic clearance of aggregate-prone proteins. *Nat Genet* 37: 771-6

Rettig J, Heinemann C, Ashery U, Sheng ZH, Yokoyama CT, et al. 1997. Alteration of Ca2+ dependence of neurotransmitter release by disruption of Ca2+ channel/syntaxin interaction. *J Neurosci* 17: 6647-56

Ridge PG, Koop A, Maxwell TJ, Bailey MH, Swerdlow RH, et al. 2013. Mitochondrial haplotypes associated with biomarkers for Alzheimer's disease. *PLoS One* 8: e74158

Rind HB, Butowt R, von Bartheld CS. 2005. Synaptic targeting of retrogradely transported trophic factors in motoneurons: comparison of glial cell line-derived neurotrophic factor, brain-derived neurotrophic factor, and cardiotrophin-1 with tetanus toxin. *J Neurosci* 25: 539-49

Roberson ED, Scearce-Levie K, Palop JJ, Yan F, Cheng IH, et al. 2007. Reducing endogenous tau ameliorates amyloid beta-induced deficits in an Alzheimer's disease mouse model. *Science* 316: 750-4

Roche KW, O'Brien RJ, Mammen AL, Bernhardt J, Huganir RL. 1996. Characterization of multiple phosphorylation sites on the AMPA receptor GluR1 subunit. *Neuron* 16: 1179-88

Roche KW, Standley S, McCallum J, Dune Ly C, Ehlers MD, Wenthold RJ. 2001. Molecular determinants of NMDA receptor internalization. *Nat Neurosci* 4: 794-802

Rogaev EI, Sherrington R, Rogaeva EA, Levesque G, Ikeda M, et al. 1995. Familial Alzheimer's disease in kindreds with missense mutations in a gene on chromosome 1 related to the Alzheimer's disease type 3 gene. *Nature* 376: 775-8

Rogaeva E, Meng Y, Lee JH, Gu Y, Kawarai T, et al. 2007. The neuronal sortilin-related receptor SORL1 is genetically associated with Alzheimer disease. *Nat Genet* 39: 168-77

Roghani M, Becherer JD, Moss ML, Atherton RE, Erdjument-Bromage H, et al. 1999. Metalloprotease-disintegrin MDC9: intracellular maturation and catalytic activity. *J Biol Chem* 274: 3531-40

Ronicke R, Mikhaylova M, Ronicke S, Meinhardt J, Schroder UH, et al. 2011. Early neuronal dysfunction by amyloid beta oligomers depends on activation of NR2B-containing NMDA receptors. *Neurobiol Aging* 32: 2219-28

Rose CR, Konnerth A. 2001. Stores not just for storage. intracellular calcium release and synaptic plasticity. *Neuron* 31: 519-22

Roselli F, Tirard M, Lu J, Hutzler P, Lamberti P, et al. 2005. Soluble beta-amyloid1-40 induces NMDA-dependent degradation of postsynaptic density-95 at glutamatergic synapses. *J Neurosci* 25: 11061-70

Rossner S, Lange-Dohna C, Zeitschel U, Perez-Polo JR. 2005. Alzheimer's disease beta-secretase BACE1 is not a neuron-specific enzyme. *J Neurochem* 92: 226-34

Rossor MN, Fox NC, Freeborough PA, Harvey RJ. 1996. Clinical features of sporadic and familial Alzheimer's disease. *Neurodegeneration* 5: 393-7

Ruben S, Perkins A, Purcell R, Joung K, Sia R, et al. 1989. Structural and functional characterization of human immunodeficiency virus tat protein. *J Virol* 63: 1-8

Saha RN, Dudek SM. 2013. Splitting hares and tortoises: a classification of neuronal immediate early gene transcription based on poised RNA polymerase II. *Neuroscience* 247: 175-81

Sanz-Clemente A, Nicoll RA, Roche KW. 2013. Diversity in NMDA receptor composition: many regulators, many consequences. *Neuroscientist* 19: 62-75

Saraceno C, Musardo S, Marcello E, Pelucchi S, Luca MD. 2013. Modeling Alzheimer's disease: from past to future. *Front Pharmacol* 4: 77

Schafer W, Stroh A, Berghofer S, Seiler J, Vey M, et al. 1995. Two independent targeting signals in the cytoplasmic domain determine trans-Golgi network localization and endosomal trafficking of the proprotein convertase furin. *EMBO J* 14: 2424-35

Scheiffele P. 2003. Cell-cell signaling during synapse formation in the CNS. *Annu Rev Neurosci* 26: 485-508

Schmeisser MJ, Grabrucker AM, Bockmann J, Boeckers TM. 2009. Synaptic cross-talk between N-methyl-D-aspartate receptors and LAPSER1-beta-catenin at excitatory synapses. *J Biol Chem* 284: 29146-57

Schmid SL. 1997. Clathrin-coated vesicle formation and protein sorting: an integrated process. *Annu Rev Biochem* 66: 511-48

Schweizer A, Ericsson M, Bachi T, Griffiths G, Hauri HP. 1993. Characterization of a novel 63 kDa membrane protein. Implications for the organization of the ER-to-Golgi pathway. *J Cell Sci* 104 (Pt 3): 671-83

Schwetz TA, Norring SA, Ednie AR, Bennett ES. 2011. Sialic acids attached to O-glycans modulate voltage-gated potassium channel gating. *J Biol Chem* 286: 4123-32

Scott DB, Michailidis I, Mu Y, Logothetis D, Ehlers MD. 2004. Endocytosis and degradative sorting of NMDA receptors by conserved membrane-proximal signals. *J Neurosci* 24: 7096-109

Seaman MN. 2004. Cargo-selective endosomal sorting for retrieval to the Golgi requires retromer. *J Cell Biol* 165: 111-22

Seki N, Hattori A, Sugano S, Muramatsu M, Saito T. 2000. cDNA cloning, expression profile, and genomic structure of human and mouse RNF10/Rnf 10 genes, encoding a novel RING finger protein. *J Hum Genet* 45: 38-42

Selkoe D, Kopan R. 2003. Notch and Presenilin: regulated intramembrane proteolysis links development and degeneration. *Annu Rev Neurosci* 26: 565-97

Selkoe DJ. 2001. Alzheimer's disease: genes, proteins, and therapy. *Physiol Rev* 81: 741-66

Seubert P, Vigo-Pelfrey C, Esch F, Lee M, Dovey H, et al. 1992. Isolation and quantification of soluble Alzheimer's beta-peptide from biological fluids. *Nature* 359: 325-7

Shankar GM, Bloodgood BL, Townsend M, Walsh DM, Selkoe DJ, Sabatini BL. 2007. Natural oligomers of the Alzheimer amyloid-beta protein induce reversible synapse loss by modulating an NMDA-type glutamate receptor-dependent signaling pathway. *J Neurosci* 27: 2866-75

Shankar GM, Li S, Mehta TH, Garcia-Munoz A, Shepardson NE, et al. 2008. Amyloid-beta protein dimers isolated directly from Alzheimer's brains impair synaptic plasticity and memory. *Nat Med* 14: 837-42

Shanks MF, Powell TP. 1981. An electron microscopic study of the termination of thalamocortical fibres in areas 3b, 1 and 2 of the somatic sensory cortex in the monkey. *Brain Res* 218: 35-47

Sheng M, Hoogenraad CC. 2007. The postsynaptic architecture of excitatory synapses: a more quantitative view. *Annu Rev Biochem* 76: 823-47

Sheng M, Pak DT. 2000. Ligand-gated ion channel interactions with cytoskeletal and signaling proteins. *Annu Rev Physiol* 62: 755-78

Shepherd JD, Huganir RL. 2007. The cell biology of synaptic plasticity: AMPA receptor trafficking. *Annu Rev Cell Dev Biol* 23: 613-43

Sherrington R, Rogaev EI, Liang Y, Rogaeva EA, Levesque G, et al. 1995. Cloning of a gene bearing missense mutations in early-onset familial Alzheimer's disease. *Nature* 375: 754-60

Shi XP, Chen E, Yin KC, Na S, Garsky VM, et al. 2001. The pro domain of beta-secretase does not confer strict zymogen-like properties but does assist proper folding of the protease domain. *J Biol Chem* 276: 10366-73

Shipton OA, Leitz JR, Dworzak J, Acton CE, Tunbridge EM, et al. 2011. Tau protein is required for amyloid {beta}-induced impairment of hippocampal long-term potentiation. *J Neurosci* 31: 1688-92

Shoji M, Golde TE, Ghiso J, Cheung TT, Estus S, et al. 1992. Production of the Alzheimer amyloid beta protein by normal proteolytic processing. *Science* 258: 126-9

Simons M, Ikonen E, Tienari PJ, Cid-Arregui A, Monning U, et al. 1995. Intracellular routing of human amyloid protein precursor: axonal delivery followed by transport to the dendrites. *J Neurosci Res* 41: 121-8

Simpson PB, Challiss RA, Nahorski SR. 1995. Neuronal Ca2+ stores: activation and function. *Trends Neurosci* 18: 299-306

Sinha S, Knops J, Esch F, Moyer ED, Oltersdorf T. 1991. Conversion of the Alzheimer's beta-amyloid precursor protein (APP) Kunitz domain into a potent human neutrophil elastase inhibitor. *J Biol Chem* 266: 21011-3

Sinha S, Lieberburg I. 1999. Cellular mechanisms of beta-amyloid production and secretion. *Proc Natl Acad Sci U S A* 96: 11049-53

Small SA, Gandy S. 2006. Sorting through the cell biology of Alzheimer's disease: intracellular pathways to pathogenesis. *Neuron* 52: 15-31

Small SA, Kent K, Pierce A, Leung C, Kang MS, et al. 2005. Model-guided microarray implicates the retromer complex in Alzheimer's disease. *Ann Neurol* 58: 909-19

Smith DO. 1980. Morphological aspects of the safety factor for action potential propagation at axon branch points in the crayfish. *J Physiol* 301: 261-9

Smith KR, Muir J, Rao Y, Browarski M, Gruenig MC, et al. 2012. Stabilization of GABA(A) receptors at endocytic zones is mediated by an AP2 binding motif within the GABA(A) receptor beta3 subunit. *J Neurosci* 32: 2485-98

Snyder EM, Nong Y, Almeida CG, Paul S, Moran T, et al. 2005. Regulation of NMDA receptor trafficking by amyloid-beta. *Nat Neurosci* 8: 1051-8

Spillantini MG, Bird TD, Ghetti B. 1998. Frontotemporal dementia and Parkinsonism linked to chromosome 17: a new group of tauopathies. *Brain Pathol* 8: 387-402

Spires TL, Hyman BT. 2005. Transgenic models of Alzheimer's disease: learning from animals. *NeuroRx* 2: 423-37

Spruston N. 2008. Pyramidal neurons: dendritic structure and synaptic integration. *Nat Rev Neurosci* 9: 206-21

Stenmark H. 2009. Rab GTPases as coordinators of vesicle traffic. *Nat Rev Mol Cell Biol* 10: 513-25

Stephan A, Laroche S, Davis S. 2001. Generation of aggregated beta-amyloid in the rat hippocampus impairs synaptic transmission and plasticity and causes memory deficits. *J Neurosci* 21: 5703-14

Stewart M. 2007. Molecular mechanism of the nuclear protein import cycle. *Nat Rev Mol Cell Biol* 8: 195-208

Stine WB, Jr., Dahlgren KN, Krafft GA, LaDu MJ. 2003. In vitro characterization of conditions for amyloid-beta peptide oligomerization and fibrillogenesis. *J Biol Chem* 278: 11612-22

Storey GP, Opitz-Araya X, Barria A. 2011. Molecular determinants controlling NMDA receptor synaptic incorporation. *J Neurosci* 31: 6311-6

Sudhof TC. 2004. The synaptic vesicle cycle. *Annu Rev Neurosci* 27: 509-47

Sudhof TC, Rothman JE. 2009. Membrane fusion: grappling with SNARE and SM proteins. *Science* 323: 474-7

Suh YH, Terashima A, Petralia RS, Wenthold RJ, Isaac JT, et al. 2010. A neuronal role for SNAP-23 in postsynaptic glutamate receptor trafficking. *Nat Neurosci* 13: 338-43

Sutton MA, Ito HT, Cressy P, Kempf C, Woo JC, Schuman EM. 2006. Miniature neurotransmission stabilizes synaptic function via tonic suppression of local dendritic protein synthesis. *Cell* 125: 785-99

Suzuki N, Cheung TT, Cai XD, Odaka A, Otvos L, Jr., et al. 1994. An increased percentage of long amyloid beta protein secreted by familial amyloid beta protein precursor (beta APP717) mutants. *Science* 264: 1336-40

Takahashi RH, Capetillo-Zarate E, Lin MT, Milner TA, Gouras GK. 2010. Co-occurrence of Alzheimer's disease ss-amyloid and tau pathologies at synapses. *Neurobiol Aging* 31: 1145-52

Talantova M, Sanz-Blasco S, Zhang X, Xia P, Akhtar MW, et al. 2013. Abeta induces astrocytic glutamate release, extrasynaptic NMDA receptor activation, and synaptic loss. *Proc Natl Acad Sci U S A* 110: E2518-27

Tanaka H, Grooms SY, Bennett MV, Zukin RS. 2000. The AMPAR subunit GluR2: still front and center-stage. *Brain Res* 886: 190-207

Tanaka J, Horiike Y, Matsuzaki M, Miyazaki T, Ellis-Davies GC, Kasai H. 2008. Protein synthesis and neurotrophin-dependent structural plasticity of single dendritic spines. *Science* 319: 1683-7

Tanaka S, Nakamura S, Ueda K, Kameyama M, Shiojiri S, et al. 1988. Three types of amyloid protein precursor mRNA in human brain: their differential expression in Alzheimer's disease. *Biochem Biophys Res Commun* 157: 472-9

Terasaki M, Slater NT, Fein A, Schmidek A, Reese TS. 1994. Continuous network of endoplasmic reticulum in cerebellar Purkinje neurons. *Proc Natl Acad Sci U S A* 91: 7510-4

Terry RD. 1996. The pathogenesis of Alzheimer disease: an alternative to the amyloid hypothesis. *J Neuropathol Exp Neurol* 55: 1023-5

Terry RD, Masliah E, Salmon DP, Butters N, DeTeresa R, et al. 1991. Physical basis of cognitive alterations in Alzheimer's disease: synapse loss is the major correlate of cognitive impairment. *Ann Neurol* 30: 572-80

Texido L, Martin-Satue M, Alberdi E, Solsona C, Matute C. 2011. Amyloid beta peptide oligomers directly activate NMDA receptors. *Cell Calcium* 49: 184-90

Thompson KR, Otis KO, Chen DY, Zhao Y, O'Dell TJ, Martin KC. 2004. Synapse to nucleus signaling during long-term synaptic plasticity; a role for the classical active nuclear import pathway. *Neuron* 44: 997-1009

Tong G, Shepherd D, Jahr CE. 1995. Synaptic desensitization of NMDA receptors by calcineurin. *Science* 267: 1510-2

Torre ER, Steward O. 1996. Protein synthesis within dendrites: glycosylation of newly synthesized proteins in dendrites of hippocampal neurons in culture. *J Neurosci* 16: 5967-78

Traynelis SF, Hartley M, Heinemann SF. 1995. Control of proton sensitivity of the NMDA receptor by RNA splicing and polyamines. *Science* 268: 873-6

Traynelis SF, Wollmuth LP, McBain CJ, Menniti FS, Vance KM, et al. 2010. Glutamate receptor ion channels: structure, regulation, and function. *Pharmacol Rev* 62: 405-96

Trinidad JC, Thalhammer A, Specht CG, Lynn AJ, Baker PR, et al. 2008. Quantitative analysis of synaptic phosphorylation and protein expression. *Mol Cell Proteomics* 7: 684-96

Tsukita S, Ishikawa H. 1980. The movement of membranous organelles in axons. Electron microscopic identification of anterogradely and retrogradely transported organelles. *J Cell Biol* 84: 513-30

Tytell M, Black MM, Garner JA, Lasek RJ. 1981. Axonal transport: each major rate component reflects the movement of distinct macromolecular complexes. *Science* 214: 179-81

Valderrama F, Babia T, Ayala I, Kok JW, Renau-Piqueras J, Egea G. 1998. Actin microfilaments are essential for the cytological positioning and morphology of the Golgi complex. *Eur J Cell Biol* 76: 9-17

van Vliet C, Thomas EC, Merino-Trigo A, Teasdale RD, Gleeson PA. 2003. Intracellular sorting and transport of proteins. *Prog Biophys Mol Biol* 83: 1-45

Vassar R, Bennett BD, Babu-Khan S, Kahn S, Mendiaz EA, et al. 1999. Beta-secretase cleavage of Alzheimer's amyloid precursor protein by the transmembrane aspartic protease BACE. *Science* 286: 735-41

Vedrenne C, Klopfenstein DR, Hauri HP. 2005. Phosphorylation controls CLIMP-63-mediated anchoring of the endoplasmic reticulum to microtubules. *Mol Biol Cell* 16: 1928-37

Vogt DL, Gray CD, Young WS, 3rd, Orellana SA, Malouf AT. 2007. ARHGAP4 is a novel RhoGAP that mediates inhibition of cell motility and axon outgrowth. *Mol Cell Neurosci* 36: 332-42

Von Bartheld CS, Altick AL. 2011. Multivesicular bodies in neurons: distribution, protein content, and trafficking functions. *Prog Neurobiol* 93: 313-40

Wade RH. 2007. Microtubules: an overview. *Methods Mol Med* 137: 1-16

Walsh DM, Klyubin I, Fadeeva JV, Cullen WK, Anwyl R, et al. 2002a. Naturally secreted oligomers of amyloid beta protein potently inhibit hippocampal long-term potentiation in vivo. *Nature* 416: 535-9

Walsh DM, Klyubin I, Fadeeva JV, Rowan MJ, Selkoe DJ. 2002b. Amyloid-beta oligomers: their production, toxicity and therapeutic inhibition. *Biochem Soc Trans* 30: 552-7

Walsh DM, Selkoe DJ. 2004. Deciphering the molecular basis of memory failure in Alzheimer's disease. *Neuron* 44: 181-93

Walsh DM, Selkoe DJ. 2007. A beta oligomers - a decade of discovery. *J Neurochem* 101: 1172-84

Walsh DT, Montero RM, Bresciani LG, Jen AY, Leclercq PD, et al. 2002c. Amyloid-beta peptide is toxic to neurons in vivo via indirect mechanisms. *Neurobiol Dis* 10: 20-7

Walter J, Fluhrer R, Hartung B, Willem M, Kaether C, et al. 2001. Phosphorylation regulates intracellular trafficking of beta-secretase. *J Biol Chem* 276: 14634-41

Wan XZ, Li B, Li YC, Yang XL, Zhang W, et al. 2012. Activation of NMDA receptors upregulates a disintegrin and metalloproteinase 10 via a Wnt/MAPK signaling pathway. *J Neurosci* 32: 3910-6

Wang Z, Edwards JG, Riley N, Provance DW, Jr., Karcher R, et al. 2008. Myosin Vb mobilizes recycling endosomes and AMPA receptors for postsynaptic plasticity. *Cell* 135: 535-48

Wang ZC, Zhao J, Li S. 2013. Dysregulation of synaptic and extrasynaptic N-methyl-D-aspartate receptors induced by amyloid-beta. *Neurosci Bull* 29: 752-60

Washburn MS, Numberger M, Zhang S, Dingledine R. 1997. Differential dependence on GluR2 expression of three characteristic features of AMPA receptors. *J Neurosci* 17: 9393-406

Watanabe I, Zhu J, Recio-Pinto E, Thornhill WB. 2004. Glycosylation affects the protein stability and cell surface expression of Kv1.4 but Not Kv1.1 potassium channels. A pore region determinant dictates the effect of glycosylation on trafficking. *J Biol Chem* 279: 8879-85

Weingarten MD, Lockwood AH, Hwo SY, Kirschner MW. 1975. A protein factor essential for microtubule assembly. *Proc Natl Acad Sci U S A* 72: 1858-62

Wente SR. 2000. Gatekeepers of the nucleus. *Science* 288: 1374-7

Weskamp G, Kratzschmar J, Reid MS, Blobel CP. 1996. MDC9, a widely expressed cellular disintegrin containing cytoplasmic SH3 ligand domains. *J Cell Biol* 132: 717-26

Westerman MA, Cooper-Blacketer D, Mariash A, Kotilinek L, Kawarabayashi T, et al. 2002. The relationship between Abeta and memory in the Tg2576 mouse model of Alzheimer's disease. *J Neurosci* 22: 1858-67

Westphalen RI, Scott HL, Dodd PR. 2003. Synaptic vesicle transport and synaptic membrane transporter sites in excitatory amino acid nerve terminals in Alzheimer disease. *J Neural Transm* 110: 1013-27

Wolfe MS, Xia W, Ostaszewski BL, Diehl TS, Kimberly WT, Selkoe DJ. 1999. Two transmembrane aspartates in presenilin-1 required for presenilin endoproteolysis and gamma-secretase activity. *Nature* 398: 513-7

Wolfsberg TG, Primakoff P, Myles DG, White JM. 1995. ADAM, a novel family of membrane proteins containing A Disintegrin And Metalloprotease domain: multipotential functions in cell-cell and cell-matrix interactions. *J Cell Biol* 131: 275-8

Wolosker H, Blackshaw S, Snyder SH. 1999. Serine racemase: a glial enzyme synthesizing D-serine to regulate glutamate-N-methyl-D-aspartate neurotransmission. *Proc Natl Acad Sci U S A* 96: 13409-14

Wu J, Petralia RS, Kurushima H, Patel H, Jung MY, et al. 2011. Arc/Arg3.1 regulates an endosomal pathway essential for activity-dependent beta-amyloid generation. *Cell* 147: 615-28

Wu Z, Guo H, Chow N, Sallstrom J, Bell RD, et al. 2005. Role of the MEOX2 homeobox gene in neurovascular dysfunction in Alzheimer disease. *Nat Med* 11: 959-65

Wyszynski M, Lin J, Rao A, Nigh E, Beggs AH, et al. 1997. Competitive binding of alpha-actinin and calmodulin to the NMDA receptor. *Nature* 385: 439-42

Xiao B, Tu JC, Petralia RS, Yuan JP, Doan A, et al. 1998. Homer regulates the association of group 1 metabotropic glutamate receptors with multivalent complexes of homer-related, synaptic proteins. *Neuron* 21: 707-16

Yaar M, Zhai S, Pilch PF, Doyle SM, Eisenhauer PB, et al. 1997. Binding of beta-amyloid to the p75 neurotrophin receptor induces apoptosis. A possible mechanism for Alzheimer's disease. *J Clin Invest* 100: 2333-40

Yan R, Han P, Miao H, Greengard P, Xu H. 2001. The transmembrane domain of the Alzheimer's beta-secretase (BACE1) determines its late Golgi localization and access to beta -amyloid precursor protein (APP) substrate. *J Biol Chem* 276: 36788-96

Yan S, Tso J. 2004. Temperature may influence and regulate NF-YB expression in toad oocyte. *Biochem Biophys Res Commun* 313: 802-11

Yang Y, Wang XB, Frerking M, Zhou Q. 2008. Spine expansion and stabilization associated with long-term potentiation. *J Neurosci* 28: 5740-51

Yao PJ, Zhu M, Pyun EI, Brooks AI, Therianos S, et al. 2003. Defects in expression of genes related to synaptic vesicle trafficking in frontal cortex of Alzheimer's disease. *Neurobiol Dis* 12: 97-109

Yoshii A, Constantine-Paton M. 2010. Postsynaptic BDNF-TrkB signaling in synapse maturation, plasticity, and disease. *Dev Neurobiol* 70: 304-22

Yuste R, Majewska A, Holthoff K. 2000. From form to function: calcium compartmentalization in dendritic spines. *Nat Neurosci* 3: 653-9

Zempel H, Thies E, Mandelkow E, Mandelkow EM. 2010. Abeta oligomers cause localized Ca(2+) elevation, missorting of endogenous Tau into dendrites, Tau phosphorylation, and destruction of microtubules and spines. *J Neurosci* 30: 11938-50

Zerial M, McBride H. 2001. Rab proteins as membrane organizers. *Nat Rev Mol Cell Biol* 2: 107-17

Zhai S, Ark ED, Parra-Bueno P, Yasuda R. 2013. Long-distance integration of nuclear ERK signaling triggered by activation of a few dendritic spines. *Science* 342: 1107-11

Zhang J, Ito H, Wate R, Ohnishi S, Nakano S, Kusaka H. 2006. Altered distributions of nucleocytoplasmic transport-related proteins in the spinal cord of a mouse model of amyotrophic lateral sclerosis. *Acta Neuropathol* 112: 673-80

Zhao MG, Toyoda H, Lee YS, Wu LJ, Ko SW, et al. 2005. Roles of NMDA NR2B subtype receptor in prefrontal long-term potentiation and contextual fear memory. *Neuron* 47: 859-72

Zhao WQ, Alkon DL. 2001. Role of insulin and insulin receptor in learning and memory. *Mol Cell Endocrinol* 177: 125-34

Zhao WQ, Chen H, Quon MJ, Alkon DL. 2004. Insulin and the insulin receptor in experimental models of learning and memory. *Eur J Pharmacol* 490: 71-81

Zhao WQ, Santini F, Breese R, Ross D, Zhang XD, et al. 2010. Inhibition of calcineurin-mediated endocytosis and alpha-amino-3-hydroxy-5-methyl-4-isoxazolepropionic acid (AMPA) receptors prevents amyloid beta oligomer-induced synaptic disruption. *J Biol Chem* 285: 7619-32

Zheng H, Koo EH. 2006. The amyloid precursor protein: beyond amyloid. *Mol Neurodegener* 1: 5

Zhu JJ, Esteban JA, Hayashi Y, Malinow R. 2000. Postnatal synaptic potentiation: delivery of GluR4-containing AMPA receptors by spontaneous activity. *Nat Neurosci* 3: 1098-106

Zuber B, Nikonenko I, Klauser P, Muller D, Dubochet J. 2005. The mammalian central nervous synaptic cleft contains a high density of periodically organized complexes. *Proc Natl Acad Sci U S A* 102: 19192-7